

Soils and Rocks

An International Journal of Geotechnical
and Geoenvironmental Engineering



Volume 41, N. 2
May-August 2018

SOILS and ROCKS

An International Journal of Geotechnical and Geoenvironmental Engineering

Editor Paulo Scarano Hemsí - Aeronautics Institute of Technology, Brazil

Co-editor José Couto Marques - University of Porto, Portugal

Executive Board

Waldemar Coelho Hachich
University of São Paulo, Brazil
António Topa Gomes
University of Porto, Portugal

Gustavo Ferreira Simões
Federal University of Minas Gerais, Brazil
Rafaela Cardoso
University of Lisbon, Portugal

Associate Editors

H. Einstein
MIT, USA
John A. Hudson
Imperial College, UK
Kenji Ishihara
University of Tokyo, Japan
Michele Jamiolkowski
Studio Geotecnico Italiano, Italy
Willy A. Lacerda
COPPE/UFRJ, Brazil

E. Maranha das Neves
Lisbon Technical University, Portugal
Nielen van der Merve
University of Pretoria, South Africa
Paul Marinos
NTUA, Greece
James K. Mitchell
Virginia Tech., USA
Lars Persson
SGU, Sweden

Harry G. Poulos
University of Sidney, Australia
Niek Rengers
ITC, The Netherlands
Fumio Tatsuoka
Tokyo University of Science, Japan
Luiz González de Vallejo
UCM, Spain
Roger Frank
ENPC-Cermes, France

Editorial Board Members

Roberto F. Azevedo
Federal University of Viçosa, Brazil
Milton Kanji
University of São Paulo, Brazil
Kátia Vanessa Bicalho
Federal University of Espírito Santo, Brazil
Omar Y. Bitar
IPT, Brazil
Lázaro V. Zuquette
University of São Paulo at São Carlos, Brazil
Fabio Taioli
University of São Paulo, Brazil
Tarcisio Celestino
University of São Paulo at São Carlos, Brazil
Edmundo Rogério Esquivel
University of São Paulo at São Carlos, Brazil
Nilo C. Consoli
Federal Univ. Rio Grande do Sul, Brazil
Sandro S. Sandroni
Consultant, Brazil
Sérgio A.B. Fontoura
Pontifical Catholic University, Brazil
Ennio M. Palmeira
University of Brasília, Brazil
Luciano Décourt
Consultant, Brazil
Faïçal Massad
University of São Paulo, Brazil
Marcus Pacheco
University of the State of Rio de Janeiro, Brazil
Paulo Maia
University of Northern Rio de Janeiro, Brazil
Renato Cunha
University of Brasília, Brazil

Orencio Monje Vilar
University of São Paulo at São Carlos, Brazil
Maria Eugenia Boscov
University of São Paulo, Brazil
Eda Freitas de Quadros
BGTECH, Brazil
Tácio de Campos
Pontifical Catholic University of Rio de Janeiro, Brazil
Richard J. Bathurst
Royal Military College of Canada
Robert Mair
University of Cambridge, UK
Serge Leroueil
University of Laval, Canada
Mario Manassero
Politécnico di Torino, Italy
Luis Valenzuela
Consultant, Chile
Jorge G. Zornberg
University of Texas/Austin, USA
Andrew Whittle
MIT, USA
Pierre Bérest
LCPC, France
Peter Kaiser
Laurentian University, Canada
He Manchao
CUMT, China
Teruo Nakai
Nagoya Inst. Technology, Japan
Claudio Olalla
CEDEX, Spain
Frederick Baynes
Baynes Geologic Ltd., Australia

R. Kerry Rowe
Queen's University, Canada
R. Jonathan Fannin
University of British Columbia, Canada
Laura Caldeira
LNEC, Portugal
António S. Cardoso
University of Porto, Portugal
José D. Rodrigues
Consultant, Portugal
António G. Coelho
Consultant, Portugal
Luís R. Sousa
University of Porto, Portugal
Rui M. Correia
LNEC, Portugal
João Marcelino
LNEC, Portugal
António C. Mineiro
University of Lisbon, Portugal
António P. Cunha
LNEC, Portugal New
António G. Correia
University of Minho, Portugal
Carlos D. Gama
Lisbon Technical University, Portugal
José V. Lemos
LNEC, Portugal
Nuno Grossmann
LNEC, Portugal
Luís L. Lemos
University of Coimbra, Portugal
Ricardo Oliveira
COBA, Portugal

“Ad hoc” Reviewers (2018)

Soils and Rocks is indebted to all “ad hoc” reviewers.

A complete list of reviewers that contributed to the current volume of Soils and Rocks will be published here in the December issue.

Soils and Rocks publishes papers in English in the broad fields of Geotechnical Engineering, Engineering Geology and Geoenvironmental Engineering. The Journal is published in April, August and December. Subscription price is US\$ 90.00 per year. The journal, with the name “Solos e Rochas”, was first published in 1978 by the Graduate School of Engineering, Federal University of Rio de Janeiro (COPPE-UFRJ). In 1980 it became the official magazine of the Brazilian Association for Soil Mechanics and Geotechnical Engineering (ABMS), acquiring the national character that had been the intention of its founders. In 1986 it also became the official Journal of the Brazilian Association for Engineering Geology and the Environment (ABGE) and in 1999 became the Latin American Geotechnical Journal, following the support of Latin-American representatives gathered for the Pan-American Conference of Guadalajara (1996). In 2007 the journal acquired the status of an international journal under the name of Soils and Rocks, published by the Brazilian Association for Soil Mechanics and Geotechnical Engineering (ABMS), Brazilian Association for Engineering Geology and the Environment (ABGE) and Portuguese Geotechnical Society (SPG). In 2010, ABGE decided to publish its own journal and left the partnership.

Soils and Rocks

1978,	1 (1, 2)
1979,	1 (3), 2 (1,2)
1980-1983,	3-6 (1, 2, 3)
1984,	7 (single number)
1985-1987,	8-10 (1, 2, 3)
1988-1990,	11-13 (single number)
1991-1992,	14-15 (1, 2)
1993,	16 (1, 2, 3, 4)
1994-2010,	17-33 (1, 2, 3)
2011,	34 (1, 2, 3, 4)
2012-2017,	35-40 (1, 2, 3)
2018,	41 (1, 2,

ISSN 1980-9743

CDU 624.131.1

SOILS and ROCKS

An International Journal of Geotechnical and Geoenvironmental Engineering

Publication of**ABMS - Brazilian Association for Soil Mechanics and Geotechnical Engineering****SPG - Portuguese Geotechnical Society****Volume 41, N. 2, May-August 2018****Table of Contents***VICTOR DE MELLO LECTURE**Geotechnical Risk, Regulation, and Public Policy*

N.R. Morgenstern

107

*ARTICLES**The Up-Hole Seismic Test Together with the SPT: Description of the System and Method*

R.A.A. Pedrini, B.P. Rocha, H.L. Giacheti

133

Durability of RAP-Industrial Waste Mixtures Under Severe Climate Conditions

N.C. Consoli, H.C. Scheuermann Filho, V.B. Godoy, C.M.D.C. Rosenbach, J.A.H. Carraro

149

Effects of the Addition of Dihydrate Phosphogypsum on the Characterization and Mechanical Behavior of Lateritic Clay

M.M.A. Mascarenha, M.P. Cordão Neto, T.H.C. Matos, J.V.R. Chagas, L.R. Rezende

157

Stress-Strain Analysis of a Concrete Dam in Predominantly Anisotropic Residual Soil

M.F. Leão, M.P. Pacheco, B.R. Danziger

171

Assessment of the Stress History of Quaternary Clay from Piezocone Tests

E. Odebrecht, F. Schnaid

179

*CASE STUDIES**Heterogeneity Evaluation of Soil Engineering Properties Based on Kriging Interpolation Method. Case Study: North East of Iran, West of Mashhad*

M. Etemadifar, N.S. Vaziri, I. Aghamolaie, N.H. Moghaddas, G.R. Lashkaripour

193

Case Study: Stability Assessment in Underground Excavations at Vazante Mine - Brazil

L.T. Figueiredo, A.P. Assis

203

A Case History with Combined Physical and Vacuum Preloading in Colombia

D.G. Yanez, F. Massad

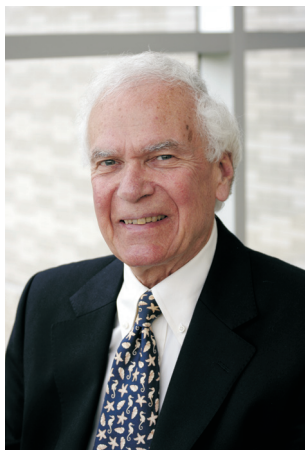
217

Victor de Mello Lecture



The Victor de Mello Lecture was established in 2008 by the Brazilian Association for Soil Mechanics and Geotechnical Engineering (ABMS), the Brazilian Association for Engineering Geology and the Environment (ABGE) and the Portuguese Geotechnical Society (SPG) to celebrate the life and professional contributions of Prof. Victor de Mello. Prof. de Mello was a consultant and academic for over 5 decades and made important contributions to the advance of geotechnical engineering. Every second year a worldwide acknowledged geotechnical expert is invited to deliver this special lecture, on occasion of the main conferences of ABMS and SPG.

This 6th Victor de Mello Lecture is delivered by a prestigious geotechnical engineer and a good friend of Victor de Mello. Prof. Nordie Morgenstern is an internationally-renowned professor, author, consultant, practitioner and researcher. Following slope instability disasters in Hong Kong in the 1970s, Prof. Morgenstern and Prof. de Mello worked for the Government of Hong Kong advising on the causes and implications of the recent landslides, and recommended the establishment of an organization to support the Government in managing the stability of HK slopes, which became the Geotechnical Engineering Office, GEO. The intensively productive relationship between these good friends encouraged Prof. Morgenstern to become President of the ISSMGE, in what became a very productive period for our international society. Prof. Morgenstern shares with us, in his Victor de Mello Lecture, his immense experience on the crucial interface between geotechnical risk, regulation and public policy, so important in these times.



Prof. N.R. MORGENSTERN, Distinguished University Professor Emeritus at the University of Alberta, is an international authority on geotechnical engineering and a highly sought-after consultant. As an educator, researcher and practitioner, the international scope of his experience spans over 40 countries on 6 continents. Among his recognitions, he is an elected Fellow of the Royal Society of Canada and the Canadian Academy of Engineering. He is also a Foreign Associate of the US National Academy of Engineering, a Foreign Member of the Royal Academy of Engineering (UK) and a Foreign Fellow of the National Academy of Engineering of India. He has been inducted into the Alberta Order of Excellence and the Order of Canada for his outstanding achievements and life-long contributions to geotechnical engineering. He has received honorary degrees from the University of Toronto, Queen's University and the University of Alberta. Moreover, he is an Honorary Professor at Zhejiang University, PRC.

Soils and Rocks
v. 41, n. 2

Geotechnical Risk, Regulation, and Public Policy

N.R. Morgenstern

Abstract. At this time, there is a crisis associated with concern over the safety of tailings dams and lack of trust in their design and performance. This crisis has resulted from recent high-profile failures of dams at locations with strong technical experience, conscientious operators, and established regulatory procedures. It is the primary intent of this Lecture to assess the underlying cause(s) for this crisis, review the response to it by various agencies, and to make recommendations on how to overcome it. The Lecture begins with a review of the evolving safety culture associated with slope stability problems as exemplified by the achievements in Hong Kong. This is particularly relevant here because Victor de Mello was a key contributor to the recommendations made in 1976 that initiated the development of the Hong Kong Slope Safety System. The Lecture then addresses the evolution of the safety culture associated with water dams. While there is a long history of concern with respect to water dam safety, these concerns were intensified by several catastrophic dam failures that occurred in the USA in the 1970s. The evolution of regulatory systems from that time is recorded, as is the later trend to adopt risk-based safety assessment and regulation. However, the process that has emerged has been much affected by the Oroville Dam Spillway incident, and dam safety practice is being re-assessed by many. This Lecture summarizes some of the major findings arising from the analysis of this incident and makes recommendations to move to more performance-based risk-informed design and safety reviews that are constrained by reliable evidence to a greater degree than is currently the case. Turning to the evolving safety culture for tailings dams, this emerged with rational dam design procedures in the 1970s, more or less as an appendage to water dam design. The growth of environmental legislation related to surface water quality had a considerable impact as well. Hence, a twin regulatory regime emerged in the 1970s. The regulatory regime for tailings dams is typically more regional than national. The failure rate for tailings dams has generally been proportionately higher than water dams and thus has received considerable attention in the technical literature, however without measurable results. The recent failures of major dams in technically advanced regions of the world, operated by mature mining organizations and designed by recognized consulting engineers, has created a crisis in terms of a loss of confidence and trust associated with the design, construction, operation, and closure of tailings storage facilities. Responses to these failures are analyzed, and all are found wanting, particularly since the widespread evidence for weak engineering is inadequately recognized. The Lecture proposes a system for Performance-Based Risk-Informed Safe Design, Construction, Operation, and Closure of tailings storage facilities. It further urges the International Council on Mining and Metals (ICMM) to support the proposed system and facilitate its adoption in practice.

Keywords: safety culture, slopes, water dams, tailings dams, risk analysis, performance-based design.

In Memoriam

Like my predecessors who have delivered this Lecture, I too was much influenced by my relationship with Victor de Mello. Victor was inspiring in his breadth of interests, his enthusiasm, and his accomplishments. Reading the list of his consulting assignments is almost like reading the history of modern Brazil. This relates not only to his prowess as a consulting engineer, but also to his dedication to our profession as both a teacher and a researcher.

Over the years we engaged in numerous discussions on both technical and professional matters. I owe much to his guidance and support that encouraged me to become President of our International Society (ISSMGE). While we discussed a number of technical challenges over the years, the one in which we collaborated closely was the assignment from the Government of Hong Kong to partici-

pate in an Independent Review Panel on Fill Slopes, in 1976. The photo below (Fig. 1) shows Victor in characteristic field-work mode. As will be discussed subsequently in this paper, our report had a significant impact on slope safety in Hong Kong and subsequently on international practice.

Through engineering, Victor devoted his life to the betterment of the people not only of Brazil, but also the world at large. The central theme of this Lecture is public safety. I like to think that Victor would have approved of it.

1. Safe Slopes

1.1. Hong Kong slope safety management

The history of slope instability in Hong Kong is well-documented. In the 1970s, during a period of intensive construction, catastrophic landslides occurred in 1972 and

Norbert R. Morgenstern, Distinguished University Professor (Emeritus), University of Alberta, Edmonton, Alberta, Canada. e-mail: norbert.morgenstern@ualberta.ca.
Intituted Lecture, no discussions.
DOI: 10.28927/SR.412107



Figure 1 - Victor de Mello, 1976.

1976. They are portrayed vividly in videos and animation reconstructions online (GEO, 2011). Following the 1976 disaster, the Government of Hong Kong appointed an Independent Review Panel on Fill Slopes to advise on the cause and implications of the Sau Mau Ping failure. In addition to responding to the technical issues, the Panel also recommended “that a central organization be established within the Government to provide continuity throughout the whole process of investigation, design, construction, monitoring, and maintenance of slopes in Hong Kong” (Knill *et al.*, 1976, republished in 1999). The Government accepted this recommendation and established the Geotechnical Control Office (GCO), which later became the Geotechnical Engineering Office (GEO).

The GEO was set up in 1977 to regulate slope engineering in Hong Kong. The initial efforts of the GEO were based on the application of the then current state of practice in slope engineering in order to enhance the safety of man-made slopes in Hong Kong, at a territory-wide level. Over the ensuing years this involved cataloguing slopes and development of suitable prescriptive design measures and soil testing procedures, supported by considerable checking of designs proposed for construction, all of which contributed to the evolution of a safety culture of excellence. Advances were made in characterizing regional soils and geology, as well as carrying out slope stabilization works that were needed to bring priority slopes up to the newly declared standards. Within a decade, enormous progress had been made as reflected in a marked decline in the annual landslide fatality rate. It was recognized early that to reduce risk, a Slope Safety System had to evolve that not only set standards for new slopes, but also embraced retrofitting substandard slopes, issued landslide warnings, advanced emergency disaster services, and encourage public education on slope safety. This has been described in detail by Malone (1997).

Although considerable progress in reducing the risk from landslides had been made by the mid-1990s, Hong Kong continued to grow and public expectations of slope safety increased as the quality of life continued to improve. Unfortunately, several landslides occurred in the early to mid-1990s that generated a strong negative reaction from the community and the government administration. I returned to Hong Kong at that time to review the investigation into the Kwun Lung Lau landslide and to comment on the slope safety system as a whole (Morgenstern, 1994). This report resulted in a number of changes to GEO’s practice, leading to more outward-looking perspectives in evaluating slope stability assessments. Of far-reaching implications, it also supported the adoption in Hong Kong of the development and application of Quantitative Risk Assessment (QRA) as a tool for landslide risk quantification, evaluation, and mitigation. This was particularly timely as the GEO was beginning to address landslide hazards from natural slopes where traditional approaches based on prescribed Factors of Safety are of limited value. Malone (2005) recounts the circumstances that preceded this important step and the challenges associated with gaining acceptance for it within public policy. The outcome for the GEO and Hong Kong has been entirely positive.

Figure 2 plots the history of landslide fatalities in Hong Kong from 1948 to 2016. This history embraces a period of population rise, from about 2,000,000 to over 7,000,000 today. The threat of extreme storms and cyclones is ever present. Yet the impact of the GEO and its efforts on the key fatality metric is clear. This remarkable achievement is highlighted by the plot of the 15-year rolling average annual fatality rate, recently updated by Wong (2017), that emphasizes the near elimination of fatalities due to landslides in Hong Kong.

1.2. Learning from Hong Kong

The Hong Kong Slope Safety System increased its effectiveness as it progressed through traditional geotechnical considerations to risk-based decision-making, together with a parallel commitment to risk communication and enhancing public awareness. Are there lessons to be learnt from this experience that can be applied to enhancing safety of water and tailings dams?

Hong Kong was the first jurisdiction that put into regulation quantified tolerable risk criteria embracing geotechnical hazards associated with slope stability. While the methodology for QRA was well-established, and in some instances was a recommended practice, making it a required evaluation process in the law is much more complex than adopting it to aid decision-making in the private sector. Figure 3 presents the risk tolerance criteria adopted after considerable evaluation, and many examples exist in the literature to illustrate the calculations for risk associated with various scenarios.

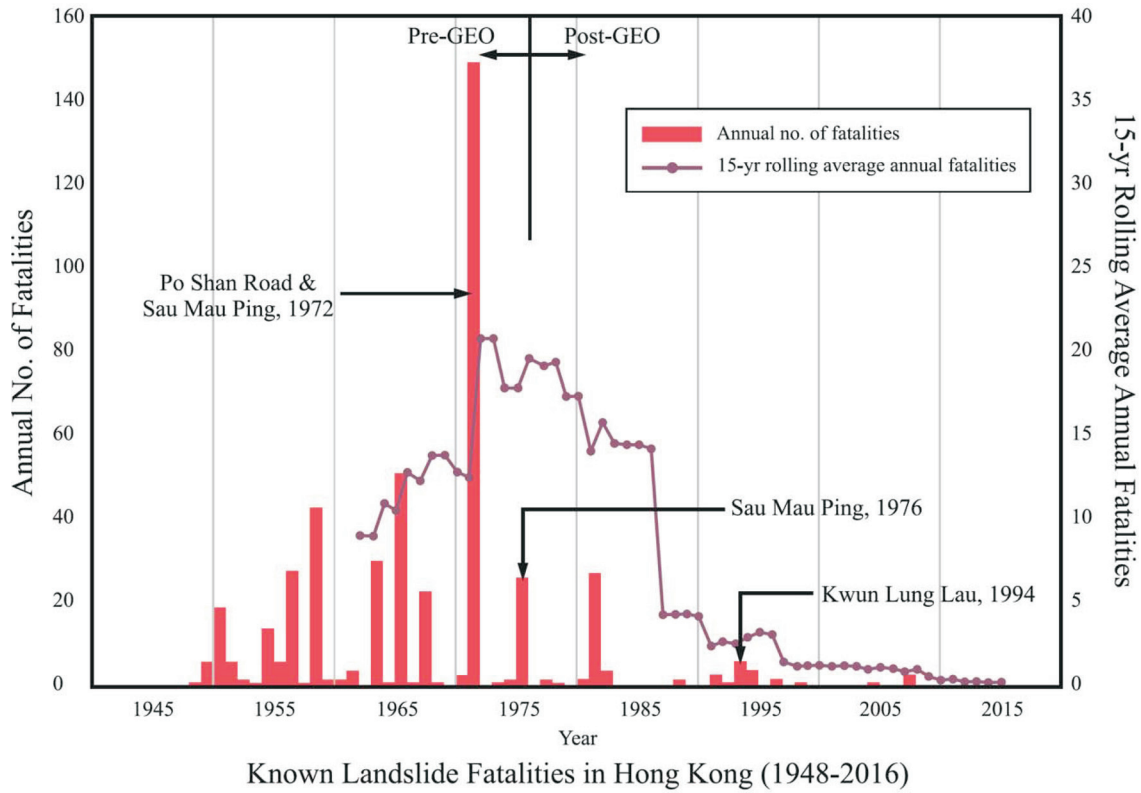


Figure 2 - History of landslide fatalities in Hong Kong from 1948 to 2016 (Wong, 2017).

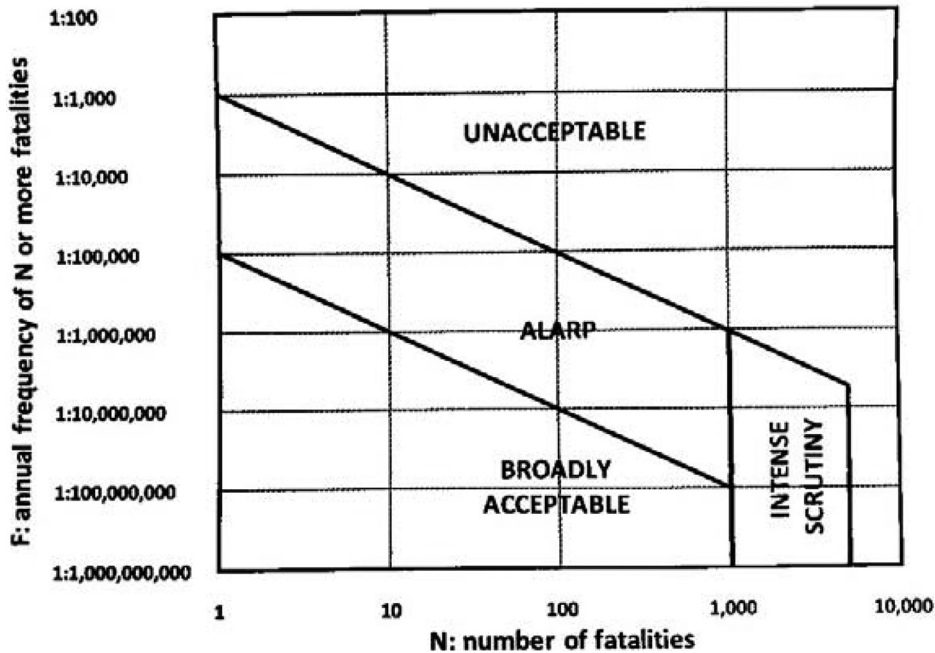


Figure 3 - Societal risk tolerance criteria for landslides in Hong Kong (GEO, 1998).

Hungr *et al.* (2016) undertook a review of current practice in various parts of the world related to landslide risk management and found wide differences between the current scientific understanding of risk acceptance and ac-

tual applications in practical circumstances. This is particularly marked by the absence of public jurisdictions to follow Hong Kong's lead. Examples of legally binding regulation in public policy were found only in Canada.

Two cases in Canada involving QRA are summarized in Morgenstern (2017). Both adopt the Hong Kong risk tolerability criteria (Fig. 3) and both relate to debris flows. In order to calculate risk in terms of “Potential Loss of Life” (PLL) in both cases, it was necessary to develop the hazard magnitude/frequency relationship based on complex geological and geomorphological studies; conduct debris flow runout analyses using advanced computational models; determine the spatial vulnerability reflecting both spatial and temporal probabilities; and convert the outcome into PLL metrics. QRA calculations are challenging undertakings but carry considerable weight if conducted carefully. While we found in both cases that the utilization of the Hong Kong criteria made sense, ultimately the stakeholders, jurisdictions and decision-makers have to select, ideally by means of a suitable public process, the appropriate risk evaluation parameters for a particular situation or jurisdiction. This selection of risk tolerance has to balance the risks from landslides with other societal values. Societal values include such things as public safety, affordable residential land, and return on investment. The geotechnical risk assessment can only inform this process.

While quantifying risk is challenging, communicating risk to inform public policy is equally challenging. In the case of the debris flow in North Vancouver, Canada, which was the first jurisdiction outside of Hong Kong to formally adopt the Hong Kong QRA criteria, extensive public involvement was a part of the process which ultimately resulted in legislation that places restrictions on increases of habitable area, rezoning, or redevelopment where tolerable risk criteria are violated. Tappenden (2014) has summarized these processes that successfully utilized a community task force approach. The District of North Vancouver received international recognition for its innovation and community engagement.

Similar circumstances were encountered in Canmore, Canada, the second jurisdiction in Canada to formally adopt QRA in legislation. This followed a catastrophic debris flow that created considerable damage, although, fortunately, no loss of life. Future risk mitigation was based on QRA. Risk communication had to be directed not only to the population affected, but also to three levels of government who would fund risk mitigation measures. The decisions affecting public policy required consideration of “feasibility, fairness, and affordability.”

The limited adoption of QRA in public policy related to managing landslide risk is better understood by reference to a Maturity Matrix for Assessing Community Engagement. This was published in studies undertaken to foster community resilience after the Katrina disaster in New Orleans (National Research Council, 2012). The matrix is presented in Fig. 4. As indicated by the Table, adoption of QRA into public policy requires a high level of Maturity (IV-V). Most jurisdictions worldwide operate in the range of I-III. Even with high levels of Maturity, the penetration

of QRA related to slope stability and related land management is slow.

In recognition of the fact that by far the greatest impact of landslide hazards occurs in the developing world, Hungr *et al.* (2016) were prompted to reflect that our approach towards landslide hazard and risk control should be made simpler and more transparent, so that it can be more easily exported to help people who most need it.

2. Safe Water Dams

2.1. History

A history of dams in society and their implications for public safety has been presented by Jansen (1980). Jansen observes that about 200 notable reservoir failures occurred in the world in the 20th century to the date of publication, with more than 8,000 fatalities. Catastrophic loss of life is always of great public concern, and, albeit in a reactive manner, this has resulted in a wide recognition of the need for governmental involvement in the supervision of dams and reservoirs.

Jansen (*op. cit.*) records how, in 1929, following the failure of the St. Francis Dam, California placed dams under an effective system of governmental supervision with jurisdiction over all dams, except those owned by the federal government.

In the United Kingdom, reservoir safety legislation came into effect in 1930 (The Reservoirs (Safety Provisions) Act, 1930) following two major dam failures in 1925 which led to the deaths of 21 people. This was subsequently updated with the Reservoirs Act of 1975. The Malpas (1959) and the Vajont (1963) disasters also contributed to the trend in a number of countries to enact new or revised laws for the supervision of dams and reservoirs. However, it was the failure in the United States (US) of the Buffalo Creek Dam, in West Virginia, with 125 deaths and the failure of the Teton Dam in 1976, with 11 deaths and \$1 Billion in losses, which accelerated this process, not only in the US, but also elsewhere.

The Buffalo Creek Dam which failed in 1972, was actually a coal slurry impoundment that burst four days after having been declared “satisfactory” by a federal mine inspector. The effects were catastrophic for the local community, not only due to fatalities and injuries, but also due to devastating property damage. One of the results of this event, together with the near failure of the Van Norman Dam due to the San Fernando Earthquake and the failure of the Canyon Lake Dam, South Dakota, was the passage of the National Dam Inspection Act in 1972 which would have authorized the US Army Corps of Engineers (USACE) to compile an inventory of all dams in the US and inspect them. For both financial reasons and other, this was never completed.

The Teton Dam, Idaho, designed and constructed by the Bureau of Reclamation, failed during first filling. Fail-

Elements	Level I	Level II	Level III	Level IV	Level V	Examples of Possible Outcomes
Dam or levee safety reviews	No activity	Standards-based only	Introduction of additional review criteria (e.g., failure mode analysis)	Application of quantitative risk assessment by using criteria developed by owner or regulator with input from community members and stakeholders	Application of quantitative risk assessment by using criteria that reflect the community's societal values	Community is fully apprised of current level of risk
<i>Other programs related to conventional dam/levee safety activities</i>	<i>Each tool is defined at different levels to show progression from minimum activity (Level I) through best industry practice to full community member and stakeholder engagement and collaboration (Level V)</i>					
Emergency action plans	No activity	EAPs developed internally by owner	EAPs developed with input from emergency management agency	EAPs developed with input from community members and stakeholders and emergency management agency and shared with selected community representatives	Community collaboration with owners or operators to develop integrated EAPs that reflect community values	Community collaboration results in EAPs that minimize consequences of defined emergencies by incorporating community values and the potential for community resilience
<i>Specific tools related to emergency planning response, including development of community preparedness measures, warning and evacuation procedures, and recovery plans</i>	<i>Each tool is defined at different levels showing progression from minimum activity (Level I) through best industry practice to community member and full stakeholder engagement and collaboration (Level V)</i>					
Floodplain management	No floodplain management plans	Floodplain management plans in place	Floodplain management plans accommodate shadow floodplain associated with catastrophic dam or levee failure	Floodplain management plans integrated into community comprehensive or general plans	Floodplain management plans fully integrated into dam and levee owners' planning processes	Full participation by both community and dam and levee owners in floodplain management facilitates adoption of complementary resilience-enhancing measures
<i>Specific tools such as those related to land-use planning and floodplain management, including initiatives for financial incentives and zoning reform</i>	<i>Each tool is defined at different levels showing progression from minimum activity (Level I) through best industry practice to community member and full stakeholder engagement and collaboration (Level V)</i>					

Figure 4 - Maturity Matrix for Assessing Community Engagement (National Research Council, 2012).

ure was rapid. Fortunately, it occurred during the day. The population affected by the flood was estimated to be around 10,000, and, had the failure occurred at night, it is believed that the majority of those people would have been killed. This failure, the responsibility of one of the premier dam design, construction, and operation organizations in the world, sent shockwaves through the dam engineering community.

One positive outcome from the failure was the creation by the Bureau of Reclamation of one of the most rigorous and comprehensive dam safety programs in the US.

2.2. Evolution of regulatory systems

Public policy related to dam safety is established by regulations. It is of interest to observe the contrasting frameworks that have evolved. Some of the variations arise from differences in the legal structures in various countries, *i.e.*, the common law system vs. the Napoleonic legal system. Scaletta *et al.* (2012) provide some concise summaries.

In the US there are both federal and state dam safety regulations. Federal guidelines for privately owned hydropower dams are summarized in the Engineering Guidelines for Hydropower Projects (FERC, 2010). The guidelines were developed in conjunction with the Federal

Power Act. Dams that are owned and operated by the federal government through the USACE and the Bureau of Reclamation are regulated by their respective organizations. State or privately owned dams that do not support hydropower production, including tailings dams, are the jurisdiction of the individual state where the dam is located. All states in the US, with the exception of Alabama, have dam safety regulations.

US regulations typically have a hazard classification based on the consequences of failure. This classification commonly relates the loading conditions and the required Factors of Safety for design as well as requirements for monitoring and inspection. For high-hazard, FERC-regulated dams, the engineering guidelines also require the following:

- i. Supporting Technical Information Document
- ii. Emergency Action Plan
- iii. Probable Failure Mode Analysis
- iv. Dam Safety and Surveillance Monitoring Plan
- v. Dam Safety and Surveillance Report
- vi. Dam Safety Inspection Reports.

Similar requirements are required for high hazard dams from other federal and state agencies. The tenor of this phase of regulatory development is decidedly prescriptive and standards based. In more recent years, risk-infor-

med decision making has entered into federal dam safety evaluation processes, and this will be discussed below.

In Canada, the regulation of dams is on a provincial/territorial basis. The federal government has no mandate to regulate in this area. However, national dam safety guidelines have been published by the Canadian Dam Association (CDA), a professional organization which has no regulatory authority. A province may choose to adopt CDA guidelines which would then make them official standards in the specific jurisdiction. Matters are made more complex because regulations may differ in some provinces between water storage dams and tailings dams. CDA (2012) summarizes Canadian dam safety regulations by jurisdiction. Technical Bulletins published by the CDA provide additional detail on suggested methodologies and procedures for dam analyses and assessments.

While Brazil contains a large number of dams of considerable economic importance in terms of water supply, power generation, and support for industry and mining, prior to 2010 Brazil did not have any laws or regulations that addressed dam safety at either the federal or state levels. However, guidelines such as CDA and US federal agencies were available as a general reference for dam owners and hydropower plant operators. The lack of policy was remedied at the federal level in 2010 by the establishment of the National Policy on Safety of Dams and creation of the National System on Safety of Dams in Brazil (Presidente da República, 2010). The objectives of this law are to ensure compliance with dam safety standards, regulate dam safety requirements during various phases of the dam project, promote monitoring and oversight, institute public involvement, establish technical guidance, and foster dam safety culture and risk management. Comprehensive dam safety plans are required for dams assessed to be in higher risk categories.

The evolution of the regulatory system in Australia is of special interest. Like Canada, dam safety in Australia is covered by state legislation, and there is no role for the Australian federal government. Design methods were traditional until 1994 when the Australian National Committee on Large Dams (ANCOLD) produced Guidelines on Risk Assessment, followed by revised Guidelines in 2003. The Dams Safety Act was passed in New South Wales (NSW) in 1978, and it established the Dam Safety Committee (DSC) as regulator. By 2002, the DSC had officially decided to pursue a risk-based approach to dam safety regulation. This was endorsed by the NSW Government in 2006, and in 2010 it was fully implemented by the DSC. It is noteworthy that the DSC appears to have been the first regulator in the world to successfully incorporate the inclusion of public safety tolerability criteria into regulatory practice (Graham, 2016).

2.3. Evolution of risk-based regulation

The first phase of regulatory control of dam safety relied primarily on a prescribed standards approach supported by visual observations of behaviour amplified by instrumentation. USACE criteria dominated much of the practice. Spillway capacities were designed to safely pass an inflow design flood; Factors of Safety were calculated to meet required minimum values depending on various recognized loading conditions; and stress in components or the structure itself were compared with allowable levels and/or ultimate strengths. Dam failures were rare, and the methodology was underpinned by substantial experience. Brinded (2000) has provided an insightful analysis of the framework associated with risk-informed decision-making processes, summarized in Fig. 5. The description of the first phase of regulatory control fits well with Type A.

As summarized by France & Williams (2017), the evolution of risk analysis has strengthened the dam safety community in many ways by:

- i. Recognizing in a formal manner the many ways that a dam can fail and the consequences of the failures;
- ii. Using risk as a tool for prioritizing risk reduction actions, particularly for dam portfolio analyses; and
- iii. Focusing monitoring programs and remediation efforts on the highest risk dams and potential failure modes.

These are all laudable advances, although the means of achieving them are not without pitfalls.

As pointed out by France & Williams (*op. cit.*), dam safety risk analysis in the US has its roots in the Bureau of Reclamation's adoption of failure modes and effects analysis (FMEA) in the 1980s, which evolved into PFMA (potential failure modes analysis). This transformed the dam safety evaluation process into one of critically assessing the way dams could fail, along with the relative likelihoods of the different failure modes and their consequences. Steps in the process vary from qualitative to semi-quantitative. Detailed descriptions are found in Hartford & Baecher (2004) and FERC (2017). This methodology is utilized in practice both at the design stage and at subsequent performance evaluation stages. The requirement of FERC to conduct PFMA as part of its mandatory inspection for hydropower dams within its regulatory jurisdiction has resulted in widespread understanding and adoption of the procedures.

PFMA follows thought processes familiar to engineers; it can be applied to a variety of consequences (fatalities, property damage, environmental, etc.) with ease, and it can be conducted in a timely and economic manner under the right circumstances.

In the 1990s the Bureau of Reclamation advanced from PFMA to quantitative risk analysis as a key tool in dam safety decision making. This aided them in assessing the urgency of dam safety concerns and, particularly, the relative priority of concerns for different dams. Quantitative risk analysis consists of estimating annual probabilities

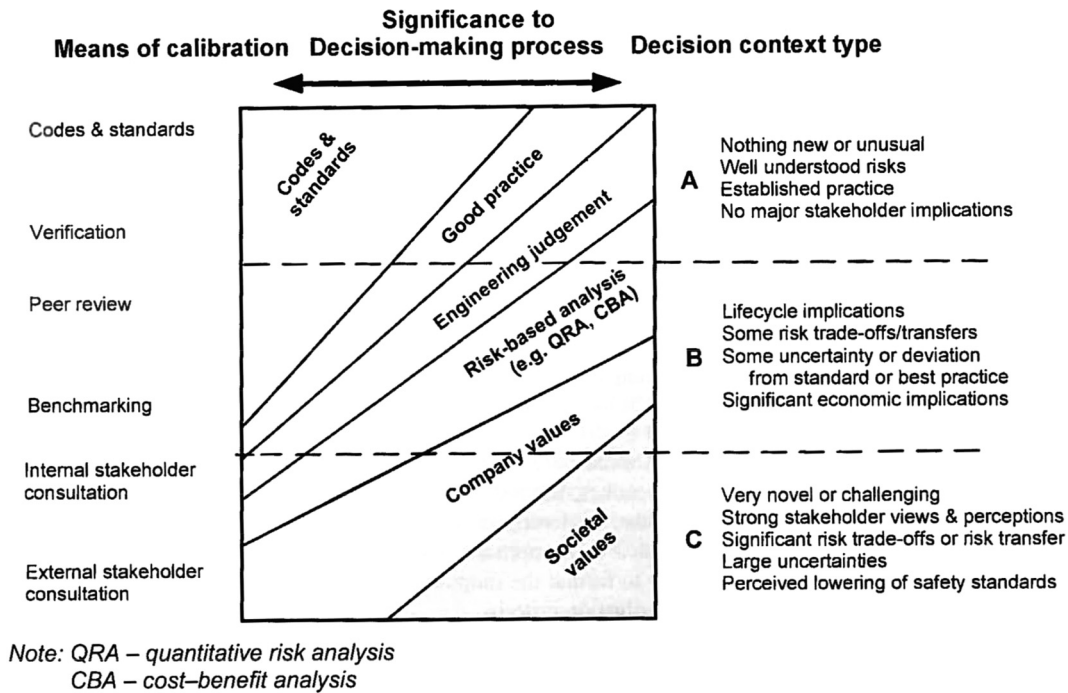


Figure 5 - Risk decision framework (Brinded, 2000).

of failure, failure consequences such as expected life loss, and annual life loss risks for failure modes of significance. Guidelines were needed to help evaluate the results of the analyses, typically expressed in terms of tolerable loss of life. This marks a significant change in metrics that might be acceptable internally to a large dam owner, but they should require extensive consultation if the criteria are to be adopted by the public at large. As observed by Bowles (2007):

“From the outset it is emphasized that judgements about the adequacy of dam safety, which are fundamentally judgements about public safety, are intrinsically value judgements and not technical matters, although they should be informed by sound technical information.”

The vocabulary of “tolerable loss of life” is provocative and should require stakeholder engagement as well as special risk communication efforts before the criteria become legal regulations. The appropriate balance between “value judgements” and technical matters also requires reflection.

While quantitative risk-informed decision making is undoubtedly informative, it involves its own, sometimes large, uncertainties. It is also time-consuming and costly. Embracing these uncertainties in a regulatory framework is challenging. This observation is also a finding arising from the previous discussion on the contribution of quantified risk analysis and its application to slope safety.

2.4. Dam safety after the Oroville Dam spillway incident

“Although the practice of dam safety has certainly improved since the 1970s, the fact that this incident hap-

pened to the owner of the tallest dam in the United States, under regulation of a federal agency, with repeated evaluation by reputable outside consultants, in a state with a leading dam safety regulatory program, is a wake-up call for everyone involved in dam safety. Challenging current assumptions on what constitutes “best practice” in our industry is long overdue” (Independent Forensic Team Report, 2018).

After the Oroville Dam Spillway incident in February 2017, FERC required the California Department of Water Resources (DWR) to engage an Independent Forensic Team (IFT) to develop findings and opinions on the causes of the incident. Anyone who cares about dam safety and is interested in the theme of this Lecture owes an enormous debt of gratitude for the outstanding report that has been produced. It is neither practical nor necessary to summarize the report in any detail before drawing conclusions from it. However, a brief description of the event is necessary before doing so.

The following points are extracted from the summary of the IFT report of the Incident which led to the mandatory evacuation of at least 188,000 people on February 13, 2017:

- i. The inherent vulnerability of the service spillway design and as-constructed conditions reflect lack of proper modification of the design to fit the site conditions.
- ii. Almost immediately after construction, the concrete chute slab cracked above and along underdrain pipes, and high underdrain flows were observed. The slab cracking and underdrain flows, although originally thought of as unusual, were quickly deemed to be “normal” and as simply requiring on-going repairs.

- iii. The seriousness of the weak as-constructed conditions and lack of repair durability was not recognized during numerous inspections and review processes over the almost 50-year history of the project.
- iv. Over time, a number of factors contributed to progressive deterioration (see Report for details).
- v. Due to the unrecognized inherent vulnerability of the design and as-constructed conditions and the chute slab deterioration, the spillway chute slab failure, although inevitable, was unexpected.
- vi. Once the initial section of the chute slab was uplifted, the underlying poor-quality foundation materials were directly exposed to high-velocity flows and were quickly eroded.
- vii. Although the poor foundation conditions at both spillways were well documented in geology reports, those conditions were not properly addressed in the original design and construction, and all subsequent reviews mischaracterized the foundation as good quality rock. As a result, the significant erosion of the service spillway foundation was also not anticipated.
- viii. In limiting service spillway discharge to reduce the likelihood of powerhouse flooding, the additional dam safety risk associated with use of the emergency spillway was not appropriately considered. Once the emer-

gency spillway was allowed to overtop, this additional risk was soon realized, and the evacuation order became a necessary precaution.

Figure 6 presents a picture of the net result of the Incident.

The IFT report makes a number of observations and recommendations related to the operation of DWR related to dam safety evaluation and with respect to the process as a whole. Two are particularly germane to the contents of this Lecture:

- i. “Shortcomings of the current PFMA processes in dealing with complex systems must be recognized and addressed. Evolution of ‘best practice’ must continue by supplementing current practice with new approaches, as appropriate.
- ii. Compliance with regulatory requirement is not sufficient to manage risk and meet dam owners’ legal and ethical responsibilities.”

Vick (2017) has made a timely and important contribution by emphasizing how “normalization of deviance” (Vaughan, 1996) has been a major contributing factor in a number of dam failures or near failures. The Oroville Incident is clearly another example to be added to the list. Improvements to dam safety evaluation processes must



Figure 6 - Oroville Dam Spillway incident (Independent Forensic Team, 2018).

recognize this organizational risk and measures must be imposed to eliminate it.

2.5. Toward safer water dams

In the previous presentation summarizing the evolution in practice of risk-based perspectives for evaluating dam safety, the common regulatory requirements were described as standards based, albeit supported by observation. This is not an accurate description of geotechnical practice in design and construction for all but the simplest structures. It is common risk management in geotechnical engineering to employ the observational method, which requires not only making observations, but also planning for intervention and mitigation of risk if needed. As discussed in Morgenstern (1995), the observational method implies risk analysis, but of a consequential kind. Its application enhances robustness, adaptability, and the capacity for intervention which are important considerations to enhance reliability.

Current practice does require conformance to certain standards, some prescribed and some recognized empirically as sound practice. As such, the design process based on the observational method is precautionary and would best be described as a “*precautionary risk-informed design process*.”

The geotechnical aspects of current dam design, at least for major projects, is rapidly being transformed by advances in instrumentation, real-time monitoring, and interpretation of data, all supported by increased capacity, in real-time, to model and interpret deformation and seepage regimes. As observed by Morgenstern (2017), this will lead to design procedures that overcome some of the conceptual limitations associated with the Factor of Safety concept and, by sequential history-matching of performance and implicit Bayesian updating, will result in a more reliable basis for projecting future performance. This can be described as a “*performance-based risk-informed design process*.”

Whether precautionary or performance-based, or even utilizing subjective judgements based on experience, it is essential that the risk assessment process be constrained by evidence and its evaluation to a higher degree than is currently the case. Based on the IFT report on the Oroville Dam Spillway Incident and experience from forensic investigations into two major tailings dam failures (Mount Polley Internal Panel, 2015; Fundão Tailings Dam Review Panel, 2016), the following are recommended:

i. Design Basis Memorandum (DBM): The DBM contains the design criteria for all aspects of the facility and the methods of analysis. It should contain enough detail to support a forward projection of all observational performance data once the project is complete and in service. Such an analysis should be undertaken to provide a reference basis for in-service expectations.

- ii. Construction Record: Experience reveals that when problems occur, the record is everything. Construction recordings should be expanded to develop a comprehensive GIS-based retrievable system that will document all aspects of construction history chronologically, as well as any written or photographic documents associated with the specific components.
- iii. Quality Assurance (QA): The role of QA is to document whether the facility has been constructed as intended. This is much more than simply collecting as-built drawings and some corroboration of laboratory procedures. More extensive reporting is needed tied to the expanded Construction Record.
- iv. Deviations: Deviation from the design/specifications are common. Major deviation may result in a formal design change which would be captured in the QA report and changes to the DBM. However minor deviations may accumulate. To avoid the risks associated with normalization of deviation, a Deviation Accountability Report (DAR) should be implemented to validate the acceptance of the deviations.

Implementing the above and carrying the related documentary references and criteria through the future dam safety evaluation process should contribute to improve reliability, accountability, and transparency, and thereby strengthen the safety cultures associated with the long-term performance of water dams.

3. Safe Tailings Dams

3.1. Regulatory framework

The industrial antecedents for the development of tailings dams differ markedly from those for water dams. Water dams, for millennia, created value by facilitating flood control, enhancing water supply, and subsequently expanding power supply. The disposal of tailings was a necessary evil in the mining industry, to be carried out at minimal cost. This typically meant disposal in streams or other bodies that would minimize accumulation. As production capacity increased in the mining industry, or aqueous disposal was not economical, surface stacking evolved. All aspects of tailings disposal added to the cost of production, and it was natural, at the time, to adopt procedures that were as economical as possible. This resulted in the upstream method of construction which became the standard procedure for many decades. By the mid-1960s changes were becoming evident.

The transformation is evident in the paper by Casagrande & McIver (1971). It provides a clear recognition of the differences between tailings and water dams as well as special geotechnical risks associated with upstream construction. The references reveal considerable related geotechnical studies being undertaken in the years preceding publication.

Klohn (1972) summarizes the evolution of tailings dams in British Columbia (BC, Canada), where methods of tailings dam design and construction were coming under critical review as both government regulatory bodies and the mining industry became more aware of the need for better tailings dams. This culminated in the Government of British Columbia enacting regulations which, historically, were precedent setting in North America. The BC regulations appeared in 1971, but were preceded by the Chilean decree in 1970 that banned upstream construction of tailings dams (Valenzuela, 2016).

In BC, two separate approvals were necessary: the first from the Department of Mines which was specifically concerned with the design, construction, and operation of tailings dam; and the second from the Department of Lands, Forests, and Water Resources, Pollution Control Branch which was concerned that the effluent escaping from a tailings storage pond would not cause pollution. The early guidelines related to dam safety were not prescriptive in any way, retaining confidence in the professional community to meet its obligations. At the time, practice procedures and other supporting documentation were being published to indicate what was considered acceptable practice.

The evolution of tailings dam regulation was much influenced by these two emerging regulatory concerns: i) environmental concern over pollution of water bodies, and ii) concern with respect to safety of dams. The history of the development of the Grizzly Gulch Tailings Dam, in South Dakota, is an example of the first, while Tar Island Dyke, the first tailings dam in the Alberta oil sands industry, is an example of the second.

In the US, the enactment of the Federal Water Pollution Control Act Amendment of 1972 brought an end to the standard practice of merely depositing tailings in the most convenient place. This legislation set a deadline of 1977 for compliance with standards that totally precluded disposal of industrial waste into the waters of the US. The Homestake Mine, which had at the time been operating for about 100 years, had been depositing most tailings into local creeks. To comply with these regulations, the Mine undertook the design and construction of an impoundment to water dam standards with an ultimate storage capacity of 50 years of gold production. Inflow flood design criteria were declared by the Mine Enforcement Safety Administration (MESA), but geotechnical design criteria relied on the experience of the dam design engineers. Site investigation was performed in the mid-1970s. The design was finalized in 1975, and the facilities were completed in 1977, with subsequent raises at later times. Details are provided in Carrigan & Shaddrick (1977). I was involved with this facility at the end of its service life and was pleased to assess the safe design created at the outset.

A contrasting evolution of tailings dam regulation is provided by the experience in the Province of Alberta arising from the expansion of dam safety regulation, discussed

in Section 2, above. In 1978, the Government of Alberta enacted specific dam and canal safety regulation establishing the first formal dam safety regulatory program in Canada to ensure safety of the public and the environment. This followed from recommendations of a Committee formed by the then Association of Professional Engineers, Geologists and Geophysicists of Alberta in 1972, that recommended that the Province of Alberta take action in this regard. The initial application of this new regulatory program was to Tar Island Dyke, the first tailings dam under construction in what was a relatively young oil sands industry. This first comprehensive safety review conducted by a team of well-known experts in the field expressed concern about movements in the foundations of the structure that had been detected by inclinometers that had been installed, and recommendations were made to restrict rate of construction by observational means. As noted by McRoberts *et al.* (2017): “This first review significantly strengthened the ability of the geotechnical engineers to insert on the budgetary support for appropriate monitoring with such new-fangled devices such as slope inclinometers and pneumatic piezometers.”

The positive interaction between the new regulatory process and the growing challenges in the oil sands industry contributed to the evolution of dam safety reviews, now regularly being undertaken, and the early adoption in the industry of external tailings review boards.

Both the catastrophic failure of the Aberfan Coal Waste Dump in England in the 1960s and the equally catastrophic failure of the Buffalo Creek Coal Waste Dam in the US in 1972 resulted in the recognition in the dam design community that tailings dams and related structures required better design to increase their safety. A committee to address these issues was formed by the International Commission on Large Dams (ICOLD) in 1976 which produced a design manual in 1982 (ICOLD, 1982). This publication (Bulletin No. 40) contained a summary of the status of international regulations that revealed that only limited progress had been made related to tailings dam safety by the time of completion of the manual.

ICOLD (1989) issued Bulletin No. 74 in response to the increasing number of large tailings dams that were being constructed around the world and in recognition of the severe consequences that would result from failure. The Stava catastrophe that occurred in Italy in 1985 was cited as an example. This publication, in an Appendix on Guidelines on Tailings Dam Legislation, recognized that while regulation of water dams had advanced, only a few countries had similar measures for tailings dams and that the jurisdictional issues for regulation of tailings dams were complex. They could vary from national to regional and even local responsibilities. Recommended guidelines were published but, to my knowledge, are not commonly cited.

Failures persisted in the following years and the environmental impact of tailings dams also attracted the atten-

tion of the United Nations Environmental Programme (UNEP) who joined forces with ICOLD to support a substantial revision of Bulletin No. 40 in the form of ICOLD/UNEP (1996). Progress was identified in recognizing jurisdictions that had regulations covering tailings dams, particularly with respect to environmental matters. Regional jurisdictions were the norm in North America and Australia where strong mining industries existed. However, national regulations also prevailed elsewhere at this time, such as in Chile.

3.2. The emerging crisis

Recorded failures of tailings dams persisted through the 1980s and 1990s with even an increase in rate in the mid-1990s as reflected in the WISE inventory (www.wise-uranium.org/mdaf.html). This attracted the attention of not only geotechnical and mining engineers, but also other organizations such as the UNEP.

In 1996, I presented an overview of the multiple contributions that geotechnical engineering can make to the challenges of mine waste management (Morgenstern, 1996). This presentation emphasized the changes in design and performance requirements that have evolved in recent years, and it provided examples of complex tailings dam behaviour, both favourable and not, as illustrations of the need to avoid over-simplification.

Toward the end of the decade, the UNEP combined resources with the International Council on Metals and the Environment (ICME; now the International Council on Mining and Metals, ICMM) to convene international meetings on managing the risks of tailings disposal. At the meeting in 1998, I drew on the previously published assessment, aided by additional experience, to conclude the following (Morgenstern, 1998):

- i. The standard of care associated with mine waste retention structure was too low.
- ii. The standard of care associated with mine waste retention structures should move towards those of water-retaining structures.
- iii. Establishing the standard of care is the responsibility of senior mine management who should set design objectives, risk management policy, and the associated levels of safety.
- iv. Consultants should involve Failure Modes/Effects Analysis or equivalent risk analyses at an early state of project development.
- v. Regulatory Agencies should devote more concern to the details of corporate policy regarding mine waste management procedure as opposed to being risk driven.
- vi. ICME (now ICMM), as the industrial interface, should contribute to improved risk management by drafting model corporate policy codes of practice and model regulations for consideration by individual corporations and regulatory agencies.

As will be borne out by this Lecture, it is disappointing to reflect that these recommendations are as meaningful to-day (2018) as they were when presented twenty years ago (1998).

I re-visited the issue of the safety of mine waste impoundments in 2010 (Morgenstern, 2010). In the preceding decade, failures continued to accumulate at approximately the same rate as in the recent past although some analysis suggested the possibility of a correlation between the time of failure with commodity price peaks. The inference implied here would be the suggestion that economic prizes create compromises in the diligent management of tailings. There was no socio-economic pattern among the cases, with regulatory environments ranging from weak to strong.

I was able to draw attention to some positive developments, namely:

- i. The efforts made by the Mining Association of Canada (MAC) to foster improvements in the safe and environmentally responsible management of Tailings and mine waste. This culminated in the document “MAC Guide to the Management of Tailings Facilities” which provided a framework of management principles, policies and objectives, checklists for implementing the framework through the life cycle of a tailings facility, and lists of technical considerations. This document was followed by the guide on “Developing an Operation, Maintenance, and Surveillance Manual for Tailings and Water Management Facilities” and “A Guide to Audit and Assessment of Tailings Facilities Management.” The MAC guidelines were readily adaptable to non-Canadian jurisdictions and site conditions of any kind.
- ii. Improvements in regulatory guidance documents had been produced, particularly with respect to the coal industry in the US where serious problems with the integrity of coal waste impoundments had developed early in the decade. Nevertheless, the limitations of relying on regulatory processes alone to ensure dam safety were becoming increasingly clear.

At the time, I offered the opinion that in my experience the dam safety system that had been developed in Alberta applied to the oil sands industry was the best in the world. It is worth repeating its components:

- i. Each owner is cognizant of its responsibilities to provide a tailings management consistent with the MAC guidelines.
- ii. Each owner has staff qualified in the management of tailings dams.
- iii. Owners retain consulting engineers for design and construction supervision who are well-known for their expertise in tailings dam design with special reference to the circumstances associated with the oil sands industry; the designer acts as the Engineer-of-Record at least for design; senior internal review of design submissions is expected.

- iv. Designs rely on the detailed application of the observational method for risk management.
- v. Designs are reviewed by the Alberta Dam Safety Branch, the regulator, who have staff well-versed in dam design and construction.
- vi. An annual report is submitted to the regulator by the owner, supported by the Engineer-of-Record, that the dam is behaving as intended; if not, actions that have been or need to be taken are indicated.
- vii. In accordance with CDA Guidelines, approximately every five years the owner retains an engineer, other than the Engineer-of-Record, to undertake an independent assessment of dam safety.
- viii. Each owner retains an Independent Geotechnical Review Board, comprised of senior specialists, to provide on-going third-party review of geotechnical issues of significance to the operation. One of the major responsibilities of such Boards is to review all aspects related to safety of tailings dams over the life cycle from design, construction, operation, and closure.

The success of the dam safety system applied to the Alberta oil sands industry relies on responsibilities shared by the owner, the Engineer-of-Record, the regulator, and various levels of independent review. I am aware that in many jurisdictions, not all of these components will be mature. Under these circumstances, the remainder of the safety management team should exercise additional caution to compensate for regional limitations. As many case histories continue to remind us, a permit to operate is not a guarantee against failure.

It is of interest to note that this same regulator has not had the same degree of success with a different set of industrial clients, strengthening my view that improving the safety of mine waste impoundments relies on shared responsibilities and cannot be achieved by regulation alone.

In this same presentation, following my experience with the oil sands industry and with water dams, I advocated for increased use of Independent Tailings Dam Review Boards (ITRB) in the mining industry and provided some guidance on their operations. It is of interest to note that McRoberts *et al.* (*op. cit.*) confirm the value of ITRBs in their experience in the oil sands industry.

Following on from 2010, tailings impoundment failures continued to recur at approximately a constant rate, as reflected by the WISE catalogue, which is recognized to be incomplete. For example, Li *et al.* (2016) report four major failures of upstream dams in China over the period 1962-2010 that involved 249 fatalities and are not included in the WISE catalogue. Moreover, Li *et al.* (2017) reveal that following a period of eliminating particularly hazardous facilities, at the end of 2015, 8,869 tailings facilities existed in China. Most are upstream constructions with design Factors of Safety less than commonly used elsewhere. Details are not readily available.

However, outside of China, the record for 2010 to 2018 was not “business as usual.” In 2014, the Mount Polley Mine tailings dam in British Columbia failed, fortunately with no loss of life, but with substantial outflow of both water and tailings. This was followed by the failure of Samarco’s Fundão tailings dam in 2015, with multiple fatalities and huge environmental and social consequences. It is located in Minas Gerais, Brazil. These two events attracted special attention not only because of their scale of consequences, but perhaps more so, because of their provenance. Both were operated by responsible mining companies, retaining experienced consulting engineers, and both were located in regions with mature mining experience and advanced regulatory regimes. The conjunction of the two events, building on a long history of inadequate performance has created to-day’s crisis. There is a loss of confidence and a loss in trust in the safety of tailings dams. Moreover, there is a lack of transparency in the way that safety-related issues are communicated to stakeholders.

In its commentary on risk reduction in the Mount Polley Report (Independent Expert Panel, 2015), the Panel expressed the following:

“In risk-based dam safety practice for conventional water dams, some particular level of tolerable risk is often specified that, in turn, implies some tolerable failure rate. The Panel does not accept the concept of a tolerable failure rate for tailings dams. To do so, no matter how small, would institutionalize failure. First Nations will not accept this, the public will not permit it, government will not allow it, and the mining industry will not survive it.”

As this manuscript is being written, Newcrest Mining Limited (NML) has just announced the failure of a portion of its tailings dam at the Cadia Mine in New South Wales, Australia. NML is one of the largest and most experienced gold mining companies in the world; its Cadia Mine is its flagship producer; and New South Wales has had for some time one of the most comprehensive dam safety regulatory processes in the world. Clearly the crisis is not over.

3.3. Responding to the crisis

3.3.1. Introduction

As a result of the two main incidents a few years ago, many commentators and agencies addressed the issues and provided guidance to resolve the crisis. This involved individuals, mining organizations, NGOs, government, and the UNEP. This section summarizes and comments on the most noteworthy of these recommendations and actions and asks the overarching question whether enough has been done.

3.3.2. Prescriptive recommendations

Examples of prescriptive recommendations follow with commentary on their effectiveness.

3.3.2.1. “Ban upstream dams, particularly where subjected to seismic loads.”

This prescriptive solution has appeal because of the large number of upstream failures in the case history records, and it is policy in Chile where, since 1970, the construction of upstream dams has been prohibited. This results in higher costs. Nevertheless, the policy was reaffirmed in 2007 with no exceptions. Valenzuela (2015) summarizes the successful performance of downstream tailings dams in Chile when subjected to large earthquakes, hence, apparently, vindicating the policy.

However, I side with the views of Martin & McRoberts (1999) and others before them (*e.g.*, Lenhart, 1950; Vick, 1992) that there is nothing wrong with upstream tailings dams provided that key principles are adhered to in the design, construction, and operation of such dams. Some 12 principles are outlined that should be recognized when upstream dams are proposed. In my practice, I advocate for purposes of preliminary design that liquefiable deposits that can liquefy be assumed to do so and that containment be provided by a buttress of non-liquefiable unsaturated tailings and/or compacted dilatant material. In addition, it is essential to continually demonstrate by monitoring that the assumed unsaturated conditions in the buttress persist if relied upon in the design and that the buttress is behaving as intended.

Some upstream dams are surprisingly seismic resistant. Morgenstern (1996) cites studies into the Dashihe Dam that survived the catastrophic Tangshan earthquake in 1996. At the time of the earthquake, this dam was 36 m high and the downstream slope was 5:1. It developed some cracking and sand boils during the earthquake, but did not collapse. Investigation carried out by a joint Sino-Canadian research team revealed surprisingly high densities. These were attributed to the low solids content during deposition and long beach slopes facilitating enhanced seepage-induced densification. The capacity to pump higher solids content slurry did not exist in China at that time. While a rational explanation of behaviour exists, the survival of the Dashihe Dam was more accidental than founded in geotechnical principles.

If upstream construction can be executed safely, even in seismic areas, does that contradict the logic of the Chilean regulation? The Chilean regulation, as with most national/regional regulation, reflects more than design principles. It must reflect the maturity of the design community, procurement policies, quality assurance, land tenure, the degree of seismicity, and many other aspects of practice. Only the Chileans have the capacity to make these integrated judgments with respect to public safety in their own country.

3.3.2.2. “Ban clay foundations.”

There are numerous examples of successful construction of large tailings dams on clay foundations. From the oil

sands industry alone, one can cite the successful completion of Tar Island Dyke, 90 m high, in part on a normally consolidated alluvial clay and other structures, albeit with flat slopes, on some of the weakest foundation ever encountered.

The application of geotechnical principles adequately provides for accommodating clay foundations. The challenge resides in ensuring that these principles are properly understood and applied in design.

3.3.2.3. “Require a Factor of Safety of at least 1.5 during operations.”

The prescription of the Factor of Safety (F of S) is attractive to regulators, but experience with case histories, such as Samarco, reveal that over-reliance on prescribed values is not adequate to eliminate failure. In my experience, we have been using F of S = 1.3 during operations on very challenging sites in the oil sands industry for many years. At the other end of the spectrum, I have encountered cases where F of S = 1.5 may not be adequate due to either enhanced ductility or enhanced brittleness. The prescription of F of S in regulation, if necessary, requires thoughtful input from experienced designers and recognition of the characteristics of regional practice.

This leads to a wide choice in regulatory perspectives from that adopted in Chile where upstream construction is banned regardless of calculated F of S, to that currently being adopted in the revised Alberta Dam Safety Guidelines where no specification of minimum F of S is made. In this instance, existing industry guidelines are referenced, but the selection of the F of S must consider influencing factors such as:

- i. Consequence of failure
- ii. Uncertainty of material properties and subsurface conditions
- iii. Variable construction and operating conditions
- iv. Comprehensive site investigation, and geotechnical monitoring
- v. Soil response (contractive/dilatative) and its variation with confining stress and shear stress laws), including potential for brittle failure
- vi. Time-dependent, deformation-dependent, and stress-path dependent processes that may affect the critical material properties
- vii. Strain incompatibility of different materials
- viii. Seismic loading as appropriate
- ix. Implementation of an effective risk management system (*e.g.*, observational method).

3.3.2.4. Concluding remark

No set of simple prescriptions will resolve the crisis. As emphasized by McRoberts *et al.* (2017): “One of the most important learnings can be seen in failure of other structures in the world. This is that a highly integrated team effort and success of an individual structure relies on the

operational discipline of planning, technology, operations, geotechnical engineering, and regulatory bodies.”

3.3.3. Response in British Columbia (BC) to the Mount Polley incident (2014)

The breach in the Mount Polley Tailings Storage Facility (TSF) resulted in two inquiries:

- i. Independent Expert Engineering Investigation and Review Panel (<https://www.mountpolleyreviewpanel.ca/final-report>).
- ii. Investigation Report of the Chief Inspector of Mines (<https://www2.gov.bc.ca/gov/content/industry/mineral-exploration-mining/further-information/directives-alerts-incident-information/mount-polley-tailings-breach/mount-polley-investigation>).

The first had terms of reference to report on the cause of failure of the tailings storage facility and to make recommendations to government on actions that could be taken to ensure that a similar failure does not occur at other mine sites in BC. The Panel concluded that the dominant contributions to the failure resided in its design and operation. In addition, it recommended that the industry establish a path to zero failure, as opposed to some tolerable failure rate. To do so, it should adopt a combination of Best Available Technology (BAT) and Best Available Practices (BAP). BAT argued for an emphasis on technologies that minimize the consequence of failure by reducing fluidity and/or provide more positive containment. BAP included a number of recommendations to reduce the probability of failure by improved governance, expanded sensitivity to risk assessment in design, the introduction of Quantitative Performance Objectives in the declared design, the increased utilization of independent tailings review boards, and other related aspects of professional practice.

The Chief Inspector of Mines has the statutory authority to investigate any incident that occurs on mine sites in the Province of British Columbia. His investigation differed from that of the Independent Panel in that it included the determination of the root and contributory causes of the event as well as developing findings to address the accountability of the industry, the regulator, engineering practices, and any other contributions to the event. The investigation was also concerned with reducing the risk of such an event in the future, as well as making recommendations for regulatory changes.

The technical explanation of the failure was similar to that presented by the Independent Panel, but it went further in attributing the root cause to weak engineering, waste management issues, and risk management. It is of interest to note that the facility, from a structural perspective, was apparently not in contravention with the then-extant regulations, clearly prompting a need for a reassessment. Arising from the lessons learned from this inquiry, multiple recommendations for improved practice were made to mining op-

erations, the mining industry, professional organizations, and the regulator. There was a strong alignment between the recommendations arising from the two investigations.

The Government of British Columbia responded positively to the recommendations from the two inquiries. In particular all of the recommendations arising from the Independent Panel have been addressed, and a major revision of the Code has been completed and published (Health, Safety and Reclamation Code for Mines in British Columbia; revised June 2017 <https://www2.gov.bc.ca/assets/gov/driving-and-transportation/transportation-infrastructure/contracting-with-the-province/documents/12811-2018/t3-10-health-safety-and-reclamation-code-for-mines-in-british-columbia-2008.pdf>). Chapter 10 (Permitting, Reclamation and Closure) in the Code deals with tailings storage facilities. The revised Code reflects the response of a multi-stakeholder committee to the findings from the inquiries. This is an important document and, in my view, constitutes the best revision of any regulatory document in response to the crisis. It is evident that both BAT and BAP need formalized response and that regulation needs to be more prescriptive than in the past to minimize recurrence of the failures that are being encountered. This Code strikes a sensible balance in this regard without intruding into the responsibilities of both the operator and the design engineer.

It is of interest that it is having influence elsewhere. For example, the State of Montana has recently adopted a regulatory process that draws considerably from the example of the BC Code.

3.3.4. Response in Brazil to the Samarco incident (2015)

The Report on the failure of the Fundão Dam (Fundão Tailings Dam Review Panel, 2016) was limited to an evaluation of the technical causes of failure. It drew attention to flaws in both design and operation. However, it consciously did not address roles and responsibilities. Public discussion of these issues is limited by ongoing litigation. However, this has not prevented agencies in Brazil from assessing changes in both professional practice and regulation, intended to prevent future reoccurrences of such incidents.

The Brazilian National Dam Safety Policy was first established in 2010 and constitutes the regulatory framework for dams in the country. Oliveira & Kerbany (2016) provide a brief summary of the evolution of tailings dam risk in Brazil and their regulations up to the Samarco incident. ABNT NBR 13028:2006 appears to have been the first regulatory instrument explicit for tailings storage facilities. Following Samarco, a committee was formed to revise the existing regulations, and in November 2017, a new version 13028:2017 was produced. It expands considerably on the technical requirements to support approval of the design of a tailings dam and draws on relevant international practice in this regard. In addition, the National Department

of Mineral Production (DNPM) has expanded substantially its regulatory requirements with respect to the operation of tailings facilities (Alves, 2017) and additional requirements may be forthcoming.

The role of the State in Brazil from a regulatory aspect is not immediately clear. Bogossian (2018) reflects disappointment with the rate of change of regulations governing tailings dam safety.

3.3.5. *Response of United Nations Environment Programme (UNEP)*

The UNEP has demonstrated a long-term concern regarding the high incidence of inadequate performance of mine tailings storage facilities. In response to the emerging crisis, it undertook a Rapid Response Assessment to look at why existing engineering and technical knowhow to build and maintain safe tailings storage facilities is insufficient to meet the target of zero catastrophic incidents. It examined the ways in which the established best practice solutions to international collaborative governance, enhanced regulations, more resource-efficient approaches, and innovation could help to ensure the elimination of tailings dam failures. Case histories were utilized to highlight efforts in this regard (Roche *et al.*, 2017).

This report has not been prepared by technical specialists, and it has been obliged to adopt some of the published literature at face value. Nevertheless, it is generally balanced, well-produced with helpful photographs, referencing, and historical summations. It concludes with two recommendations and identifies a number of actions to improve regulation and practice. The two recommendations are:

- i. The approach to tailings storage facilities must place safety first, by making environmental and human safety a priority in management actions and on-the-ground operations. Regulators, industries, and communities should adopt a shared zero-failure objective in tailings storage facilities where “safety attributes should be evaluated separately from economic considerations, and cost should not be the determining factor” (citation from Mount Polley Expert Panel Report, p. 125).
- ii. Establish a UN Environment stakeholders report to facilitate international strengthening of tailings dam regulation.

A number of actions recommended in past publications are also summarized. Clearly the first recommendation is consistent with the emerging safety culture within the mining industry. However, it is difficult to envisage much support for the second recommendation, given the complexity of jurisdictions responsible for tailings dam regulation and widespread evidence that failures continue even with mature and experienced regulators. This will be discussed in more detail in a subsequent section of this Lecture.

3.3.6. *Response of Mining Association of Canada (MAC)*

The first edition of MAC’s Guide to the Management of Tailings Facilities was released in 1998 in response to a series of international tailings-related incidents that occurred in the 1990s, several involving Canadian mining companies. The overarching objective of this document was to help mining companies to implement safe and environmentally responsible management of tailings facilities. This was followed in 2003 with a companion document on “Developing an Operation, Maintenance, and Surveillance Manual for Tailings and Water Management Facilities.” Tailings management was further embedded in the “Towards Sustainable Mining” (TSM) initiative established in 2004, which provided clear guidance on governance issues. There has been strong external recognition that implementing the tailings management component of TSM is a best practice for tailings management. This was recognized in the report on the Mount Polley failure.

Following the Mount Polley incident, the Board of Directors of MAC initiated a review of the tailings management component of TSM which culminated in the revised Guide to the Management of Tailings Facilities (Third Edition), issued in November 2017 (MAC, 2017). This is an outstanding document particularly in its contribution to governance structure within companies which is necessary to underpin a commitment to safe design, construction, operation, and closure of tailings storage facilities.

MAC processes emphasize the value of conducting audits to verify commitment and effectiveness. There are the three levels that corporations aspire to. Numerous commitments are required to achieve each level. In the new edition, new guiding principles are introduced to include:

- i. Risk-based approaches
- ii. BAT and BAP for tailings management
- iii. The roles of independent review
- iv. Design and operating for closure
- v. Revised roles and responsibilities.

This new Guide provides an outstanding document to influence the organization and governance protocols needed to ensure safe tailings management from the conceptual stages through to closure.

3.3.7. *Response of International Council on Mining and Metals (ICMM)*

The ICMM and its predecessor organization, the ICME, has long recognized the significant role that mine tailings management plays in the overall risk profile of mining operations worldwide. This is of special significance since the ICMM represents the majority of the world’s largest mining and metals companies. In response to the crisis, ICMM undertook a global review of tailings storage facility standards, guidelines, and risk controls. The review was conducted by member company representatives, assisted by external experts. The focus was on corporate-level surface tailings management across the

membership, including standards, guidelines, risk controls, and governance and emergency preparedness related to the prevention of and response to sudden catastrophic failure of tailings storage facilities. The report arising from this important review and the recommendations based on its findings has been produced by Golder Associates (2016).

Before engaging in the review that concentrated on governance issues, the study team reflected on learning from recent high-profile failures and concluded:

“If one were to focus on these and other such case histories through consideration of a greater number of failure and investigation results over the last 20 or so years, and ask the question is there anything missing from existing standards and guidance documentation that if known and applied could have forestalled such events, then the answer might be as follows:

“Existing published guidance and standards documentation fully embrace the knowledge required to embrace such failures. The shortcoming lies not in the state of knowledge, but rather in the efficiency with which that knowledge is applied. Therefore, efforts moving forward should focus on improved implementation and verification of controls, rather than restatement of them.”

Based on this justification, it was concluded that a higher level of governance and assurance is required for the effective implementation of good practice. To this end, the study focussed on the following core elements of good practice:

- i. Tailings management framework
- ii. Governance
- iii. Minimum requirements for design, construction, operation, decommissioning, and closure (including post-closure management).

Arising from the review of member company documents, five areas of improvement were identified and recommendations were made with respect to the following (see Report for details):

- i. The need for a tailings storage facility classification system based on the consequences of failure.
- ii. The need for a formal change management process related to material changes to the life of the facility plan.
- iii. The need for improved communication between the Engineer-of-Record and operator/owner.
- iv. Expanded utilization of formal risk assessment processes.
- v. The need for more independent review by suitably qualified and experienced professionals.

Additional details were provided regarding the recommended governance and tailings management framework, supported by the necessary assurance protocols.

Assisted by the Golder Associates (2016) study, ICMM also issued a Position Statement on Preventing Catastrophic Failure of Tailings Storage Facilities (ICMM, 2016). All members of ICMM are obliged to implement in their businesses the ten principles associated with the

ICMM Sustainable Development Framework. A number of these principles are of particular relevance to the need for preventing catastrophic failure of tailings storage facilities. The specific commitments related to an enhanced tailings governance framework require the following:

- i. Accountabilities, responsibilities, and associated competencies are defined to support appropriate identification and management of tailings storage facilities risk.
- ii. The financial and human resources needed to support continued tailings storage facilities management and governance are maintained throughout a facility’s life cycle.
- iii. Risk management associated with tailings storage facilities, including risk identification, an appropriate control regime, and the verification of control performance.
- iv. Risks associated with potential changes are assessed, controlled, and communicated to avoid inadvertently compromising facility integrity.
- v. Processes are in place to recognize and respond to impending failure of facilities and mitigate the potential impacts arising from a potentially catastrophic failure.
- vi. Internal and external review and assurance processes are in place so that controls for facilities risks can be comprehensively assessed and continually improved.

It is of interest to note that members of ICMM are expected to implement the commitments required by this position statement by November 2018.

3.3.8. Commentary

Positive and productive responses to the crisis have been made by revisions of regulatory requirements at both the regional and national levels as well as recommendations for improved corporate practice, with emphasis on governance, as made by both MAC and ICMM. All are welcome. However, the question remains whether they are adequate to overcome the crisis.

3.4. The causes of catastrophic tailing incidents

3.4.1. Introduction

One cannot answer the question that asks whether the measures taken so far by the industry and the various regulators are sufficient to address the crisis and resolve it without understanding the causes of catastrophic tailings incidents.

I have been involved to various degrees in 15 public tailings incidents over the last 30 years, not all involving dam failures, but all involving safe tailings management. In the following, I have personally assessed the basic causes of each incident in terms of whether it was engineering, operations, or regulatory related. By engineering related, I mean related to the matters of design, construction, quality control, and quality assurance. By operations related, I mean deviations from an operation manual that would

guide such matters as water management, tailings placement, and care and maintenance and would usually be covered by an Operations, Maintenance, and Surveillance manual (OMS). By regulatory related, I mean decisions made, or not made, by a regulatory authority that contributed significantly to the incident that occurred. In some instances, it is not possible to discriminate clearly between one or the other basic cause, and in such cases, I nominate both (see Table 1).

It should be made clear that these attributions are personal judgments and are not to be confused with root causes that are more complicated to assess. I make no attribution of roles and responsibilities in the basic cause assessment. In most cases, a brief Internet search will provide supporting details and photographs. Therefore, in general, no detailed references are provided here. Where this is not the case, a brief commentary and extra referencing is provided. My involvement in these cases covers the range from participating in detailed forensic investigations through knowing enough from files managed by others to form an opinion.

3.4.2. Commentary

The first case, Tyrone, is mentioned in Martin & McRoberts (1999) who reference a more-detailed back analysis of the failure first presented by Carrier (1991), which is neither well-known nor readily accessible. It deserves wide-spread recognition because it highlights the limited understanding of the role of undrained analysis applied to tailings dam stability, which was extant at that time and continues to this day.

The second case, Ok Tedi, was not a failure of an operating tailings storage facility, but a failure during construction due to a large landslide that occurred in the eastern abutment of the dam. As a result, tailings storage concepts were abandoned in favor of riverine discharge solutions. This decision had disastrous environmental, social, and financial consequences, which are a matter of public record. Substantial litigation developed with respect to liability associated with the abandonment of the tailings storage site with conflicting expert reviews. Respected expert opinions varied from the view that the circumstances around the landslide were too complex, given the local conditions, for the hazard to be identified, to the alternative, that the studies were deficient. Fookes & Dale (1992) provide a summary of alternate views. It is not the intent here to favour one side or the other, but to draw attention to the fact that geological and geotechnical complexity in some instances may be too great to support site selection at all, which is not a comforting observation.

The third case, Stava, resulted in the loss of 269 lives, the destruction of two villages, and extensive property damage. This incident has received considerable attention in the literature and was the subject of extensive litigation. It will come as a surprise to many that I attribute the basic cause to regulatory decisions. The detailed support of this attribution is presented in Morgenstern (1996). This paper records that the mine was shut down in 1978, and the dams were abandoned, except for a pond in both dams to manage precipitation runoff. The local authorities encouraged new ownership, and mining recommenced in 1982 by an organization with, limited mining experience. Construction and

Table 1 - Basic causes of tailings incidents.

Name	Year	Place	Basic causes		
			Engineering	Operations	Regulators
Tyrone	1980	New Mexico, USA	✓		
Ok Tedi	1984	Papua New Guinea	✓		
Stava	1985	Italy			✓
Omai	1995	Guyana	✓		
Golden Cross	1995	New Zealand	✓		
Marcopper	1996	Philippines	✓		
El Porco	1996	Bolivia	✓		
Pinto Valley	1997	Arizona, USA	✓	✓	
Los Frailes	1998	Spain	✓		
Inez	2000	Kentucky, USA	✓	✓	
Kingston	2008	Tennessee, USA	✓		
Keephills	2008	Alberta, Canada	✓		
Obed	2013	Alberta, Canada		✓	✓
Mount Polley	2014	British Columbia, Canada	✓	✓	
Samarco/Fundão	2015	Minas Gerais, Brazil	✓	✓	

tailings operations were substantially modified by the new operator. In particular, mobile cyclone placement of tailings was abandoned in favor of single point discharge which allowed pond water to encroach on the beach of the dam, ultimately triggering static liquefaction. It appears that had the regulator not interfered in the fate of the facility, without prescribing operational restraints, the failure would not have occurred.

Not much information regarding the Pinto Valley failure is available in the public domain. It involved the static liquefaction of an old tailings facility that had been decommissioned in the 1970s while the second lift of a waste dump was being placed on it. From my limited familiarity with the files, both engineering and operational issues contributed to the incident.

The failure of the Inez coal tailings impoundment in Kentucky, USA, reflected technological and operational perspectives that appear peculiar to the coal industry in that part of the US. The technical challenges have been evaluated by a special committee established by the US National Research Council (Committee on Coal Waste Impoundments, 2002).

The Keephills incident is not well-known, primarily because it did not result in loss of containment. Instability of the wall of the impoundment occurred during dyke raising. Fortunately, the crest of the slide did not penetrate into the fluid contents of the pond. The slide was attributed to deficiencies in assessing the shear strength of the complex foundation conditions beneath the embankment.

The Obed incident is also associated with the coal industry. A water retaining dyke failed due to inadequacies in site-wide fluid management, indicating an operational Basic Cause. However, even though the operation was licensed as a mine, the retaining structure had not been reviewed by the dam safety regulator. This appears to have been a lapse in the approval of mine operations and hence a contribution from the regulator to the basic cause of failure.

3.4.3. Reflection

From a technical perspective, it is of interest to note that inadequate understanding of undrained failure mechanisms leading to static liquefaction with extreme consequences is a factor in about 50% of the cases. Inadequacies in site characterization, both geological and geotechnical, is a factor in about 40% of the cases. Regulatory practice, considered appropriate for its time and place, did not prevent these incidents. However, the most important finding is that the dominant cause of these failures arises from deficiencies in engineering practice associated with the spectrum of activities embraced by design, construction, quality control, quality assurance, and related matters. This is a very disconcerting finding.

There is an unwritten covenant in our professional practice with the assumption on the part of an operator that, given reasonable resources, and on the part of the regulator

that, given technical guidelines and a modicum of inspection, the engineering team can be relied upon to produce a tailings storage facility that will perform as intended. The experience summarized here leads to the conclusion that this covenant is broken.

The conclusions in the ICMM-sponsored study of tailings management guidelines (Golder Associates, 2016) and the recommendations embraced in the Tailings Governance Framework issued by ICMM (2016) are not adequate to resolve the crisis.

3.5. Toward zero failures

3.5.1. Introduction

The responsibility for improving the safety culture associated with the performance of tailings storage facilities through all cycles of their life resides primarily with the operators. While regulators also have a role, it is necessarily subordinate to the role of operators. Experience reveals that the advance of this safety culture to the goal of zero failures requires intrusion into not only the activities of the operator, but also into the activities of the engineer(s). However, this intrusion must not be so prescriptive that it needlessly limits the creative input from both the operator and the engineer. To this end, it is recommended for any specific project that the operator be required to develop, for regulatory approval and subsequent execution, a tailings management system for Performance-Based, Risk-Informed, Safe Design, Construction, Operation, and Closure of the proposed tailings storage facility (PBRISD). Many single elements combined in PBRISD have been identified before, but the required integration presented in the following is perceived as necessary to impose more rigorous direction, supported by critical levels of review at various stages of the process.

3.5.2. Outline of PBRISD

For convenience, the organization of PBRISD is broken down into various stages of the life cycle of the project. Actual projects will develop the proposed system with reference to their own specific details.

3.5.2.1. Stage 1: (Conceptual)

This stage is associated with site and technology selections that generally are intended for application for approval by a regulatory process. The following elements are part of this stage:

- i. Qualified Operator (QO). Any proponent must establish itself as a QO. This is achieved by declaring that its safe management system will be compatible with the MAC 2017 Guide. In addition to prescribing to this excellent guide to the management of tailings facilities, the establishment of the following three critical positions becomes a commitment: i) Accountable Executive Officer, ii) Responsible Person(s), and iii) Engineer-of-Record.

- ii. Establish Independent Review Board. This will require creating a risk-based classification of facilities to provide guidance on the extent to which external review boards are required. Clearly there are instances where, either by past experience or by limited risk, no external independent review is necessary. At the other extreme, a three- to four-person board is required. Guidance is also required to assist the QO in forming such a board. Examples of terms of references are needed as well as a discussion on dealing with confidential matters, while also assessing safety issues that should be available in the public domain. Hence, reporting structures for boards need summarizing as do legal/commercial issues such as indemnification of board members for potential legal actions beyond their remit.
- iii. Uncertainty Assessment. It should be recognized at this early stage that safe design and operation relies on a large number of models (*e.g.*, the geological model, the hydrogeological model, the geochemical model, the geomechanical model, the stability model). All of these models possess uncertainties which either are addressed or become irrelevant with time. A first assessment of all uncertainties should be conducted in this stage for all options under consideration.
- iv. Potential Problems Analysis (PPA). The first formal risk analysis for all options under consideration should be a PPA which is a systematic method for determining what could go wrong in a plan under development. It is not anticipated that all issues would be addressed in Stage 1. However, the analysis might influence the recommendations arising from Stage 1 and residual concerns would be addressed in Stage 2.
- v. Multiple Account Analysis (MAA). The options for tailings technology and site selection considered in Stage 1 and recommendations arising from the assessments should be supported by an MAA. This is a structured decision-making process that makes transparent how both corporate and other stakeholder values have been considered in the assessment process. It is of considerable value in both documenting process as well as promoting trust. The MAA procedure has long been advocated by the federal regulators in Canada and is also outlined in MAC (2017).

3.5.2.2. Stage 2: (Feasibility)

This stage is associated with advancing the design of the selected option to a level both appropriate for making a financial commitment to proceed and to submit a design in sufficient detail to receive approval from the dam safety regulator. The following elements are part of this stage:

- i. Engineer-of-Record (EoR). The position of EoR is widely recognized as an integral part of the tailings management team dedicated to safety performance of the facility. The role of the EoR is to verify that the

facility has been designed in accordance with performance objectives and is supported by applicable guidelines, standards, and regulatory requirements. When constructed, it will perform, throughout the life cycle, in accordance with the design intent, performance objectives, applicable guidelines, standards, and regulatory requirements. The EoR is generally perceived to be a person and not a firm. While the functions of the EoR are important, there is still some debate in practice as to how these functions are best fulfilled, particularly if the QO has substantial in-house geotechnical and construction capability, as well as increasingly automated instrumentation and interpretation capacity. This is made more complex when the life of the facility is long and change of the EoR is inevitable. Guidance is required to assist the QO in evaluating the best way to fulfill the requirements of the EoR.

- ii. Designer. The designer selected for Stage 2 has a crucial role in all aspects of this stage. Some regional procurement practice places a strong emphasis on competitive costs which can result in breaking the design into small segments for either economic or other perceived management objectives. The QO needs guidance on procurement policy and the risks that might be generated by multiplying design interfaces.
- iii. Design Basis Memorandum (DBM). The DBM is the critical document that supports all design criteria and related methodology. It is subject to change based on evolving experience and methodologies. Documentation of change to the DBM must be formalized in a comprehensive manner. While the review board will participate throughout this stage, it is expected that review of the DBM and related matters will receive special attention. It is expected that all geotechnical design will adopt the observational method where possible. This is a precautionary-based design, to verify that no significant departures from design assumption have been identified. It requires prior identification of practical mitigation measures in the event that observations reveal that they are prudent or necessary. It is also expected that geotechnical design, at least for the more challenging undertakings, will increasingly utilize performance-based design. With advances in performance modeling, monitoring, and interpretation in a timely manner, it is now practical to move in this direction. The outcome is improved safety assessment and increased opportunities for optimization. Morgenstern (2017) discusses the merits of this transformation in more detail.
- iv. Risk Assessment. Risk assessments will be carried out as the schedule for Stage 2 dictates. For planning purposes, risk assessments at 30% and 70% completion should be in the development plan. The PFMA methodology is recommended. Some guidance is provided

in the MAC 2017 Guide, but additional documentation may be warranted for the QO.

- v. **Quality Management.** Detailed quality management plans will be developed distinguishing between Quality Control (QC) and Quality Assurance (QA). When construction is performed by the mine itself, ambiguities often arise. It is necessary to emphasize the independence of QA and, if conflicts arise with QC, to have resolutions at a senior level to ensure that production concerns do not overwhelm quality concerns. QA should also be responsible for the construction report which is an indispensable document, both for supporting the EoR requirements as well as constituting a basic resource to inform future long-term safety assessments.
- vi. **Documentation.** Experience with recent failure investigations highlights the need to have complete as-built data and other records compiled, preferably on a GIS platform, and accessible so that a technical audit could be conducted at any time. This is a valuable insurance document for all involved in the project and merits dedicated planning and support.

3.5.2.3. Stage 3: (Construction and operations)

Both construction and operations tend to overlap in the evolution of tailings storage facilities. Managing the construction follows naturally from the processes that evolved in Stage 2. However, additional considerations are needed to guide safe operations.

- i. **Operations.** Both safe construction and safe operation are guided by an Operation, Maintenance, and Surveillance Manual (OMS). This document requires critical reviews from the review board and periodic updating. The MAC 2017 Guide also provides valuable guidance on the development of this document.

3.5.2.4. Stage 4: (Closure implementation)

Modern project planning recognizes the need to integrate mine planning, tailings planning, water planning, and closure planning at the outset. It is assumed here that in PBRISD closure planning will be considered in all of the previous stages, at increasing levels of detail with time. From a geotechnical perspective, the primary concern is with the physical and chemical integrity of the ultimate landforms and release fluids. Closure design should recognize that the construction as-built record constitutes a basic reference for landform design under closure conditions. The evolution of closure design should emphasize the need for a new DBM to identify closure design criteria and methodology for the physical and chemical aspects of the closure landscape. Ongoing safety assessments must be able to rely on the as-built record as reliable to avoid the circumstances that occurred at Oroville Dam.

3.6. Guidance

The design, construction, operation, and closure of modern tailings facilities to acceptable standards of safety and environmental impact is a complex undertaking. Both experience and system analysis indicate clearly that it is not possible to meet acceptable standards by regulations alone. It is the primary responsibility of the proponent to put forward an acceptable waste management plan that meets these standards. The evolving crisis related to trust and confidence, discussed here, has also revealed a high rate of technical deficiencies as a significant factor in the failures that have been documented. It is tempting to conclude that increased prescriptive measures controlling the engineering works are required. However, the intrinsic complexity and diversity of the undertakings reduces the reliability of this perspective. Instead, the underlying principle for the tailings management system advocated here (PBRISD) is accountability. This is achieved by multiple layers of review, recurrent risk assessment, and performance-based validation from construction through closure.

The regulator also has a vital role. It is the responsibility of the regulator to review the proposed waste management plan and indicate how it is to be validated. This will involve some combination of inspections concentrating on quantified performance objectives, receiving review board reports, and other measures deemed necessary. The regulator is also the custodian of prescribed regional practice. For example, the regulator in Chile may continue to ban upstream construction even though technical arguments can be advanced that they can be designed and operated in a safe manner.

3.7. Recommendations

In order to turn the system recommended here into a reality, it is necessary to expand the skeleton outline into a guidance document that would help individual operators in developing a tailings management system for their specific operations based on PBRISD. The principles involved in PBRISD are entirely consistent with the ten principles that are the foundation of ICMM's Sustainable Development Framework. In addition, supporting the adoption of PBRISD can be regarded as a natural extension of the action already taken by ICMM in their 2016 Position Statement.

This Lecture concludes with the recommendation that ICMM support the tailings management system based on PBRISD, as outlined here, and fund the development and publication of a guidance document that would facilitate its adoption in mining practice.

4. Concluding Remarks

This Lecture has explored the evolution in practice of a safety culture in several important aspects of geotechnical practice. The range covers examples of success to examples of failure related to public aspects of geotechnical practice.

The example of success is the Slope Safety System in Hong Kong, to which Victor de Mello contributed in its early development.

The intermediate example relates to water dam safety where the recent Oroville Dam incident in California has exposed disconcerting practice in dam safety evaluation. Some of the learnings from this incident are presented and recommendations have been made to improve practice in water dams safety assessment.

Currently, the weakest safety culture is associated with tailings dams. Here, several high-profile failures have, in recent years, created a crisis due to loss of trust and confidence in the design, construction, and operation of such facilities. The Lecture reveals that this appears to be justified, particularly due to weak engineering in many instances (design, construction, QC, QA). Recommendations are made, primarily to operators, as to how to develop an improved tailings management system to maximize reliable performance.

Acknowledgments

I would like to recognize the valuable discussions on these matters with numerous colleagues in both professional practice and academic studies over the years. They are too numerous to list in detail, but important to remember. In the short term, the preparation of this Lecture and publication owes much to the organizational and communication skills of Vivian Giang to whom I am grateful.

References

- Alves, F. (2017). Com regras mais rigorosas, DNPM espera evitar novos acidentes. *Brasil Mineral*, 372:2-7.
- Bogossian, F. (2018). Accidents of tailings dams. *Jornal de Brasil*, May 11.
- Bowles, D.S. (2007). Tolerable risk for dams. How safe is safe enough? Proc. 27th USSD Conference, Philadelphia.
- Brinded, M. (2000). Perception vs analysis. How to handle risk. The 2000 Lloyd's Register Lecture, Royal Academy of Engineers, London.
- Canadian Dam Association. (2012). Canadian Regulations, available at https://www.cda.ca/EN/Dams_in_Canada/Regulation/EN/Dams_In_Canada_Pages/Regulation.aspx
- Carrier, W.D. (1991). Stability of tailings dams. Proc. XV Ciclo di Conferenze di Geotecnica di Torino, Italy, 48 p.
- Carrigan, M.C. & Shaddrick, D.R. (1977). Homestake's Grizzly Gulch tailings disposal project. Proc. 28th Annual Highway Geology Symposium, South Dakota School of Mines and Technology, Rapid City, pp. 1-16.
- Casagrande, L. & McIver, B.N. (1971). Design and construction of tailings dams. Brawner, C.O. & Milligan, V. (eds), *Stability in Open Pit Mining*: Proc. 1st International Conference on Stability in Open Pit Mining, American Institute of Mining, Metallurgical and Petroleum Engineers, New York, pp. 181-204.
- Federal Energy Regulatory Commission (FERC). (2010). *Engineering Guidelines for the Evaluation of Hydro-power Projects*, Washington, DC.
- Federal Energy Regulatory Commission (FERC). (2017). Chapter 14, *Dam Safety Monitoring Program*, Washington, DC, Revision 2, January 3. (Original publication in 2003).
- Fookes, P.G. & Dale, S.G. (1992). Comparison of interpretations of a major landslide at an earthfill dam site in Papua New Guinea. *Quarterly Journal of Engineering Geology*, 25:313-330.
- France, J.W. & Williams, J.L. (2017). Risk analysis is fundamentally changing the landscape of dam safety in the United States. Proc. GeoRisk 2017, ASCE, Denver, p. GSP282.
- Fundão Tailings Dam Review Panel. (2016). Report on the Immediate Causes of the Failure of the Fundão Dam available at <http://fundaoinvestigation.com/wp-content/uploads/general/PR/en/FinalReport.pdf>.
- Geotechnical Engineering Office, Hong Kong Government (GEO). (1998). *Landslides and Boulder Falls from Natural Terrain: Interim Risk Guidelines*. Government of the Hong Kong Special Administrative Region, Geotechnical Engineering Office, GEO Report No.75.
- Geotechnical Engineering Office, Hong Kong Government (GEO). (2011). Computer animation of the 1972 & 76 Sau Mau Ping landslides, available at <https://www.youtube.com/watch?v=tbCX9NKdEwo>.
- Golder Associates. (2016). *Review of Tailings Management Guidelines and Recommendations for Improvement*. Submitted to International Council on Mining and Metals (ICMM).
- Graham, E. (2016). *Patching the Gaps: Improving the Regulatory Capacity of British Columbia's Waste Dam Safety Program*. Master of Public Policy Thesis, Simon Fraser University, Vancouver, Canada.
- Hartford, D.N.D. & Baecher, G.B. (2004). *Risk and Uncertainty in Dam Safety*. Thomas Telford Ltd., London.
- Hungr, O.; Clague, J.; Morgenstern, N.R.; VanDine, D. & Stadel, D. (2016). A review of landslide risk acceptability practices in various countries. Aversa *et al.* (eds), *Proc. Landslides and Engineered Slopes: Experience, Theory and Practice*, Associazione Geotecnica Italiana, Rome, pp. 1121-1128.
- Independent Expert Engineering Investigation and Review Panel. (2015). Report on Mount Polley Tailings Storage Facility Breach available at <https://www.mountpolleyreviewpanel.ca/sites/default/files/report/ReportonMountPolleyTailingsStorageFacilityBreach.pdf>.

- Independent Forensic Team. (2018). Report on Oroville Dam Spillway Incident. Department of Water Resources, Sacramento.
- International Commission on Large Dams (ICOLD). (1982). Manual on Tailings Dams and Dumps. Bulletin No. 40, Paris, France.
- International Commission on Large Dams (ICOLD). (1989). Tailings Dam Safety. Bulletin No. 74, Paris, France.
- International Commission on Large Dams/United Nations Environment Programme (ICOLD/UNEP). (1996). A Guide to Tailings Dams and Impoundments. Bulletin No. 106, Paris, France.
- International Council on Mining and Metals (ICMM). (2016). Position Statement on Preventing Catastrophic Failure of Tailings Storage Facilities, London, UK.
- Jansen, R.B. (1980). Dams and Public Safety. Water and Power Resources Service. Superintendent of Documents, US Government Printing Office, Washington, DC.
- Klohn, E.J. (1972). Tailings dams in British Columbia. C.O. & Milligan, V. (eds), Geotechnical Practice for Stability in Open Pit Mining: Proc. 2nd International Conference on Stability in Open Pit Mining, Society of Mining Engineers, pp. 151-172.
- Knill, J.L.; Lumb, P.; Mackey, S.; de Mello, V.F.B.; Morgenstern, N.R. & Richards, B.G. (1976). Report of the Independent Review Panel on Fill Slopes. Published as GEO Report No. 86, 1999, CEDD, Hong Kong.
- Lenhart, W. (1950). Control of tailings from washing plants. Rock Products July, p. 72-80.
- Li, Q.; Zhang, H. & Li, G. (2017). Tailings pond life cycle safety management system. Proc. 8th International Conference on Sustainable Development in the Minerals Industry, p. 95-100.
- Li, S.; Chen, Q. & Wang, X. (2016). Superiority of filtered tailings storage facility to conventional tailings impoundment in southern rainy regions of China. Sustainability, 8:1-22.
- Malone, A.W. (1997). Risk management and slope safety in Hong Kong. HKIE Transactions, 4(2-3):12-21.
- Malone, A.W. (2005). The story of quantified risk and its place in slope safety policy in Hong Kong. Glade, T.; Anderson, M.G. & Crozier, M.J. (eds), Landslide Hazard and Risk, John Wiley and Sons Ltd., pp. 643-974.
- Martin, T.E. & McRoberts, E.C. (1999). Some consideration in the stability analysis of upstream tailings dams. Proc. Tailings and Mine Waste '99, Fort Collins, pp. 287-302.
- McRoberts, E.C.; MacGowan, T.; Eenkooren, N. & Pollock, G. (2017). 50 years of successful learnings by experience: Suncor tailings geotechnical. Proc. 21st International Conference on Tailings and Mine Waste, University of Alberta Geotechnical Centre, Banff, pp. 229-239.
- Mining Association in Canada (MAC) (2017). A Guide to the Management of Tailings Facilities. Third Edition, Ottawa, Canada.
- Morgenstern, N.R. (1994). Report on the Kwun Lung Lau Landslide, Volume 1: Causes of the Landslide and Adequacy of Slope Safety Practice in Hong Kong. GEO Report No. 103, CEDD, Hong Kong.
- Morgenstern, N.R. (1995). Managing risk in geotechnical engineering. Third Casagrande Lecture. Proc. 10th Pan-American Conference on Soil Mechanics and Foundation Engineering, v. 4, pp. 102-126.
- Morgenstern, N.R. (1996). Geotechnics and mine waste management. Proc. International Symposium on Seismic and Environmental Aspects of Dam Design: Earth, Concrete and Tailings Dams, Sociedad Chilena de Geotécnica, Santiago, v. 2, pp. 5-26.
- Morgenstern, N.R. (1998). Geotechnics and mine waste management – an update. Proc. Workshop on Risk Management and Contingency Planning in the Management of Mine Tailings, ICME and UNEP, Buenos Aires, pp. 171-175.
- Morgenstern, N.R. (2010). Improving the safety of mine waste impoundments. Proc. Tailings and Mine Waste '10, Vail, pp. 3-10.
- Morgenstern, N.R. (2017). The evaluation of slope stability: A further 25-year perspective. Distinguished Lecture, Hong Kong Institution of Engineers, available at <http://mail3.hkie.org.hk/distinguishedlectures2017/index.asp>.
- National Research Council (US). (2002). Coal Waste Impoundments: Risks, Responses and Alternatives. The National Academic Press, Washington, DC.
- National Research Council (US). (2012). Dam and Levee Safety and Community Resilience: A Vision for the Future. The National Academic Press, Washington, DC.
- Oliveira, M.G.S. & Kerbany, M.T.M. (2016). Environmental vulnerability and technological risks in collapse and break of dams in Brazil: Lessons for Mariana (MG) disaster. Proc. 15th Conference Global Spatial Data Infrastructure (GSDI) Association, Taipei, pp. 539-546.
- Presidente da República. (2010). Política Nacional de Segurança de Barragens, Lei nº 12.334, de 20 de setembro de 2010. Casa Civil – Subchefia para Assuntos Jurídicos, Brazil.
- Roche, C.; Thygesen, K.; Baka, E. (eds). (2017). Mine Tailings Storage: Safety is No Accident. United Nations Environment Programme and GRID-Arendal.
- Scaletta, M.; Mesania, F.; Osterle, J.P. & Deible, J. (2012). Regulatory framework for dam safety – comparative assessment. Proc. Hydrovision Brazil, September 25-27.
- Tappenden, K.M. (2014). The District of North Vancouver's landslide management strategy: Role of public involvement for determining tolerable risk and increasing community resilience. Natural Hazards, 72:481-501.

- Valenzuela, L. (2015). Tailings dams and hydraulic fills. Casagrande Lecture. Proc. 15th Pan-American Conference on Soil Mechanics and Geotechnical Engineering, Buenos Aires, v. 5, pp. 5-49.
- Valenzuela, L. (2016). Design, construction, operation and the effects of fines content and permeability on the seismic performance of tailings sand dams in Chile. *Obras y Proyectos*, 19:6-22.
- Vaughan, D. (1996). *The Challenges Launch Decision: Risky Technologies, Culture and Deviance at NASA*. University of Chicago Press, Chicago.
- Vick, S.G. (1992). Stability evaluation during staged construction – a discussion. *Journal of Geotechnical Engineering*, 118:1282-1289.
- Vick, S.G. (2017). Dam safety risk – from deviance to diligence. Proc. GeoRisk 2017, ASCE, pp. 19-30, GSP282.
- Wong, H.N. (2017). Forty years of slope engineering in Hong Kong. HKIE Geotechnical Division Annual Seminar, Hong Kong Institution of Engineering, p. 1-10.

Articles

Soils and Rocks
v. 41, n. 2

The Up-Hole Seismic Test Together with the SPT: Description of the System and Method

R.A.A. Pedrini, B.P. Rocha, H.L. Giacheti

Abstract. A proper geotechnical site characterization has to identify the geometry of relatively homogeneous zones and define indices, strength and stiffness properties of the soils within these zones. The most widely used *in situ* test to define the stratigraphical profile and to estimate geotechnical parameters is the Standard Penetration Test (SPT). Although it is widely used, this test provides a single index to define a great number of parameters, a peculiar characteristic criticized by many authors. Some authors have shown that it is possible to incorporate the measurement of shear wave velocity (V_s) using the SPT and the up-hole seismic test. This hybrid test can be called the seismic SPT (S-SPT), combining stratigraphic logging, and estimation of geotechnical parameters and determination of shear wave velocity (V_s) values. This paper describes a system to carry out the seismic SPT and the approach to interpret the seismic data. Seismic SPT was carried out at three research sites in the state of São Paulo, Brazil to assess its applicability. The V_s values determined by this hybrid test were compared with V_s reference values determined through cross-hole, down-hole and seismic cone penetration tests. The differences between V_s values were, on average, 8.5%, 9.0% and 16.0% for each research site. The hybrid S-SPT test can be used to define the V_s and, consequently G_0 profile, together with the N -value determination.

Keywords: in situ testing, seismic, shear wave velocity, site investigation, SPT, up-hole.

1. Introduction

Geotechnical site characterization is the first step for adequate geotechnical and geo-environmental projects. It has to present the stratigraphic profile, including soil variability and genesis, the ground water level and the mechanical and hydraulic parameters. It is also required to define the chemical distribution and source and/or receptor for potential or existing contaminants for the geo-environmental site characterization (US EPA, 1989).

The SPT has been recognized as the most commonly used *in situ* test for geotechnical site characterization in Brazil, as well as in most countries worldwide (Anderson *et al.*, 2007; Santana *et al.*, 2014; Lukiantchuki, 2012). As a result, there are several empirical correlations to determine geo-mechanical soil properties (shear strength and compressibility soil parameters). However, some authors such as Mayne *et al.* (2009) have questioned the use of a single number to estimate so many soil parameters. In the 1980s, there was an increase in *in situ* testing techniques that allowed performing more than one measurement using the same test. These test techniques are known as hybrid.

Some authors have demonstrated the possibility of incorporating the measurement of shear wave velocity in the SPT by the up-hole technique (Ohta *et al.*, 1978; Bang & Kim, 2007; Pedrini, 2012). This hybrid test, called seismic SPT (S-SPT), allows verifying the stratigraphic profile, es-

timating the geotechnical parameters and determining the shear wave velocity (V_s) profile. The V_s value is used to calculate the maximum shear modulus (G_0) via Theory of Elasticity (Atkinson, 2000). The most used and appropriate hybrid test to determine V_s profiles is the seismic cone test (SCPT). However, it requires using special equipment, which sometimes is not available. In such cases, the S-SPT could be an alternative test, at least to obtain a preliminary estimative of G_0 profiles.

Tropical soils are formed mainly by chemical weathering of the rock and their peculiar behavior cannot be explained by the principles of classical soil mechanics. The term tropical soil includes both lateritic and saprolitic soils. The surface horizon, lateritic soil, is characterized by intensive pedogenetic evolution, while the horizon below the lateritic soil is the so-called saprolitic soil. Saprolitic soils are necessarily residual soils and retain the characteristics of the parent rock. They have very heterogeneous mechanical behavior, according to the matrix rock and the level of weathering to which they were submitted (Committee on Tropical Soils of ISSMFE, 1985).

The objective of this paper is to describe a system and a method to carry out and interpret the up-hole seismic tests together with the SPT. Three S-SPT campaigns were carried out at different research sites located in the cities of Bauru, São Carlos and Campinas, in the state of São Paulo, Brazil. The results were compared with V_s reference val-

Rubens Amaral Antonio Pedrini, M.Sc. Student, Departamento de Engenharia Civil e Ambiental, Universidade Estadual Paulista "Júlio de Mesquita Filho", Bauru, SP, Brazil. e-mail: rubenspedrini@gmail.com.

Breno Padovezi Rocha, Ph.D. Student, Departamento de Geotecnia, Universidade de São Paulo, São Carlos, SP, Brazil. e-mail: brenop@sc.usp.br.

Heraldo Luiz Giacheti, D.Sc., Full Professor, Departamento de Engenharia Civil e Ambiental, Universidade Estadual Paulista "Júlio de Mesquita Filho", Bauru, SP, Brazil. e-mail: h.giacheti@unesp.br.

Submitted on October 25, 2017; Final Acceptance on June 6, 2018; Discussion open until December 31, 2018.

DOI: 10.28927/SR.412133

ues, which were determined by cross-hole, down-hole and seismic cone tests, in accordance with the results available at the different research sites.

2. The Seismic SPT

The system for the up-hole seismic test together with the SPT consists of hardware (geophones, trigger, grounding, seismic source and data acquisition system) and software to record and to interpret the seismic data. They were adapted by Pedrini (2012) based on the Bang & King (2007) proposal to carry out and to interpret the Seismic SPT. The differences from each approach will be pointed out in the next items.

2.1. Equipment

Bang & Kim (2007) proposed the up-hole method for use with the mechanical SPT equipment currently used in North America, Europe, Japan and other countries. The SPT equipment currently used in Brazil is standardized by ABNT (2001). It is carried out using a manual system and lightweight tripod. Bang & Kim (2007) pointed out some problems due to the use of the mechanical SPT equipment, such as the seismic noise caused by the vibration of the boring machine, the trigger installation and the exact definition of the depth where the seismic signal was generated by the SPT sampler. These problems are overcome with the system used in this study.

The seismic SPT is basically the same currently used in a manual system, complemented with a data acquisition

system (DAQ) and an arrangement of six boxes attached onto the ground surface with two geophones inside each box (one in the vertical and another in the horizontal direction). The DAQ system records the seismic data from the waves generated at 1 m depth intervals. Seismic data were recorded up to 20 m depth immediately after the N-value determination. The trigger and the seismic source, which is the SPT sampler itself impacted by a small sledgehammer, integrate the seismic SPT.

The software was developed using the LabVIEW Platform and the data interpretation software used the Matlab Platform.

2.1.1. The SPT equipment

The Standard Penetration Test (SPT) currently used in Brazil is a manual system described in the Brazilian Standard (ABNT, 2001). This system was used in this research and it has a tripod, a rotating cathead, a typically 25 mm diameter manila rope, a crown sheave (or pulley), a guide pipe, an anvil, a drill rod, a thick-walled sampler tube and a hammer (Fig. 1). The operator pulls the rope towards himself until the hammer is lifted to the prescribed fall height. He rapidly slackens the rope on the cathead to drop the weight. The operator is in charge of ensuring a 750 mm fall, usually with the aid of a mark on the rod for guiding the drop of a free-falling hammer weighing 65 kg. Another way to lift and release the hammer is by manually lifting and releasing the rope passing over the crown sheave, without using the winch cathead (Robertson *et al.*, 1992).

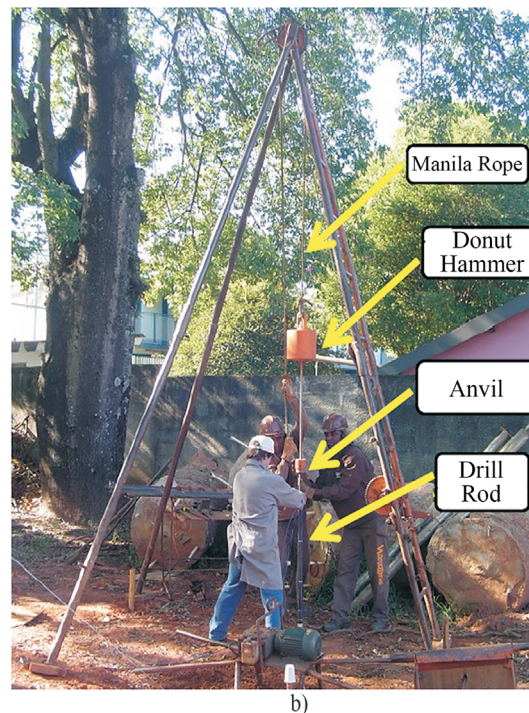
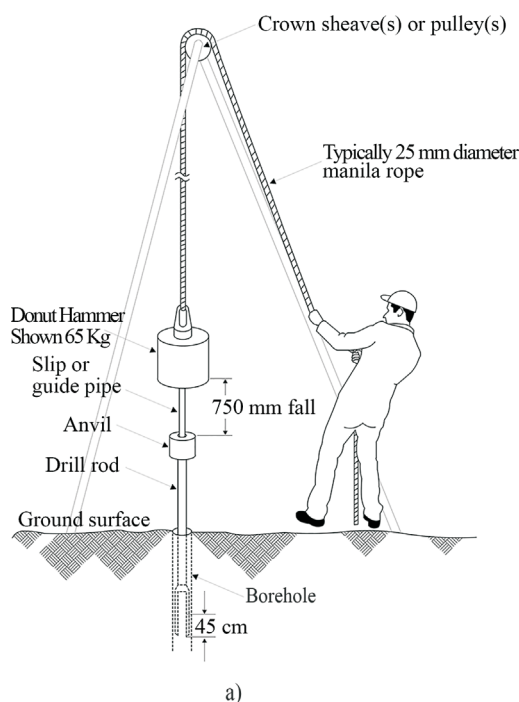


Figure 1 - a) Schematic representation of a typical SPT system with manual release and a donut hammer (adapted from Robertson *et al.*, 1992). b) Photo of the SPT system (adapted from Lukiantchuki, 2012).

2.1.2. Source

The seismic SPT described by Bang & Kim (2007) uses the SPT blow itself to generate the seismic waves. Tests were carried out at the Bauru research site to assess the quality of the seismic traces using this approach. A sledgehammer was also used to generate the seismic waves. In this case, the blow was delivered right after ending the driving of the sampler, as described by Pedrini (2012). Figure 2a presents the seismic traces registered by vertical geophones for the last blow after driving the SPT sampler at several distances from the borehole. Figure 2b shows similar traces recorded with a 2 kg sledgehammer blow.

It was observed that the sledgehammer generated better traces than the SPT hammer (Fig. 2). This can be explained by the high energy of the SPT hammer, which causes noise and moves too much the sampler in the soil during driving. Another important aspect is the inaccuracy in defining the depth where the wave is generated, since the SPT sampler penetrated a lot with just one blow from the SPT hammer at the first meters for the studied sites. On the other hand, the traces recorded with the sledgehammer are better, since the energy is much lower and it causes little sampler movement and lower disturbance. It was also noted in all test sites that the sledgehammer generated enough en-

ergy, even for greater depths (up to 20 m) providing good quality seismic traces to identify the shear waves arrival.

2.1.3. Trigger

A trigger system was used to start recording the wave generated in the ground by the SPT sampler. This device allows recording signals with high accuracy and it is easily implemented in the seismic SPT. The signal starts recording when the sledgehammer reaches the anvil head and the circuit closes (Fig. 3).

The wave signal generated on the anvil propagates down along the shaft to the sampler, which will transmit the signal through the soil. The time delay to reach the SPT sampler has to be considered in order to calculate the shear wave velocity due to wave signal propagation down along the rods. It will depend on the rod length assuming the theoretical velocity on steel of 5123 m/s.

2.1.4. Geophones and installation

The geophones' main factory specifications are: natural frequency of 28 Hz, sensitivity of 35.4 V/(m/s) and spurious frequency of 400 Hz. This type of geophone is the same used by Campanella & Stewart (1992). Bang & Kim (2007) recommend using geophones with a lower natural frequency (4.5 to 10 Hz). The geophones were placed in six

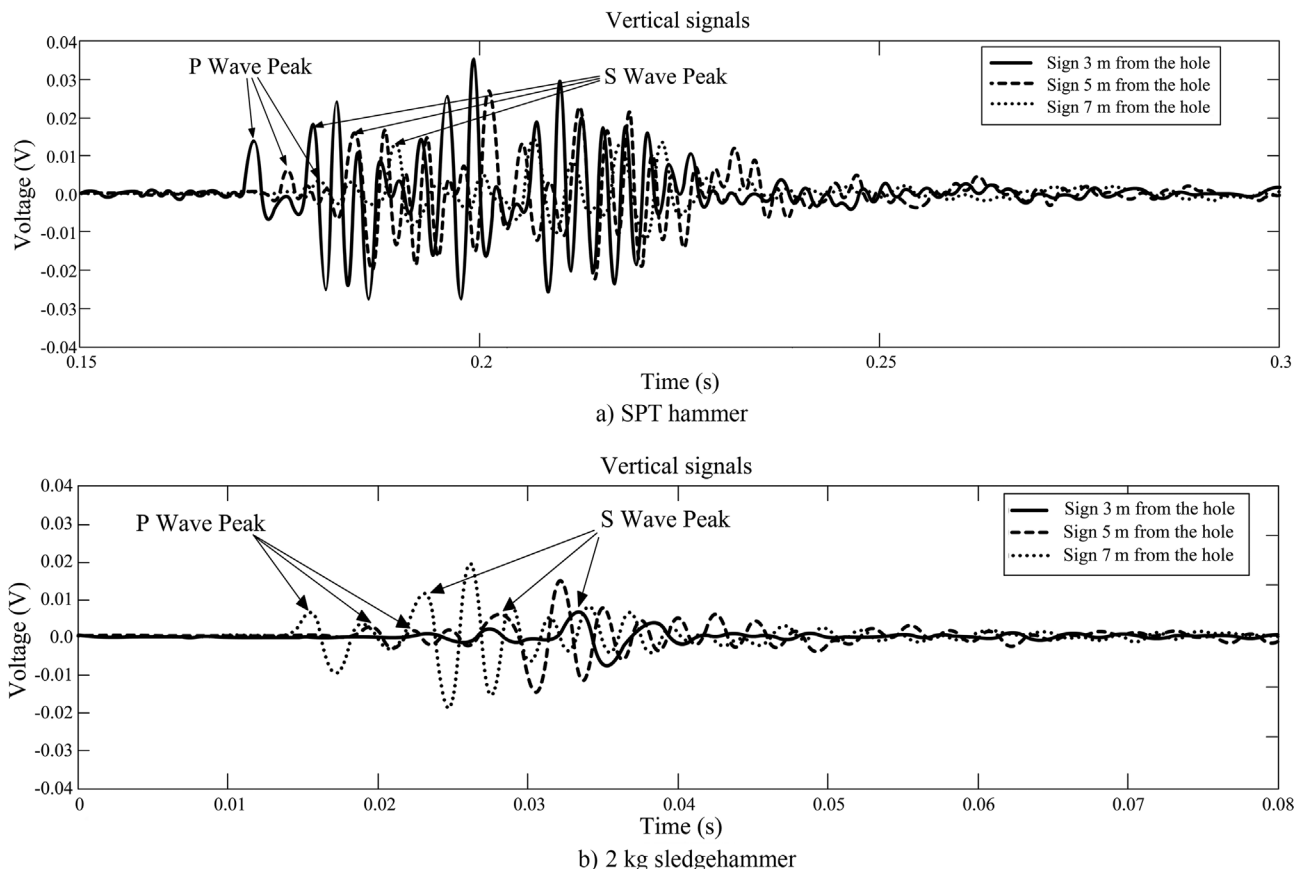


Figure 2 - Illustration of the seismic traces for the blow generated by different sources.

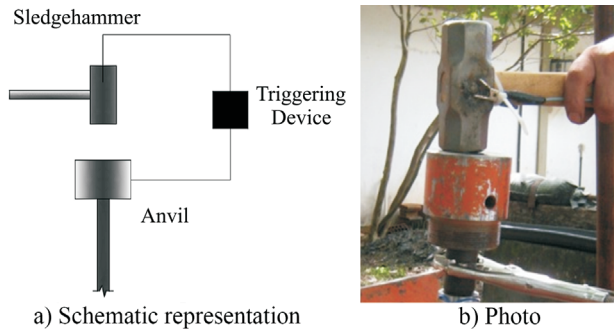


Figure 3 - Schematic representation and photo of the source and the trigger device.

boxes. It is possible to place up to three triaxial geophones inside each box: one vertical and two horizontal. The vertical and the horizontal geophones were used similarly to the Bang & Kim (2007) approach.

The quality of the received signal depends on the installation procedure. Figure 4 shows the correct procedure to achieve the best signals. Figure 4a shows the tip attachment which must be tightly threaded to the box containing the geophones. Figure 4b shows the box, which must be firmly bolted to the ground but without touching it. Moreover, all the boxes must be leveled. Figure 4c shows a red line indicating the alignment of the boxes with the borehole. Six boxes with two geophones (one vertical and another horizontal) were used to carry out the seismic SPT.

2.1.5. Data acquisition system

The data acquisition system is from National Instruments, model NI-USB-6353. The main characteristics of this system are: 16 bit resolution, 32 single ended channels and 16 differential channels, analogue and digital triggers and a receiving rate of 1.25 ms/s.

2.1.6. Software

The data acquisition software was developed using the LabVIEW platform to trigger, capture the traces and

generate the data files. It was also developed the data interpretation software in the Matlab platform. This software allows signal processing, represents the traces, analyzes the recorded data and calculates velocities by using the refracted wave pathway through an interactive method, as described later in item 2.3.3.

The main objective of this software is to provide a simple and functional method to identify and determine the first arrival of S and P waves, and determine the time lag between subsequent waves. The software also has a module implemented that uses the DTS (delay time between serial sources) method developed by Bang & Kim (2007).

2.2. Test procedure

The procedure of this hybrid test incorporates the up-hole seismic technique for V_s measurement in addition to the traditional SPT. A seismic wave is generated, and it can be recorded at the ground surface for each sampler depth (usually every meter). Figure 5 shows a schematic representation of the seismic SPT. An arrangement of 6 boxes is placed onto the ground to carry out the test, with

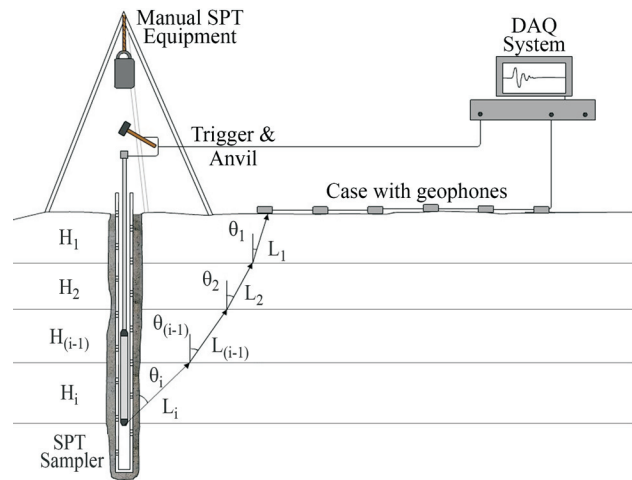


Figure 5 - Schematic representation of Seismic SPT and a seismic refracted path.

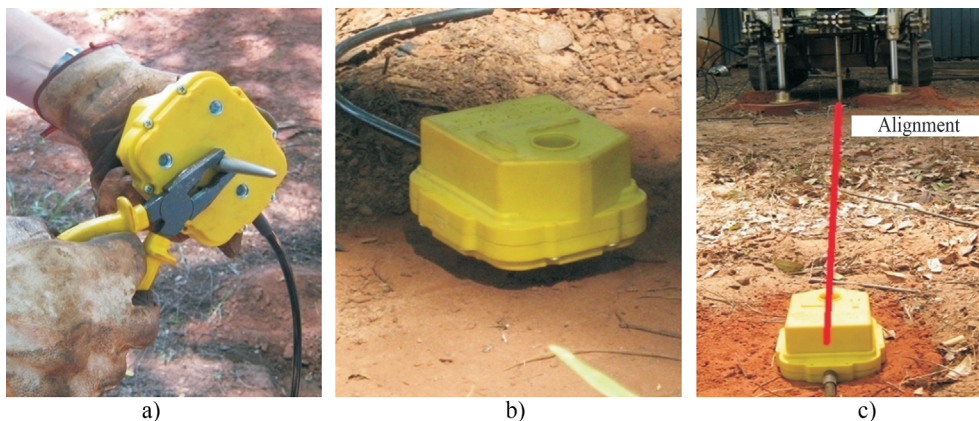


Figure 4 - Setup of the geophone boxes placed on the ground.

the first box positioned at 2.0 m from the SPT borehole and the others 2.0 m further away. Seismic data are recorded from waves generated at one meter depth intervals, right after the N-value determination.

2.3. Data reduction and interpretation

2.3.1. V_s methods

The wave velocity can be calculated dividing the pathway between the source (the SPT sampler) and the receptors (geophones) by the time for the first wave arrival (t_s) for the SPT up-hole test, as discussed by Bang & Kim (2007). Refraction occurs during wave propagation inside a stratified media and consequently Snell's law should be considered. The refracted ray cannot be neglected due to the difference between the straight and the refracted pathways, as represented in Fig. 5.

There are two methods for calculating V_s . First, the DTR (delay time between serial receivers) and second, the DTS (delay time between serial sources). Bang & Kim (2007) demonstrated that the DTS method is the best to determine V_s . This method starts with the determination of the time interval from wave generation at the SPT sampler up to its arrival to the geophones at the ground surface. It is defined by identifying the exact moment of the shear wave arrival. It can be done by plotting the wave receptions generated at different depths as the SPT test is carried out, and identifying the minimum point of the waves, as shown in Fig. 6 (Rocha, 2013).

2.3.2. The arrival time of the S waves

The wave velocity calculation by the DTS method requires determining the exact wave arrival time. Up to the previous step, only one reference time was identified for each record in a subsoil profile, but not the exact arrival time since it is difficult to determine it. An alternative to solve this issue is to use the crossover method. In this case, two signals with different polarities are generated by applying two blows in opposite directions. The arrival time of the S wave can be determined by cross referencing these two records. However, this procedure is not feasible in the seismic SPT because it would require extra time and it is very difficult to produce good data by striking the head in the upward direction. Some data like that were recorded at certain depths during this research. The application of a downward blow is shown in Fig. 7a, and the blow in the opposite direction is shown in Fig. 7b.

Figure 8 shows two typical records produced by blows with inverted polarity at a depth of 6 m captured by a horizontal geophone at the Unesp research site. Despite the amplitude difference of the signals, the crossover of the waves is identified, as shown in Fig. 8.

The arrival point of the S waves was indirectly identified in all tests in the Bauru, São Carlos and Campinas sites by first defining a reference point on the profile corre-

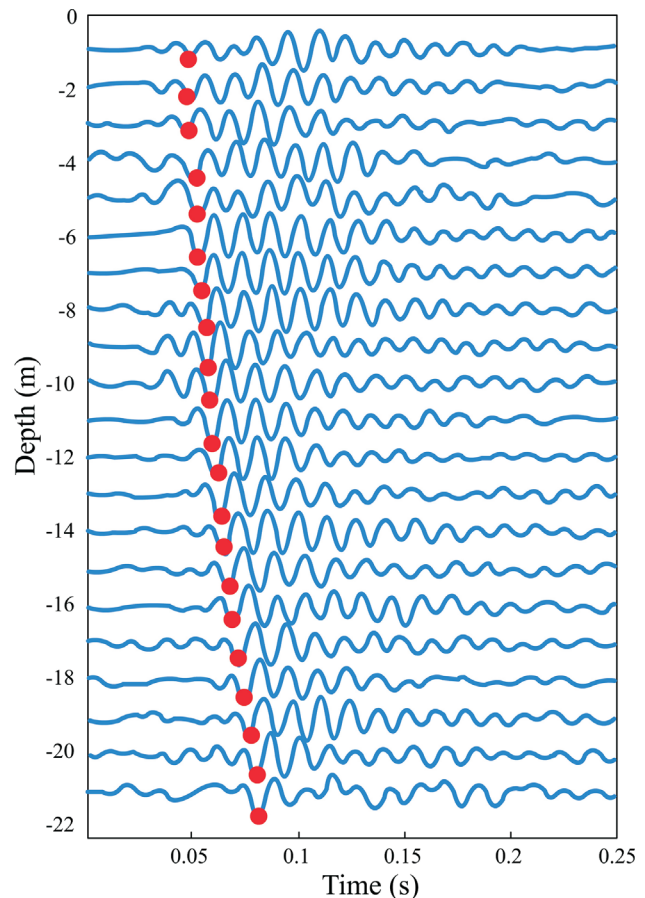


Figure 6 - Typical wave profile and the identification of the minimum point of the S waves (Rocha, 2013).

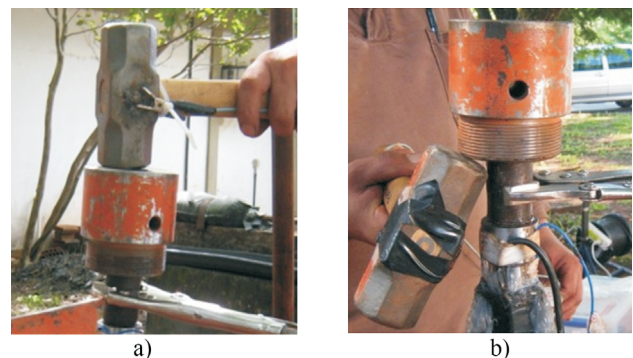


Figure 7 - Striking the drive head (a) downwards and (b) upwards (Pedrini, 2012).

sponding to the minimum point (Fig. 6). The next step was to subtract the time (Δt) until the crossing of the waves (Fig. 8), which corresponds to approximately 1/4 of the wave period. The wave period was determined by spectrum frequency analysis. It is important to point out that this analysis should be carried out for each S-SPT.

The predominant frequencies of the main pulse of the S wave were determined, as suggested by Stewart (1992).

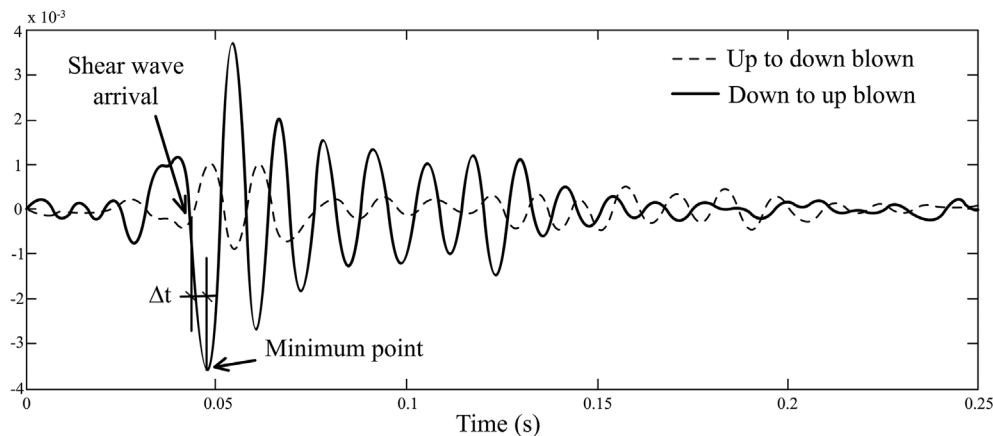


Figure 8 - Typical seismic traces obtained by the crossover method (adapted from Pedrini, 2012).

Figure 9 shows the frequency spectrum of the waves for an S-SPT carried out at the Campinas research site, which provided a dominant frequency of 61 Hz, with a time interval equal to 4.1 ms. This procedure is necessary to estimate the arrival time of the S wave, since this research adopted a method which does not determine the arrival time, but a reference time in each trace corresponding to the minimum point.

2.3.3. Vs calculation

The refracted wave path is determined from Snell’s law and a geometric criterion. The refracted wave path is defined based on the follow assumptions: a) the layer thickness of each sample is equal to the depth intervals where the SPT test is carried out (1 m); and b) each layer is homogeneous, and the propagated wave velocity will be constant. The Vs profile is determined by applying Eq. 1 of the DTS method, as presented by Bang & Kim (2007):

$$V_i = \frac{L_i}{T_i - \sum_{j=1}^{i-1} \left(\frac{L_j}{V_j} \right)} \tag{1}$$

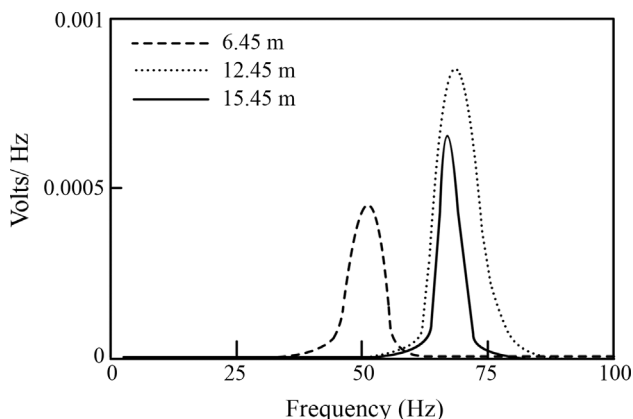


Figure 9 - Spectrum frequency (Hz) (adapted from Rocha, 2013).

where: *i* is the layer for which the velocity *V* (shear or compression waves) will be calculated; *L* is the length of the sample layer in which the wave will propagate; *T* is the total time that the wave takes to propagate from the sampler up to the surface receiver, and *V* is the wave propagation velocity. The velocity at the first layer is calculated dividing the distance from the sampler to the geophone by the time measured on the system. An interactive method was implemented in the software to calculate the wave velocities for the next layers. In this interactive method, the wave velocity for a certain layer is calculated assuming the velocity of the previous layer has been already calculated. Then, this value is assumed as the first *V* value and it is compared with the velocity calculated by Eq. 1. If the difference is within an imposed tolerance in the iterative method, the *V* value for the next layer is then calculated.

Further details for the above-mentioned calculations to determine the refracted trajectory according to Snell’s Law can be found in Bang & Kim (2007) as well as in Pedrini (2012).

2.3.4. Test layout and trend of the shear wave arrival

Identifying the first arrival of the shear wave velocity on the up-hole method is crucial for the interpretation of seismic SPT data. The SPT source generates a great amount of both compression and shear waves. The compression wave is detected mainly in a radial direction at the ground surface when the SPT source is located at a shallow depth, while it is detected mainly in the vertical direction at greater depths. In contrast, as the shear wave changes to a horizontal direction due to Snell’s law as propagating vertically to the ground surface, the shear wave is detected mainly in the vertical direction at the ground surface when the SPT source is located at shallow depth and in the radial direction when located at greater depths (Bang & Kim, 2007). In addition, the reverse polarity technique is difficult to be used because the source (the SPT sampler) is inside a borehole. For this reason, vertical and horizontal geophones were used, similarly to what was done by Bang & Kim (2007).

The trend of the shear wave arrival was evaluated through a qualitative interpretation of the seismic SPT data. It was observed that the vertical geophones can better record the P waves in all locations, compared to the horizontal ones. Moreover, it was also noted that, depending on the location of the geophones, the farther away from the SPT borehole, the lower the P wave amplitude, especially for waves generated at shallower depths. For greater depths, the horizontal geophones also record P waves, especially those closest to the SPT borehole. Figure 10a shows vertical geophone signals located 4.9 m away from the borehole. This figure shows that trend 1 represents the arrival of the P waves and trend 2 represents the arrival of the S waves.

It was found that S waves were more easily identified by the horizontal geophones and that at shallower depths, the horizontal geophones closest to the SPT borehole can better identify the S wave, while, at greater depths, the farthest geophones better recorded these waves. It was noted that at 7.5 m and 10.5 m from the SPT borehole, the arrival of S waves could also be identified with the vertical geophones, but with lower amplitude and poorer quality than the horizontal ones. Figure 10b shows the signals from the horizontal geophone located at 7.5 m from the SPT borehole. In this case, it is much easier to identify the trend of the S wave arrivals (trend 2) and quite difficult to identify the P waves (trend 1). Therefore, the V_s values were determined using only horizontal geophone records for the S-SPT performed at the three research sites, since these data better characterized the S waves.

2.3.5. Frequency filters

According to Campanella & Stewart (1992), identifying the arrival of the S wave and determining the shear wave propagation velocity can be influenced by the presence of noise in the seismic signal recorded by the geophones and the DAQ System during the SCPT signal analysis. Filters are often required to eliminate distortion in the S waves and resonance of the geophones. The P waves often also interfere with the signal of the S waves, mainly in unsaturated soils and at greater depths, where the amplitude of the S waves is close to that of the P waves due to the attenuation effect. Digital low-pass filters with three cutoff frequencies (400 Hz, 120 Hz and 80 Hz) to register seismic vibrations captured by geophones located 7.5 m from the SPT borehole were evaluated.

The most suitable digital filter was the one with 120 Hz cutoff frequency, as that used by Campanella & Stewart (1992) in down-hole tests. Figure 11 shows the vertical (Fig. 11a) and horizontal (Fig. 11b) records captured by the geophones. The vertical records show that tendency 1 (P-wave arrivals) was noticeably damaged. The same can be observed when the horizontal records are analyzed. Tendency 2 (arrival of S waves) clearly shows the arrival of this wave in the horizontal record, with a dominant amplitude when compared to the entire record. It is also possible to identify it in the vertical geophone traces, even though with some subjectivity. It is therefore concluded that:

- The P waves traces were quite minimized due to the applied filter, which attenuates the predominant frequencies of these waves; and

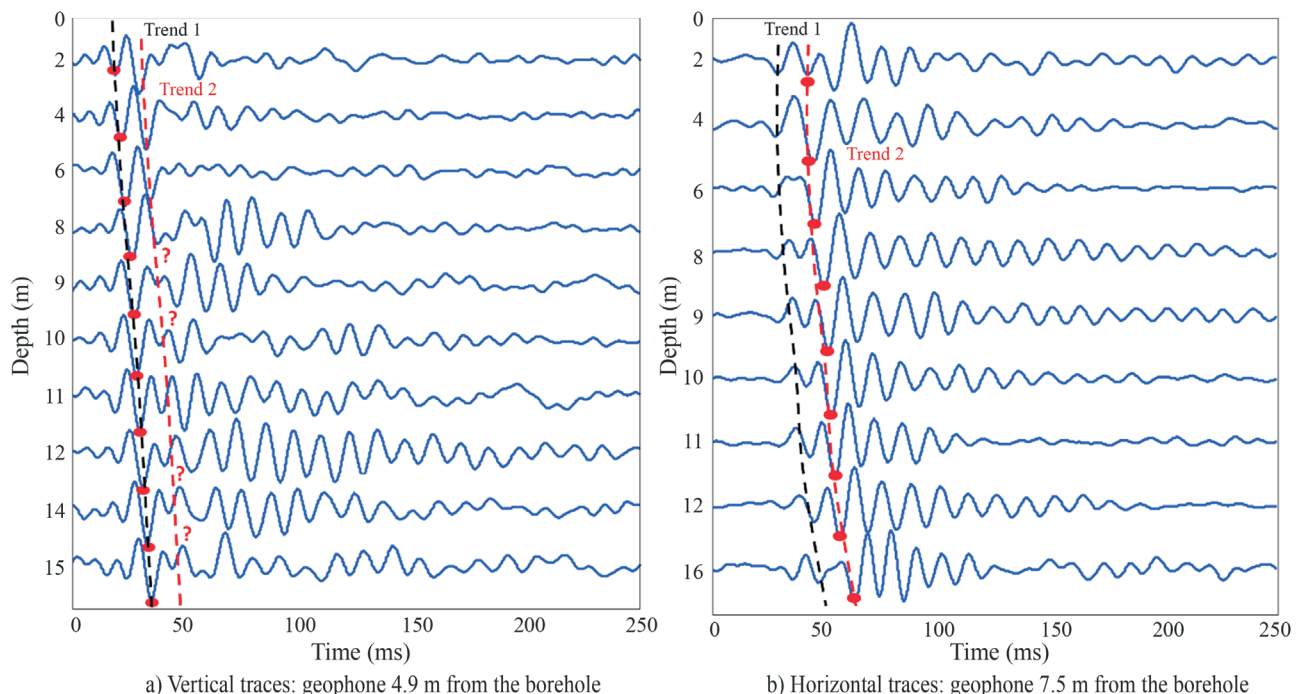


Figure 10 - Identification of the arrival of (a) compression waves - P and (b) shear waves - S.

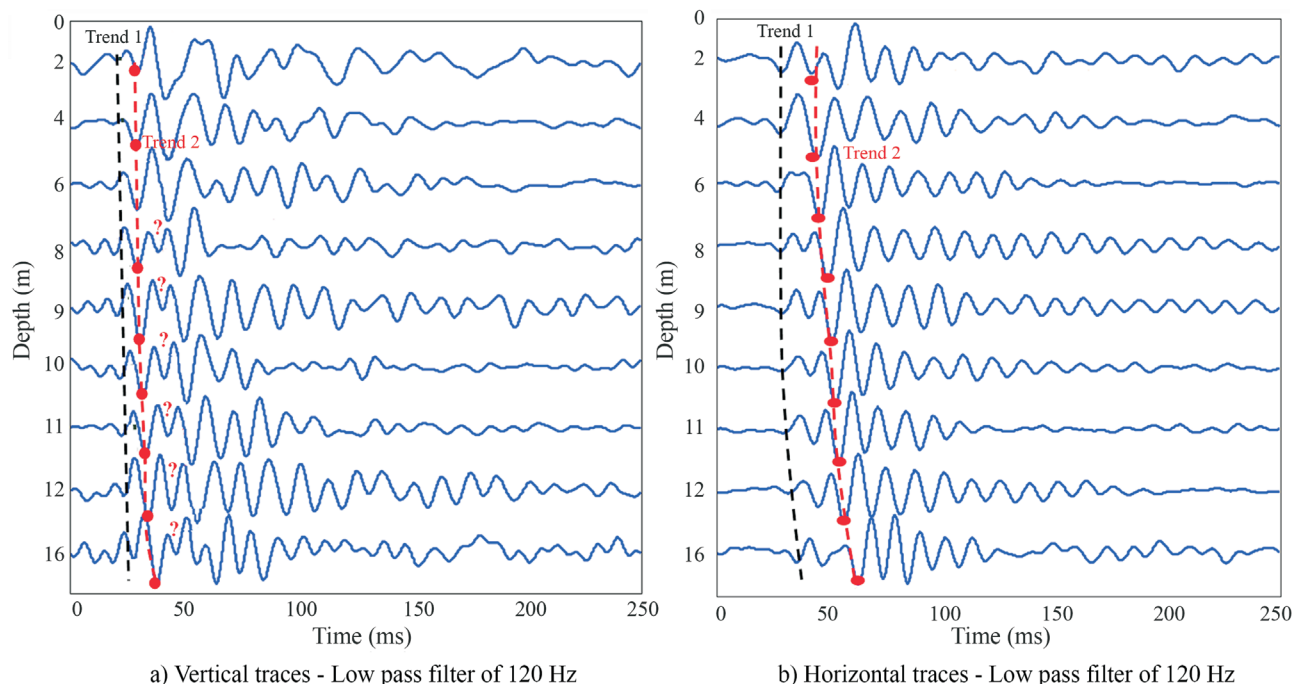


Figure 11 - Wave profile at 7.5 m from the borehole - Filter of 120 Hz.

- The records captured by the geophone in the horizontal direction clearly identify the arrival of the S waves.

3. Test Data and Discussion

Three S-SPT campaigns were conducted at the research sites of Unesp, USP and Unicamp to validate the system and the methodology. These sites were chosen because cross-hole, SCPT and down-hole test data were available (Giacheti, 1991; Giacheti *et al.*, 2006a; Giacheti *et al.*, 2006b, Giacheti *et al.*, 2007; Vitali *et al.*, 2012). They were used as a reference for comparison with the up-hole data from the S-SPTs.

The cross-hole tests were carried out in three boreholes, one for the seismic source and the other two for the triaxial geophones. PVC casing was grouted in the borehole according to ASTM D4428 (2007).

Down-hole tests were carried out using a seismic probe, with three geophone compartments, spaced at 0.5 m from each other. This probe allows to record at three different depths. The main characteristics of these geophones are: natural frequency of 28 Hz, sensitivity of 35.4 V/(m/s) and spurious frequency of 400 Hz. The geophones were installed in a uniaxial configuration, where it is essential to maintain the axis of vibration of the geophones parallel to the direction of the strike; this factor is considered as the most important factor for the success of the test (Vitali *et al.*, 2012). The seismic source in down-hole tests consists of a steel bar placed on the ground by the pushing equipment, which was positioned 0.3 and 1.8 m away from the CPT hole. The data were interpreted using the cross-correlation method and the true interval.

SCPT tests were carried out close to the cross-hole tests and up to 20 m depth by De Mio (2005). The seismic cone presents a triaxial array of geophones and the seismic waves were generated by blows applied on the side of a steel bar placed on the ground and loaded with weights, generating predominantly S_H type waves. The seismic wave velocities were calculated by the pseudo time interval with cross-over technique.

An error analysis was performed to verify the accuracy of V_s values determined with the S-SPT. The relative error was used (Eq. 2) to assess the quality of the measurement process and the accuracy in the determined V_s values (ISO 5725-1, 1994).

$$\delta_x = \left(\frac{\Delta x}{x} \right) \cdot 100 = \left(\frac{x_i - x}{x} \right) \cdot 100 \quad (2)$$

where δ_x : relative error; Δx : absolute error; x : true value of V_s (the assumed reference values from cross-hole, down-hole and SCPT); x_i : measured value of V_s (S-SPT).

3.1. USP research site

The soils at the USP research site, located in São Carlos, São Paulo State, Brazil, consist of porous and collapsible fine clayey sand up to a depth of about 6.5 m (colluvium), followed by a residual soil of Bauru sandstone. Both layers classify as clayey sand (SC) according to the Unified Soil Classification System (ASTM, 2003). These two distinct layers are separated by a 0.3 m thick layer of pebbles (Giacheti, 2001, Costa *et al.*, 2003, De Mio, 2005, Rocha, 2013). Figure 12 shows the grain size distribution,

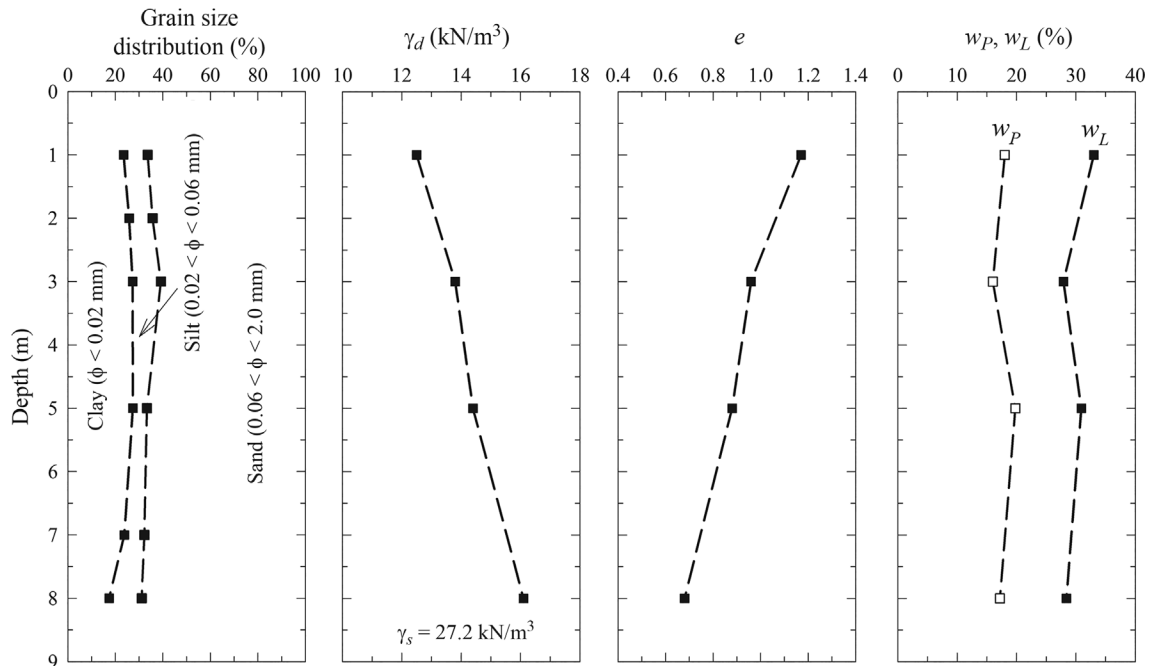


Figure 12 - Grain size distribution and indices properties for the USP research site (adapted from Machado, 1998).

dry unit weight (γ_d), void ratio, and Atterberg limits (w_L and w_p) up to 8.0 m depth. The particle unit weight (γ_s) can be considered constant along depth.

As previously argued (item 2.3.2), the reference point (minimum point) determination and frequency spectral analysis were performed. The average frequency of approximately 72 Hz was found at this site, which represents a time interval of approximately 3.47 ms. This value was subtracted from those defined from the reference point of each signal. It was observed that the signals from the horizontal geophones located at 2.0 and 4.0 m from the SPT borehole were not able to provide good quality seismic signals (surrounding noise) and they were not used to determine shear wave velocities (V_s).

Figure 13 shows all the test location at this research site. Figure 14 shows the test data of two cross-hole tests (CH1 and CH2), two seismic cone tests (SCPT1 and SCPT2), two down-hole tests (DH1 and DH2) and one S-SPT carried out using the described system and method. Figure 14 also shows that the average V_s difference between the S-SPT and the average cross-hole (CH1 and CH2) test data was 12.8%. It is also observed that the average relative difference between cross-holes CH1 and CH2 was 10.4%, which is in the same range for the S-SPT. It indicates that the S-SPT and the cross-hole provided comparable results. This difference was more significant at the top 6 m and by the pebble layer. One reason to explain it is the position of the seismic source, 1.8 m apart from the CPT hole, which can lead to higher V_s values determined by the down-hole tests, as explained by Butcher & Powell (1996) and Vitali *et al.* (2012). Another reason for the higher dif-

ference can be the soil suction, which could affect soil stiffness and the shear wave velocity (Giacheti, 1991; Barros, 1997; Georgetti *et al.*, 2015). It was also observed a lower quality of seismic S-SPT data nearby the pebble layer. It can be associated with the interference from this layer in the pathway of the seismic waves.

The average difference between S-SPT and average down-hole (DH1 and DH2) tests was 9.1%. Similarly, the main differences occurred up to about 7.0 m. The average difference between V_s from S-SPT and average V_s from SCPT (SCPT1 and SCPT2) tests was 6.4%. Once again, the main difference occurred in the upper layer, up to a depth of 7.0 m.

3.2. Unesp research site

The Unesp research site is in the city of Bauru, São Paulo State, Brazil. According to De Mío (2005), the typical soil profile at this site consists of a red clayey sand

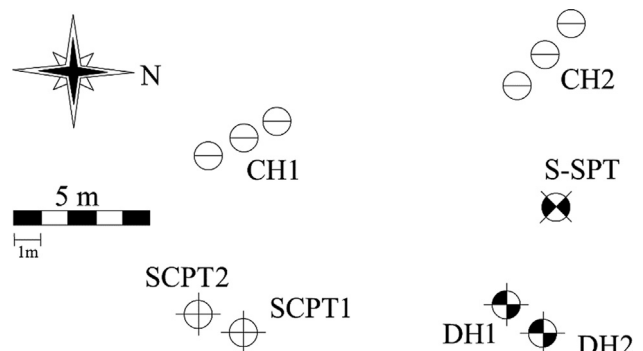


Figure 13 - Test locations at the USP research site.

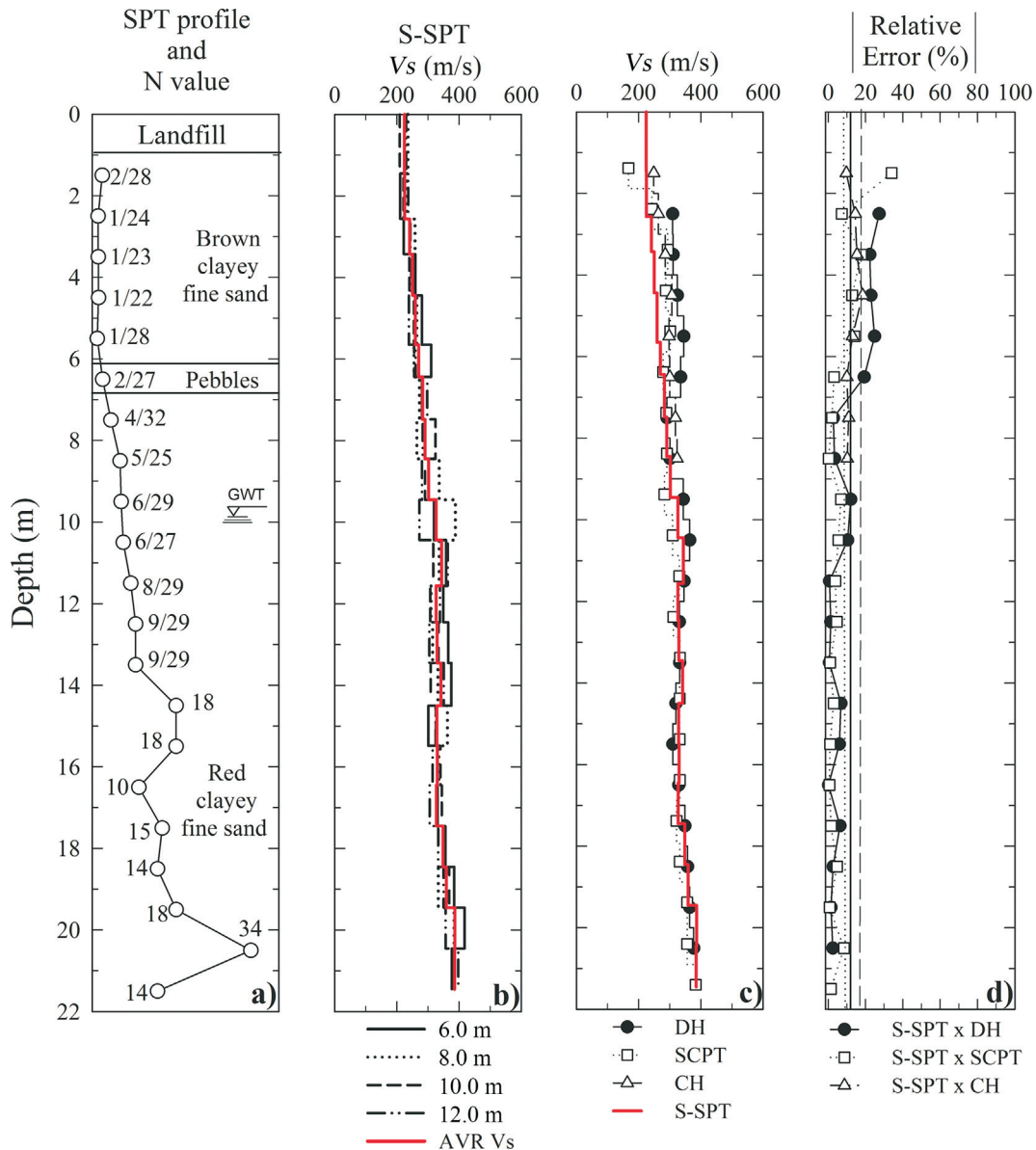


Figure 14 - SPT, V_s values from S-SPT, cross-hole, down-hole and SCPT tests at the USP research site.

(residual soil), classified as SM-SC in the Unified Soil Classification System (ASTM, 2003). Giacheti (2001) described this research site as a porous and collapsible soil, the density increases with depth and the soil has a lateritic behavior to about a depth of 13 m. Giacheti *et al.* (2006a) highlight the variability of the soil profile, observed throughout the electrical CPT testing data. Figure 15 shows the grain size distribution, dry unit weight (γ_d), void ratio, and Atterberg limits (w_L and w_p) up to 9.0 m depth. The particle unit weight (γ_s) can be considered constant along depth.

The identification of the minimum point (reference) and frequency spectral analysis were carried out for shear wave velocity profile definition. An average frequency of approximately 61 Hz was found at this site, which repre-

sents a time interval of approximately 4.20 ms. This value was subtracted from those defined from the reference point of each signal.

The signals recorded by boxes located at 2.0 and 4.0 m from the SPT borehole (horizontal geophones) were also not used to determine shear wave velocities (V_s) due to the horizontal signals being relatively weak and infected by surrounding noise.

Figure 16 shows the location of the *in situ* tests conducted at this site. One S-SPT, one cross-hole (CH), two seismic cone tests (SCPT1 and SCPT2) and two down-hole tests (DH1 and DH2) were carried out at this site.

Figure 17 shows the V_s values determined via S-SPT, cross-hole, SCPT and down-hole tests. The S-SPT provided equivalent results, with an average difference of

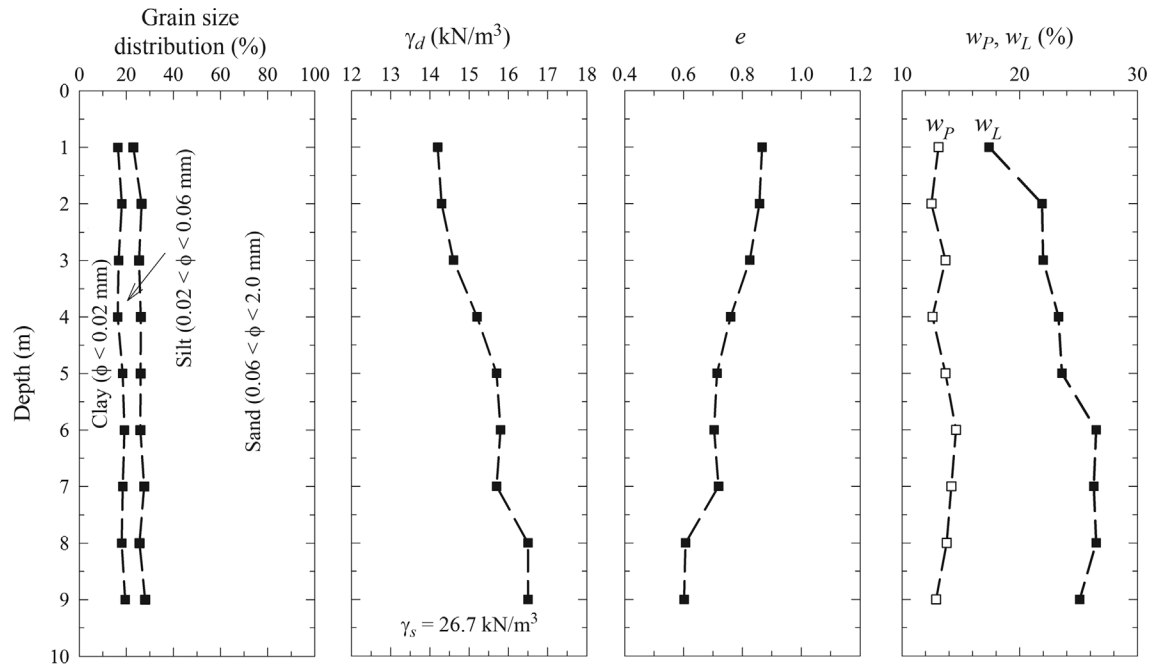


Figure 15 - Grain size distribution and indices properties for the Unesp research site (adapted from Giacheti *et al.*, 1998).

6.3% from the down-hole (Vitali *et al.*, 2012), 10.9% from the SCPT (Giacheti *et al.*, 2006a) and 7.0% from cross-hole test (Giacheti, 1991).

These differences were associated to soil variability as well as to possible soil anisotropy (Giacheti *et al.*, 2006a). The variability and the possible anisotropy are mainly due to the morphological and pedogenetic processes that occurred at this site, as mentioned by Giacheti *et al.* (2003) and by Giacheti & De Mio (2008), as well as the characteristics of the S-SPT, in which the interpretation of the up-hole technique is more complex than in the cross-hole and down-hole tests.

3.3. Unicamp research site

The Unicamp research site is in the city of Campinas, São Paulo State, Brazil. This site is also described by De Mio (2005) and it presents basic intrusive rocks of the Serra Geral Formation.

This research site is formed by two distinct layers: porous sand-silty clay, with lateritic and collapsible behavior up to 6 m depth (colluvium) followed by a transition zone with possible presence of lateritic crusts (from 6 to 7 m depth) and mature residual soil to depths that vary from 15 to 18 m. The highest clay concentration can be found in the mature residual soil at the upper part of the soil profile (between depths of 6 and 10 m). Despite such depth, this indicates the occurrence of a pedogenetic process that concentrates clay minerals at the horizon B. At depths greater than 18 m there is the occurrence of younger residual soils and the usual occurrence of fewer unaltered rock cores (De Mio, 2005 and Miguel *et al.*, 2007). CPT tests performed by Giacheti *et al.* (2003) exhibited varied tip resistance values (q_c) indicating the soil variability at this site.

Figure 18 shows the grain size distribution, dry unit weight (γ_d), void ratio, and Atterberg limits (w_L and w_p) up

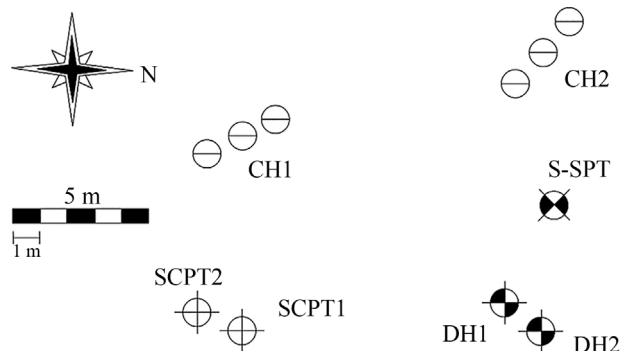


Figure 16 - Test location at the Unesp research site.

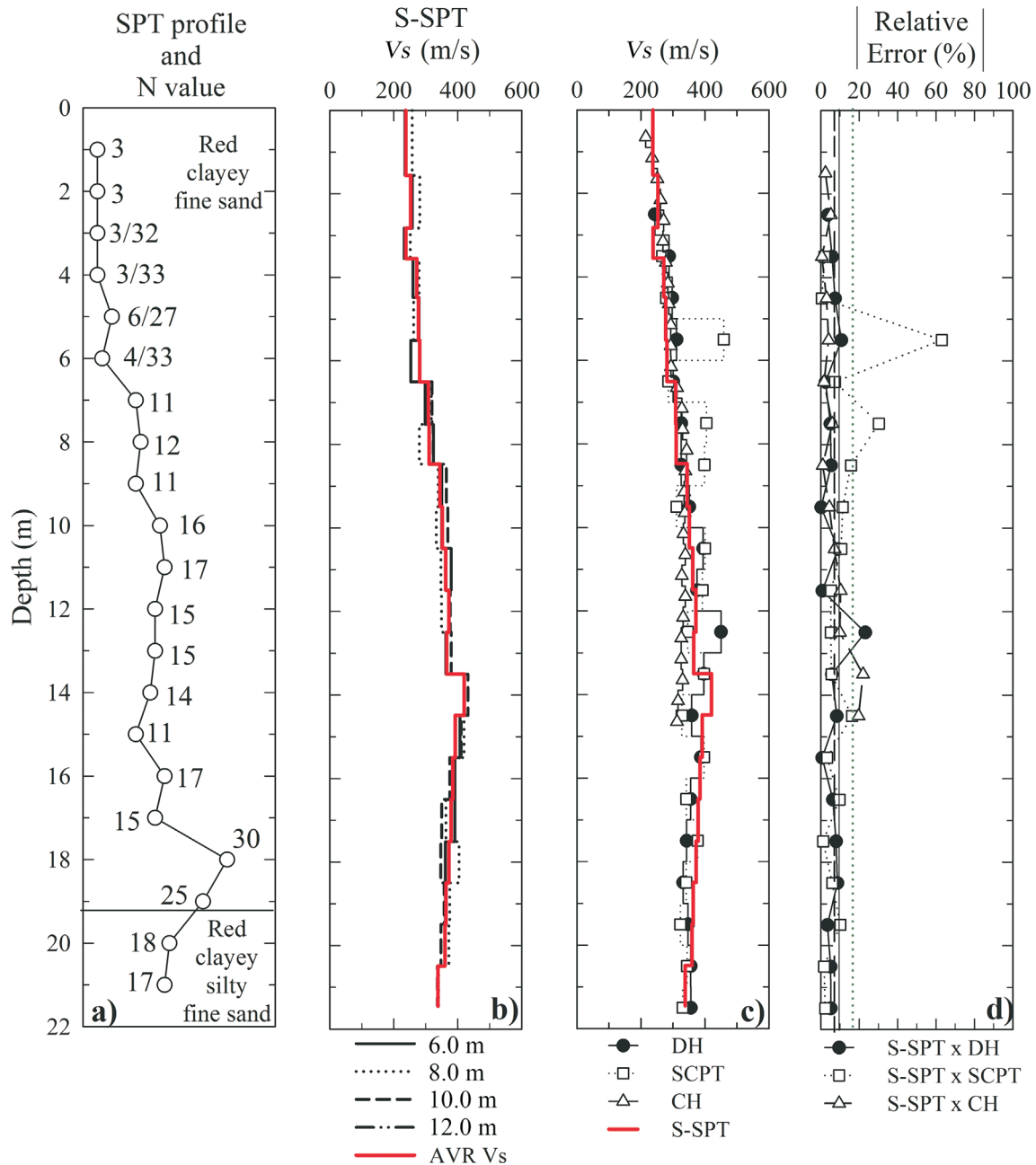


Figure 17 - SPT, Vs values from S-SPT, cross-hole, down-hole and SCPT tests at the Unesp research site.

to 9.0 m depth. The particle unit weight (γ_s) can be considered constant along depth.

Similarly to the USP and Unesp research sites, the identification of the minimum point and frequency spectral analysis (Fig. 11) were also carried out at the Unicamp research site. An average frequency of approximately 61 Hz was found, which represents a time interval of approximately 4.20 ms. Moreover, as previously mentioned for the USP and Unesp research sites, the signals recorded by horizontal geophones located at 2.0 and 4.0 m from the SPT borehole were not used to determine shear wave velocities (V_s).

Figure 19 shows the location of the seismic tests carried out in the Campinas research site. Figure 20 shows the differences between the average V_s values determined in the S-SPT and the average values of CH (21.9%), SCPT (16.2%) and DH (11.2%) tests. The greatest differences were found up to the depth of 5.0 m. Giacheti *et al.* (2007) discussed the great variability at this site based on CPT test data. The greatest difference was observed at the highest surface layer, which can be associated to the different test methods (the source position in the down-hole test, as discussed by Vitali *et al.* (2012) and to a possible influence of soil suction variation, since these tests were conducted at

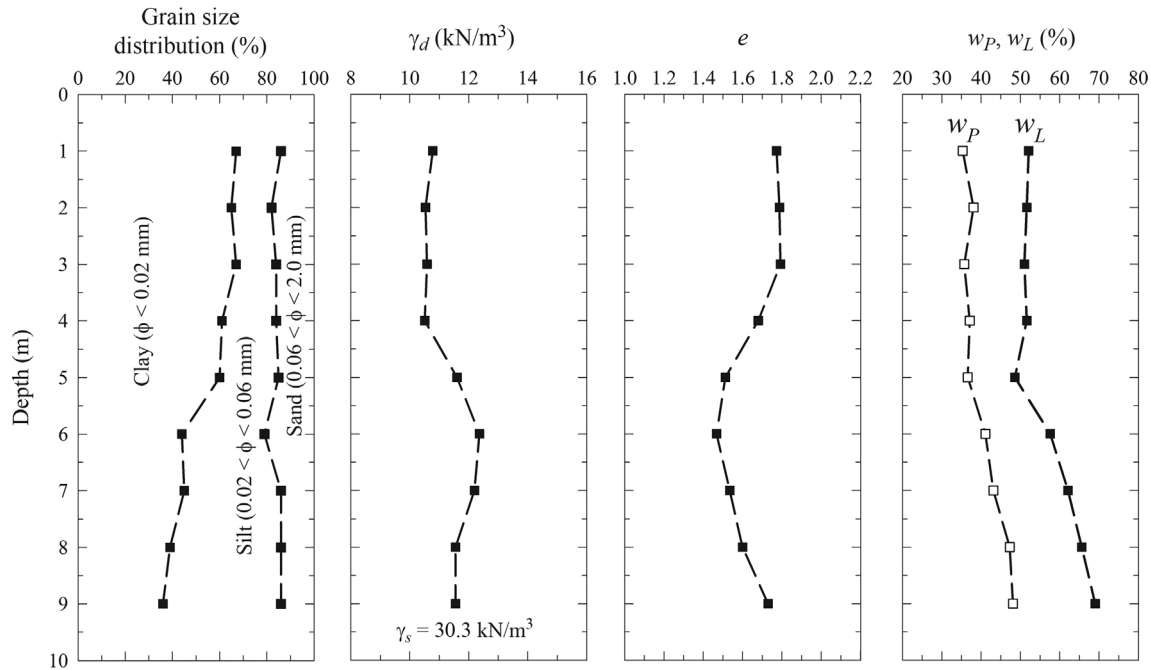


Figure 18 - Grain size distribution and index properties for the Unicamp research site (adapted from Gon, 2011).

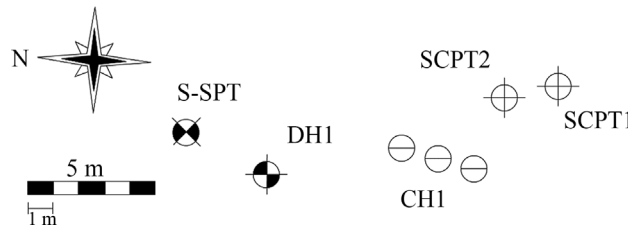


Figure 19 - Test locations at the Unicamp research site.

various times of the year, as discussed in Giacheti (1991), Barros (1997), Miguel & Vilar (2009) and Benatti *et al.* (2013).

The difference observed for the diabase residual soil layer (9.0 to 17.0 m) was smaller, of 9.4% for the SCPT tests and 8.0% for the DH. In this section of the soil profile a smaller variability was also observed by Giacheti *et al.* (2007) by the higher similarity of q_c profiles, indicating greater homogeneity of the geotechnical characteristics at this horizon. The variegated fine silty sand layer (at depths of 17.0 to 21.0 m) has the smallest difference in V_s values: average of 8.5% in the S-SPT and SCPT results, and 6.6% for the S-SPT and DH results.

4. Conclusions

This paper presents a system to carry out the Seismic SPT (S-SPT) and a method to interpret the seismic test data. The tests carried out at three research sites allowed to conclude the following:

- The S waves were mainly recorded by horizontal geophones during the up-hole SPT. It was also found that the

geophones installed at 2 m and 4 m from the borehole were not able to record good quality seismic signals.

- It is recommended to place the geophones at intervals of 2 m, starting 6 m away from the borehole. It was also observed that with increasing depth, the signals are better captured by the sensors placed further away.
- The low-pass frequency filters of 120 Hz worked well for the up-hole test together with SPT.
- The S-SPT proved to be an interesting tool for site characterization, since the differences from the reference V_s values are in the same order of magnitude as that observed for other seismic tests. The differences between V_s values were, in average, 8.5%, 9.0% and 16.0% for each research site.
- The S-SPT can be used as an alternative method for determining the shear wave velocity via the up-hole technique. SCPT and SDMT are the most used and appropriate hybrid tests to determine V_s profiles via down-hole technique. However, it requires using special equipment, which sometimes is not available. In such cases, the S-SPT could be an alternative hybrid test, at least to

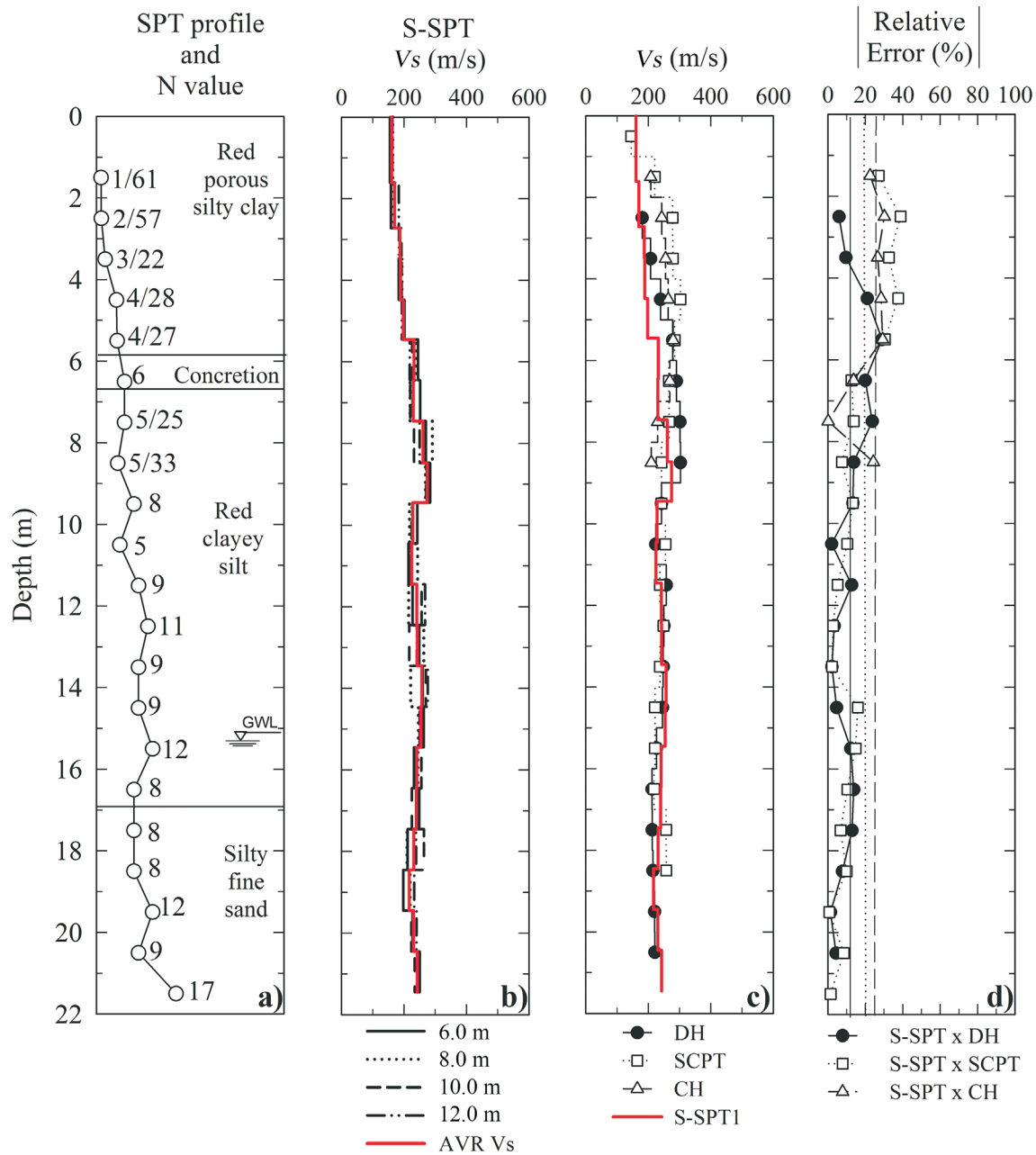


Figure 20 - SPT, V_s values from S-SPT, cross-hole, down-hole and SCPT tests at the Unicamp research site.

obtain a preliminary estimative of maximum shear modulus profiles.

Acknowledgments

The authors gratefully acknowledge the São Paulo Research Foundation - FAPESP (Grants # 2009/12428-0 and # 2010/50650-3), National Council for Scientific and Technological Development - CNPq (Grants # 481752/2010-2 and # 310867/2012-6) and Coordination for the Improvement of Higher Education Personnel - CAPES for their financial support.

References

ABNT (2001). Standard Penetration Test (SPT). NBR 6484, Rio de Janeiro, 17 p. (in Portuguese).

Anderson, J.B.; Townsend, F.C. & Rahelison, L. (2007). Load testing and settlement prediction of shallow foundation. *Journal of Geotechnical and Geoenvironmental Engineering*, 133(12):1494-1502.

ASTM (2007). Standard Test Method for Crosshole Seismic Testing – D 4428. ASTM International, West Conshohocken, Pennsylvania, USA, 11 p.

- ASTM (2003). Standard Practice for Classification of Soils for Engineering Purposes (Unified Soil Classification System) – D 2487. ASTM International, West Conshohocken, Pennsylvania, USA, 10 p.
- Atkinson, J.H. (2000). Non-linear soil stiffness in routine design. *Géotechnique*, 50(5):487-508.
- Bang, E.S. & Kim, D.S. (2007). Evaluation of shear wave velocity profile using SPT based up-hole method. *Soil Dynamics and Earthquake Engineering*, 27(8):741-758.
- Barros, J.M.C. (1997). Dynamics Shear Modulus for Tropical Soil. Ph.D. Dissertation, Department of Civil Engineering, University of São Paulo, São Paulo, 437 p. (in Portuguese).
- Benatti, J.C.B.; Rodrigues, R.A. & Miguel, M.G. (2013). Aspects of mechanical behavior and modeling of a tropical unsaturated soil. *Geotechnical and Geological Engineering*, 31(5):1569-1585.
- Butcher, A.P. & Powell, J.J.M. (1996). Practical Considerations for Field Geophysical Techniques Used to Assess Ground Stiffness. *Advances in Site Investigation*. Thomas Telford, London, p. 701-714.
- Campanella, R.G. & Stewart, W.P. (1992). Seismic cone analysis using digital signal processing for dynamic field characterization. *Canadian Geotechnical Journal*, 29(3):477-486.
- Committee on Tropical Soils of ISSMFE (1985). Peculiarities of Geotechnical Behavior of Tropical Lateritic and Saprolitic Soils: Progress Report (1982-1985). Edile, São Paulo.
- Costa, Y.D.; Cintra, J.C. & Zornberg, J.G. (2003). Influence of matric suction on the results of plate load tests performed on a lateritic soil deposit. *Geotechnical Testing Journal*, 26(2):219-227.
- De Mio, G. (2005). Geological Conditioning Aspects for Piezocone Test Interpretation for Stratigraphical Identification in Geotechnical and Geo-Environmental Site Investigation. Ph.D. Dissertation, Department of Geotechnical Engineering, University of São Paulo, São Carlos, 354 p. (in Portuguese).
- Georgetti, G.B.; Vilar, O.M. & Hoyos, L.R. (2015). Shear and compression wave velocities of an unsaturated sandy soil. *Proc. 15th Pan-American Conference on Soil Mechanics and Geotechnical Engineering*, v. 1, pp. 2204-2211.
- Giacheti, H.L. (1991). Experimental Study of Dynamics Parameters of some Tropical Soils from the State of São Paulo. Ph.D. Dissertation, University of São Paulo, São Carlos, 232 p. (in Portuguese).
- Giacheti, H.L. (2001). In situ Tests for Site Characterization: Studies and Thoughts for Tropical Soils. Department of Civil and Environmental Engineering, São Paulo State University, Bauru, 327 p. (in Portuguese).
- Giacheti, H.L. & De Mio, G. (2008). Seismic cone penetration tests on tropical soils and the ratio G_s/q_c . *Proc. 3rd Geotechnical and Geophysical Site Characterization Conference ISC'3*, Taiwan, v. 1, pp. 1289-1295.
- Giacheti, H.L.; Coelho, V. & Carvalho, David de (1998). Geotechnical characterization of two tropical soils based on laboratory tests. *Proc. 11th Brazilian Conference on Soil Mechanics and Geotechnical Engineering*, ABMS, v. 1, pp. 195-202. (in Portuguese).
- Giacheti, H.L.; Peixoto, A.S.P. & Marques, M.E.M. (2003). Cone penetration testing on Brazilian tropical soils. *Proc. 12th Pan-American Conference on Soil Mechanics and Geotechnical Engineering*, MIT, Cambridge, v. 1, pp. 397-402.
- Giacheti, H.L.; De Mio, G.; Dourado, J.C. & Malagutti, W. (2006a). Comparing down-hole and cross-hole seismic tests results on the Unesp Bauru research site. *Proc. 13th Brazilian Congress of Soil Mechanics and Geotechnical Engineering*, Curitiba, v. 2, pp. 669-674. (in Portuguese).
- Giacheti, H.L.; De Mio, G. & Peixoto, A.S.P. (2006b). Seismic cross-hole and CPT Tests in the Tropical Soil Site. *Proc. ASCE Geo-Congress*, Atlanta, pp. 1-6.
- Giacheti, H.L.; Peixoto, A.S.P. & De Mio, G. (2007). Cross-hole and SCPT tests in a tropical soil from Campinas, SP, Brazil. *Proc. 13th Pan-American Conference on Soil Mechanics and Geotechnical Engineering*, Venezuela, p. 1-6.
- Gon, F.S. (2011). Geotechnical Site Characterization by Laboratory Tests for a Diabasic Soil from Campinas-SP Region. M.Sc. Thesis, School of Civil Engineering, University of Campinas, Campinas, 166 p. (in Portuguese).
- ISO 5725-1 (1994). Accuracy (Trueness and Precision) of Measurement Methods and Results - Part 1: General Principles and Definitions, 17 p.
- Lukiantchuki, J.A. (2012). Interpretation of SPT Test Results based on Dynamic Instrumentation. Ph.D. Dissertation, Department of Geotechnical Engineering, University of São Paulo, São Carlos, 365 p. (in Portuguese).
- Machado, S.L. (1998). Application of Elasto-Plasticity Concepts to Unsaturated Soils. Ph.D. Dissertation, Department of Geotechnical Engineering, University of São Paulo, São Carlos, 361 p. (in Portuguese).
- Mayne, P.W.; Coop, M.R.; Springman, S.M.; Huang, A.B. & Zornberg, J.G. (2009). Geomaterial behavior and testing. State of the Art (SOA) paper. In: 17th International Conference on Soil Mechanics and Geotechnical Engineering, Alexandria, pp. 1-96.
- Miguel, M.G.; Albuquerque, P.J.R.; Azevedo, G.S.; Silva, G.S.V. & Carvalho, D. (2007). Lateritic behavior of the colluvial soil from Campinas-SP-Brasil. *Proc. 13th Pan American Conference on Soil Mechanics and Geotechnical Engineering*, Isla de Margarita, Venezuela. CD-ROM.

- Miguel, M.G. & Vilar, O.M. (2009). Study of the water retention properties of a tropical soil. *Canadian Geotechnical Journal*, 46(9):1084-1092.
- Ohta, Y.; Goto, N.; Kagami, H. & Shiono, K. (1978). Shear wave velocity measurement during a standard penetration test. *Earthquake Engineering & Structural Dynamics*, 6(1):43-50.
- Pedrini, R.A.A. (2012). Developing a System for Up-Hole Seismic Testing together with the SPT. M.Sc. Thesis, Department of Civil and Environmental Engineering, São Paulo State University, Bauru, 127 p. (in Portuguese).
- Robertson, P.K.; Woeller, D.J. & Addo, K.O. (1992). Standard penetration test energy measurements using a system based on the personal computer. *Canadian Geotechnical Journal*. 29(4):551-557.
- Rocha, B.R. (2013). The Use of Seismic SPT for Site Investigation of Tropical Soils. M.Sc. Thesis, Department of Geotechnical Engineering, University of São Paulo, São Carlos, 116 p. (in Portuguese).
- Santana, C.M.; Danziger, F.A.B. & Danziger, B.R. (2014). Energy measurement in the Brazilian SPT system. *Soils & Rocks*, 37(3):243-255.
- Stewart, W.P. (1992). In situ Measurement of Dynamic Soil Properties with emphasis on Damping. Ph.D. Dissertation, University of British Columbia, Vancouver, Canada, 379 p.
- US EPA, (1989). Seminar on Field Characterization for subsurface Remediation, United States Environmental Protection Agency, Technology Transfer, Report CERI-89-224, Sept, 350 p.
- Vitali, O.P.M.; Pedrini, R.A.A.; Giacheti, H.L. & Oliveira, L.P.R. (2012). Developing a system for down-hole seismic test together with the CPTU. *Soils & Rocks*, 35(2):75-88.

Durability of RAP-Industrial Waste Mixtures Under Severe Climate Conditions

N.C. Consoli, H.C. Scheuermann Filho, V.B. Godoy, C.M.D.C. Rosenbach, J.A.H. Carraro

Abstract. The sustainable use of industrial wastes such as coal fly ash and carbide lime is an effective procedure to enhance the long-term performance of reclaimed asphalt pavement (RAP) under extreme freeze-thaw and wet-dry conditions. This study evaluates the impact of lime content (L) and dry unit weight (γ_d) on the durability and long-term performance of compacted RAP-fly ash-carbide lime mixes. For all mixtures tested, specimens were statically compacted inside a cylindrical mould to their target dry unit weights. Single-level variables used in the stabilisation process included: fly ash (FA) content of 25% (in relation to the RAP), optimum water content of 9% (modified compaction effort) and seven days of curing. Three target dry unit weights equal to 17, 18 and 19 kN/m³ (the last one determined using the modified Proctor energy) as well as three different lime contents (3, 5 and 7%) were also used in the analysis. Both the accumulated loss of mass (ALM) after wetting-drying and freezing-thawing cycles and the splitting tensile strength (q_t) of the specimens tested were evaluated as a function of the porosity/lime ratio index (η/L_n). Compacted RAP-fly ash-carbide lime mixtures performed better when subjected to wetting-drying cycles than to freezing-thawing cycles. The results indicate that the porosity/lime ratio index controls not only the mechanical response but also the long-term performance of compacted RAP-fly ash-carbide lime mixes, which substantially broadens the applicability of the index.

Keywords: durability, industrial wastes, porosity/lime index, reclaimed asphalt pavement, soil stabilisation.

1. Introduction

The road network is a fundamental element for the supply and distribution chains, since it promotes the integration of regions, states, ports, railways, waterways and airports. With time, pavements start to present defects, such as irregularities in pavement surface, holes, interconnected, longitudinal and transverse cracks, landslides, absence of shoulder, among others. These factors may increase the risk of road accidents. Moreover, the quality of the pavement is one of the main determinants of the users' performance during their travels and in addition to the increase of the road costs when one has roads with precarious functionality.

One of the ways currently used to correct defects in pavements is the restoration of the cutting off of the old asphalt pavement and recomposition with a new asphalt coating. This operation (cutting off the asphalt coating) produces a great amount of residue in the works of restoration of highways (FHWA, 2011). The problem arises since there is no specification in the project for using this waste, which ends up generating problems in its final disposal, and is usually deposited in inappropriate places, such as along the highways, in landfills or mistakenly used as a primary coating, when its use can become an environmental liability,

as the rains end up carrying this residue to streams and rivers. One viable alternative to road maintenance and rehabilitation is the use of cement stabilised reclaimed asphalt pavement (RAP) in the base or sub-base layers of a pavement (e.g., Puppala *et al.*, 2011). Recently, Consoli *et al.* (2017) carried out research on the mechanical properties (unconfined compressive strength - q_u and splitting tensile strength - q_t) and the viscoelastic behavior (dynamic modulus - E^* and phase angle - δ) of RAP - powdered rock - Portland cement blends. These authors found out that the porosity/cement index (η/C_n) is a proper parameter to predict q_u , q_t , E^* and δ of RAP - powdered rock - Portland cement mixes. Such studies were based mainly in the mechanical behaviour (unconfined compressive strength, resilient and dynamic modulus) of such blends. However, the durability and long-term performance of compacted RAP treated industrial wastes has received reduced attention. One of the few investigations on this topic was carried out by Avirneni *et al.* (2016), who assessed the loss of mass after wetting-drying cycles on reclaimed asphalt pavements mixed with fly ash and sodium hydroxide. As present research is being developed in southern Brazil, where seasons are quite well defined, with temperatures reaching extremes of about -15 °C in winter and over 40 °C in summer (INPE, 2017),

Nilo Cesar Consoli, Ph.D., Full Professor, PPGEC, Universidade Federal do Rio Grande do Sul, Porto Alegre, RS, Brazil. e-mail: consoli@ufrgs.br.

Hugo Carlos Scheuermann Filho, M.Sc. Student, PPGEC, Universidade Federal do Rio Grande do Sul, Porto Alegre, RS, Brazil. e-mail: hugocsf@gmail.com.

Vinicius B. Godoy, Ph.D. Student, PPGEC, Universidade Federal do Rio Grande do Sul, Porto Alegre, RS, Brazil. e-mail: vinigodoy@msn.com.

Caroline M. De Carli Rosenbach, M.Sc. Student, PPGEC, Universidade Federal do Rio Grande do Sul, Porto Alegre, RS, Brazil. e-mail: carolmomoli@gmail.com.

J. Antonio H. Carraro, Ph.D., Associate Professor, Department of Civil and Environmental Engineering, Imperial College London, UK.

e-mail: antonio.carraro@imperial.ac.uk.

Submitted on November 22, 2017; Final Acceptance on May 16, 2018; Discussion open until December 31, 2018.

DOI: 10.28927/SR.412149

there is a need to search for the endurance of newly developed blends under severe climate conditions.

This research aims to investigate the performance under extreme wet-dry (cycles reaching 71 °C for 42 h followed by 23 °C for 5 h) and freeze-thaw (cycles reaching -23 °C for 24 h followed by 21 °C for 23 h) conditions of a RAP treated with coal fly ash and carbide lime to assess its potential use as road embankment, as well as sub-base material for low volume road. Besides, this study seeks to establish possible relationships between the porosity/lime index (η/L_v) and accumulated loss of mass (ALM) after wet-dry and freeze-thaw cycles for compacted RAP-fly ash-lime blends. Such index has already been correlated to strength and durability performance of lime treated clayey soils, lime-fly ash improved sands and in the stabilization of fly ash through the use of carbide lime (Consoli *et al.*, 2011, 2014, 2016a).

Consoli *et al.* (2018) performed an initial analysis of the effect of sodium chloride addition on blends with RAP, only indicating the accumulated loss of mass for wet-dry cycles, without relating such loss with the index $\eta/(L_v)^{0.11}$. The present article does not analyze the addition of salt, but the increase of compaction effort and lime content in relation to the splitting tensile strength (q_t). This enabled to establish a direct relationship for the accumulated loss of mass of both types of cycle (wet-dry and freeze-thaw cycles) with the index $\eta/(L_v)^{0.11}$, which demonstrated that such index controls the long-term behavior (durability) of the analyzed mixtures.

2. Experimental Program

The materials and methods used in present research are discussed below.

2.1. Materials

RAP grain size distribution is presented in Table 1 and in Fig. 1. Such recycled aggregate was reclaimed from the BR 290 highway, which connects the city of Porto Alegre (located in southern Brazil) to the seashore. RAP samples were collected in sufficient amount to complete all tests. The bitumen content (SBS Modified - PG 70-22S) found in the RAP was about 5.0%, having been determined according to ASTM D 2172 (ASTM, 2011a). Specific gravity of RAP for coarse aggregate was determined according to NBR NM 53 (ABNT, 2009b), for the fine aggregate was determined according to NBR NM 52 (ABNT, 2009a) and the relationship between them results in ($\gamma_{S_{RAP}}$) of 2.505. It is important to notice that the RAP grain size distribution is influenced, amongst other factors, by the milling machine process, so it can spatially vary, being therefore essential to particularly characterize the granulometry for each case. It is possible to adopt a control of the grain size of the selected milling, as was done in this research: 70% of the material retained in the 4' (4.75 mm opening) sawmill and 30% of the material passed through this same sieve.

The type F fly ash (FA) selected, according to ASTM C 618 (ASTM, 2008), is a residue of coal burning from a thermal power station. The results of the FA characterization tests are also presented in Table 1. The material is nonplastic and its specific gravity ($\gamma_{S_{FA}}$) was determined according to ASTM D 854 (ASTM, 2014), being equal to 2.18. Due to its granulometry, the FA is classified as silt (ML) according to the Unified Soil Classification System, presented in ASTM D 2487 (ASTM, 2006). As a result of X-Ray fluorescence spectrometry (XRF), it was possible to identify the main components of the FA, among which stand out SiO₂ (64.8%), Al₂O₃ (20.4%), Fe₂O₃ (4.8%) and CaO (3.1%).

Table 1 - Physical properties of the RAP and coal fly ash samples.

Properties	RAP	Coal fly ash
Liquid limit (%)	-	-
Plastic limit (%)	-	-
Plasticity index (%)	Nonplastic	Nonplastic
Specific gravity	2.505	2.180
Fine gravel (4.75 mm < diameter < 20 mm) (%)	52.0	-
Coarse sand (2.00 mm < diameter < 4.75mm) (%)	24.0	-
Medium sand (0.425 < diameter < 2.00 mm) (%)	19.0	0.1
Fine sand (0.075 mm < diameter < 0.425 mm) (%)	5.0	13.5
Silt (0.002 mm < diameter < 0.075 mm) (%)	-	84.1
Clay (diameter < 0.002 mm) (%)	-	2.3
Mean particle diameter (mm)	5.0	0.022
USCS class	GW (well-graded gravel)	ML (silt)

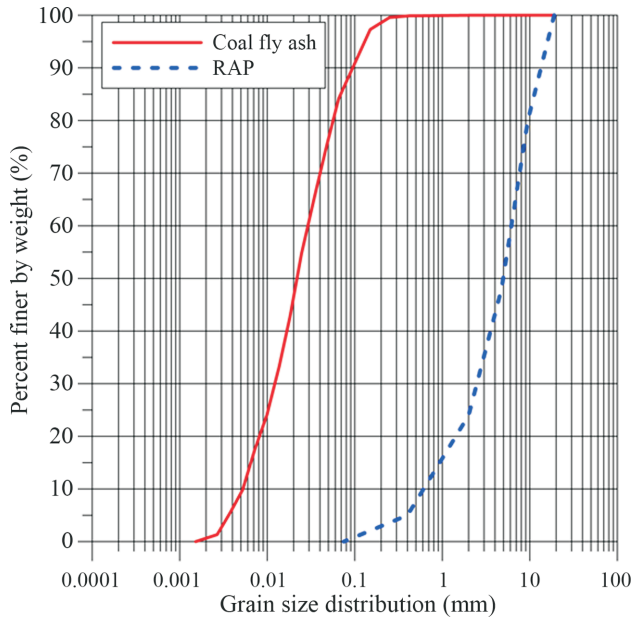


Figure 1 - Grain size distribution of studied RAP and coal fly ash.

The carbide lime (L), a by-product of the manufacture of acetylene gas, obtained from one source, was used throughout this investigation as the alkaline activator agent. The determination of calcium oxide established a value of 96%. In addition, its specific gravity ($\gamma_{s_{cl}}$) was, likewise, measured in accordance to ASTM D 854 (ASTM, 2014) and is 2.12.

Distilled water was employed both for characterization tests and moulding specimens for the mechanical tests.

2.2. Methods

2.2.1. Moulding and curing of specimens

For (split tensile) strength tests, cylindrical specimens 100 mm diameter and 60 mm from top to bottom were employed. For durability (wet-dry and freeze-thaw) tests, cylindrical specimens 100 mm diameter and 127.3 mm from top to bottom were utilized. A target dry unit weight for a particular specimen was then instituted as a result of the dry compacted RAP-fly ash-lime mix divided by the total volume of the specimen. As exhibited in Eq. 1 (Consoli *et al.*, 2017), porosity (η) is a function of dry unit weight (γ_d) of the mix, fly ash (FA) and carbide lime contents (L). The volumetric lime content (L_v), on the other hand, is defined as the ratio between the volume of lime and the total volume of the specimen, where the volume of lime was obtained through the ratio between added mass of lime and specific gravity of carbide lime.

Each substance (RAP, fly ash and lime) has a unit weight of solids ($\gamma_{s_{RAP}}$, $\gamma_{s_{FA}}$ and γ_{s_L}), which also requires to be pondered for computing porosity.

$$\eta = 100 - 100 \left\{ \left[\frac{\gamma_d}{1 + \frac{L}{100}} \right] \left[\frac{\frac{RAP}{100}}{\gamma_{s_{RAP}}} + \frac{\frac{FA}{100}}{\gamma_{s_{FA}}} + \frac{\frac{L}{100}}{\gamma_{s_L}} \right] \right\} \quad (1)$$

Once the RAP, fly ash and carbide lime were weighed, they were blended for about 10 min, until the mix visually attained uniformity. Moisture content (w) of 9% [optimum moisture content for modified Proctor compaction effort (ASTM, 2012)] for the blends was then supplemented, and mixing was resumed until a homogeneous paste in appearance was generated. The amount of fly ash (25%) was referenced to the dry mass of RAP + FA, based on previous research (Consoli *et al.*, 2018). Dry unit weights of 19 kN/m³ [maximum dry unit weight for modified Proctor compaction effort (ASTM, 2012)], and two other lower values below (18 kN/m³ and 17 kN/m³) were employed. The lime content applied to the mixtures was based on the ICL (Initial Consumption of Lime), method proposed by Rogers *et al.* (1997). Such method performs pH measurements of the blend with different lime contents. The minimum value indicated for use in the mixture is the percentage at which the pH reaches a maximum and constant value. Thus obtaining the values of 3%, 5% and 7% in this research [same values as those adopted for soil-cement mixtures (Consoli *et al.*, 2009, 2016a, 2016b; Mitchell, 1981)]. Specimens were statically compacted in the interior of a cylindrical mould in 3 strata, for the durability tests, and in 1 stratum for the split tensile strength tests. Subsequently to moulding, specimens were removed from the moulds and their weights, diameters and heights measured with precisions of nearly 0.01 g and 0.1 mm, respectively. The specimens were then sealed in plastic bags and cured in a humid room at 23° ± 2 °C with relative moisture of about 95%, in consonance with ASTM C 511 (ASTM, 2013), for a period of 7 days, which is the minimum time required by ASTM D 7762 (ASTM, 2018). Before all tests, specimens were put underwater for 24 h to reduce suction (Consoli *et al.*, 2011).

2.2.2. Splitting tensile tests

Splitting tensile tests were performed with a rate of loading equal to 1.14 mm/min, in agreement with the standard ASTM C496 (ASTM, 2011b). The split tensile strength was determined through the following relation, which is a function of the specimen diameter (D), height (H) and applied load (P).

$$q_t = \frac{2P}{\pi DH} \quad (2)$$

2.2.3. Durability tests

Durability tests of compacted RAP-fly ash-carbide lime blends were carried out according to standards ASTM D 559 (ASTM, 2015) for wet-dry cycles and ASTM D 560 (ASTM, 2016) for freeze-thaw cycles.

2.2.3.1. Wet-dry (ASTM D 559)

Test procedures determine mass losses produced by twelve recurrent wet-dry series followed by brushing strokes. Every cycle begins by full immersion of the specimens in water for 5 h at 23 ± 2 °C followed by oven drying during 42 h at 71 ± 2 °C. Lastly, specimens are brushed a number of times using a force of approximately 13.3 N.

2.2.3.2. Freeze-thaw (ASTM D 560)

Test procedures determine mass losses produced by twelve repeated freeze-thaw series followed by brushing strokes. Every cycle begins by introducing specimens in a freezing cabinet having a constant temperature not higher than -23 °C for 24 h and after removing. Next, placing the assembly in the moist room under a temperature of 21 °C and a relative humidity of 100% for 23 h and removing. Finally, specimens are brushed a number of times using a force of approximately 13.3 N.

3. Results and Analysis

3.1. Influence of the porosity/lime index on splitting tensile strength (q_t)

Figure 2 presents the splitting tensile strength (q_t) as a function of $\eta/(L_{iv})^{0.11}$ [quantified as porosity (η) divided by the volumetric lime content (L_{iv}), the latter expressed as a percentage of carbide lime volume to the total volume of the specimen (Consoli *et al.*, 2014). Fig. 2 indicates that the adjusted porosity/lime index is helpful in normalizing strength results for RAP-fly ash-carbide lime mixtures. A very good correlation ($R^2 = 0.95$) can be perceived concern-

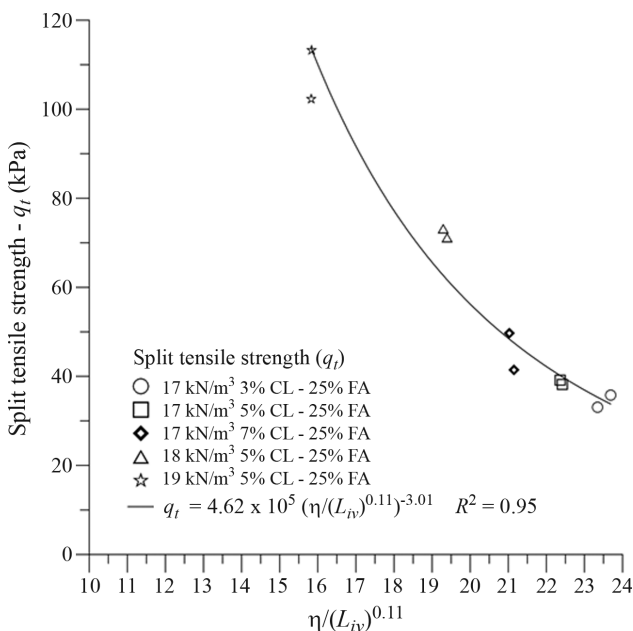


Figure 2 - Variation of splitting tensile strength (q_t) with porosity/lime index for RAP-fly ash-carbide lime blends for 7 days of curing.

ing $\eta/(L_{iv})^{0.11}$ and q_t [see Eq. 3] of the RAP-fly ash-carbide lime mixtures studied.

$$q_t \text{ (kPa)} = 4.62 \times 10^5 \left[\frac{\eta}{(L_{iv})^{0.11}} \right]^{-3.0} \quad (3)$$

The capability of the adjusted porosity/lime index to normalize strength of lime treated soils has been shown by Consoli *et al.* (2014, 2016a,b). They have shown that rates of change of strength with porosity (η) and the inverse of the volumetric lime content ($1/L_{iv}$) are as a rule not the same. Thus, the application of a power (as a rule 0.11 - Consoli *et al.*, 2014) to L_{iv} is required for the rates of η and $1/L_{iv}$ to be compatible.

3.2. Influence of the carbide lime content, porosity and porosity/lime index on durability (wetting-drying cycles and freezing-thawing cycles) of RAP-coal fly ash-carbide lime blends

Figure 3 presents relations of accumulated loss of mass (*ALM*) vs. number of wetting-drying and freezing-thawing cycles for compacted RAP-coal fly ash-lime blends (for a curing period of 7 days) in view of distinctive dry unit weights (17, 18 and 19 kN/m³) and carbide lime contents (5 and 7%). It can be seen in Fig. 3 that the *ALM* of each specimen is reduced with the increase of carbide lime content and with increase in dry unit weight. Similar specimens submitted to wetting-drying and freezing-thawing show distinct accumulated loss of mass (*ALM*), always occurring larger values of *ALM* brushing specimens submitted to freezing-thawing. The reason for different losses is due to distinct effects of temperature during wetting-drying and freezing-thawing cycles. For freezing-thawing testing conditions, after curing for 7 days at a standard temperature of about 23 °C the pozzolanic reactions are periodically stopped during freezing at temperature below -23 °C. On the contrary, under dry-wet conditions, after curing for 7 days at a normal temperature of about 23 °C the pozzolanic reactions are accelerated during drying at temperature 71 °C (Consoli *et al.*, 2014). As a consequence, specimens submitted to wetting-drying cycles have stronger bonds and so, smaller loss of mass during brushing.

Figure 4a exhibits compacted RAP-coal fly ash-carbide lime blends accumulated loss of mass (*ALM*) vs. adjusted porosity/lime index [$\eta/(L_{iv})^{0.11}$] after 1 [$R^2 = 0.93$ - see Eq. 4], 3 [$R^2 = 0.94$ - see Eq. 5], 6 [$R^2 = 0.94$ - see Eq. 6], 9 [$R^2 = 0.93$ - see Eq. 7] and 12 [$R^2 = 0.93$ - see Eq. 8] wetting-drying cycles (during durability tests).

$$ALM(\%) = 150 \times 10^{-3} \left[\frac{\eta}{(L_{iv})^{0.11}} \right]^{2.20} \quad (4)$$

$$ALM(\%) = 184 \times 10^{-3} \left[\frac{\eta}{(L_{iv})^{0.11}} \right]^{2.20} \quad (5)$$

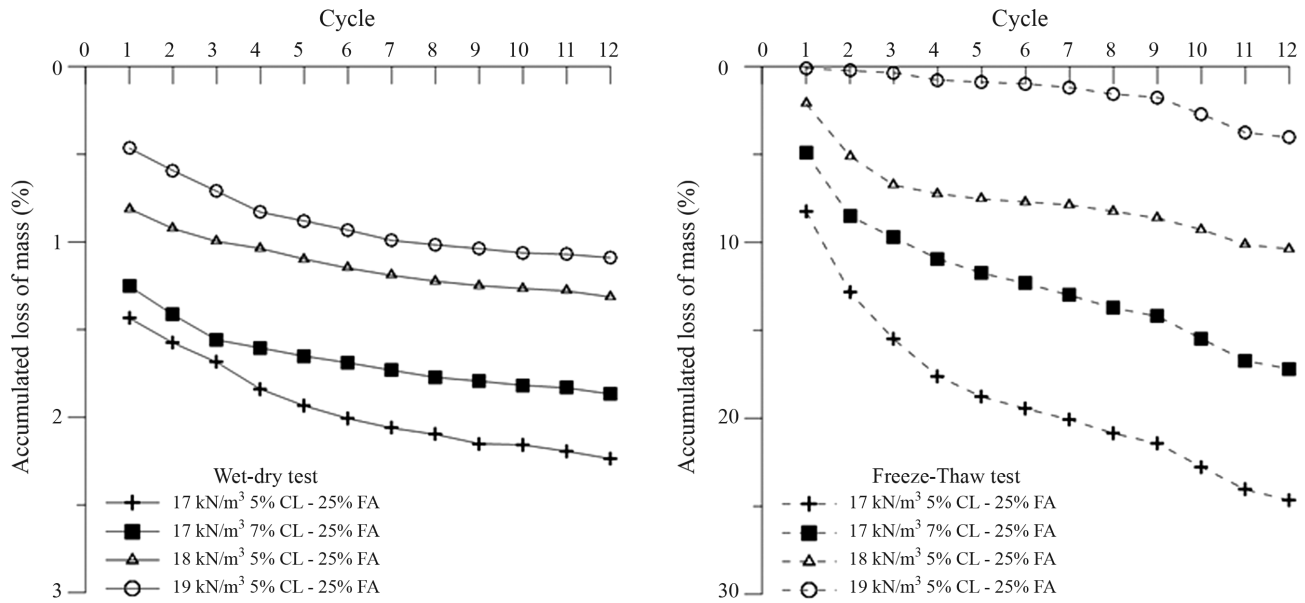


Figure 3 - Accumulated loss of mass after (a) wet-dry and (b) freeze-thaw cycles considering RAP-fly ash-carbide lime specimens moulded with dry unit weights of 17, 18 and 19 kN/m³, carbide lime contents of 5% and 7% specimens and 7 days as curing period.

$$ALM(\%) = 2.14 \times 10^{-3} \left[\frac{\eta}{(L_{iv})^{0.11}} \right]^{2.20} \quad (6)$$

$$ALM(\%) = 2.30 \times 10^{-3} \left[\frac{\eta}{(L_{iv})^{0.11}} \right]^{2.20} \quad (7)$$

$$ALM(\%) = 2.40 \times 10^{-3} \left[\frac{\eta}{(L_{iv})^{0.11}} \right]^{2.20} \quad (8)$$

Similarly, Fig. 4b exhibits compacted RAP-coal fly ash-carbide lime blends accumulated loss of mass (*ALM*) vs. adjusted porosity/lime index [$\eta/(L_{iv})^{0.11}$] after 1 [$R^2 = 0.98$ - see Eq. 9], 3 [$R^2 = 0.98$ - see Eq. 10], 6 [$R^2 = 0.99$ - see Eq. 11], 9 [$R^2 = 0.99$ - see Eq. 12] and 12 [$R^2 = 0.97$ - see Eq. 13] freezing-thawing cycles.

$$ALM(\%) = 1.08 \times 10^{-12} \left[\frac{\eta}{(L_{iv})^{0.11}} \right]^{9.50} \quad (9)$$

$$ALM(\%) = 2.10 \times 10^{-12} \left[\frac{\eta}{(L_{iv})^{0.11}} \right]^{9.50} \quad (10)$$

$$ALM(\%) = 2.66 \times 10^{-12} \left[\frac{\eta}{(L_{iv})^{0.11}} \right]^{9.50} \quad (11)$$

$$ALM(\%) = 2.97 \times 10^{-12} \left[\frac{\eta}{(L_{iv})^{0.11}} \right]^{9.50} \quad (12)$$

$$ALM(\%) = 3.49 \times 10^{-12} \left[\frac{\eta}{(L_{iv})^{0.11}} \right]^{9.50} \quad (13)$$

It is clear in Figs. 4a and 4b that the accumulated loss of mass (*ALM*) is controlled by $\eta/(L_{iv})^{0.11}$ for all cycles in both wetting-drying and freezing-thawing tests. The existence of such relationships is shown for the first time ever for compacted RAP-coal fly ash-carbide lime blends. Looking at such figures, it might be observed that for the specimens with $\eta/(L_{iv})^{0.11} \sim 15$ (smaller studied value) the *ALM* under wetting-drying conditions varies from about 0.5% to 1.0% after one and twelve cycles while it varies only from about 0.4% to 4.0% under freezing-thawing conditions. For specimens in which $\eta/(L_{iv})^{0.11} \sim 22.5$ (larger studied value) the *ALM* under wetting-drying conditions varies from about 1.2% to 2.4% after one and twelve cycles while it varies only from about 8% to 25% under freezing-thawing conditions. These results also show that the long-term performance of compacted RAP-fly ash-lime blends is a function of $\eta/(L_{iv})^{0.11}$ and that such material is more durable under wetting-drying than freezing-thawing conditions.

It was expected that the dry unit weight vary along the test, particularly for the freeze-thaw tests. Nonetheless, it was also expected that the specimens with lower initial $\eta/(L_{iv})^{0.11}$ values perform better than those with higher values, which is one of the explanations for the correlation between the porosity/lime index and the accumulated loss of mass (in each cycle). The change in the porosity along the cycles can be one of the reasons for the not so good fitting observed in Fig. 4b (even with high values of R^2), although further studies, such as micro structural, combined with a

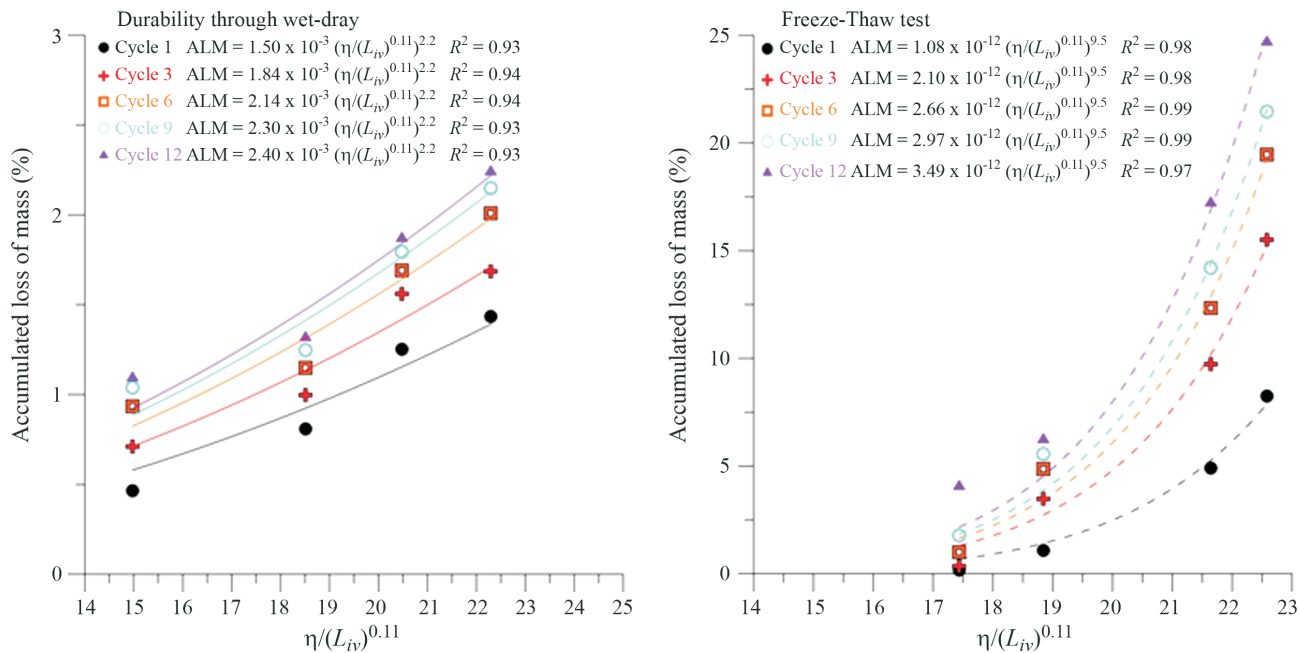


Figure 4 - Accumulated loss of mass for (a) wet-dry and (b) freeze-thaw for 1, 3, 6, 9 and 12 cycles vs. $\eta/(L_{iv})^{0.11}$ of RAP-fly ash-carbide lime blends considering distinct dry unit weight (17, 18 and 19 kN/m³) and carbide lime content (5 and 7%) specimens and 7 days curing period.

statistical analysis, should be performed to reach up definitive conclusions.

Finally, relationships of accumulated loss of mass (*ALM*) (after twelve cycles under wetting-drying and freezing-thawing conditions) vs. splitting tensile strength (q_t) for compacted RAP-coal fly ash-carbide lime blends are presented in Fig. 5. Unique non-linear relations ALM_{WD} vs. q_t and ALM_{FT} vs. q_t are presented in Eq. 14 and Eq. 15, respectively. Both have high correlations ($R^2 \geq 0.96$).

$$ALM_{WD} (\%) = 1.47 \times 10^4 \times q_t^{-1.77} \quad (14)$$

$$ALM_{FT} (\%) = 25.92 \times q_t^{-0.68} \quad (15)$$

Further research is still necessary to enhance the understanding of such materials, specially in what concerns the microstructural level and the effect of addition of other binders. Even so, in the future, this kind of relationships might enable researchers to reduce time in assessing durability of RAP-binder blends, as wetting-drying and freezing-thawing durability are time and effort consuming tests.

4. Concluding Remarks

From the studies described in this manuscript the following conclusions can be drawn:

- The accumulated loss of mass (*ALM*) (long term performance) of individual wetting-drying and freezing-thawing cycles of compacted RAP-coal fly ash-carbide lime blends was observed in the present research to be directly associated with the adjusted porosity/lime index;

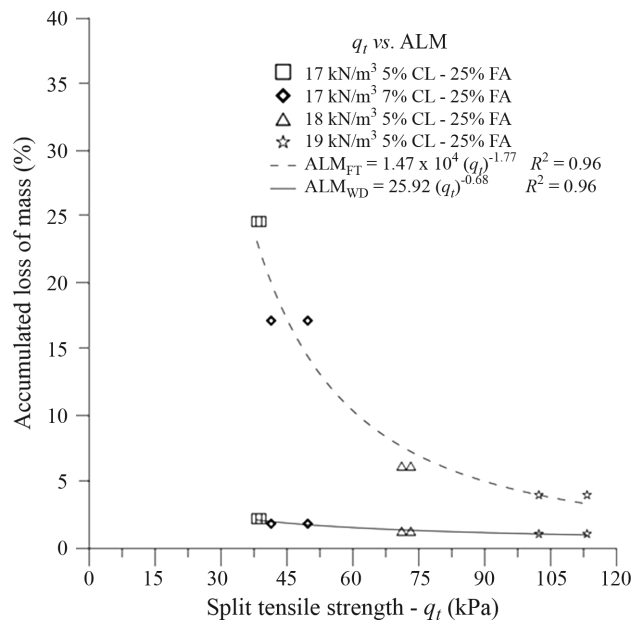


Figure 5 - Accumulated loss of mass considering twelve wetting-drying (and freezing-thawing) vs. q_t for RAP-coal fly ash-carbide lime blends in view of distinct dry unit weight (17, 18 and 19 kN/m³) and carbide lime content (3, 5 and 7%) specimens and 7 days curing period.

- Long term performance of compacted RAP-fly ash-lime blends is a function of $\eta/(L_{iv})^{0.11}$. Such material is more durable under wetting-drying than freezing-thawing conditions;

- The porosity/lime index controls strength and endurance of the compacted RAP-coal fly ash-carbide lime blends. So, according to the strength and durability requirements, the earthwork designer can establish the adjusted porosity/lime index that fulfils the design needs.

Acknowledgments

The authors desire to express their gratitude to Edital 12/2014 FAPERGS/CNPq - PRONEX (project # 16/2551-0000469-2) and CNPq (INCT-REAGEO and Produtividade em Pesquisa) for funding the research group.

References

- ABNT (2009a). Fine Aggregate - Determination of the Bulk Specific Gravity and Apparent Specific Gravity. NBR NM 52, Rio de Janeiro, Brazil (in Portuguese).
- ABNT (2009b). Coarse Aggregate - Determination of the Bulk Specific Gravity, Apparent Specific Gravity and Water Absorption. NBR NM 53, Rio de Janeiro, Brazil (in Portuguese).
- ASTM (2006). Standard Classification of Soils for Engineering Purposes. ASTM D 2487, West Conshohocken, Philadelphia.
- ASTM (2008). Standard Specification for Coal Fly Ash and Raw or Calcined Natural Pozzolan for Use in Concrete. ASTM C 618, West Conshohocken, Philadelphia.
- ASTM (2011a). Standard Test Methods for Quantitative Extraction of Bitumen from Bituminous Paving Mixtures. ASTM D 2172, West Conshohocken, Philadelphia.
- ASTM (2011b). Standard Test Method for Splitting Tensile Strength of Cylindrical Concrete Specimens. ASTM C 496, West Conshohocken, Philadelphia.
- ASTM (2012). Standard Test Methods for Laboratory Compaction Characteristics of Soil Using Modified Effort (2,700 kN-m/m³). ASTM D 1557, West Conshohocken, Philadelphia.
- ASTM (2013). Standard Specification for Mixing Rooms, Moist Cabinets, Moist Rooms, and Water Storage Tanks Used in the Testing of Hydraulic Cements and Concretes. ASTM C 511, West Conshohocken, Philadelphia.
- ASTM (2014). Standard Test Methods for Specific Gravity of Soil Solids by Water Pycnometer. ASTM D 854, West Conshohocken, Philadelphia.
- ASTM (2015). Standard Test Methods for Wetting and Drying Compacted Soil-Cement Mixtures. ASTM D 559, West Conshohocken, Philadelphia.
- ASTM (2016). Standard Test Methods for Freezing and Thawing Compacted Soil-Cement Mixtures. ASTM D 560, West Conshohocken, Philadelphia.
- ASTM (2018). Standard Practice for Design of Stabilization of Soil and Soil-Like Materials with Self-Cementing Fly Ash. ASTM D 7762, West Conshohocken, Philadelphia.
- Avirneni, D.; Peddinti, P.R.T. & Saride, S. (2016). Durability and long-term performance of geopolymer stabilized reclaimed asphalt pavement base courses. *Construction and Building Materials*, 121:198-209.
- Consoli, N.C.; Lopes Jr., L.S. & Heineck, K.S. (2009). Key parameters for the strength control of lime stabilized soils. *Journal of Materials in Civil Engineering*, 21(5):210-216.
- Consoli, N.C.; Dalla Rosa, A. & Saldanha, R.B. (2011). Variables governing strength of compacted soil-fly ash-lime mixtures. *Journal of Materials in Civil Engineering*, 23(4):432-440.
- Consoli, N.C.; Rocha, C.G. & Saldanha, R.B. (2014). Coal fly ash-carbide lime bricks: An environment friendly building product. *Construction and Building Materials*, 69:301-309.
- Consoli, N.C.; Quiñónez Samaniego, R.A. & Kanazawa Villalba, N.M. (2016a). Durability, strength and stiffness of dispersive clay-lime blends. *Journal of Materials in Civil Engineering*, 28(11):04016124.
- Consoli, N.C.; Quiñónez Samaniego, R.A.; Marques, S.F.V.; Venson, G.I.; Pasche, E. & González Velázquez, L.E. (2016b). A single model establishing strength of dispersive clay treated with distinct binders. *Canadian Geotechnical Journal*, 53(12):2072-2079.
- Consoli, N.C.; Pasche, E.; Specht, L.P. & Tanski, M. (2017). Key parameters controlling dynamic modulus of crushed reclaimed asphalt paving-powdered rock-Portland cement blends. *Road Materials and Pavement Design*, (published online) DOI: 10.1080/14680629.2017.1345779.
- Consoli, N.C.; Giese, D.N.; Leon, H.B.; Mocelin, D.M.; Wetzel, R. & Marques, S.F.V. (2018). Sodium chloride as a catalyser for crushed reclaimed asphalt pavement - fly ash - carbide lime blends. *Transportation Geotechnics* 15:13-19.
- Federal Highway Administration (FHWA) (2011). Publication No. FHWA-PL-11-028, U.S. Department of Transportation, Washington, DC.
- INPE (2017). <http://www.inpe.br/>. Brazilian Institute of Spatial Research, Brasília, Brazil.
- Mitchell, J.K. (1981). Soil improvement - State-of-the-art report. Proc. 10th Int. Conf. on Soil Mechanics and Foundation Engineering. International Society of Soil Mechanics and Foundation Engineering, Stockholm, pp. 509-565.
- Puppala, A.J.; Hoyos, L.R. & Potturi, A.K. (2011). Resilient moduli response of moderately cement treated reclaimed asphalt pavement aggregates. *Journal of Materials in Civil Engineering*, 23(7):990-998.
- Rogers, C.D.F.; Glendinning, S. & Roff, T.E.J. (1997). Lime modification of clay soils for construction expediency. *Proc. Inst. Civil Eng., Geotech. Eng.*, 125(3):242-249.

List of Symbols

ALM: accumulated loss of mass

D: specimen diameter

*E**: dynamic modulus

FA: fly ash

H: specimen height

L: lime content (expressed in relation to mass of RAP + fly ash)

L_v : volumetric lime content (expressed in relation to the total specimen volume)

P: applied load

q_u : unconfined compressive strength

q_t : splitting tensile strength

R^2 : coefficient of determination

RAP: reclaimed asphalt pavement

η : porosity

η/C_w : porosity/cement index

η/L_v : porosity/lime index

γ_d : dry unit weight

γ_s : unit weight of solids

δ : phase angle

w: moisture content (ratio of mass of water to mass of solids)

Effects of the Addition of Dihydrate Phosphogypsum on the Characterization and Mechanical Behavior of Lateritic Clay

M.M.A. Mascarenha, M.P. Cordão Neto, T.H.C. Matos, J.V.R. Chagas, L.R. Rezende

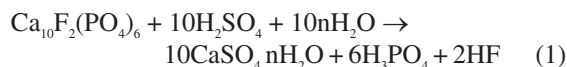
Abstract. This paper presents the effect of adding dihydrate phosphogypsum, which is a byproduct of the production of phosphate fertilizers, on the mechanical behaviour of a lateritic clay typical of Brazil's Midwest region. Because of the distinction of the mechanical behaviours of both materials, laboratory experiments were conducted with soil, phosphogypsum and mixtures with 10%, 20% and 50% phosphogypsum content. One-dimensional consolidation, direct shear and scanning electron microscopy (SEM) tests were conducted on optimally compacted specimens to show the effect of the loading time on the mechanical parameters of the materials. Water percolated through the materials was chemically analysed to verify the groundwater level contamination potential due to cation lixiviation in phosphogypsum. The results show that the addition of phosphogypsum to the soil increases the compressibility without significant effect on the strength parameters, and the broken phosphogypsum particles make the mixture deformability depend on the loading time. With this study, one can conclude that the dihydrate phosphogypsum content in geotechnical works must be maintained below 20%, since higher ratios negatively affect the soil mechanical behaviour and ground water contamination potential. This study also presents an option to reuse and dispose of the most commonly produced phosphogypsum type in Brazil.

Keywords: deformation, environment, grain breakage, loading time, reuse, strength parameters.

1. Introduction

The main output of the industries in Catalão, which is a city in the state of Goiás (GO), Brazil, is phosphate fertilizer with local phosphate rocks as the raw material. One of the production outputs is a solid industrial byproduct known as phosphogypsum. Its chemical composition is identical to natural gypsum ($\text{CaSO}_4 \cdot n\text{H}_2\text{O}$) except for impurities such as fluorides, phosphates, organic matter, aluminium and iron minerals, toxic heavy metals and radioactive elements.

According to Hull & Burnett (1996) and Lapido-Loureiro & Nascimento (2009), the chemical process to obtain phosphogypsum as a byproduct is as follows:



where $\text{Ca}_{10}\text{F}_2(\text{PO}_4)_6$ is fluorapatite, H_2SO_4 is sulfuric acid, H_2O is water, $\text{CaSO}_4 \cdot n\text{H}_2\text{O}$ is phosphogypsum, H_3PO_4 is phosphoric acid, and HF is hydrofluoric acid.

In Eq. 1, the coefficient n is related to the temperature during the process to obtain phosphoric acid, which can have the values of 0 (null) for anhydrous phosphogypsum (anhydrite), 1/2 for hemihydrate phosphogypsum (HH) and 2 for dihydrate phosphogypsum (DH). HH phosphogyp-

sum is also known as bassanite, and DH is known as gypsum. The dihydrate process is used by the industries in Catalão and is the most common process in Brazil. It has low production costs because of the low temperature required in the reaction between phosphatic rock and sulfuric acid. However, the phosphogypsum produced in this process has more impurities such as residual sulfuric acid, phosphoric acid and toxic heavy metals, which may contaminate the environment (Canut, 2006).

For every ton of phosphoric acid produced across the industries in Goiás, approximately five tons of dihydrate phosphogypsum are also produced, which amounts to 60 thousand tons of this byproduct monthly and requires large areas for storage (Chagas, 2014). According to the NBR 10004 (ABNT, 2004), this phosphogypsum is classified as Class II A: not dangerous and not inert (Mesquita, 2007).

According to Jacomino *et al.* (2009), when analysing dihydrate phosphogypsum collected from a phosphoric acid industry in the city of Uberaba (MG), Brazil, the concentrations of ^{226}Ra (251 Bq kg^{-1}) and ^{228}Ra (226 Bq kg^{-1}) in the phosphogypsum samples were greater than the limits advised by the 402-R-98-008 document published in 1988 by the Environmental Protection Agency. The concentrations of ^{210}Pb and ^{210}Po were similar to those obtained for

Márcia Maria dos Anjos Mascarenha, D.Sc., Associate Professor, Escola de Engenharia Civil e Ambiental, Universidade Federal de Goiás, Goiânia, GO, Brazil. e-mail: marciamascarenha@gmail.com.

Manoel Porfírio Cordão Neto, D.Sc., Associate Professor, Departamento de Engenharia Civil e Ambiental, Universidade de Brasília, Brasília, DF, Brazil. e-mail: mporfirio76@gmail.com.

Tubal Henrique Cândido de Matos, Auditor of CODEVASF, Brasília, DF, Brazil. e-mail: tubal.matos@gmail.com.

Juliana Verônica Ribeiro das Chagas, M.Sc., Engineer of Sete Engenharia, Goiânia, GO, Brazil. e-mail: juvribeiro@hotmail.com.

Lilian Ribeiro de Rezende, D.Sc., Associate Professor, Escola de Engenharia Civil e Ambiental, Universidade Federal de Goiás, Goiânia, GO, Brazil. e-mail: rezende.lilian@gmail.com.

Submitted on November 28, 2017; Final Acceptance on May 16, 2018; Discussion open until December 31, 2018.

DOI: 10.28927/SR.412157

^{226}Ra and ^{228}Ra , whereas the concentration of ^{238}U was less than that obtained for a local clay soil (latosol). The authors also noted that the concentrations of toxic heavy metals and metalloids were less than the limits established by Resolution 375 (2006) from the Brazilian National Environmental Council (CONAMA).

Thus, Campos *et al.* (2017) analysed the ^{226}Ra emission rate of eighteen samples of plates and fifteen samples of brick manufactured with phosphogypsum produced in the cities of Cajati (SP), Cubatão (SP) and Uberaba (MG). The authors concluded that the use of these building materials for house construction posed no health risk because of the exhalation of radon.

Mesquita (2007) showed results from radiometry evaluations conducted both in the industrial plant and in specimens produced in the laboratory with the Goiás dihydrate phosphogypsum. The average exposition rate obtained at the plant was $0.09 \mu\text{R/h}$ or $2.32 \times 10^{-8} \text{ C/kg/h}$, whereas in the specimens compacted in the laboratory, the rate was $0.00 \mu\text{R/h}$. Thus, there is no radioactive problem when this material is used in on-site pavement construction.

Many studies were conducted on the reuse of phosphogypsum in the cement industry (Altun & Sert 2004; Shen *et al.*, 2012), brick production (Yang *et al.*, 2009), concrete production (Smadi *et al.*, 1999), soil stabilization (Degirmenci *et al.*, 2007; James & Pandian, 2014), pavement layers (Parreira *et al.*, 2003; Oliveira, 2005; Mesquita, 2007; Rufo 2009; Metogo, 2011; Kumar *et al.*, 2014; Rezende *et al.*, 2016) and asphalt mixture (Cuadri *et al.*, 2014). Altun & Sert (2004) used weathered phosphogypsum. Yang *et al.* (2009), Smadi *et al.* (1999) and Rezende *et al.* (2016) used HH phosphogypsum. Degirmenci *et al.* (2007), Cuadri *et al.* (2014), James & Pandian (2014) and Kumar *et al.* (2014) did not specify the phosphogypsum type, and other studies used DH phosphogypsum. Generally, these studies proved the technical and environmental viability of reusing this byproduct in its different types.

The studies performed by Degirmenci *et al.* (2007), James & Pandian (2014), Mesquita (2007), Rufo (2009), Metogo (2011) and Rezende *et al.* (2016) discuss the behaviour changes that occur when phosphogypsum is mixed with soils because of the flocculation, carbonation, and cementing compound formation, such as ettringite and calcite, as mentioned by Ahmed (2015). These reactions depend on the phosphogypsum type, the soil type, the presence of a stabilizer and its type, and the contents of each material in the mixture.

In these studies, because of their intended use, the following mechanical tests were conducted: unconfined compression, California bearing ratio and dynamic triaxial. Mechanical tests (one-dimensional consolidation, direct shear, among others) that are frequently performed in geotechnical works (*e.g.*, landfills, embankments and dams) were not performed and published before. Thus, this ap-

proach is the advancement of this study in relation to other earlier studies.

In this context, the present study aims to evaluate the effect of adding dihydrate phosphogypsum on the mechanical behaviour of a lateritic clay, which broadens the possibilities of its use. In addition, water percolated through the materials, obtained from permeability tests, was chemically analysed to verify the water table contamination potential due to cation lixiviation in phosphogypsum.

2. Materials and Methods

This section describes the studied materials and the methods used to execute the laboratory tests.

2.1. Materials

The soil used in the laboratory tests was obtained from Aparecida de Goiânia, GO, Brazil; it was collected at 0.8-1.2 m depth in the lateritic residual layer. It is classified as a low-plasticity silt according to the Unified Soil Classification System and as lateritic clay according to the typical soil classification proposed by Nogami & Villibor (2009). According to Rezende *et al.* (2016), the mineralogical constitution of the soil is quartz, gibbsite, haematite and kaolinite. This soil was selected because of its use in an experimental roadway construction with the local soil and phosphogypsum.

The dihydrate phosphogypsum is classified as a low-plasticity silt according to the Unified Soil Classification System. According to Rezende *et al.* (2016), its main mineral is gypsum.

The mixtures analysed in this study were made with three phosphogypsum contents: Mixture A (10%), Mixture B (20%) and Mixture C (50%). Mixture A's content was set to evaluate the effect of the low phosphogypsum content on the soil behaviour. Mixture B was determined because it was used in the experimental roadway's construction assessed by Metogo (2011). Mixture C's content was set to be the most suitable to evaluate the effect of the high phosphogypsum content addition on the soil's mechanical properties. The amounts of soil and phosphogypsum in each mixture were calculated according to the dry mass, and these materials were mixed in a concrete mixer for 10 min to obtain homogeneous mixtures. The geotechnical characterization of these materials is presented in Table 1 and the grain size distribution curves are shown in Fig. 1.

Matos (2011) showed that in the grain size distribution carried out with dispersant, sand content of mixtures are higher than soil and phosphogypsum content. The phosphogypsum added to the soil changes its *pH* and causes a reaction among the soil, phosphogypsum and dispersant agent, which prevents the breakdown of particle aggregations. Similar phenomena were observed in the particle size analyses of the soil and phosphogypsum mixtures in Mesquita (2007), Rufo (2009) and Metogo (2011).

Table 1 - Geotechnical characterization of materials (modified from Matos, 2011).

Materials	w_L (%)	w_p (%)	PI (%)	γ_s (kN/m ³)	Classification	
					USCS	AASHTO
Soil	38	25	13	27.4	ML	A-6
Mixture A	36	24	12	27.0	ML	A-6
Mixture B	35	23	12	26.9	ML	A-4
Mixture C	30	-	NP	26.5	ML	A-4
Phosphogypsum	-	-	NP	25.5	ML	A-4

Materials	Grain size distribution							
	Without dispersant				With dispersant			
	% G	% S	% M	% C	% St	% S	% M	% C
Soil	0.2	87.4	11.1	1.3	0.2	34.4	22.9	42.6
Mixture A	0.1	75.9	23.6	0.4	0.0	60.3	31.7	8.0
Mixture B	0.1	60.9	38.2	0.8	0.1	58.9	37.0	4.0
Mixture C	0.1	45.9	53.2	0.8	0.1	36.8	59.5	3.6
Phosphogypsum	0.0	16.6	81.7	1.7	0.0	16.5	78.3	5.2

Note: w_L = liquid limit; w_p = plastic limit; PI = plasticity index; γ_s = specific gravity of grains; USCS = Unified Soil Classification System; AASHTO = American Association of Highway and Transportation Officials; G = gravel; S = sand; M = silt; C = clay.

The chemical composition of the studied mixtures is shown in Table 2 and was obtained from the initial studies of Matos (2011). The incorporation of phosphogypsum into the soil increases the cation exchange capacity (CEC) and reduces the pH . The low pH value for phosphogypsum corroborates the acidic characteristics, which were obtained by Ghafoori & Chang (1993), Rabelo *et al.* (2001) and Parreira *et al.* (2003).

Figure 2a shows SEM images of the phosphogypsum. The SEM images of the optimally compacted mixtures, which were obtained by Matos (2011) using Zeiss' SteREO Discovery V20 with digital image capture, are presented in Figs. 2b, 2c and 2d. The studied phosphogypsum particles clearly exhibit plates with tabular format and large dimen-

Table 2 - Chemical analysis of the materials (modified from Matos, 2011).

Sortive complex	Phosphogypsum content (%)				
	0	10	20	50	100
pH in H ₂ O	5.4	5.4	5.3	4.9	35
P (meq/100 mL)	0.10	53.4	180.0	554.0	888.0
Ca (meq /100 mL)	2.50	64.9	55.1	66.2	69.9
Mg (meq /100 mL)	0.20	0.20	0.20	0.20	0.20
K (meq /100 mL)	0.10	0.06	0.06	0.08	0.06
Na (meq /100 mL)	0.02	0.39	0.40	0.49	0.31
Al (meq /100 mL)	0.10	0.40	0.70	0.90	1.30
CEC (meq /100 mL)	9.0	69.0	59.0	69.0	73.0
C (g/kg)	2.5	5.3	0.9	2.9	1.5
MO (g/kg)	4.3	9.1	1.5	5.0	2.6
B	0.4	0.6	0.8	0.6	0.4
Cu	0.9	0.9	0.7	0.8	0.5
Fe	22.0	27.9	30.8	31.8	89.8
Mn	31.3	23.0	19.7	13.7	4.5
Zn	2.0	3.4	5.8	3.2	9.8
S	139	186.0	160.0	154.0	145.0
As	< 0.01	< 0.01	< 0.01	< 0.01	< 0.01

Note: pH = hydrogen potential; meq = milliequivalents; mL = milliliter; P =phosphor; Ca = calcium; Mg = magnesium; K = potassium; Na = sodium; Al = aluminium; CEC = cation exchange capacity ; C = carbon; MO = organic matter; B = barium; Cu = copper ; Fe = iron; Mn = manganese ; Zn = zinc; S = sulfur; As = arsenic.

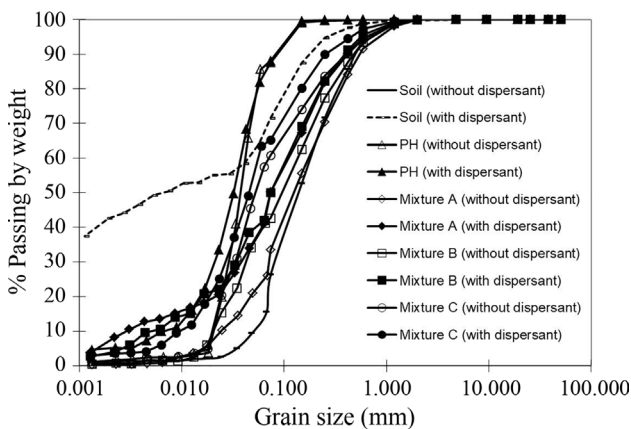


Figure 1 - Grain size distribution curves (modified from Matos, 2011).

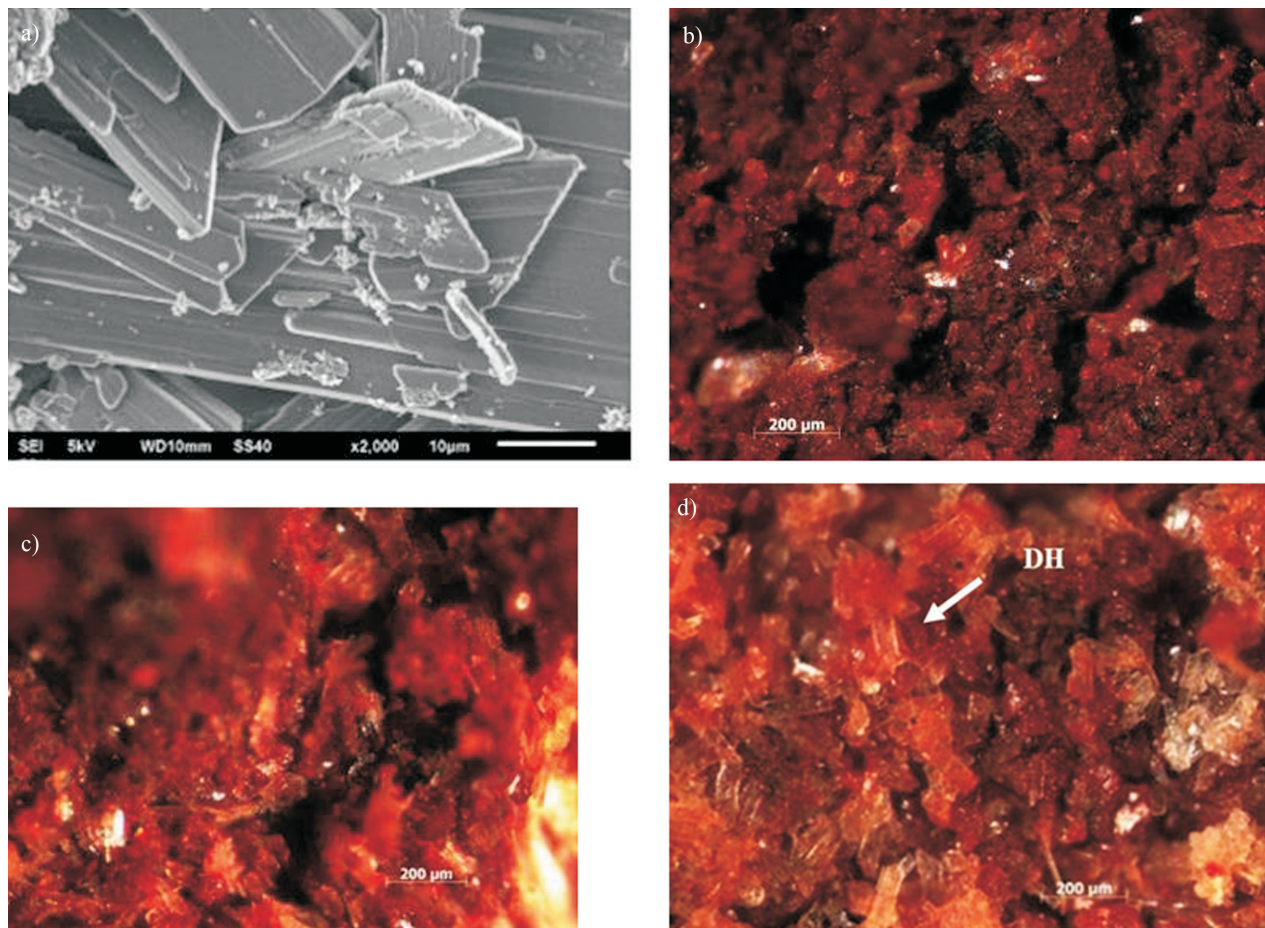


Figure 2 - Microphotographs of compacted samples: (a) Phosphogypsum (Alves, 2015); (b) Mixture A (Matos, 2011); (c) Mixture B (Matos, 2011); (d) Mixture C (Matos, 2011).

sions (Fig. 2a), which is typical of dihydrate phosphogypsum, as ascertained by Yang *et al.* (2009), Roy *et al.* (1996), Rutherford *et al.* (1993), Shen *et al.* (2012) and Alves (2015). There are small amounts of phosphogypsum crystals in Mixture A (Fig. 2b). When the content increases to 20% (Mixture B), more concentrated phosphogypsum crystals are observed, and phosphogypsum grains do not interact with the soil (Fig. 2c). The microscopy of Mixture C, which was obtained by Matos (2011), exhibits identical characteristics to Mixture B with a higher phosphogypsum crystal content (Fig. 2d).

The specimens for the mechanical tests of this study were molded from the compacted samples at optimal moisture content (w_{opt}) and maximal dry density ($\gamma_{dm\acute{a}x}$) using Proctor compaction test, as presented by Matos *et al.* (2012). These values are presented in Table 3. The phosphogypsum addition reduces the maximal dry density and increases the optimal water content. According to Sivapullaiah *et al.* (1998) *apud* Lovato (2004), the reason is the occurrence of flocculation, which is caused by the replacement of monovalent ions from soil by calcium, which creates a more porous structure and more water absorption.

2.2. Methods

One-dimensional consolidation tests were performed in a saturated condition according to NBR 12007 (ABNT, 1990) to understand the effect of phosphogypsum addition on the deformability parameters of the soil. The tests were made with pressures of 13.5 kPa, 32 kPa, 50 kPa, 100 kPa, 200 kPa, 400 kPa, 800 kPa and 1000 kPa in 48 h.

To verify the deformability of phosphogypsum over time, consolidation tests were performed in saturated conditions in the soil, Mixture A and phosphogypsum with three different loading conditions: 48 h stages to 800 kPa stress and direct loading to 800 kPa stress, which was maintained constant for 7 and 15 days.

After the saturated consolidation tests, which were conducted for loading times from 48 h to 15 days, the phosphogypsum samples were analysed using scanning electron microscopy (SEM) tests in the Multiuser Laboratory of High Definition Microscopy (LabMic) of the Federal University of Goias (UFG). The test aimed to verify the changes that the loading time induced on the structural matrix of the material. It was not possible to perform the SEM test with compacted phosphogypsum and phosphogypsum

after 7 days of consolidation because the samples suffered defragmentation during the metallization process.

Grain size tests were also performed according to NBR 7181 (ABNT, 2016) on phosphogypsum samples prior to compaction, after compaction and after submission to 800 kPa compression stress for 15 days. This test aimed to verify the occurrence of phosphogypsum particle fracture.

To understand the effect of the phosphogypsum addition on the soil, direct shear tests were performed according to D3080 - 04 (ASTM, 2004). The shear tests were of the consolidated and drained type (CD). To determine the Mohr-Coulomb failure envelope, the tests were conducted with four levels of normal stress: 50 kPa, 100 kPa, 200 kPa and 400 kPa. The consolidation time for each stress level was 37 h. To analyse how the specimen consolidation time can affect the strength parameters, direct shear tests with consolidation time of 12.5 h were also conducted on Mixture C.

To verify the ground water contamination potential caused by cation lixiviation in phosphogypsum in geotechnical constructions, water percolated through the soil samples, phosphogypsum and mixtures under hydraulic gradients of 2 and 10 was chemically analysed. For metals and boron, the chemical analyses were performed using MP AS 4200 with procedures described by SMEWW 3120 (APHA, 1992). The amount of water percolated through the soil and Mixture A under a hydraulic gradient of 2 was insufficient to perform the chemical analysis. The water samples were kept below 0 °C to eliminate any biological activity that could occur. The pure water in the test was collected and chemically analysed.

Table 3 - Summary of the compaction test results (modified from Matos *et al.*, 2012).

Materials	w_{opt} (%)	γ_{dmax} (kN/m ³)
Soil	22.7	15.40
Mixture A	22.7	15.30
Mixture B	22.9	15.10
Mixture C	24.0	13.70
Phosphogypsum	28.0	12.10

Note: w_{opt} = optimum water content; γ_{dmax} = dry maximum density.

3. Results and Discussion

This section presents and analyses the results of the conducted laboratory tests, which studied the deformability and shear strength of the lateritic clay, phosphogypsum and mixtures, considering the effect of the phosphogypsum content and loading time.

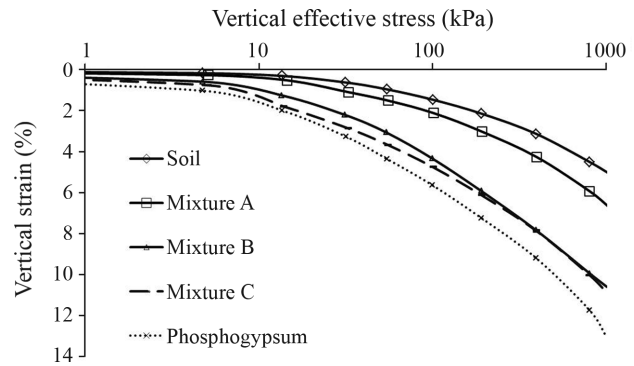


Figure 3 - Compression curves of materials (modified from Matos *et al.*, 2012).

3.1. Materials deformation

The deformation curves of the materials are presented in Fig. 3. It is verified that samples with 20% (Mixture B), 50% (Mixture C) and 100% phosphogypsum content have similar behaviour and can be explained by the SEM images in Fig. 2. The phosphogypsum grains do not interact with soil in the mixture with 20% phosphogypsum content (Fig. 2b), so the material has a greater effect on the deformability of the mixture.

Considering the 200 kPa stress, which is commonly used in earthworks, and the 1000 kPa stress, which is the maximum stress applied in the tests, phosphogypsum has less volumetric deformation than the recycled asphalt shingles (RAS), whose volumetric deformations were 17.5-30% for the stress of 200 kPa and 1000 kPa, according to Soleimanbeigi *et al.* (2013). By stabilizing the RAS with a fly ash (FA) content of 50%, the deformability of this mixture (RAS; FA) reduced to 2% and 5% for 200 kPa and 1000 kPa, respectively. These results are similar to values obtained for Mixture A and lateritic clay and presented in this study. RAS and FA are classified as well graduated sand and poorly graduated sand according to the Unified Soil Classification System (USCS).

Under 200 kPa stress, volumetric deformations as low as 5% were obtained for many recycled materials studied by Soleimanbeigi & Tuncer (2015), such as recycled concrete aggregate, bottom ash, foundry slag, foundry sand and recycled pavement material, which are classified by SUCS as well graduated gravel, poorly graduated sand, well graduated sand, sandy loam and gravel, respectively. This range of deformation was also assessed by Kim *et al.* (2005) for fly ash (0, 25, 50 and 100%) and bottom ash mixtures, which are classified as low-compressibility silt or silty sand. The recycled asphalt pavement (RAP), which is classified as poorly graduated sand and was studied by Soleimanbeigi & Tuncer (2015), had similar volumetric deformation values to the soil in this study.

Figure 4 presents the variation of the deformability parameters according to the phosphogypsum content,

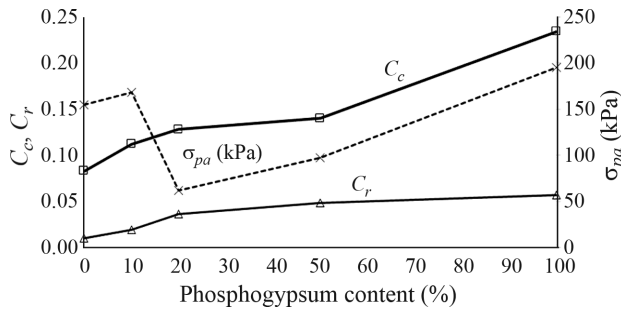


Figure 4 - Relationship between compressibility parameters and phosphogypsum content.

where σ_{pa} is the pre-consolidation stress, C_c is the compression index, and C_r is the recompression index. Increasing the phosphogypsum content also increases C_c and C_r . With the suggested C_c values and soil compressibility classification by Coduto (1999) *apud* Soleimanbeigi *et al.* (2013), the soil in this study is slightly compressible, phosphogypsum is notably compressible, and the mixtures are moderately compressible. The values found for phosphogypsum and mixtures are greater than the values observed for RAS (0.07) by Soleimanbeigi *et al.* (2013).

There is no logical relation between the reduction in pre-consolidation stress and the increase in phosphogypsum content. The obtained values are greater than the value of RAS, which is approximately 60 kPa according to Soleimanbeigi *et al.* (2013).

To evaluate the effect of the loading time on soil deformation, the soil compression curves for Mixture A and phosphogypsum samples submitted to different loading times are presented in Fig. 5. The deformation increases because the loading time changed from 48 h to 15 days and was 1.54%, 0.68% and 3.64% for soil, Mixture A, and phosphogypsum, respectively. The loading time has a greater effect on soil than on Mixture A.

Figure 6 presents the deformations of soil, Mixture A and phosphogypsum through time when the samples were loaded with 800 kPa stress regardless of previous deformations. In the 48 h tests, the stress was applied in stages; in this case, when 800 kPa stress was applied, the material had deformed because of previous stress, whereas in the 7- and 15-day tests, the 800 kPa stress was directly applied. Therefore, there are differences in the initial deformations in both situations, which were more notable for phosphogypsum.

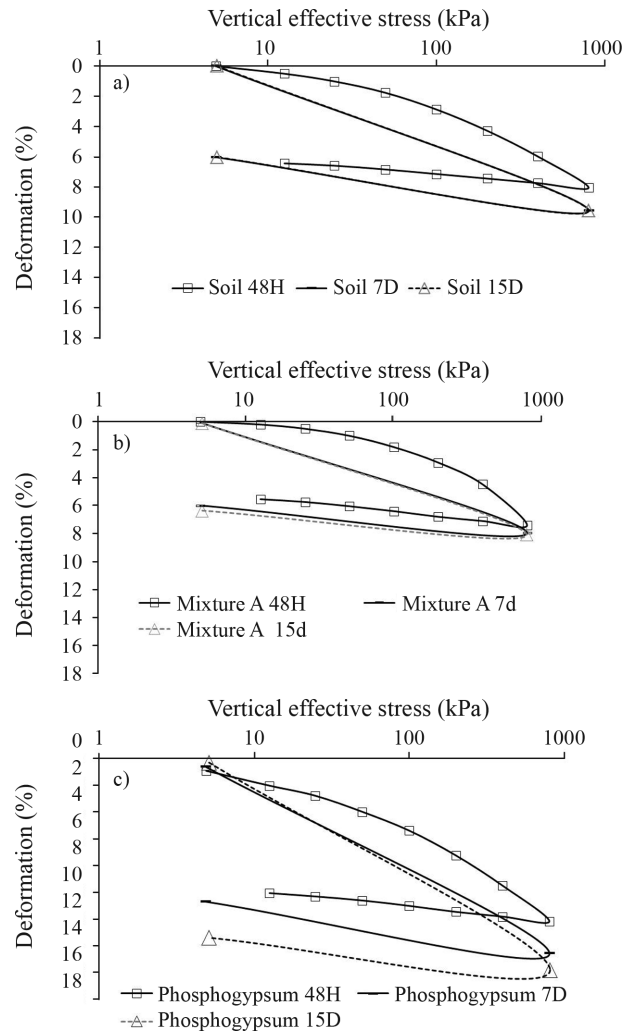


Figure 5 - Compression curves for different loading times: (a) Soil; (b) Mixture A; (c) Phosphogypsum DH (modified from Chagas *et al.*, 2014).

It is verified that there is no stabilization trend for the phosphogypsum and Mixture A samples; after 500 min, there is a variation in inclination of the curve and an increase in deformation rate because of secondary consolidation, which is more notable with phosphogypsum. The secondary consolidation does not depend on the increase in effective stress and is characterized by the deformations of the material structure.

Table 4 - Phosphogypsum grain size distribution before and after compaction and after the compression test.

Type	Grain size (mm)	PG before compaction (%)	PG after compaction (%)	PG after compression (%)
Sand	0.6 a 0.2	54.34	41.28	31.31
Silt	0.002 a 0.06	41.17	56.87	64.33
Clay	< 0.002 mm	4.49	1.85	4.35

Note: PG = phosphogypsum.

The non-stabilization of the deformations over time was also ascertained by: 1) Soleimanbeigi & Tuncer (2015) by analysing the recycled asphalt pavement (RAP) and its mixtures with glacial outwash sand (GOS) and fly ash (FA) when the samples were submitted to 100 kPa effective stress for 20 days; 2) Soleimanbeigi *et al.* (2013) by analysing the recycled asphalt shingles (RAS) and its mixtures with fly ash (FA) when the samples were submitted to the effective stress of 100 kPa for 150 days.

To verify whether the non-stabilization of the deformations is related to phosphogypsum grain breakage, which is favoured by the grain tabular format (Fig. 2c), grain size distribution analyses were made with phosphogypsum prior to compaction, after compaction and after submission to 800 kPa load during 15 days. The observed clay, silt and sand percentages in phosphogypsum under these conditions are shown in Table 4.

Compaction and consolidation break the sand-sized grains and reduce them to silt-sized grains. There was a 13% and 10% increase of fines due to compaction and compression, respectively. Soleimanbeigi & Tuncer (2015) observed this behaviour for foundry slag: the fines ratio increased from 3% to 6% after compaction and 11% after consolidation (under 200 kPa load during 24 h).

The SEM images verify the occurrence of phosphogypsum grain breakage. Figures 7 and 8 show SEM images of phosphogypsum after consolidation in 48 h and 15 days, respectively. These figures show the grain breakage evolution relative to the loading time.

Because of the non-stabilization of phosphogypsum deformations over time, which results from grain breakage, the consolidation time is a primordial factor when one analyses the settlements that may occur in mixtures of soil and phosphogypsum.

3.2. Shear strength

The strength parameters of the studied materials (effective friction angle and effective cohesion) were obtained using shear tests at 50 kPa, 100 kPa, 200 kPa and 400 kPa normal stress and are presented in Table 5. The values were

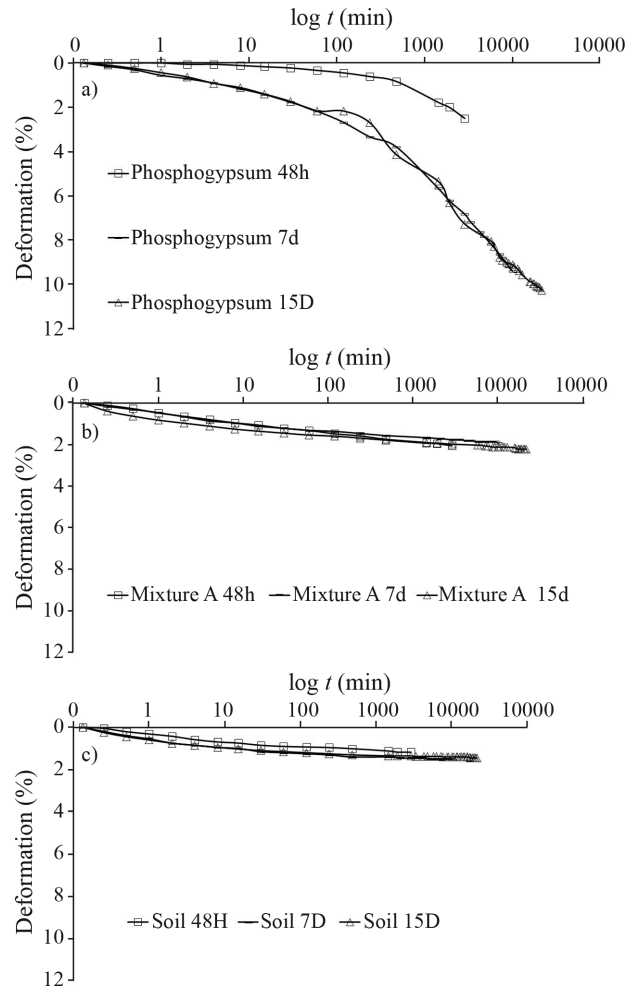


Figure 6 - Time-deformation curves for different loading times: (a) Soil; (b) Mixture A; (c) Phosphogypsum DH (modified from Chagas *et al.*, 2014).

obtained with Mohr-Coulomb failure criterion considering the maximum strength and residual strength.

Small changes of the maximum and residual strengths of each mixture were observed as opposed to the observation of Haeri *et al.* (2005), who obtained different failure modes when using maximum or residual strength, where

Table 5 - Shear strength parameters (modified from Matos *et al.*, 2012).

Material	Maximum shear strength		Residual shear strength	
	ϕ' (°)	c' (kPa)	ϕ' (°)	c' (kPa)
Soil	38	37.5	40	11.0
Mixture A	38	14.0	39	4.2
Mixture B	38	9.1	39	4.9
Mixture C	41	2.1	41	0.1
Phosphogypsum	40	1.0	40	1.7

Note: ϕ' = effective friction angle; c' = effective cohesion intercept.

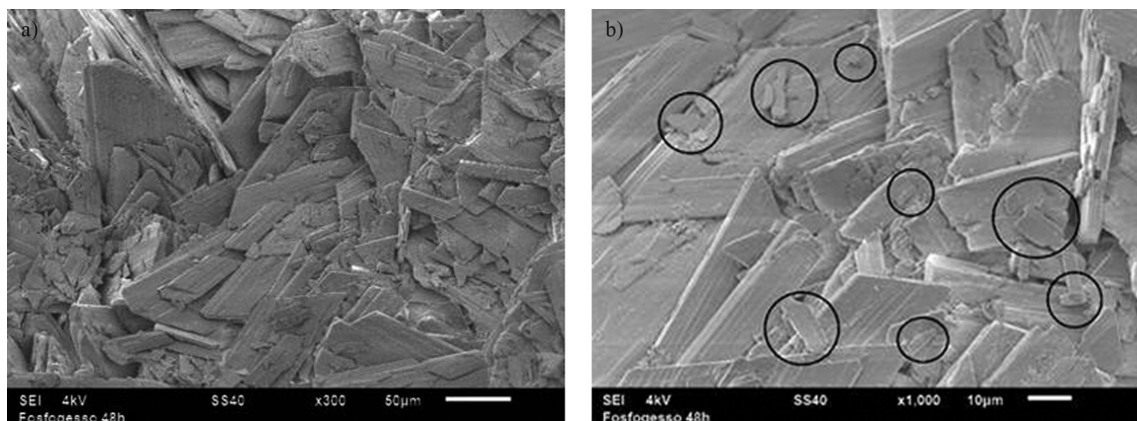


Figure 7 - SEM images of phosphogypsum after 48 h of consolidation (a) 300x; (b) 1000x (Chagas, 2014). Note: broken particles are outlined.

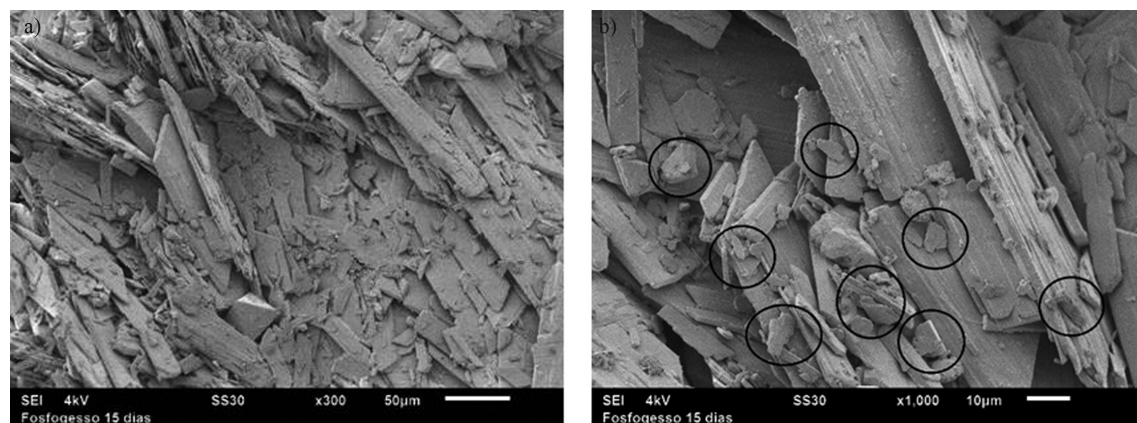


Figure 8 - SEM images of phosphogypsum after 15 days of consolidation (a) 300x; (b) 1000x (Chagas, 2014). Note: broken particles are outlined.

the differences increase with more stabilizer (gypsum plaster).

Vakili *et al.* (2016) performed direct shear tests drained in kaolinitic clay ($c' = 12.5$ kPa and $\phi' = 19.9^\circ$) and mixtures of sodium silicate, ground granulated blast fur-

nace slag (composed of gypsum and bassanite) and cement. In these mixtures, the cement content was maintained constant (2%), the sodium silicate contents were 1%, 1.5% and 2.5%, and the slag contents were 3%, 4% and 5%; the curing times were 7, 14 and 28 days. In this study, increasing

Table 6 - Shear strength parameters of cemented gravelly sand and recycled asphalt shingles.

Author	Materials	% Stabilizer									
		Gypsum plaster									
Haeri <i>et al.</i> (2005)	Cemented gravelly sand	0		1.5		3.0		4.5		6.0	
		c' (kPa)	ϕ' ($^\circ$)	c' (kPa)	ϕ' ($^\circ$)	c' (kPa)	ϕ' ($^\circ$)	c' (kPa)	ϕ' ($^\circ$)	c' (kPa)	ϕ' ($^\circ$)
		25	36	136	39	167	40	229	41	296	42
Soleiman-beigi1 <i>et al.</i> (2013)	Recycled asphalt shingles	Fly ash									
		0		10		20		-	-	-	-
		c' (kPa)	ϕ' ($^\circ$)	c' (kPa)	ϕ' ($^\circ$)	c' (kPa)	ϕ' ($^\circ$)	-	-	-	-
		0	36	42	31	102	30	-	-	-	-

Note: ϕ' = effective friction angle; c' = effective cohesion intercept.

Table 7 - Shear strength parameters of the recycled materials researched by Soleimanbeigi & Tuncer (2015).

Materials	RAP	RCA	RPM	FSD	BA	FSG
c' (kPa)	12	0	2	15	0	0
ϕ' (°)	42	46	44	37	44	36

Note: RAP = recycled asphalt pavement; RCA = recycled concrete aggregate; RPM = recycled pavement material; FSD = foundry sand; BA = bottom ash; FSG = foundry slag; c' = effective cohesion intercept; ϕ' = effective friction angle.

slag also increased the cohesion and soil friction angle, possibly because of the presence of cement, low shear strength of soil, presence of bassanite in the slag and effect of the curing time. The best parameters ($c' = 60$ kPa and $\phi' = 44^\circ$) were found in the mixture with 1% sodium silicate, 2% cement and 5% slag after 28 days of curing.

Table 6 shows the strength parameters of a well graduated silty sand stabilized with gypsum plaster contents of 1.5%, 3.0%, 4.5% and 6.0%, as presented by Haeri *et al.* (2005) and obtained using triaxial undrained tests in saturated conditions. Table 6 also shows the strength parameters for recycled asphalt shingles stabilized with 10% and 20% fly ash, which were obtained using triaxial drained tests in saturated condition performed by Soleimanbeigi *et al.* (2013). The shear strength parameters of the recycled materials researched by Soleimanbiegil & Tuncer (2015) are summarized in Table 7.

The effective friction angles for all recycled materials (including phosphogypsum) are 31-45°, which are typical of compacted sandy soils according to Soleimanbeigi & Tuncer (2015) and are considered sufficient to provide stability for typical highway embankments. Similarly, Kim *et al.* (2005) observed a friction angle range of 28-48° (depending on the origin and content of each material) using triaxial drained tests for mixtures of fly ash and bottom ash.

As expected, like phosphogypsum, the recycled materials researched by Soleimanbeigi & Tuncer (2015), recycled asphalt shingles and cemented gravely sand, have low cohesion values, since the materials are granular. In this case, adding fly ash to recycled asphalt shingles increases the cohesion value possibly because of a better particle interaction.

Table 8 - Shear strength parameters of Mixture C for different sample consolidation times.

Material	Consolidation time (h)	Maximum shear strength		Residual shear strength	
		ϕ' (°)	c' (kPa)	ϕ' (°)	c' (kPa)
Mixture C	37.0	41	2.1	41	0.1
	12.5	33	24.0	34	7.0

Note: ϕ' = effective friction angle; c' = effective cohesion intercept.

As verified in Table 5, phosphogypsum has a subtle effect on the friction variation between the sample particles because the addition or removal of 50% phosphogypsum grains in mass causes a maximum variation of 3° in the friction angle. However, adding phosphogypsum to the studied soil can significantly decrease its cohesion. This behaviour is related to the silt contents in the samples, as verified in Fig. 9, because soils mostly constituted by this particle size fraction have low cohesion.

The strength parameters of Mixture C, which was consolidated for 12.5 h and 37 h, are presented in Table 8, to analyse the effect of the consolidation time on the materials' strength. The increase in consolidation time varied the maximum and residual effective friction angles by 8° and 7°, respectively. One reason for this behaviour is the occur-

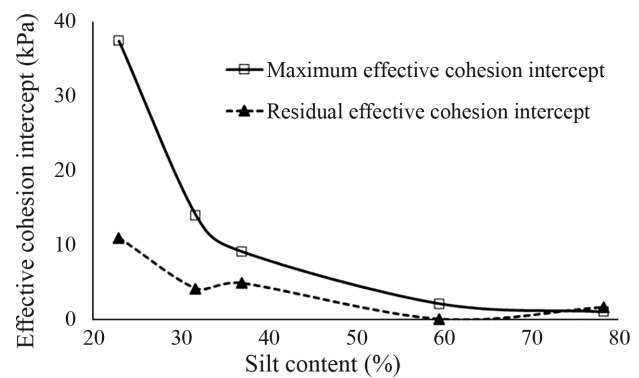


Figure 9 - Relationship between effective cohesion intercept and silt content (modified from Matos, 2011).

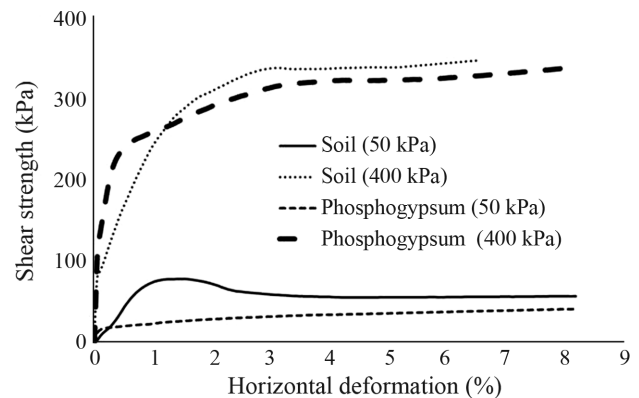


Figure 10 - Shear strength and horizontal deformation curves of soil and phosphogypsum (modified from Matos *et al.*, 2012).

rence of void closures because of grain breakage (verified in Table 4 and Figs. 7 and 8) and the consequent interlacing of phosphogypsum crystals.

Figure 10 shows the soil and phosphogypsum shear curves in the saturated condition under 50 kPa and 400 kPa normal stress. It is verified that the soil has peak strength, which is typical of pre-consolidated soils and coherent with the pre-consolidation stress in Fig. 4. Phosphogypsum behaved as a normally consolidated material, which is inconsistent with its pre-consolidation stress values (Fig. 4) because of the phosphogypsum plate breakage in this case.

When the loading stress increases, the residual stress curves of soil and phosphogypsum approach each other because the phosphogypsum plates break under high confining stress. This failure promotes an interlacing among the phosphogypsum grains and demands a great energy for overcoming the friction created among these particles. However, this question must be better addressed using microscopy tests.

3.3. Potential for groundwater contamination

The chemical analysis results of the water samples percolated through the specimen with hydraulic gradients of 10 and 2 are shown in Tables 9 and 10, respectively. Resolution 396 (CONAMA, 2008) was used to interpret the results because it provides the classification and environmental guidelines for the composition of groundwaters. The boldfaced values in Tables 9 and 10 indicate the concentrations of chemical elements in the percolated water that exceeded the maximum value allowed by the referred resolution.

The cadmium, copper and lead concentrations are above the reference values, but the water in the Geotechnical Laboratory of the University of Brasília had these concentrations above the allowed limit. The manganese concentration is above the limit established by the referred regulation, including soil. Only iron does not exhibit surpassing values in soil, but they exceed the allowed limit in Mixtures B, C and phosphogypsum.

Mixture A did not present metals with higher concentrations than the permitted values by Resolution 396 (CONAMA, 2008) beyond the original content in water and soil. Instead, the presence of phosphogypsum diminished the cadmium and copper concentrations in water and maintained an almost constant lead concentration. However, tests with water percolated under hydraulic gradient 2 were not performed for this mixture. Therefore, we suggest performing these tests with the samples submitted to clear water percolation under hydraulic gradient 2 for a more definitive conclusion of the environmental viability of this material.

4. Conclusions

In this paper, the mechanical behaviour of soil and phosphogypsum mixtures was analysed using one-dimen-

Table 9 - Chemical analysis results of percolated water in the permeability tests: hydraulic gradient = 10 (modified from Matos, 2011).

Chemical element	Water Caesb	Soil	Mix. A	Mix. B	Mix. C	Phosph.	Maximum value allowed (VMP) - CONAMA n° 396			
							Cons. human	Cons. animals	Irriga-tion	Recrea-tion
Arsenic	< 0.01	< 0.01	< 0.01	< 0.01	< 0.01	< 0.01	0.01	0.2	-	0.05
Cadmium	3.8	0.9	0.4	< 0.01	4.6	< 0.01	0.005	0.05	0.01	0.005
Lead	2.3	1.8	2.5	2.3	3.1	3.1	0.01	0.1	5	0.05
Copper	0.6	0.4	0.2	0.3	0.1	0.5	2	0.5	0.2	1
Nickel	< 0.01	< 0.01	< 0.01	< 0.01	< 0.01	< 0.01	0.02	1	0.2	0.1
Iron	< 0.01	< 0.01	< 0.01	1.6	0.8	0.2	0.3	-	5	0.3
Manganese	< 0.01	0.5	4.3	4.1	10.1	3	0.1	0.05	0.2	0.1
Zinc	0.7	0.1	0.3	< 0.01	1.9	1.8	5	24	2	5
Barium	< 0.01	< 0.01	< 0.01	< 0.01	0.2	0.1	0.7	-	-	1
Silver	< 0.01	< 0.01	< 0.01	< 0.01	< 0.01	< 0.01	0.1	-	-	0.05
Boron	0.01	0.07	0.17	0.01	0.06	0.13	0.5	5	0.5	1

Note: Unit: mg/L; Caesb = Environmental Sanitation Company of the Federal District; CONAMA = Brazilian National Council for the Environment.

Table 10 - Chemical analysis results of percolated water in the permeability tests: hydraulic gradient = 2 (modified from Matos, 2011).

Chemical element	Water Caesb	Mix. B	Mix. C	Phosph.	Maximum value allowed (VMP) - Conama n° 396			
					Cons. human	Cons. animals	Irrigation	Recreation
Arsenic	<0.01	<0.01	<0.01	<0.01	0.01	0.2	-	0.05
Cadmium	3.8	2.2	2.1	5.4	0.005	0.05	0.01	0.005
Lead	2.3	2.4	2.3	2.3	0.01	0.1	5	0.05
Copper	0.6	0.3	0.5	2.0	2	0.5	0.2	1
Nickel	<0.01	<0.01	<0.01	0.7	0.02	1	0.2	0.1
Iron	<0.01	<0.01	1.2	0.6	0.3	-	5	0.3
Manganese	<0.01	3.1	3.7	9	0.1	0.05	0.2	0.1
Zinc	0.7	<0.01	0.6	16.3	5	24	2	5
Barium	<0.01	0.4	<0.01	0.5	0.7	-	-	1
Silver	<0.01	<0.01	<0.01	<0.01	0.1	-	-	0.05
Boron	0.01	0.21	0.4	0.23	0.5	5	0.5	1

Note: Unit: mg/L; Caesb = Environmental Sanitation Company of the Federal District; Conama = Brazilian National Council for the Environment.

sional consolidation and direct shear tests, highlighting the effect of the loading time, which changes the material structure by grain breakage. In addition, water percolated through the materials was chemically analysed to verify the water table contamination potential. From the results, we conclude that:

The dihydrate phosphogypsum content in the mixtures affects the mechanical behaviour of the soil because the tabular crystal shape of this byproduct interferes in the interactions between the grains and facilitates its breakage. The SEM images show that starting at 20% phosphogypsum content, the phosphogypsum particles are not involved by soil grains. Therefore, the mechanical behaviour of mixtures with phosphogypsum content above 20% is affected by phosphogypsum. In other words, there is a critical content of dihydrate phosphogypsum for use in geotechnical constructions.

The breakage of phosphogypsum particles was verified by a granulometric analysis of *in natura* material after compaction and after consolidation using scanning electron microscopy. The consolidation was under 800 kPa load, which was applied during different loading times (48 h and 15 days).

The breakage of phosphogypsum particles affects the deformability of the mixtures. Thus, the compressibility parameters are generally superior to the values in the literature for residue stabilized soils, and the pre-consolidation values cannot be obtained using standard methods because the particles are not incompressible. In addition, the deformations depend on the loading time. These behaviours are more noticeable above 20% phosphogypsum content.

The volumetric deformation due to only secondary consolidation must be considered when one analyses the use of phosphogypsum or soil and phosphogypsum mixtures in geotechnical conditions. The 800 kPa stress is high and not commonly observed in geotechnical works.

The friction angle values of the mixtures are typical of compacted sandy soils and exhibit subtle alterations with the variation in phosphogypsum content and their method of determination (if the maximum or residual strength is used). The cohesion values decrease with the increase in phosphogypsum content because of the increase in silt content.

The effect of phosphogypsum plate breakage is verified in the change of the stress-deformation curves, which present a typical behaviour of normally consolidated soil in phosphogypsum, and in the approach of the residual curves of soil and phosphogypsum for elevated loading stress.

In the water samples percolated through the specimen, the cadmium, copper, lead and manganese elements showed higher values than the permitted value according to Resolution 396 (CONAMA, 2008). Moreover, water (for the first four elements) and soil (for manganese) already presented these inadequate concentrations, whereas iron presented values above the established value by the re-

ferred Resolution for the mixtures with at least 20% dihydrate phosphogypsum content. Thus, a phosphogypsum content of 20% or more is not recommended in geotechnical works where the mixtures are submitted to water flow because of the risk of contaminating the groundwater.

The mixture with the best mechanical behaviour is Mixture A with 10% of phosphogypsum content, due to the entanglement between soil grains and phosphogypsum plates and the low content of added phosphogypsum, which does not negatively interfere with the behaviour of this material. Nevertheless, in this mixture, there is no significant improvement of the mechanical behaviour compared to soil.

Although the use of 10% of phosphogypsum doesn't improve the soil mechanical behaviour, it is important to highlight that these study results can indicate one important way to encourage the reuse of this by-product and minimize environmental problems.

Furthermore, the research group has been continuing this study scope to find other ways to make feasible the use of a higher phosphogypsum content, such as the thermal treatment technique to transform the dihydrate in the hemihydrate phosphogypsum.

Acknowledgments

The authors thank CAPES, CNPq, CMOIC International Brasil and FAPEG for the financial support for the study and LabMic/UFG for performing the mineralogical tests.

References

- ABNT (1990). Solo - Ensaio de Adensamento Unidimensional. NBR - 12007, Rio de Janeiro, Brasil, 15 p.
- ABNT (2004). Resíduos Sólidos - Classificação. NBR - 10004, Rio de Janeiro, Brasil, 71 p.
- ABNT (2016). Análise Granulométrica. NBR - 7181, Rio de Janeiro, Brasil, 13 p.
- Ahmed, A. (2015). Compressive strength and microstructure of soft clay soil stabilized with recycled bassanite. *Applied Clay Science*, 104:27-35.
- Altun, I.A. & Sert, Y. (2004). Utilization of weathered phosphogypsum as set retarder in Portland cement. *Cement and Concrete Research*, 34:677-680.
- Alves, K.C.S.K. (2015). Efeito do Tratamento Térmico no comportamento Comportamento Ambiental e Hidromecânico de Misturas Solo, Fosfogesso e Cimento. Dissertação de Mestrado. Departamento de Engenharia Civil e Ambiental, Universidade Federal de Goiás, Goiânia, 122 p.
- ASTM (2004). Standard Test Method for Direct Shear Test of Soils under Consolidated Drained Conditions - D 3080, ASTM International, West Conshohocken., Philadelphia, USA, 9 p.
- APHA (1992). Standard Methods for the Examination of Water and Wastewater - SMEWW 3120, Washington, USA, 6 p.
- Campos, M.P.; Costa, L.J.P.; Nisti, M.B & Mazzilli, B.P. (2017). Phosphogypsum recycling in the building materials industry: assessment of the radon exhalation rate. *Journal of Environmental Radioactivity*, 172:232-236.
- Canut, M.M.C. (2006). Estudo da Viabilidade do Uso do Resíduo Fosfogesso como Material de Construção. Dissertação de Mestrado. Departamento de Construção Civil, Universidade Federal de Minas Gerais, Belo Horizonte, 154 p.
- Chagas, J.V.R. (2014). Análise da Deformabilidade do Fosfogesso. Dissertação de Mestrado, Departamento de Engenharia Civil e Ambiental, Universidade Federal de Goiás, Goiânia, 130 p.
- Chagas, J.V.R.; Mascarenha, M.M.A. & Cordão Neto, M.P. (2014). Análise da deformabilidade do fosfogesso Anais XVII Congresso Brasileiro de Mecânica dos Solos e Engenharia Geotécnica, COBRAMSEG, Goiânia, Brasil, v. 1. pp. 1-8.
- CONAMA (2008). Resolução n° 396 de 3 de abril de 2008 Publicada no DOU n° 66, de 7 de abril de 2008, Seção 1, pp. 64-68.
- Cuadri, A.A.; Navarro, F.J.; García-Morales, M. & Bolívar, J.P. (2014). Valorization of phosphogypsum waste as asphaltic bitumen modifier. *Journal of Hazardous Materials*, 279:11-16.
- Degirmenci, N.; Okucu, A. & Turabi, A. (2007). Application of phosphogypsum in soil stabilization. *Building and Environment*, 42:3393-3398.
- Ghafoori, N.; & Chang, W.F. (1993). Investigation of phosphate mining waste for construction materials. *Journal of Materials in Civil Engineering*, 5(2):249-264.
- Haeri, S.M; Hamidi, A. & Tabatabaee, N. (2005). The effect of gypsum cementation on the mechanical behavior of gravely sands. *Geotechnical Testing Journal*, 28(4):1-11.
- Hull, C.D. & Burnett, W.C. (1996). Radiochemistry of Florida phosphogypsum. *J. Environ Radioactivity*, 32(3):213-238.
- Jacomino, V.M.F.;Oliveira, K.A.P.; Taddei, M.H.T.; Siqueira, M.C.; Carneiro, M.E.D.P.; Nascimento, M.R.L.; Silva, D.F. & Mello, J.W.V. (2009). Radionuclides and heavy metal contents in phosphogypsum in comparison to cerrado soils. *R. Ci. Solos*, 33:1481-1488.
- James, J. & Pandian P.K (2014). Effect of phosphogypsum on strength of lime stabilized expansive soil. *Gradevinar*, 12:1109-1116.
- Kim, B.; Prezzi, M. & Salgado, R. (2005). Geotechnical properties of fly and bottom ash mixtures for use in highway embankments. *J. Geotech. Geoenviron. Eng.*, 10.1061/(ASCE)GT.1943-5606.0001285.

- Kumar, S.; Dutta, R.K. & Mohanty B. (2014). Engineering properties of bentonite stabilized with lime and phosphogypsum. *Slovak Journal of Civil Engineering*, 22(4):35-44.
- Lapido-Loureiro, F.E. & Nascimento, M. (2009). O gesso nos agrossistemas brasileiros: fontes e aplicações. F.E. Lapido-Loureiro, R. Melamed & J.F. Neto (eds.) *Fertilizantes: Agroindústria e Sustentabilidade*. CETEM/MCT, Rio de Janeiro, pp. 445-478.
- Lovato, R.S. (2004). Estudo do Comportamento Mecânico de um Solo Laterítico Estabilizado com Cal, Aplicado a Pavimentação. Dissertação de Mestrado. Escola de Engenharia, Universidade Federal do Rio Grande do Sul, 144 p.
- Matos, T.H.C. (2011). Caracterização Hidro-mecânica do Fosfogesso e das Misturas Solo-Fosfogesso. Dissertação de Mestrado. Departamento de Engenharia Civil e Ambiental, Universidade de Brasília, Brasília, 118 p.
- Matos, T.H.C.; Mascarenha, M.M.A. & Cordão Neto, M. P. (2012). Caracterização mecânica do fosfogesso e das misturas solo-fosfogesso. *Anais XVI Congresso Brasileiro de Mecânica dos Solos e Engenharia Geotécnica*, Goiânia, Brasil, v. 1, pp. 1-7.
- Mesquita, G.M. (2007). Aplicação de Misturas de Fosfogesso e Solos Tropicais Finos na Pavimentação. Dissertação de Mestrado. Escola de Engenharia Civil e Ambiental, Universidade Federal de Goiás, Goiânia, 144 p.
- Metogo, D.A.N. (2011). Construção e Avaliação Inicial de um Trecho de Pavimento Asfáltico Executado com Misturas de Solo Tropical, Fosfogesso e Cal. Dissertação de Mestrado, Universidade Federal de Goiás, Goiânia, 195 p.
- Nogami, J.S. & Villibor, D.F. (2009). Pavimentação de Baixo Custo com Solos Lateríticos. Editora Vilibor, São Paulo, Brasil, 290 p.
- Oliveira, S.M.F. (2005). Estudo do Comportamento Mecânico de Misturas de Fosfogesso e Cal para Utilização na Construção Rodoviária. Dissertação de Mestrado. Escola de Engenharia de São Carlos, Universidade de São Paulo, São Carlos, 190 p.
- Parreira, A.B.; Kobayashi, A.R.K. & Silvestre Jr, O.B. (2003). Influence of Portland cement type on unconfined compressive strength and linear expansion of cement-stabilized phosphogypsum. *Journal of Environmental Engineering*, 129:956-960.
- Rabelo, A.P.B.; Soler, J.G.M. & Silva, N.C. (2001). Utilização do subproduto fosfogesso na construção civil. *Anais IV Seminário Desenvolvimento Sustentável e a Reciclagem na Construção Civil - Materiais Reciclados e suas Aplicações*, IBRACON, São Paulo, Brasil, v. 1, pp. 195-202.
- Rezende, L.R.; Curado, T.S.; Silva, M.V.; Mascarenha, M.M.A.; Metogo, D.A.N.; Cordão Neto, M.P. & Bernucci, L.L.B. (2016). Laboratory study of phosphogypsum, stabilizers and tropical soil mixtures. *Journal of Materials in Civil Engineering*, 10.1061/(ASCE)MT.1943-5533.0001711.
- Roy, A.; Kalvakaalava, R. & Seals, R.K. (1996). Microstructural and phase characteristics of phosphogypsum-cement mixtures. *Journal of Materials in Civil Engineering*, 8(11):11-18.
- Rufo, R.C. (2009). Estudos Laboratoriais de Misturas de Fosfogesso, Solo Tropical e Cal para Fins de Pavimentação. Dissertação de Mestrado. Escola de Engenharia Civil e Ambiental, Universidade Federal de Goiás, Goiânia, 155 p.
- Rutherford, P.M.; Dudas, M.J. & Samek, R.A. (1993). Environmental impacts of phosphogypsum. *The Science of the Total Environment*, 149:1-38.
- Shen, W.; Gan, G.; Dong, R.; Chen, H.; Tan, Y. & Zhou, M. (2012). Utilization of solidified phosphogypsum as Portland cement retarder. *Journal of Material Cycles and Waste Management*, 14:228-233.
- Smadi, M.M.; Haddad, R.H. & Akour, A.M. (1999). Potential use of phosphogypsum in concrete. *Cement and Concrete Research*, 29:1419-1425.
- Soleimanbeigi, A. & Tuncer, B.E. (2015). Compressibility of recycled materials for use as highway embankment fill. *J. Geotech. Geoenviron. Eng.*, 10.1061/(ASCE)GT.1943-5606.0001285.
- Soleimanbeigi, A.; Tuncer, B.E. & Berson, C. (2013). Evaluation of fly ash stabilization of recycled asphalt shingles for use in structural fills. *J. Geotech. Geoenviron. Eng.*, 25(1):94-104
- Vakili, M.V.; Chegenizadeh, A.; Nikraz, H. & Keramatikerman, M. (2016). Investigation on shear strength of stabilized clay using cement, sodium silicate and slag. *Applied Clay Science*, 124-125:243-251.
- Yang, J.; Liu, W.; Zhang, L. & Xiao B. (2009). Preparation of load-bearing building materials from autoclaved phosphogypsum. *Construction and Building Materials*, 23:687-693.

List of Symbols

- Al : aluminum
 As: arsenic
 B : barium
 C: carbon;
 Ca : calcium
 CaSO₄nH₂O : phosphogypsum
 Ca₁₀F₂(PO₄)₆: fluorapatite
 C_c: compression index
 C_r: recompression index
 CEC: cation exchange capacity
 Cu : copper
 Fe: iron
 HF: fluoridric acid
 H₂O: water
 H₃PO₄: phosphoric acid

IP : plasticity index
K: potassium
Meq: milliequivalent
mL: milliliter
Mg: magnesium
Mn: manganese
MO: organic matter
Na : sodium
P: phosphor
 pH : hydrogen potential
Pb : lead
PG: Phosphogypsum

Ra : Radio
S: sulfur
U: uranium
 w_L : liquid limit
 w_{opt} : optimum water content
 w_p : plastic limit
Zn : zinc
 ϕ' : effective friction angle
 c' : effective cohesion intercept
 σ_{pa} : pre-consolidation stress
 γ_{dmax} : dry maximum density
 γ_s : specific gravity of grains

Stress-Strain Analysis of a Concrete Dam in Predominantly Anisotropic Residual Soil

M.F. Leão, M.P. Pacheco, B.R. Danziger

Abstract. Studies of foundations for dams should take into account the study of the behavior of the rocky mass, primarily the stresses and strains expected during the construction and post-construction period. When these structures are supported on sound rock, the use of concrete dams is favored. However, when the foundation is made up of soil or soft rock, earth dams are the most commonly employed technical solution. The study investigates a concrete-gravity dam in the Dominican Republic, with a foundation comprised of alternating horizons of residual soil and weathering soft rock, presenting marked anisotropy and the presence of relict structures. A high incidence of discontinuities gave rise to a more detailed study of the stress-strain behavior of the foundation, taking into account the discontinuity attitudes and the results of direct shear tests carried out parallel to and orthogonal to the discontinuities. By means of 2-D finite element simulations, an anisotropic constitutive model was adopted (the Jointed Rock Model-JRM) capable of modeling up to two preponderant discontinuity directions. The numerical analyses clearly showed the utility of the model in the selection of foundation reinforcement options, in this case through the use of cut-offs to increase the stability conditions.

Keywords: anisotropic constitutive model, anisotropy, concrete-gravity dam, residual soil.

1. Introduction

When investigating a dam site, essential geological and geotechnical aspects must be analyzed, such as: (i) the quality of the materials existing in the abutments and the foundation, (ii) the availability of these rock and soil deposits, and (iii) their relationship to geotechnical parameters of permeability, strength and deformability. Studies of foundations for dams should take into account the behavior of the rock mass, primarily the stresses and strains expected during the construction and post-construction period. When the foundation of the dam is composed of heterogeneous residual soil and weathered rock, there is great concern about the settlement capacity due to the concentration of stresses. The dam may undergo differential settlements depending on the weight transmitted to the foundation and the stratified soil.

These characteristics are difficult to predict when the selected sites present weathering profiles that, in tropical countries, are usually very thick. The presence of transition layers, partially composed of residual soils and rocks in differing degrees of alteration, requires special treatment.

In spite of these peculiarities, several dam projects have been developed on weathering profile, such as Obruk on basalt (Kocbay & Kilic, 2006) and Keban on karst marble and shale (Ertunç, 1999), both in Turkey; Tianhuanping on rhyolite and andesite (Wang & Liu, 2005) in China; Porthimund on charnockites (Ramana & Gogte, 1982), Uri and Nathpa-Jhakri on schists (Behrestaghi *et al.*, 1996) all in India; Hickory Log Creek on mica-schist (Rogers *et al.*,

2006) in the United States; and Clyde on schists (Macfarlane, 2009) in New Zealand. However, it is important to point out that there are still only limited scientific publications on schist materials as foundation, mainly for concrete-gravity dams, which often leads to a preference for the construction of earth or rock dams.

In this context, a case study of the San Juan dam on the Samaná Peninsula, in the Dominican Republic is presented. From a geological-geotechnical point of view, the foundation and abutments are supported on highly anisotropic young residual soil, with marked relict structures, derived from schist and marble, as well as soft rock layers interbedded with young residual soil. It is a concrete-gravity type dam, approximately 12 m high, in simple concrete, with a longitudinal section around 220 m in length, and spillway walls of reinforced concrete, forming a reservoir of around 700,000 m³. It was constructed by subdividing the concrete-gravity monolith into 14 foundation blocks, separated by contraction joints, designated from Block 11 (located on the right abutment) to Block 1, and Block A3 to Block A1 (located on the left abutment). The dam was completed in 2012 and came into operation in 2013.

The dam was evaluated with focus on the influence of the geological structures on the geotechnical parameters in terms of stability and deformability, based on the marked discontinuities in the foundation. These features, although difficult to reproduce in anisotropic rock through conventional limit equilibrium methods, were satisfactorily simu-

Marcio Fernandes Leão, Ph.D. Student, Rio de Janeiro State University, Rio de Janeiro, RJ, Brazil. e-mail: marciotriton@hotmail.com.

Marcus Peigas Pacheco, Ph.D., Full Professor, Rio de Janeiro State University, Rio de Janeiro, RJ, Brazil. e-mail: marcus_pacheco@terra.com.br.

Bernadete Ragoni Danziger, D.Sc., Associate Professor, Rio de Janeiro State University, Rio de Janeiro, RJ, Brazil. e-mail: bernadeterd@hotmail.com.

Submitted on December 14, 2017; Final Acceptance on July 4, 2018; Discussion open until December 31, 2018.

DOI: 10.28927/SR.412171

lated with the Finite Element Method (FEM), employing an anisotropic constitutive model.

Figure 1 represents the blocks directly influenced by the characteristics of the foundation. Blocks 10 and 11, not shown in the figure, are influenced by the characteristics of the abutment. Figure 2 shows the longitudinal section of the dam axis, corresponding to Fig. 1, and the dimension of the foundation with respect to the estimated rock surface. Block 4, the object of the present study, is highlighted and was chosen due to its representativeness of the foundation as a whole.

This paper is based on data available from geological mapping carried out across the full extent of the San Juan dam. The geotechnical parameters were obtained through drilling and laboratory tests for application of the Jointed Rock (JRM, Plaxis 2D) constitutive model. Therefore, the stress-strain behavior in a highly discontinuous and anisotropic medium was studied based on the characteristics of Block 4.

2. Materials and Methods

The methodology can be divided into three stages. The first consisted in the geological mapping of the area of the axis of the dam and its reservoir, highlighting the main units and geological structures. In the second stage, percussion and rotary drilling were defined and executed primarily in the region of the foundation blocks. In addition, undisturbed samples of residual soil were collected at the dam foundation in order to perform characterization and direct shear tests. The third stage consisted of the choice of Block 4 for the evaluation of the stress-strain behavior of

the foundation through FEM modeling, based on the geological-geotechnical parameters obtained. The first Author has been directly involved in the three stages. The latter stage has also had the collaboration of the second and third Authors.

2.1. Geological-geotechnical parameters

From the preliminary geological-geotechnical mapping, rotary and percussion drilling have been scheduled in order to define the geological layers and representative geological-geotechnical cross sections. Out of the fourteen blocks that make up the San Juan dam, Block 4 was chosen because it represents the characteristics of the foundation in terms of geological materials and heterogeneities evidenced through subsurface investigations and field mapping.

Ten undisturbed soil samples were collected, eight in the San Juan Dam area and two in the Water Treatment Station, since the residual soils occurring in these locations are geologically similar.

To obtain the strength parameters of the residual soils, two series of direct shear tests were performed. The first series comprised samples molded with the test failure surface parallel to the foliation of the test specimen material (Fig. 3a). The second series comprised samples molded orthogonal to the foliation (Fig. 3b). The direct shear tests were performed on controlled deformation Wykeham Farrance machines, with automatic monitoring of the variables involved. The specimens were molded and placed in the shear boxes under a vertical stress close to zero, and the boxes were then inundated with distilled water.

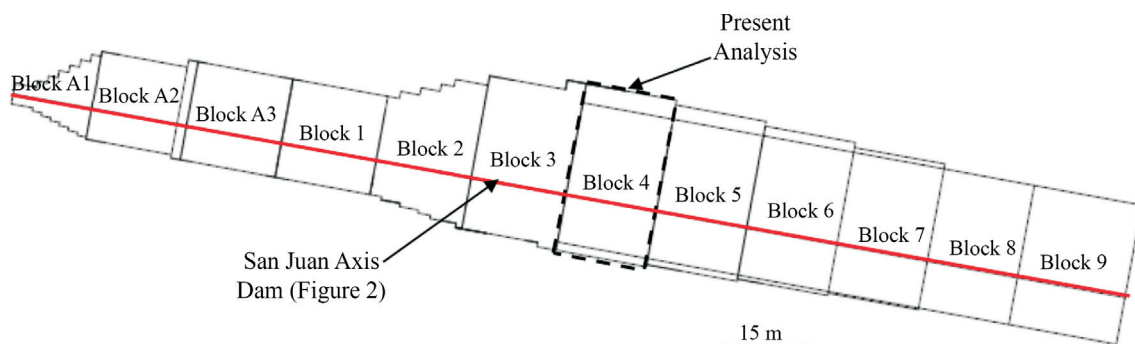


Figure 1 - General arrangement of the San Juan Dam. Original scale 1:250.

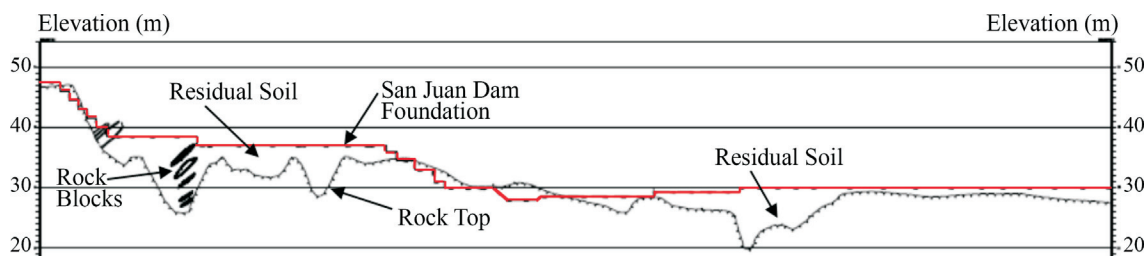


Figure 2 - San Juan Dam Axis Section (upstream) presenting the foundation elevations and the estimated bedrock surface. Original scale 1:250.



Figure 3 - Residual soil specimen in preparation for direct shear test: parallel (a) and orthogonal (b) to foliation.

The layers were grouped into three categories, according to the results of the N_{SPT} and direct shear tests, as follows: (i) F_q , for $N_{SPT} < 10$; (ii) F , for $10 < N_{SPT} < 30$; and (iii) R for $N_{SPT} > 30$. Because materials with penetration resistance $N_{SPT} > 30$ represent deformations deemed negligible for the elaborated study, the classification of the layers was simplified into three units for modeling. It should be noted that N_{SPT} refers to the number of blows for penetration of the final 30 cm of the sampler in percussion drilling according to Brazilian standards, which correlates with N_{60} , international standard, based on the relationship:

$$N_{60} = C \cdot N_{SPT} \quad (1)$$

The value of $C = 1.37$, in the above expression, instead of the value of 1.20 proposed by Décourt *et al.*, 1989, is an average value based on energy measurements performed in equipment routinely used in Brazil (*e.g.*, Belicanta, 1985, 1998; Cavalcante, 2002; Odebrecht, 2003).

2.2. Stress-strain behavior of the foundation

The geotechnical properties of the materials served as the basis for the modeling of the San Juan dam foundation, using the JRM constitutive model for the period immediately after the filling of the reservoir without seismic conditions.

The finite element method provides stress-strain analysis of continuous media representing complex behaviors and highly irregular geometries, diverse loading conditions, heterogeneities and non-linearity of materials. In addition, the JRM model takes into account the stratification and the particular directions of geological structures, such as foliations, faults and fractures. The JRM model assumes the regions between fractures as intact rock. The intact rock is linearly elastic, with transversely anisotropic behavior defined by constant Young moduli E_x and E_y and Poisson ratio ν . For the foliation and fracture planes, the shear stresses are limited according to the Mohr-Coulomb criterion. The application of the JRM model is limited to two families of joints or fractures, and is therefore a very useful and accurate model for stress-strain analysis of discontinuous rock masses (Xu *et al.*, 2015).

In this context, among the available sections for Block 4, the cross-section of the dam axis 4.1 was selected for modeling, given its representative characteristics and the geometry of the geological materials. A locally refined mesh (under the dam) was set, considering the irregularities of the foundation geometry, for soils and rocks, so that stress concentrations at these locations could be adequately modelled.

Two cases were considered for the modeling of section 4.1 (Fig. 4). In case 1 (left), the dam stability was simu-

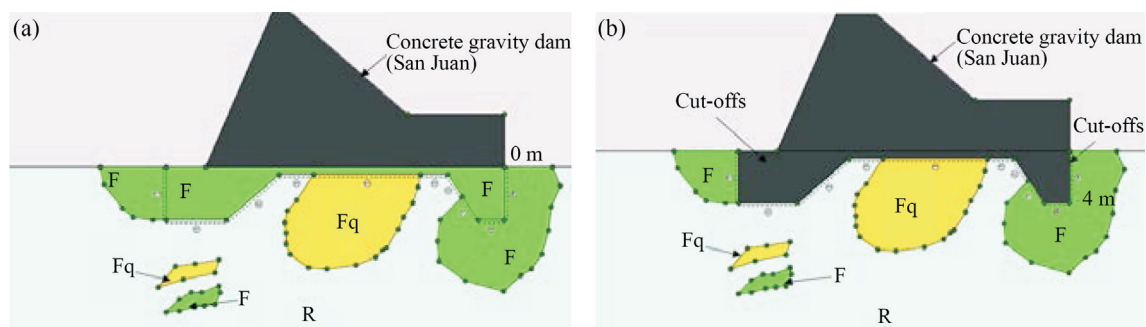


Figure 4 - Modeling the foundation of Block 4 at elevation 0 m. Case 1 (a): no cut-offs, and, Case 2 (b): with concrete cut-offs excavated to elevation -4 m.

lated with the foundation resting on a single elevation on young residual soil (el. 0 m), without reinforcement (cut-offs). Case 2 (right) simulated the foundation reinforcement with 4 m deep concrete cut-offs (base at el. - 4 m). For both cases, the water head totals 12 m upstream and 0 m downstream, representing the condition of dam operation. The dam is of an inclined bi-faceted type, that is, it forms acute and obtuse angles upstream and downstream, respectively.

The foundation was divided into three main units, based on their geotechnical properties, designated as F_q (very low resistance soil), F (low resistance soil), for young residual soils, and R (rock) for the sound rock mass. The dam body is represented by material C (concrete). The drained analyses assumed steady-state flow corresponding to the operating conditions of the dam.

3. Results and Discussion

3.1. Geological and geotechnical aspects

Geologically, the Samaná Peninsula is primarily composed of micaceous schist and marble with poorly defined boundaries (Mollat *et al.*, 2004), and occasionally occurring coverings of more recent limestone on top of the marble.

The San Juan dam is approximately 200 m downstream from a slightly narrower stretch of the river valley of the same name. Topographically, the left margin opens much more than the right, both covered by alluvial-colluvial sediments and residual soils. Basically, the geological units that occur in the studied area (Fig. 5), identified in field mappings, are: schist, marble and aluvial-colluvial soil. The materials that make up the foundation of the San Juan dam are young residual soils of schist, as well as less

altered portions of this rock, intercalated, or not, with marble.

The area is usually devoid of rocky outcrops, including the abutments, except immediately downstream, on the right bank, where there was a massive outcrop of schist, one of the only ones at that location. Field observations did not reveal evidence of infiltration zones in the riverbed. The outcrops found at the margins indicate the presence of semi-altered or partially altered sheared schist, which produces a very clayey residual soil with low permeability.

The measurements of schistosity and fractures obtained for foundation Block 4 showed a preferential direction $N75^\circ W/25^\circ SW \sim N55^\circ W/80^\circ SW$. Figure 6 shows, schematically, the principal directions of the discontinuities accounted for in the numerical model. These fracture families are parallel and make 30° and 60° angles (α) with a horizontal line, parallel to the dam foundation.

Figure 7 shows the diverse typical geological and geotechnical characteristics of the San Juan dam. In Fig. 7 (a), intercalations of schist (transitional soil / rock material) and marble with NW-SE foliation are presented in a section of the dam access road. Sometimes families of fractures are formed by the occurrence of karst cavities (Fig. 7b) in centimetric pores disseminated in the rock, and following rock foliation. The main fracture families of the rock mass are arranged in planes parallel to or normal to the foliation (Fig. 7c), and may be filled with carbonate and/or quartz material in the schist rocks.

Figure 8 shows the boundary of Block 4 in the San Juan dam, together with the geological-geotechnical sections (Fig. 9) used for the modeling process. In addition, the structural contour lines of the rock top are indicated with their respective elevations. All the geological units are re-

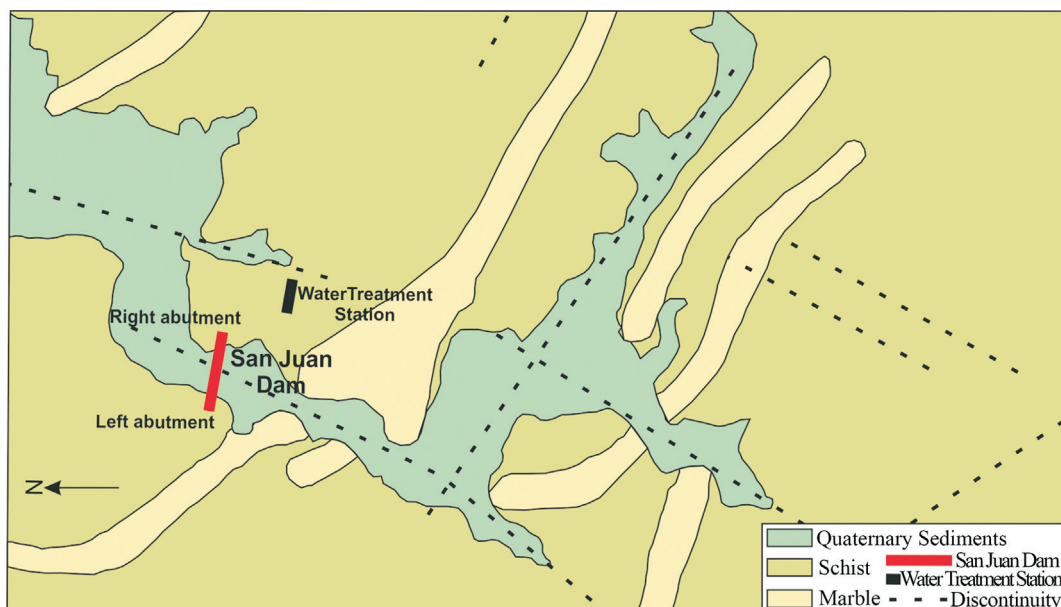


Figure 5 - Regional geological map of San Juan Dam Axis (in red) and Water Treatment Station (in black). Original scale 1:5.000.

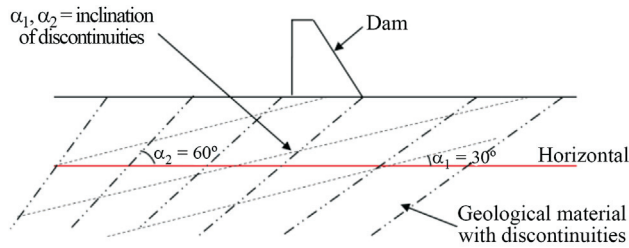


Figure 6 - Sketch showing the discontinuity family directions considered in the numerical model.



Figure 7 - Geological-geotechnical of geological materials.

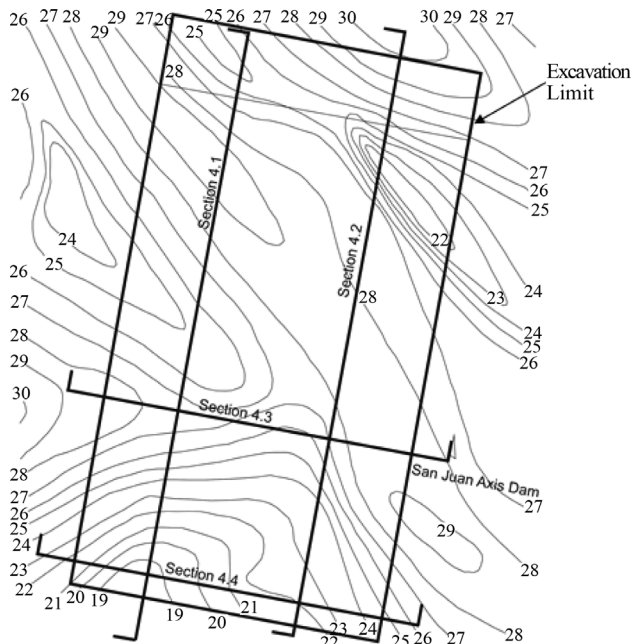


Figure 8 - Bedrock contours - Block 4, plan view.

residual soils and altered schist rocks, intercalated with passages of marble.

In addition, in the young residual soil foundation, intercalations of weathered rock occur, coming from portions that are more resistant to weathering. Stretches of low resis-

tance ($N_{SPT} = 2$) residual micaceous soil were identified in portions underlying the dam foundation.

Figure 10 shows sample boxes from a drilling survey in the region of Block 4, where passages of residual soil are noted below long rocky stretches. Figures 10 (a) and 10 (b) show intercalations of passages of mature and young residual soil and small stretches of heavily altered rock. In Fig. 10 (c) to Fig. 10 (e) it is possible to identify stretches of residual soil below extensive rocky stretches, altered or not (depths 10.45 m, 11.0 m and 18.10 m). In Fig. 10 (f), a transitional soil/rock passage (90% residual soil of schist and 10% schist rock) is evident in detail. Similar passages can be observed at points indicated by the arrows.

The results obtained from direct shear tests, both orthogonal (blue) and parallel (red), to the foliation are presented in Fig. 11. Since the foundation is very heterogeneous, composed of young residual soils of schist and heavily altered rock, a linear regression analysis was performed based on the Brazilian Standard NBR 11682 (ABNT, 2009) to obtain the effective parameters of c' and ϕ' . Confidence limits of individual strength (longer dashed lines) and mean resistance (shorter dashed lines) are included, with a 5% level of significance (two-tailed). Although the orthogonal results presented higher values than those parallel to the foliation, due to the influence of the discontinuities in the latter condition, a mean cohesion $c' = 48$ kPa and friction angle (ϕ') = 27° was adopted for the foundation in altered rock (R).

For the other materials (F_q and F), the values of c' and ϕ' , as well as the other mechanical parameters required for modeling, are presented in Table 1. The permeability values included in Table 1 have been chosen in the middle range of those related to the effective stresses occurring in the dam foundation during the filling of the reservoir.

For selection of the geomechanical parameters of the geological materials that make up the foundation, according to Table 1, the filler materials between discontinuities were considered to represent the three units (F_q , F and R). According to the JRM model, the values E_2 and G_2 for the filler materials control, respectively, the normal and the shear stiffness along the discontinuities and therefore are mutually independent. Considering that the main objective of this work was to study the influence of the anisotropy on the stability of the dam, with no primary concern on displacements, the moduli in Table 1 have been selected arbitrarily, according to typical values representing the respective materials. Since the marked foliation in these units controls the stability, the selected effective strength parameters c_1' and c_2' for each unity were those obtained from the direct shear tests. For all natural materials, a tension cut-off of 100 kN/m² was assumed to control occasional tensile stresses.

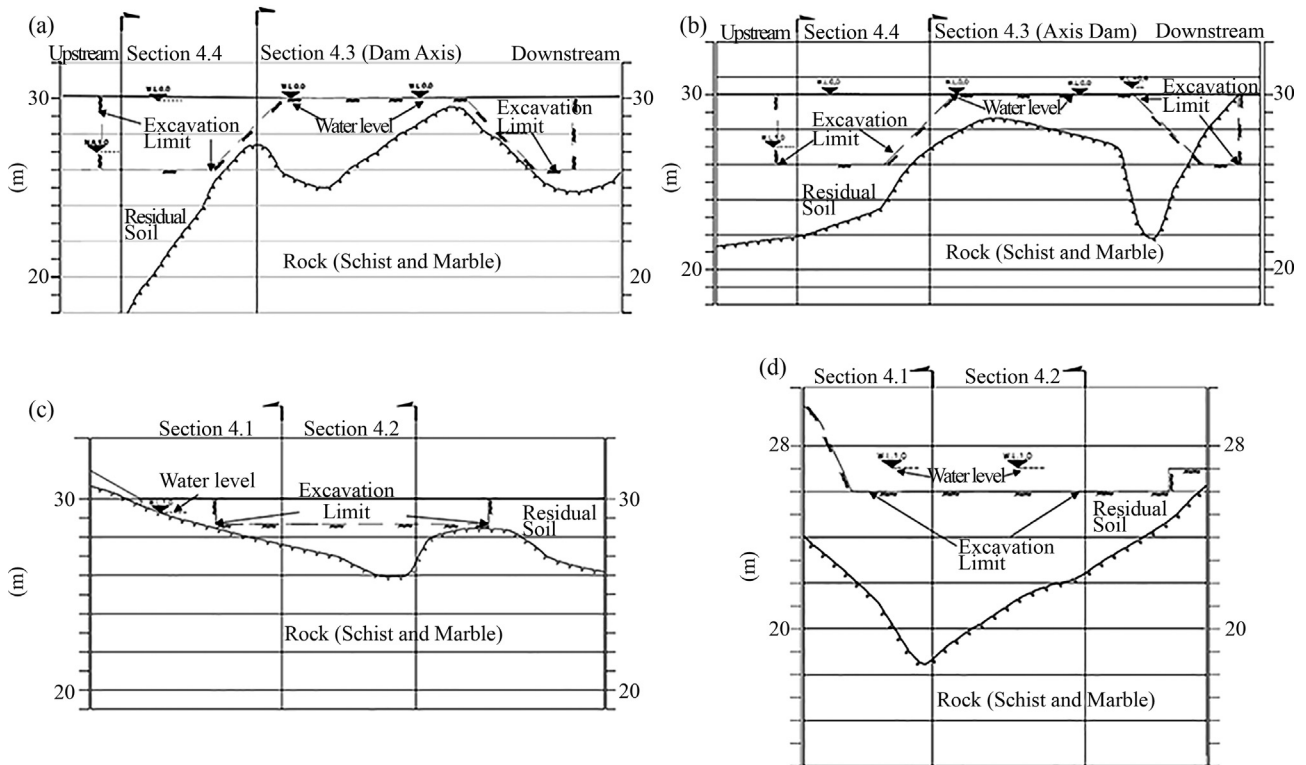


Figure 9 - Sections 4.1 (a - study object), 4.2 (b), 4.3 (c) and 4.4 (d) of Block 4. The sections show the boundary between the estimated rocky top (altered rock) and the young residual soil of the foundation. The excavation dimensions of the foundation and the water level obtained by drilling are presented.



Figure 10 - Drill core samples (a-e), in sequence, from SM-19 (rotary drilling) in Block 4 dam foundation axis. In detail (f) transitional material (soil/rock), depth 10.45 to 11.0 m.

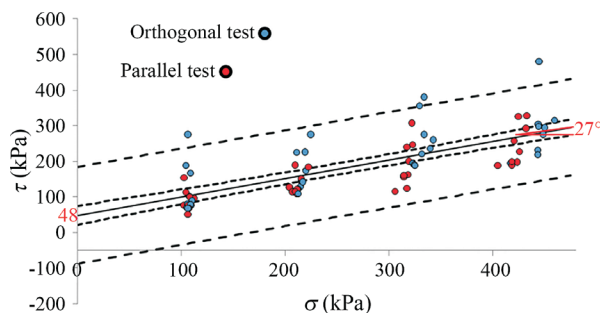


Figure 11 - Confidence limit intervals, 5% significance.

3.2. Flow, stress and strain analysis

The directions of the flow vectors are presented sequentially for Case 1 (Fig. 12a) and Case 2 (Fig. 12b).

For Cases 1 and 2, there was not much difference on the maximum pore-pressures, of 91 to 112 kN / m², respectively. Likewise, in both cases, the flow velocities presented low values, of the order of 0.005 and 0.007 m / day, due to essentially clayey soil. However, due to the head loss provided by the cut-offs, caused by the longer flow path, the output gradient is clearly smaller in Case 2. The cut-offs

Table 1 - Geological-geomechanical parameters for the FEM analysis.

Materials	γ_{sat} (kN/m ³)	E_1 (kN/m ²)	ν_1	Modeling parameters - jointed rock model									
				E_2 (kN/m ²)	ν_2	G_2 (kN/m ²)	c_1' (kN/m ²)	c_2' (kN/m ²)	ϕ' (°)	k (cm/s)	α_1 (°)	α_2 (°)	Tension cut-offs (kN/m ²)
F _q	18.6	9.5x10 ³	0.2	3.0x10 ³	0.2	1.5x10 ³	10	10	0	2.9x10 ²	30	60	100
F	20.0	2.0x10 ⁴	0.2	3.0x10 ³	0.2	1.5x10 ³	20	20	27	1.1x10 ²	30	60	100
R	22.0	3.5x10 ⁴	0.2	3.0x10 ³	0.2	1.5x10 ³	48	20	27	0.5 x10 ³	30	60	100
C	25.0	2.5x10 ⁷	0.2	-	-	-	-	-	-	-	-	-	-

Legend: F_q (very low resistance soil); F (low resistance soil); R (weathering rock) and C (concrete). γ_{sat} (saturated specific weight) E_1 (Young modulus for the intact rock), ν_1 (Poisson ratio for the intact rock), E_2 (Young modulus for the fill materials), ν_2 (Poisson ratio for the fill material), G_2 (shear modulus of the fill materials), c_1' and c_2' (cohesion of the fill materials), ϕ' (friction angle), k (permeability coefficient, obtained by Lefranc and Lugeon tests), α_1 and α_2 (angles of the discontinuities for planes 1 and 2, respectively, with the horizontal).

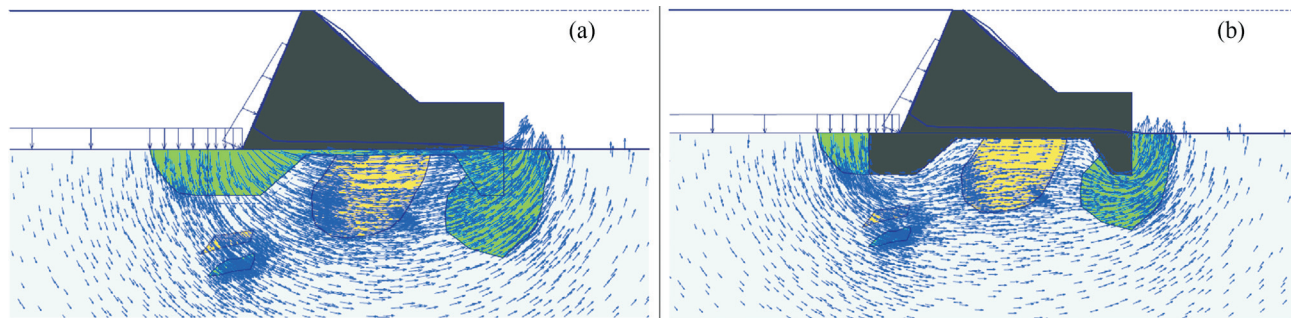


Figure 12 - Flow vectors generated for the foundation conditions for Case 1 (a) and Case 2 (b).

clearly increased the strength of the foundation mass, increasing the load capacity of the dam to withstand stress.

Figure 13 shows the total displacement contours corresponding to the deformation moduli assumed. Regardless of the values assumed for the material moduli, the highest total displacements were concentrated in the upstream toe, progressing downstream in a direction nearly perpendicular to the α_2 - inclined discontinuities. This indicates that there are no significant displacements along the discontinuities, ensuring the adequate stability of the dam. The maximum displacements found for both Cases 1 and 2 were close, around 14 mm for the F and F_q soils below the dam foundation. In terms of specific deformations, they were larger for Case 1 (5.93%) than Case 2 (2.83%), with respect to the F_q layer. This behavior was expected, since the execution of

the cut-offs removed a large portion of the deformable layers of low resistance soils (F_q), up to 4 m thick, replacing them with concrete.

The plastic points (Fig. 14), which represent points in the soil that reached the Mohr-Coulomb envelope, are mainly concentrated in the F_q and F materials, primarily near the foundation or cut-offs of the dam. In Case 2, since a portion of the materials (F and F_q) were excavated and replaced with concrete, the plastic points tended to move farther away from the dam-foundation contact (Fig. 14b).

The safety factors for Cases 1 and 2 were, respectively, 1.82 and 2.61, obtained numerically by the progressive reduction of the parameters c' and ϕ' , proving that the excavation up to the depth -4 m significantly increased the stability of the dam with a foundation of predominantly

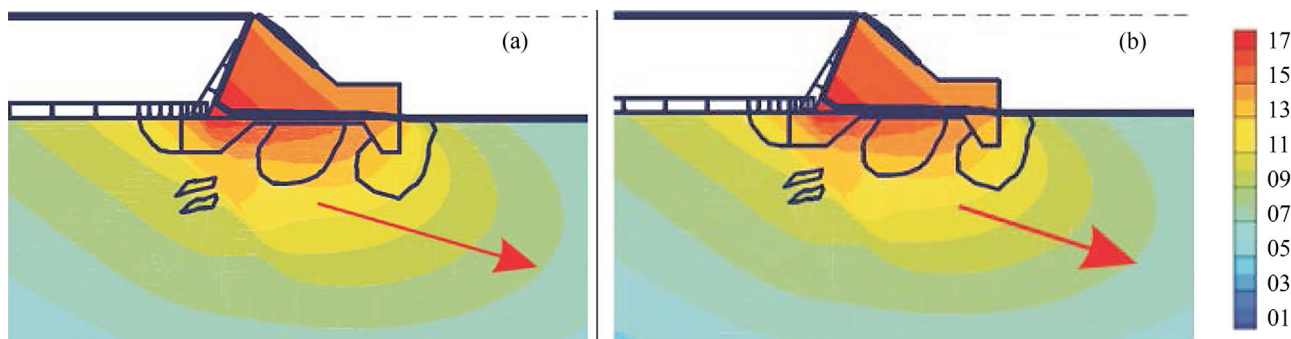


Figure 13 - Displacement contours (cm) generated for the foundation conditions for Case 1 - (a) and Case 2 - (b). The arrow in red highlights the predominant deformation direction and the color scale represents the displacements (mm).

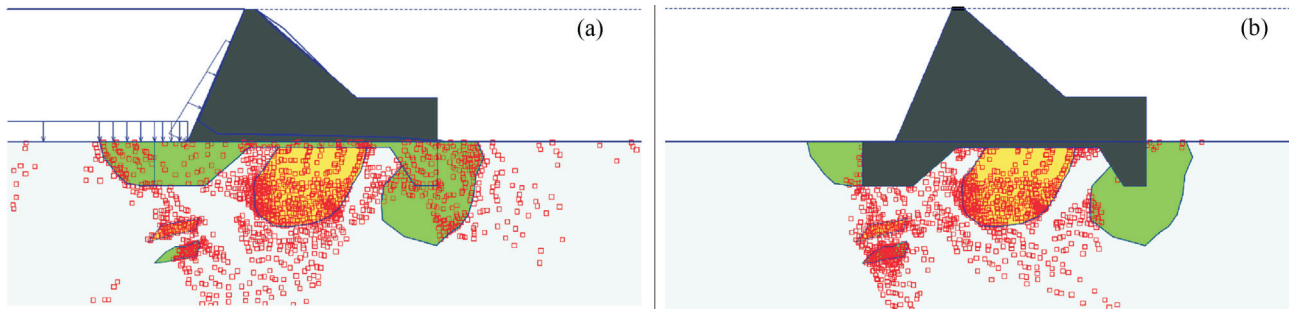


Figure 14 - Plastic points (red) obtained for Case 1 (a) and Case 2 (b).

anisotropic soil. The JRM model was therefore demonstrated to be suitable for the stress-strain analysis in question.

4. Conclusions

The methodology used for the development of this article addressed the geological and geotechnical peculiarities of the foundation material of the San Juan Dam, taking into account both its great heterogeneity and anisotropy, as well as the constitutive properties of the soils and rocks existing in the region. Materials with these characteristics are often discarded as foundation options. However, in places where weathering acts in the development of extensive alteration profiles, the understanding of the geomechanical behavior of these materials may favor the construction of more daring projects: in the case of dams, the construction of concrete dams rather than earth dams.

The strong anisotropy of the foundation materials was determinant in the choice of the constitutive model type (JRM), valid for investigating stratified layers with two dominant directions. The results obtained through FEM modeling revealed that this type of analysis is very useful in the design stages, guiding actions during construction, as well as allowing for bolder solutions for the San Juan Dam.

Acknowledgments

The authors acknowledge the financial support from FAPERJ. Thanks to Prof. Dr. Denise Gerscovich (UERJ/RJ) for the assistance with the PLAXIS 2D software.

References

- ABNT (2009). Slope Stability - NBR 11682. Associação Brasileira de Normas Técnicas, Rio de Janeiro, Rio de Janeiro, Brazil, 39 p. (in portuguese)
- Behrestaghi, M.H.N.; Seshagiri R.K. & Ramamurthy, T. (1996). Engineering geological and geotechnical responses of schistose rocks from dam project areas in India. *Engineering Geology*, 44(1):183-201.
- Belicanta, A. (1985). Dynamic Energy in SPT - Result of a Theoretical-Experimental Investigation. M.Sc. Dissertation, University of São Paulo, Department of Civil Engineering, São Paulo, SP, Brazil. (in portuguese)
- Belicanta, A. (1998). Evaluation of Factors Involved in the SPT Penetration Resistance Index. Ph.D. Dissertation, University of São Paulo, São Carlos School of Engineering, São Carlos, SP, Brazil. (in portuguese)
- Cavalcante, E.H. (2002). Theoretical-Experimental Research on SPT. Ph.D. Dissertation, Federal University of Rio de Janeiro, Department of Civil Engineering, Rio de Janeiro, RJ, Brazil. (in portuguese)
- Décourt, L.; Belicanta, A. & Quaresma FILHO, A.R. (1989). Brazilian experience on SPT. Proc. 12th Int. Conf. on Soil Mech. and Geotech. Eng., ABMS/ISSMGE, Rio de Janeiro, pp. 49-54.
- Ertunç, A. (1999). The geological problems of the large dams constructed on the Euphrates River (Turkey). *Engineering Geology*, 51(3):167-182.
- Kocbay, A. & Kilic, R. (2006). Engineering geological assessment of the Obruk dam site (Corum, Turkey). *Engineering Geology*, 87(3):141-148.
- Macfarlane, D.F. (2009). Observations and predictions of the behavior of large, slow-moving landslides in schist, Clyde Dam reservoir, New Zealand. *Engineering Geology*, 109(1):5-15.
- Mollat, H.; Wagner, B.M.; Cepek P. & Weiss W. (2004). Geological Map of the Dominican Republic 1:250.000. Schweizerbart Science Publishers. Germany, 100 p. (in spanish)
- Odebrecht, E. (2003). SPT Energy Measurements. Ph.D. Dissertation, Federal University of Rio Grande do Sul, Department of Civil Engineering, Rio Grande do Sul, RS, Brazil. (in portuguese)
- Ramana, Y.V. & Gogte, B.S. (1982). Quantitative studies of weathering in saprolitized charnockites associated with a landslip zone at the Porthimund Dam, India. *Engineering Geology*, 19(1):29-46.
- Rogers, G.D.; Kahler, C. & Deaton, S. (2006). Foundation investigation at Hickory Log Creek Dam, Canton. Proc. GeoCongress 2006, Georgia, ASCE, pp. 1-6.
- Wang, Y.S. & Liu, S.H. (2005). Treatment for a fully weathered rock dam foundation. *Engineering Geology*, 77(1):115-126.
- Xu, Q.; Chen, J.; Li, J.; Zhao, C. & Yuan, C. (2015). Study on the constitutive model for jointed rock mass. *PLoS One* 10(4):1-20.

Assessment of the Stress History of Quaternary Clay from Piezocone Tests

E. Odebrecht, F. Schnaid

Abstract. This paper highlights the importance of linking regional geology to geotechnical ground investigation when estimating the pre-consolidation pressure σ'_p of Quaternary clay deposits from piezocone tests. The work comprises a comprehensive site characterization from boring logs, piezocone tests and laboratory oedometer tests carried out at the Tubarão experimental testing site, in Southern Brazil. Geological characterization includes radiocarbon dating of samples from these clayey sediments. The approach developed at the testing site was later extended to 12 well characterized clay sites along the Brazilian coast to demonstrate that net cone penetration $q_t - \sigma_{v0}$ can provide reliable estimations of pre-consolidation pressure σ'_p in Quaternary plastic, compressible, non-fissured clays. However, the $\sigma'_p/(q_t - \sigma_{v0})$ ratio is not a constant (typically ranging from 0.1 to 0.4) and, as a consequence, pairwise parameter correlations considering σ'_p and $q_t - \sigma_{v0}$ lead to inaccurate predictions. Independent assessment of the void ratio e_0 is needed in order to produce more realistic first order estimates of σ'_p from piezocone data.

Keywords: CPT, overconsolidation ratio, pre-consolidation pressure, stress history.

1. Introduction

Geological and geotechnical assessment of the stress history of clay sediments is regarded as a key stage in the design of geo-infrastructures. Since stress history controls the strength and stiffness of geo-materials, evaluation of the depositional processes of clay deposits linked to geotechnical properties impacts the prediction of long-term consolidation settlements as well as short-term stability problems.

Given the importance of the subject, there has been considerable research developments in the past two decades. Correlations of the stress history pre-consolidation pressure and the net field penetration resistance have been reported (Wroth, 1984; Mayne & Mitchell, 1988; Mayne, 1991) and a critical appraisal of standard engineering practice has been reviewed by recent state-of-the art publications (e.g. Schnaid, 2005; Mayne *et al.*, 2009). However, few comprehensive case studies regarding geological and geotechnical data are available in the literature, and consequences are that engineering practice often adopts simplified, empirical recommendations for the estimation of the pre-consolidation pressure. The limitations of the state-of-practice are highlighted in the present paper by demonstrating that the predicted pre-consolidation pressure σ'_p from the piezocone net field penetration resistance $q_t - \sigma_{v0}$ requires independent assessment of the soil void ratio e_0 .

2. Background Information

The pre-consolidation pressure σ'_p is defined as the maximum effective vertical stress to which a soil has been

subjected along its stress history and is considered as one of the most important parameters required to assess the deformation of soft clays. Often the term is used to define the effective stress at which an undisturbed sample yields during an oedometer test, or it represents the critical stress at which a clayey soil becomes destructured and where the subsequent compression curve is initially steeper than the standard virgin line (e.g. Burland, 1990). For an idealized elasto-plastic soil, σ'_p defines the transition from overconsolidated (OC) to normally consolidated (NC) soil states, characterizing a reloading region where strains are predominantly elastic from a region of irrecoverable plastic strains.

The relative magnitude of the pre-consolidation pressure is often described by a normalized parameter termed the overconsolidation ratio $OCR = \sigma'_p/\sigma'_{v0}$, in which σ'_{v0} is the current effective vertical stress in the ground.

In addition to the oedometer test, σ'_p (or OCR) can be assessed directly from field tests such as through the use of a piezocone, vane or dilatometer following research efforts developed during the 1980s (Marchetti, 1980; Wroth, 1984; Konrad & Law, 1987; Mayne, 1987; Crooks *et al.*, 1988; Mayne & Mitchell, 1988; Mayne & Bachus, 1988; Sandven *et al.*, 1988; Sully *et al.*, 1988). Unfortunately, it is generally recognized that large strain measurements provided by cone penetration or shear torsion are not very sensitive to the *stress history* (e.g. Baldi *et al.*, 1982 Lunne *et al.*, 1997; Schnaid *et al.*, 2016) and disregarding the primary influence of past straining in field measurements in-

Edgar Odebrecht, D.Sc., Associate Professor, Departamento de Engenharia Civil, Universidade do Estado de Santa Catarina, Joinville, SC, Brazil. e-mail: edgar@geoforma.com.br.
Fernando Schnaid, Ph.D., Full Professor, Departamento de Engenharia Civil, Universidade Federal do Rio Grande do Sul, Porto Alegre, RS, Brazil. e-mail: fernando@ufrgs.br.
Submitted on July 5, 2017; Final Acceptance on May 16, 2018; Discussion open until December 31, 2018.
DOI: 10.28927/SR.412179

roduces severe limitations in the accuracy of predictive methods of *OCR*.

Acknowledging the approximate nature of the correlations between q_c and *OCR*, a recommended practice to guide engineering judgment is to estimate the *OCR* from the undrained shear strength ratio ($s_u - \sigma'_{v0}$), as suggested by Schmertmann (1978) and Ladd *et al.* (1977). The method consists simply of estimating s_u from the CPT data and σ'_{v0} from soil profile to compute ($s_u - \sigma'_{v0}$). The ratio is then compared to the corresponding normally consolidated undrained shear strength, adopting Shansep's type of approach for comparison (Ladd *et al.*, 1977). Alternatively, predictions of the *OCR* directly from piezocone data can be made using either theoretical solutions or empirically based approaches (Senneset *et al.*, 1982; Wroth, 1984; Konrad & Law, 1987; Tavenas & Leroueil, 1987; Mayne, 1991; Schneider *et al.*, 2001; Long *et al.*, 2010). A brief overview of current practice is presented and discussed herein and new recommendations are provided for Quaternary clay sediments from the experience gathered in Brazil over the last decade.

3. Tubarão Coastline Sediments

Sedimentary deposits formed along the coastline of Brazil are mainly a product of the general Eustatic sea level variations over the last 1 million years, during the so called Quaternary Period (*e.g.* Angulo & Lessa, 1997; Angulo *et al.*, 1999 and 2006; Milne *et al.*, 2005). Sediments from the upper 20 m layers were predominantly formed after the most recent glaciation, during the last 8,000 years in the Holocene Period (Giannini, 1993; Nascimento, 2011). Located in the Southern Hemisphere and relatively close to the equator, these formations in Brazil are not influenced by glacial loading and unloading.

The diverse Holocene morphological features along the coast include lagoons and residual lakes, barriers, deltas and pre-existing incised valleys that have been flooded and filled. The deposition therefore results from transgression integrated bay-lagoon sedimentary systems formed behind a transgressive barrier during the Holocene maximum flooding (Giannini, 1993; Giannini *et al.*, 2007).

The geomorphological evolution of these areas has been comprehensively investigated using a combination of morphology, stratigraphic analysis of rotary push cores, vibracores and trenches with radiocarbon dating, taxonomic determination and taphonomic characterization of Holocene fossil mollusks (Guedes *et al.*, 2011; Giannini *et al.*, 1993, 2007), as well as geotechnical site investigation testing data (*e.g.* Schnaid, 2005; Mantaras *et al.*, 2014; Jannuzzi *et al.*, 2015). Figure 1 is used to illustrate how a bay along the coast evolved over the last 8000 years (Giannini *et al.*, 2010). The Holocene sedimentary succession began with deposits of transgressive sandsheets. These deposits correspond to the initial marine flooding surface that was formed while the relative sea-level rose at a higher rate

than the input of sediments, prior to the formation of the coastal barrier (Fig. 1a). The change from a bay to a lagoon system occurred at approximately 5500 and 4000 cal BP in the mid-Holocene highstand with the formation of the barrier during the falling of the sea level and the achievement of a balance between sea-level and sedimentary supply (Fig. 1b). The presence of this barrier was followed by a gentle decline in sea level and the initial emergence of back-barrier features restricted the hydro-dynamic circulation inside the bay. This geological process transformed the bay into a lagoon system (Fig. 1c). The final stage, during the last 1700 years, was marked by the increase of the back-barrier width, with the establishment of salt marshes, the arrival of the delta in the back-barrier, and the advance of aeolian dunes along the outer lagoon margins (Fig. 1d). These marine-lacustrine environmental conditions resulted in normally consolidated to lightly overconsolidated soft soils with high water content, some organic matter content, high compressibility and low shear strength properties.

Once this geological background is properly understood, specific prediction can be made of the local ground conditions which is generally based on independent results from geotechnical site investigation. Examples of how to link the geological information with the geotechnical data are given and possible interpretations of the stress history are explored.

4. Case Study

A comprehensive site investigation in the Tubarão Lagoon system located in southern Brazil is described as a means of developing possible ways for linking geological and geotechnical sciences. Geotechnical investigation comprises both field and laboratory tests. Piezocone, vane, dilatometer, shear wave velocity and SPT measurements were performed to identify the soil type and stratigraphy. Measured cone resistance q_c , sleeve friction f_s and pore pressure u_z , as well as dilatometer readings p_0 and p_1 are shown in Fig. 2, revealing a typical soil profile with superficial sand-silty layers, overlying an approximately 20 m thick, very soft, essentially normally consolidated clay layer. The normalized soil behavior index I_c proposed by Robertson (1990) and the dilatometer material index I_b proposed by Marchetti (1980) are also shown in Fig. 2. These indices are essentially CPT and DMT predictive methods of Soil Behaviour Type based directly on q_c and f_s measurements for the CPTU or on p_0 and p_1 pressures for the DMT.

The superficial layer 2 m to 3 m in thickness is characterized as silty-sand and sandy-silt soils ($1.90 < I_c < 2.82$), from 3 to 6 m the soil is predominantly sandy-silt, and below 6 m, the soil is typically clay ($2.82 < I_c < 3.22$). The piezometric profile is approximately hydrostatic with groundwater at a depth of 1 m. Shear wave velocity measurements and cone resistance show monotonic increase with depth. The Atterberg Limits and the *in situ* water contents are shown in this figure, a common feature begin that

water content is generally slightly greater than the liquid limit, and both are relatively constant with depth.

Thin wall, *stationary piston samplers* were used to retrieve undisturbed samples at depths of 5, 9, 13 and 16 m,

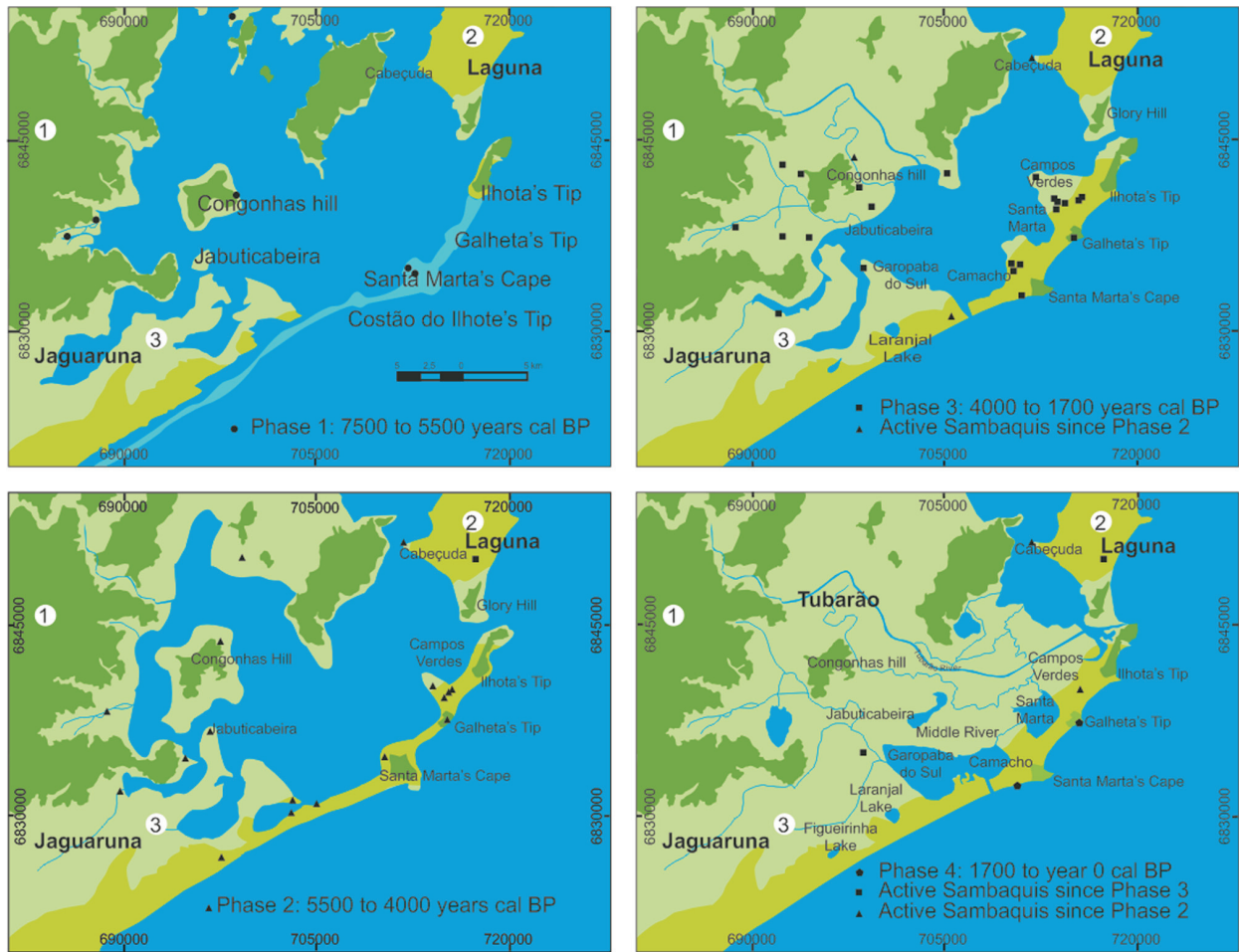


Figure 1 - The Tubarão Quaternary depositional system representative from the mid-south coast of Brazil (1-Rocky headlands or bedrock; 2-Sand Barrier and Back-barrier; 3-Delta Plain (modified from Giannini, 1993 and Carvalho do Amaral *et al.*, 2012). a) Deposits of transgressive sandsheets. b) Change from a bay to a lagoon system. c) Lagoon system. d) Current coastal conditions.

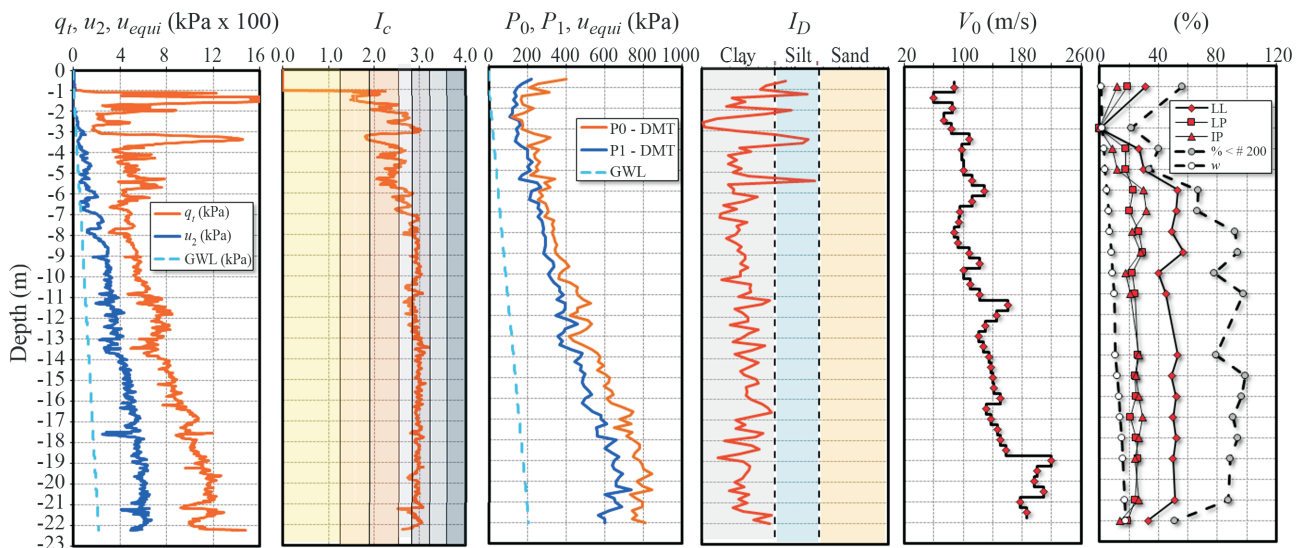


Figure 2 - Typical soil profile from CPTU and DMT measurements.

according to ASTM D1587 (2000). Incremental loading oedometer tests were performed according to the ASTM D2435 (2011) standard to determine the pre-consolidation pressure σ'_p , the compression index C_c , the recompression index C_r , and the coefficient of consolidation c_v .

Figure 3 combines the geotechnical profile to the paleoenvironmental reconstruction of the lagoon system of the area. Elemental and isotopic carbon and nitrogen analyses were conducted at the Stable Isotope Laboratory of CENA/USP (Nascimento, 2011) to characterize the sediment age of the different layers (estimated in time intervals and expressed in terms of time before measurement: BP = Before Present). The analysis performed by Giannini *et al.* (2010) is based on total organic carbon (TOC) content, total nitrogen (TN) content, and stable isotopes of carbon (d13C) and nitrogen (d15N) from peat, wood and organic matter. As previously discussed, the results suggest sedimentary processes formed by three facies, with depositions occurring during the last 8000 years (Nascimento, 2011).

A remarkable feature in the analysis of the data shown in Fig. 3 is the recognition that CPTU measurements capture the characteristic features of the three facies representative of the profile, reflecting the changes in aging and soil type. The oldest, fairly homogenous, lower clay layer, of depth ranging from 6 m to 22 m, is dated from 8013-7800 to 3838-3576 year cal BP and is identified by B_q values ranging from 0.4 to 0.6 and q_t increasing linearly with depth (representative of normally consolidated clays). The paleoenvironmental classification identifies a bay deposition

(BD) formed by clay particles with siliceous shells (Cs). Geochemical data indicative of the intermediate sediment layer is from the period of 2445-2306 year cal BP that was formed by transport sediments of the active channel of the Tubarão River (AC), deposited in sand and clay thin layers or lenses with occasional shells (SCs). These sand lenses are essentially drained reducing the B_q values to the range of 0.1 to 0.2. The superficial, recently deposited sediments (2563-2359 to 909-733 year cal BP are also layered (sand and clay), showing a predominantly drained response ($B_q \approx 0$).

5. Stress History

Correlations between the soil stress history and the piezocone measurements were established in terms of critical-state concepts, using either cone resistance or penetration pore pressure. For shoulder filter elements (u_2) the overconsolidation ratio can be expressed in terms of the normalized cone tip resistance $(q_t - u_2)/\sigma'_{v0}$ and the critical state material constants $M = (6\sin(\phi'))/(3 - \sin(\phi'))$ and $\Lambda = 1/(C_r/C_c)$ (e.g. Mayne, 1991):

$$OCR = \frac{\sigma'_p}{\sigma'_{v0}} = 2 \left[\frac{1}{1.95M + 1} \left(\frac{q_t - u_2}{\sigma'_{v0}} \right) \right]^{\frac{1}{\Lambda}} \quad (1)$$

In practice, under a number of simplifications and based on representative soil parameters, the predicted σ'_p is often expressed as:

$$\sigma'_p = k(q_t - \sigma'_{v0}) \quad (2)$$

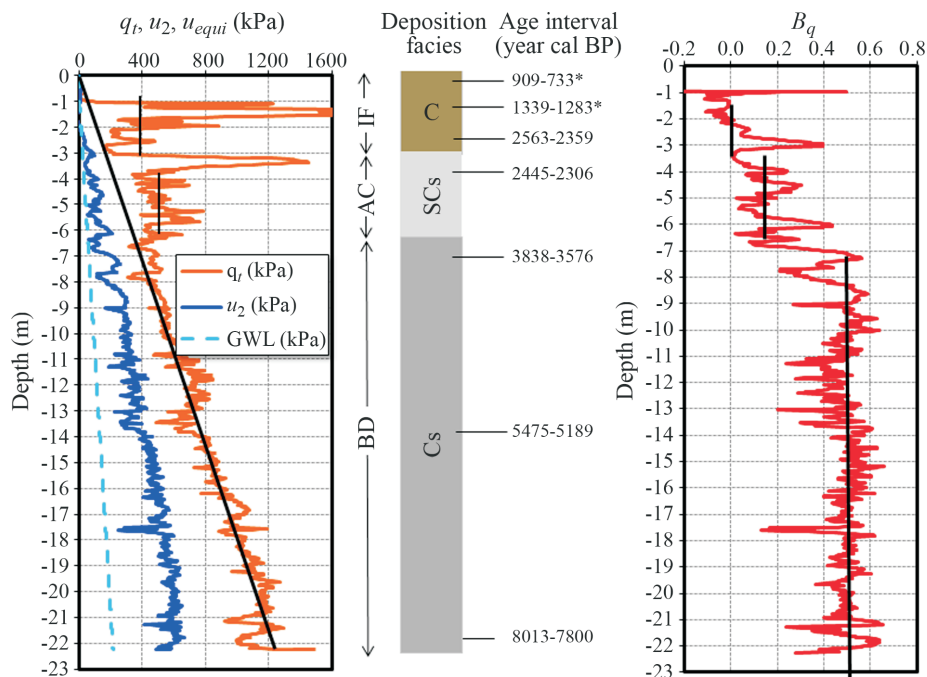


Figure 3 - CPTU profile combined to the paleoenvironmental reconstruction of the Tubarão lagoon system. (* nearby borehole; BD bay deposition; AC active channel; IF inter-channel fines; Cs clay with shells; SCs sand and clay layers with occasional shells; C clay).

where coefficient k is obtained from site specific correlations and is shown to range from 0.1 to 0.5 (e.g. Konrad & Law, 1987; Mayne & Holtz, 1988; Demers & Leroueil, 2002;).

The Tubarão case study provides a unique opportunity to evaluate this type of approach given the fact that the stress history of the deposit is known and supported by radiocarbon dating. The incremental loading oedometer test is the standard method of obtaining the pre-consolidation pressure in the laboratory and the measured values were used as a reference. Typical results of tests performed using a fixed-ring oedometer with drainage at the bottom and top of the test specimen are presented in Fig. 4. The test procedure includes overnight loadings under constant effective stress to determine the position of the virgin compression line using the Casagrande method (1936). The sample quality shown in the figure has been assessed by the $\Delta e/e_0$ ratio, where Δe is the change in void ratio during the recompression process to the *in situ* effective stresses and e_0 is the initial void ratio, as proposed by Lunne *et al.* (1997).

The field vane OCR was calculated using the lower limit of the proposed correlation of Mayne & Mitchell (1988) which, according to the authors experience, is consistent with Brazilian practice: $OCR = 4.5(s_u/\sigma'_{v0})$ for $0 < Z \leq 5$ m and $OCR = 3.8(s_u/\sigma'_{v0})$ for $5 < Z \leq 22$ m. Estimated OCR from dilatometer tests is based on Lunne *et al.* (1989), considering $OCR = (0.3K_D)^{1.17}$ for $(s_u/\sigma'_{v0}) < 0.8$ and $OCR = (0.27K_D)^{1.17}$ for $(s_u/\sigma'_{v0}) > 0.8$.

The calibrated value of the piezocone coefficient k is 0.22 for the soft clay layer (Cs). Note that $k = 0.22$ is easily justified. From the modified Cam Clay (Wroth, 1984), the relationship between s_u and OCR is expressed as:

$$\frac{s_u}{\sigma'_0} = \left(\frac{M}{2} \right) \left(\frac{OCR}{2} \right)^\lambda \quad (3)$$

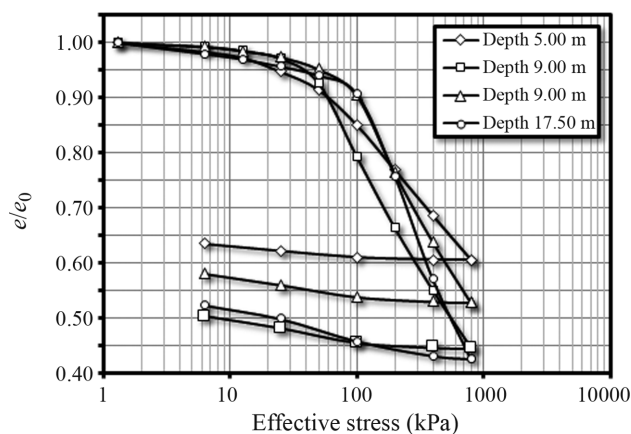
The value of s_u is calculated from the measured net penetration:

$$(q_t - \sigma'_{v0}) = s_u N_{KT} \quad (4)$$

assuming N_{KT} as derived by Baligh (1975) from the strain path method:

$$N_{KT} = 12 + \ln(I_r) \quad (5)$$

By combining these three equations and adopting $\phi' = 28^\circ$ and $I_r = 100$, the calculated value of $k = 1/(0.25MN_{KT}) = 0.22$. The rigidity index is defined as $I_r = G/s_u$, where G is the shear modulus and s_u is the undrained shear strength. In the present work an average I_r was estimated as 100 using strength and stiffness measured from the stress-strain response of unconsolidated undrained triaxial compression tests (UU). In general, s_u values from UU tests are similar to those measured by vane tests. Note that $I_r = 100$ is often adopted as the default value for soft



Depth (m)	e_0	σ'_p (kPa)	e at σ'_p (kPa)	$\Delta e/e_0$	Sample quality
5.00	0.946	20.00	0.901	0.048	Good to fair
9.00	1.664	32.00	1.600	0.038	Very good to excellent
13.00	1.110	44.00	1.080	0.027	Very good to excellent
17.50	1.734	57.50	1.620	0.066	Good to fair

Figure 4 - Incremental load oedometer test data at the Tubarão testing site.

clays and is in line with previous reported data in the region (Schnaid *et al.*, 1997). The friction angle was measured via the triaxial tests. In a similar approach, but using a different set of parameters, Mayne (2007) derived an average k value of 0.33.

The compilation of the piezocone, vane and oedometer testing data plotted together with the calculated s_u , σ'_p and OCR is shown in Fig. 5. The values of s_u and σ'_p increase linearly with depth and, in addition, the value of OCR is relatively constant and equal to unity below 6 m.

Reliable predictions of the pre-consolidation pressure and the overconsolidation ratio encouraged the use of the piezocone in other areas. Besides the Tubarão Site, similar research was performed in 12 different normally to slightly overconsolidated clay sites spread along the Brazilian coast (Fig. 6). Note that all tests were performed and supervised by the same personnel, following strictly the recommendations from the IRTP (1999) and international codes of practice (Eurocode, 1997; ASTM, 1999, ABNT, 1991) in order to minimize the possible sources of errors. The primary sources of data, as summarized in Table 1, are: (1) borehole logs with SPT and undisturbed (4" Shelby tubes) samples, (2) CPTU soundings, and (3) laboratory consolidation and shear strength tests obtained in a variety of locations. Sample quality has been assessed from the change in the void ratio during the recompression process to the *in situ* effective stresses, as already mentioned.

The collected data allowed for a direct comparison between the laboratory measured pre-consolidation pressure σ'_p and the net field penetration resistance $q_t - \sigma'_{v0}$, as presented in Fig. 6, showing that there is no unique average trend to correlate these quantities. The poor correlation in

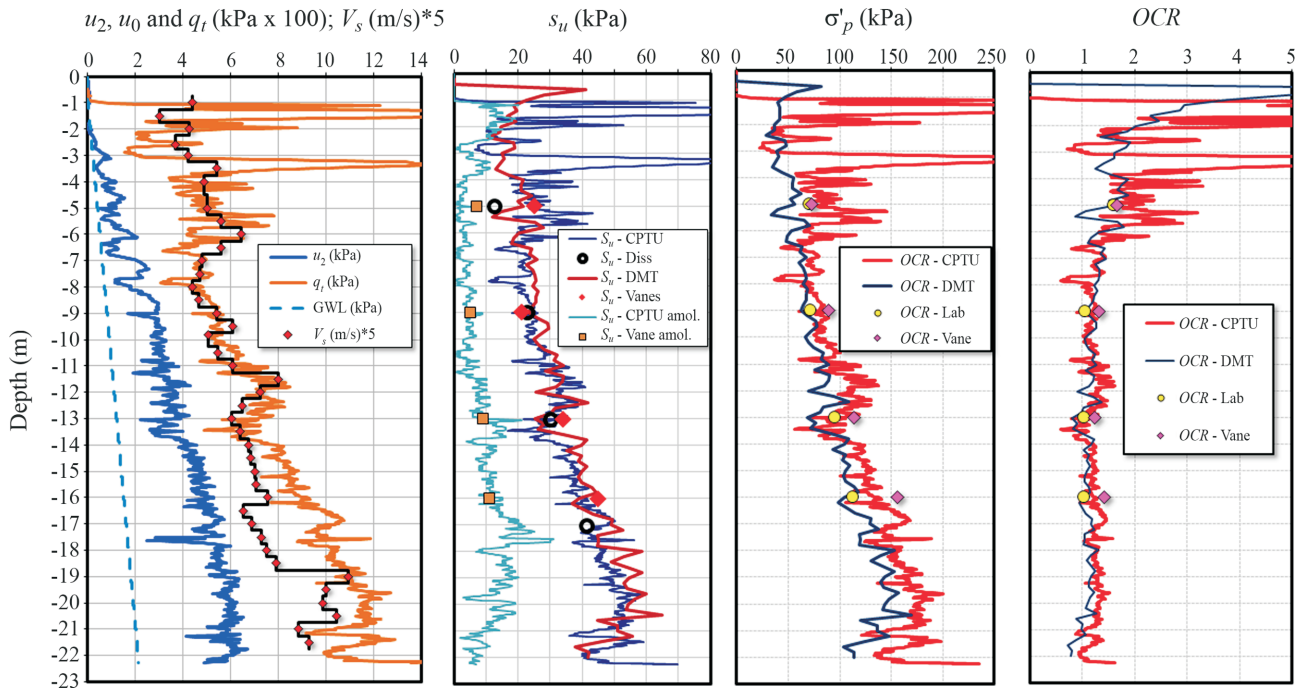


Figure 5 - Strength and stress history of the Tubarão lagoon system.

Table 1 - Summary of the site tests for 166 samples.

State	Site	Sample number	Sample quality	e_o	OCR	ω (%)	LL (%)	LP (%)	PI (%)	k	Reference
São Paulo	Santos	16	V-E = 4	{1.77}	{1.33}	{60}	{79}	{39}	{40}	{0.18}	Present work
			G-F = 9	[3.42]	[2.32]	[113]	[124]	[65]	[59]	[0.25]	
			Po = 3	(1.15)	(0.91)	(35)	(26)	(17)	(9)	(0.07)	
			V-P = 0								
Rio Grande do Sul	Porto Alegre	8	V-E = 3	{1.77}	{1.35}	{122}	{120}	{60}	{60}	{0.31}	Schnaid (2005)
			G-F = 4	[3.42]	[1.76]	[130]	[125]	[75]	[75]	[0.32]	
			Po = 1	(1.15)	(1.17)	(60)	(100)	(50)	(50)	(0.21)	
			V-P = 0								
Rio de Janeiro	Barra da Tijuca CM1 & CM2	11	V-E=	{4.84}	{1.03}	{192}	{196}	{50}	{146}	{0.14}	Baroni (2010)
			G-F = 6	[10.67]	[2.31]	[784]	[610]	[173]	[497]	[0.24]	
			Po = 5	(1.42)	(0.9)	(56)	(67)	(20)	(47)	(0.07)	
			V-P = 0								
Rio de Janeiro	Barra da Tijuca Gleba F	11	V-E = 2	{5.47}	{1.15}	{200}	{169}	{47}	{124}	{0.14}	Baroni (2010)
			G-F = 5	[12.37]	[8.77]	[670]	[521]	[212]	[308]	[0.24]	
			Po = 4	(3.84)	(0.53)	(167)	(147)	(38)	(95)	(0.11)	
			V-P = 0								
Recife	Clube Internacional	11	-	{1.66}	{1.30}	{90}	{70}	{36}	{35}	{0.28}	Coutinho <i>et al.</i> (2000)
				[2.47]	[2.08]	[125]	[99]	[44]	[63]	[0.42]	
				(1.11)	(0.89)	(51)	(45)	(24)	(17)	(0.20)	
Sergipe	Sergipe	34	-	{1.84}	{1.67}	{66}	{66}	{31}	{34}	{0.31}	Brugger <i>et al.</i> (1994)
				[2.05]	[2.26]	[75]	[85]	[34]	[50]	[0.40]	
				(1.51)	(1.01)	(53)	(52)	(25)	(28)	(0.15)	
Rio de Janeiro	Barra da Tijuca	8	V-E = 6	{5.42}	{1.45}	{166}	{128}	{45}	{86}	{0.20}	Teixeira <i>et al.</i> (2012)
			G-F = 2	[7.01]	[3.00]	[269]	[193]	[67]	[127]	[0.26]	
			Po = 0	(3.55)	(1.20)	(136)	(115)	(37)	(69)	(0.17)	
			V-P = 0								

Table 1 (cont.)

State	Site	Sample number	Sample quality	e_0	OCR	ω (%)	LL (%)	LP (%)	PI (%)	k	Reference
Rio de Janeiro	Sarapuí	37	V-E = 1 G-F = 14 Po = 22 V-P = 0	{3.38} [4.46] (2.46)	{1.70} [3.10] (1.30)	{133} [171] (106)	{113} [145] (86)	{50} [73] (33)	{59} [91] (44)	{0.19} [0.23] (0.16)	Ortigão (1980)
Santa Catarina	Navegantes	19	V-E = 2 G-F = 11 Po = 5 V-P = 1	{2.24} [2.84] (0.98)	{1.54} [3.89] (0.49)	{79} [100] (36)	-	-	-	{0.20} [0.29] (0.13)	Present work
Rio de Janeiro	Barra do Furado	3	V-E = 0 G-F = 3 Po = 0 V-P = 0	{2.32} [4.46] (1.71)	{1.40} [1.92] (1.11)	{83} [187] (56)	{91} [117] (63)	{38} [47] (32)	{58} [70] (24)	{0.20} [0.21] (0.18)	Present work
Santa Catarina	Araquari	4	V-E = 1 G-F = 1 Po = 2 V-P = 0	{1.60} [1.71] (1.41)	{1.53} [1.91] (1.04)	{59} [61] (47)	{69} [75] (55)	{32} [34] (20)	{35} [41] (28)	{0.20} [0.25] (0.15)	Present work
Santa Catarina	Tubarão	4	V-E = 1 G-F = 1 Po = 2 V-P = 0	{1.35} [1.80] (0.70)	{1.18} [1.60] (1.04)	{80} [98] (33)	{45} [27] (17)	{22} [29] (18)	{22} [32] (9)	{0.20} [0.22] (0.18)	Present work

Legend: V-E (Very good to Excellent); G-F (Good to Fair); Po (Poor); V-P (Very Poor); { average value }; [maximum value] and (minimum value).

given locations ($r^2 < 0.5$) is partially attributed to sample quality; however, as demonstrated later, sample quality is not the only factor to be considered. Part of the observed scatter may be attributed to organic matter influence on the measured q_p , inducing variations in the σ'_p vs. q_t relationship.

Because there is no unique relationship between q_t and changes in σ'_p , it becomes evident that this correlation involves a more complex measurement-property dependence. From a purely empirical basis, some attempts are made to smooth the observed trend between q_t and σ'_p (or OCR) by incorporating the influence of the void ratio e_0 .

In Quaternary clays, it is well established that σ'_p obtained in the conventional laboratory oedometer tests reduces with increasing e_0 , as shown in Fig. 7 (modified from Massad, 2009). This observation suggests that strengthening of the soil structure with time due to effects of secondary compression are not so severe in recently deposited clays and that pre-consolidation pressures can be associated to void ratio only. Departing from this experience, an attempt is made to express the coefficient k as a function of void ratio, as illustrated in Fig. 8. The values of k reduce with the increase in void ratio from 0.4 to 0.1, yielding a mean value of 0.22 (recommended by Schnaid *et al.*, 1997 and Mantaras *et al.*, 2014 and calculated from $\phi' = 28^\circ$ and $I_r = 100$). Note that the 166 samples database comprises many specimens of poor-quality retrieved from soils of

very high void ratio (greater than 4), but disregarding results from the low quality samples does not change the aforementioned conclusions. It is also worth mentioning that this range of k values is similar to that reported by Larsson & Mulabdic (1991) for 9 Swedish clays, which suggest an alternative correlation of k tracked with liquid limit.

This set of oedometer tests for the Quaternary clays yields the following equation for $(q_t - \sigma_{v0})$ and e_0 :

$$\sigma'_p = k(q_t - \sigma_{v0}) = (0.282e_0^{-0.37})(q_t - \sigma_{v0}) \quad (6)$$

that produces k values reducing typically from 0.5 to 0.1, with a mean value of 0.22 (Fig. 8).

Alternatively, Eq. 6 can be used to predict the overconsolidation ratio directly:

$$OCR = (0.282e_0^{-0.37}) \frac{(q_t - \sigma_{v0})}{\sigma'_{v0}} \quad (7)$$

To conclude, Fig. 9 exemplifies the applicability of Eqs. 7 and 8 to the described ground conditions reported from the Tubarão testing site in section 3. In this figure, the net cone resistance $(q_t - \sigma_{v0})$, overconsolidation ratio OCR and parameter k (Eq. 6) are plotted against depth. Although $(q_t - \sigma_{v0})$ increases with depth (showing a direct dependency on mean effective stress), the OCR remains approximately constant and equal to unity, representing the normally consolidated conditions reported by the sedimentation process.

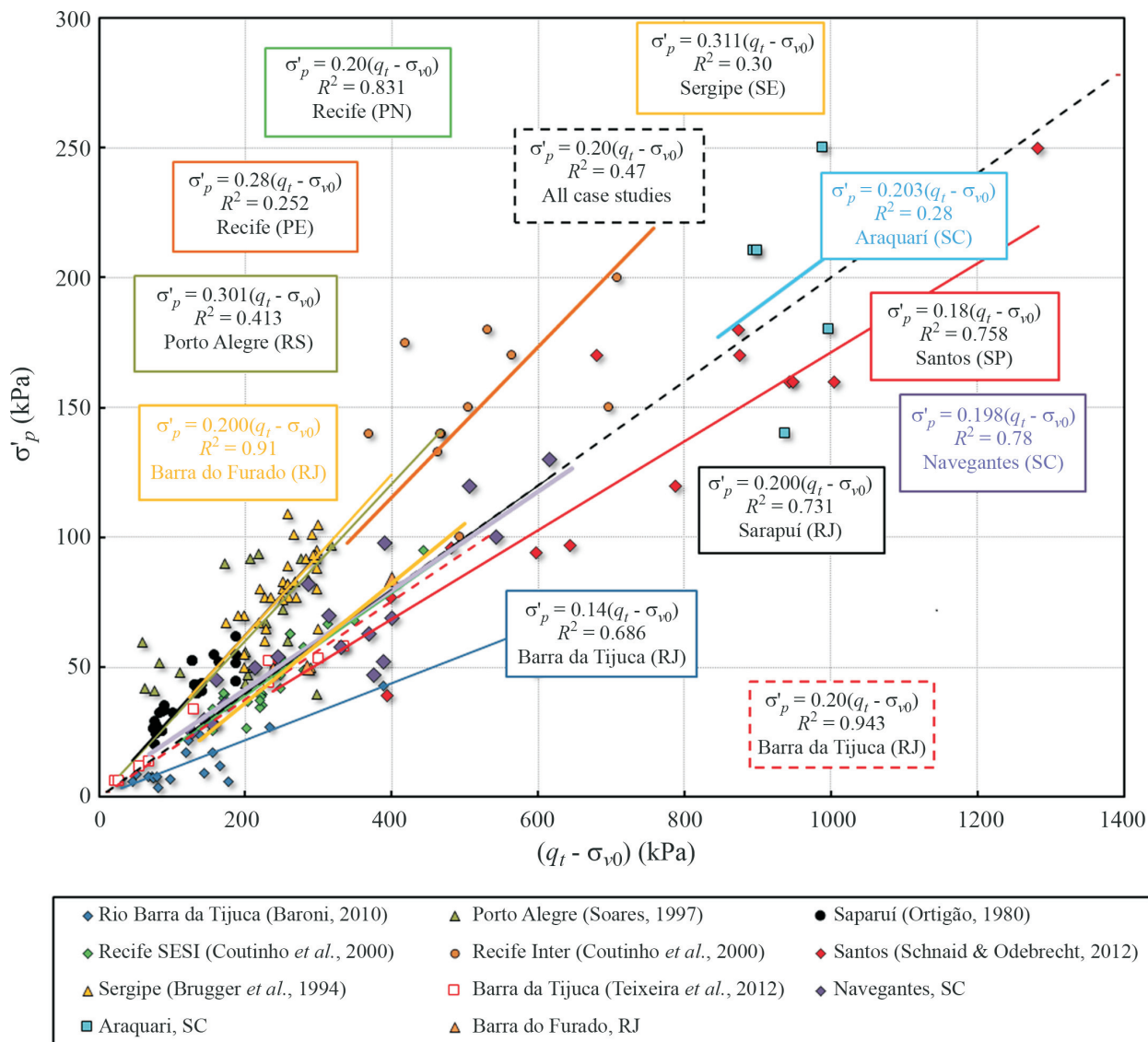


Figure 6 - Correlation of pre-consolidation pressure σ'_p and the net field penetration resistance $q_t - \sigma_{v0}$ for Quaternary Brazilian clays.

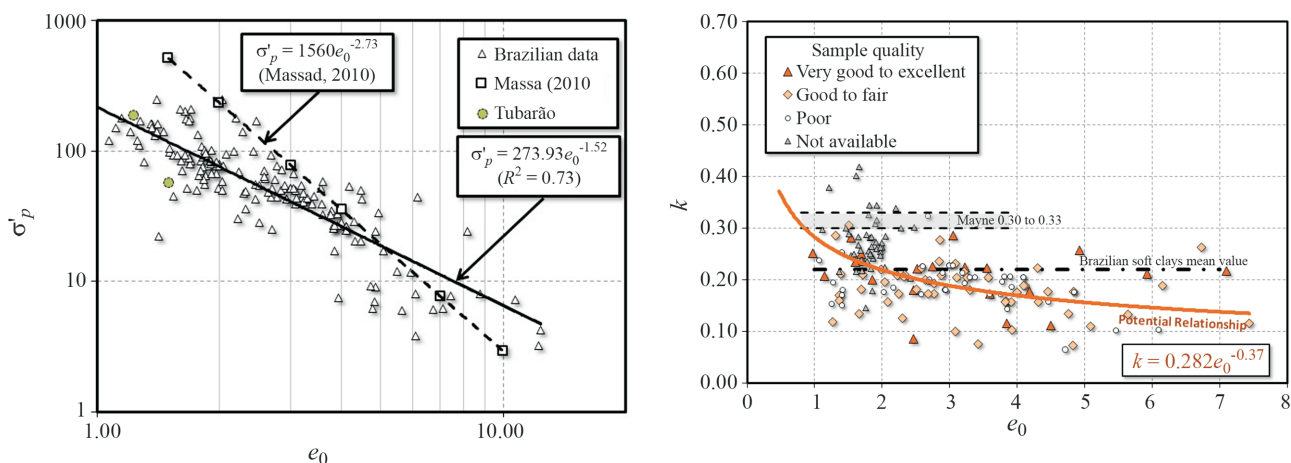


Figure 7 - Variation of e_0 vs. σ'_p (modified from Massad, 2009).

Figure 8 - Variation of k with void ratio for Brazilian low sensitivity clays.

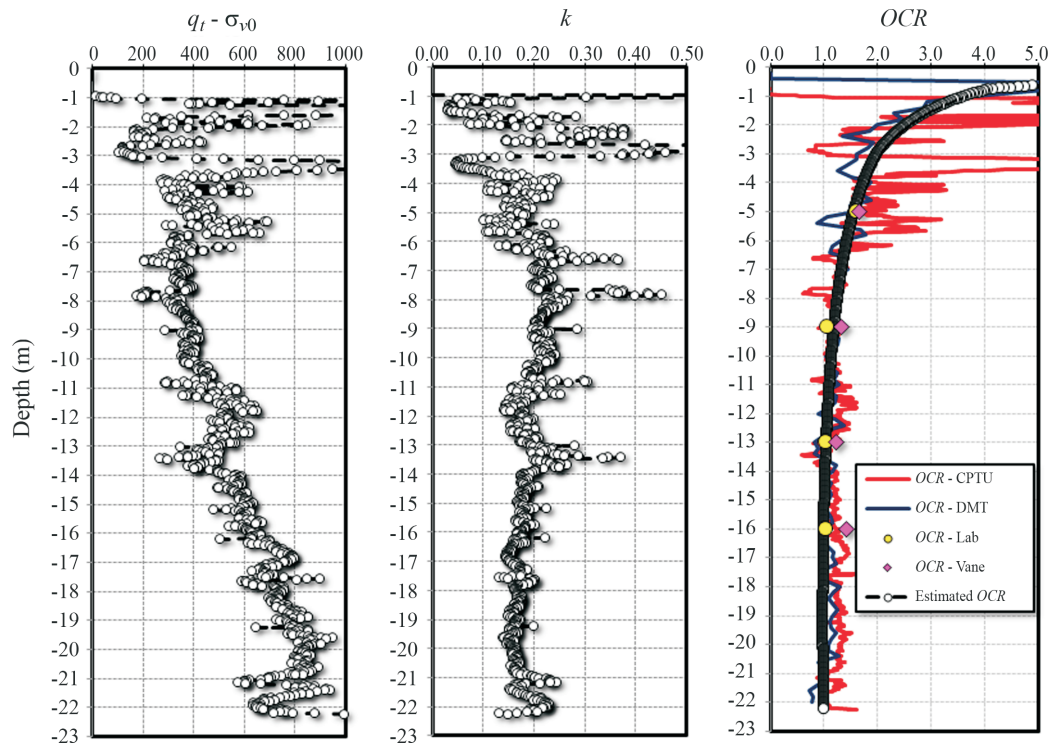


Figure 9 - Variation of k and OCR with depth for the Tubarão Experimental Testing Site.

Eq. 7 produces predicted OCR values in conformity with DMT and oedometer tests. The average k value calculated as a function of void ratio is on the order of 0.22 and is constant with depth, being lower than the 0.3 value often assumed in design (Chen & Mayne, 1996).

6. Concluding Remarks

The present paper presents detailed characterization of Quaternary, normally to slightly overconsolidated clay deposits, including high quality data from field and laboratory tests that comprises profiles with void ratios ranging from 1.0 to 12 and water contents from 30% to 400%. Based on tests from 12 well-documented sites it was found that piezocone field data should be used with caution when predicting the pre-consolidation pressure σ'_p (or OCR). A possible explanation is that σ'_p is strongly affected by soil structure emerging from the effects of secondary compression, aging and cementation, whereas q_t (as a large strain measurement) is not very sensitive to these effects. As a consequence, the ratio of σ'_p and q_t cannot be expressed as a constant, as often assumed in engineering practice. Correlations between σ'_p and q_t should be preferably expressed through the void ratio, which is an indirect form of compensating for the lack of sensitivity of cone penetration to stress history. In terms of engineering practice, an expression was proposed for interpretation of piezocone tests that provides realistic first order estimates of σ'_p .

References

- ABNT (1991). Cone Penetration Test: CPT, MB-3406. Brazilian Standard.
- Angulo, R.J. & Lessa, G.C. (1997). The Brazilian sea level curves: A critical review with emphasis on the curves from Paranaguá and Cananéia regions. *Marine Geology*, 140:141-166.
- Angulo, R.J.; Giannini, P.C.F.; Suguio, K. & Pessenda, L.C.R. (1999). Relative sea level changes in the last 5500 years in southern Brazil (Laguna-Imbituba region, Santa Catarina State), based on vermetid ^{14}C ages, Amsterdam. *Marine Geology*, 159:323-339.
- Angulo, R.J.; Lessa, G.C. & Souza, M.C. (2006). A critical review of mid-to late-Holocene sea level fluctuations on the eastern Brazilian coastline. *Quaternary Science Reviews*, 25:486-506.
- ASTM (1999). Standard Test Method for Penetration Test and Split Barrel Sampling of Soil, D1586.
- ASTM (2011). Standard Test Methods for One-Dimensional Consolidation Properties of Soils Using Incremental Loading, D2435.
- ASTM (2000). Standard Practice for Thin-Walled Tube Sampling of Soils for Geotechnical Purposes, ASTM D1587.
- Baldi, G.; Bellotti, R.; Ghionna, V.N.; Jamiolkowski, M. & Pasqualini, E. (1982) Design Parameters for sand from CPT. Proc. 2nd European Symp. On Penetration Testing, ESOPT-II, Ameterdam, v. 2, pp. 425-432.

- Baligh, M. M. (1975). "Theory of deep site static cone penetration resistance", Research Report R75-56, Dept. of Civil Engg., MIT, Cambridge, 141p.
- Baroni, M. (2010). Geotechnical site investigation on Barra da Tijuca very soft organic clay. M.Sc. Thesis, Federal University of Rio de Janeiro, Brazil (in Portuguese).
- Brugger, P.J.; Almeida, M.S.S.; Sandroni, S.S.; Brant, J.R.; Lacerda, W.A. & Danziger, F.A.B. (1994). Geotechnical parameters of the Sergipe soft clay. Proc. 10th Brazilian Conf. Soil Mech. Found. Engng., v. 1, pp. 539-546.
- Burland, J.B. (1990). On the compressibility and shear strength of natural clays. *Geotechnique*, 40(3):329-378.
- Carvalho do Amaral, P.G.; Giannini, P.C.F.; Sylvestre, F. & Pessenda, L.C.R. (2012). Paleoenvironmental reconstruction of a late Quaternary lagoon system in southern Brazil (Jaguaruna region, Santa Catarina state) based on multi-proxy analysis, *Journal of Quaternary Science*, 27(2):181-191.
- Casagrande, A. (1936). The determination of the pre-consolidation load and its practical significance. *International Conference on Soil Mechanics and Foundation Engineering*, Cambridge, v. 3, pp. 60-54.
- Chen, B.S. & Mayne, P.W. (1996). Statistical relationships between piezocone measurements and stress history of clays. *Canadian Geotech. J.*, 33(3):488-498.
- Coutinho, R.Q.; Oliveira, J.T.R. & Oliveira, A.T.J. (2000). Geotechnical properties of Recife soft clays. *Soils & Rocks*, 23(3):177-204.
- Crooks, J.H.A.; Been, D.E. & Jefferies, M.G. (1988). CPT interpretation in clays. Proc. Int. Symp. on Penetration Testing, ISOPT. Balkema Publishing., Rotterdam, v. 2, p. 715-722.
- Demers, D. & Leroueil, S. (2002). Evaluation of preconsolidation pressure and the overconsolidation ratio from piezocone tests of clay deposits in Quebec. *Canadian Geotechnical Journal*, 39(1):174-192.
- Eurocode 7 (1997). European Committee for Standardization: Geotechnical Design Part 1. Geotechnical Design General Rules, Part 3. Design Assisted by Field Testing.
- Giannini, P.C.F. (1993). The costal Quaternary Depositional system in the southern Brazil region of Jaguaruna and Imbituba region. PhD Thesis, University of São Paulo, Brazil, 439 p.
- Giannini, P.C.F.; Sawakuchi, A.O.; Martinho, C.T. & Tatum, S.H. (2007). Eolian depositional episodes controlled by late Quaternary relative sea level changes on the Imbituba-Laguna coastal zone (southern Brazil). *Marine Geology*, 237:143-168.
- Giannini, P.C.F.; Villagram, X.S.; Fornani, M.; Nascimento, D.R.; Assunção, D.C.; DeBlasis, P. & Amaral, P.G.C. (2010). Interaction between sedimentary evolution and pre-historic human occupation in the southern coast of Santa Catarina, Brazil. *Museum Emilio Goeldi Journal*, 5(1):105-128.
- Guedes, C.C.F.; Giannini, P.C.F.; Sawakuchi, A.O.; DeWitt, R.; Nascimento Jr, D.R.; Aguiar, V.A.P. & Rossi, M.G. (2011). Determination of controls on Holocene barrier progradation through application of OSL dating: The Ilha Comprida Barrier example, Southeastern Brazil. *Marine Geology*, 28(5):1-16.
- IRTP (1999) ISSMFE Technical Committee TC16 ground property characterization from in situ testing. International Reference Test Procedure (IRTP) for the cone penetration testing (CPT) and cone penetration test with pore pressure (CPTU). Proc. XIIth ESCMGE, Balkema, Amsterdam, pp. 2195-2222.
- Jannuzzi, G.M.F.; Danziger, F.A.B. & Schumann, M.M. (2015). Geological-geotechnical characterization of Sarapuí II clay. *Engineering Geology*, 190:77-86.
- Konrad, J.M. & Law, K. (1987). Preconsolidation pressure from piezocone tests in marine clays. *Geotechnique*, 37(2):177-190.
- Ladd, C.C.; Foott, R.; Ishihara, K.; Schlosser, F. & Poulos, H.G. (1977). Stress-deformation and strength characteristics: State-of-the-Art Report. Proc. 9th Int. Conf. Soil Mech. Found. Engn. Tokyo, v. 2, pp. 421-494.
- Larsson, R. & Mulabdic, M. (1991) Piezocone test in clay. Swedish Geotechnical Institute, Linköping Report, 42.
- Long, M.; Guidjonsson, G.; Donohue, S. & Hagberg, K. (2010). Engineering characterization of Norwegian glaciomarine silt. *Engineering Geology*, 110:51-65.
- Lunne, T.; Robertson, P.K. & Powell, J.J.M. (1997). Cone penetration testing in geotechnical practice. Blackie Academic & Professional, 312 p.
- Lunne, T.; Lacasse, S. & Rad, D.S. (1989). SPT, CPT, pressuremeter testing and recent developments on in situ testing of soils. General report Session. Proc. 12th Int. Conf. soil Mech. Found. Eng., pp. 2339-2404.
- Mantaras, F.M.B; Odebrecht, E. & Schnaid, F. (2014). Using piezocone dissipation test to estimate the undrained shear strength in cohesive soil. Proc. 3th Int. Symp. on the Cone Penetration Testing, Las Vegas, Nevada, pp. 323-330.
- Marchetti, S. (1980). In situ tests by flat dilatometer. *J. Geotech. Engng. Div.*, 106(GT3):299-321.
- Massad, F. (2009). São Paulo marine soils. *Oficina de Textos*, São Paulo, 248 pp.
- Mayne, P.W.; Coop, M.R.; Springman, S.; Huang, A.B. & Zornberg, J. (2009). Geotechnical behavior and testing. State-of-the-art paper (SOA-1). Proc. Int. Conf. Soil Mech. Geotech. Eng., ICSMGE, 17, Alexandria, Egypt. Proceedings Rotterdam: Millpress/IOS Press, v. 4, pp. 2777-2872.
- Mayne, P.W. (1987). Determining preconsolidation and penetration pore pressure from DMT contact pressures. *ASTM Geotech. Testing Journal*, 10(3):146-150.

- Mayne, P.W. (1991). Determination of OCR in clays by piezocone tests using cavity expansion and critical state concepts. *Soil & Foundation*, 31(1):65-76.
- Mayne, P.W. (2007). NCHRP Synthesis 368: Cone Penetration Testing. Transportation Research Board, Washington, DC, 118 p.
- Mayne, P.W. & Bachus, R.C. (1988). Profiling OCR in clays piezocone sounding. *Proc. Int. Symp. on Penetration Testing*, ISOPT 1. Balkema Publ., v. 2, pp. 857-864.
- Mayne, P.W. & Holtz, R.D. (1988). Profiling stress history from piezocone sounding. *Soil & Foundation*, 28(1):12-28.
- Mayne, P.W. & Mitchell, J.K. (1988). Profiling of overconsolidation in clays by field vane. *Canadian Geotech. J.*, 25:150-157.
- Milne, G.S.; Long, A.J. & Bassett, S.E. (2005). Modeling Holocene relative sea-level observations from the Caribbean and South America. *Quaternary Science Reviews*, 24:1183-1202.
- Nascimento Jr., D.R. (2011). The Holocene sedimentary evolution of the Tubarão river in the state of Santa Catarina, Brazil. Ph.D. Thesis, University of São Paulo, 230 pp. (in Portuguese).
- Ortigão, J.A.R. (1980). Failure of a trial embankment on Rio de Janeiro gray clay. D.Sc. Thesis, Federal University of Rio de Janeiro, Brazil (in Portuguese).
- Robertson, P.K. (1990). Soil classification using the cone penetration test. *Canadian Geotechnical Journal*, 27(1):151-158.
- Sandven, R.; Senneset, K. & Janbu, N. (1988). Interpretation of piezocone tests in cohesive soils. *Proc. Int. Symp. Penetration Testing*, ISOPT-I, Balkema, v. 2, pp. 939-953.
- Schmertmann, J.H. (1978). Guidelines for cone penetration test, Performance and Design. US Federal Highway Administration, Washington, DC, Report FHW-TS-78-209.
- Schneider, J.A.; Mayne, P.W. & Rix, G.J. (2001). Geotechnical site characterization in the greater Memphis area using cone penetration tests. *Engineering Geology*, 62:169-184.
- Schnaid, F. (2005). Geo-characterization and properties of natural soils by in situ tests. *Proc. Int. Conf. on Soil Mech. and Geotech. Engng.*, Osaka, Millpress, v. 1, pp. 3-47.
- Schnaid, F. & Odebrecht, E. (2012) Soil investigation for foundation engineering. 2nd ed. Oficina do Textos, São Paulo, 553 p. (in Portuguese).
- Schnaid, F.; Sills, G.C.; Soares, J.M. & Nyirenda, Z. (1997). Predictions of the coefficient of consolidation from piezocone tests. *Can. Geotech. J.*, 34(2):143-159.
- Schnaid, F.; Odebrecht, E.; Sosnoski, J. & Robertson, P.K. (2016). Effects of test procedure on flat dilatometer test (DMT) results in intermediate soils. *Canadian Geotechnical Journal*, 10.1139/cgj-2015-0463.
- Senneset, K.; Janbu, N. & Svano, G. (1982). Strength and deformation parameters from cone penetrometer tests. *Proc. 2nd European Symp. on Penetration Testing*. Amsterdam, v. 2, pp. 863-870.
- Soares, J.M.D. (1997). Characterization of the Porto Alegre soft clay deposits. D.Sc. Thesis, Federal University of Rio Grande do Sul, Brazil (in Portuguese).
- Sully, J.P.; Campanella, R.G. & Robertson, P.K. (1988). Overconsolidation ratio of clays from penetration pore pressure. *J. Geotech. Engng*, ASCE, 114(2):209-216.
- Tavenas, F. & Leroueil, S. (1987). State-of-the-art on laboratory and in situ stress-strain-time behavior of soft clays. *Proc. Int. Symp. on Geotech. Engng. of Soft Soil*, Mexico City, v. 2, pp. 1-46.
- Teixeira, C.F.; Sayão, A.S.F.J. & Sandroni, S.S. (2012). Evaluation of sample quality in the Barra da Tijuca soft clay. *Proc. XVI Brazilian Conference Soil Mech. Geotech. Engng*, Brazil, pp. 15-23.
- Wroth, C.P. (1984). The interpretation of in situ soil test. 24th Rankine Lecture. *Géotechnique*, 34(4):449-489.

Case Studies

Soils and Rocks
v. 41, n. 2

Heterogeneity Evaluation of Soil Engineering Properties Based on Kriging Interpolation Method. Case Study: North East of Iran, West of Mashhad

M. Etemadifar, N.S. Vaziri, I. Aghamolaie, N. Hafezi Moghaddas, G.R. Lashkaripour

Abstract. Many sciences are confronted with uncertainty in their application field. Therefore, the use of statistics plays an important role for creating a partial model of the whole in most practical cases. Preparing a dispersion map, merging spatial statistics and geographic information systems (GIS), is very useful in geotechnical engineering. Interpolation is one of the usual methods to prepare these maps that has many different types. The ordinary kriging which is used in this paper is one of the most popular interpolation methods. This method is usually used to predict possible changes of an unknown variable using known parameters. In general, geostatistical estimation is a process by which one can obtain the value of a quantity in points with unknown coordinates using the same quantity in other points with definite coordinates. In this paper with information about the boreholes drilled in West Mashhad (North East of Iran), the specification of areas without borehole log is determined using interpolation method, drawing of kriging maps including soil texture, percentage of passing No. 200 sieve, standard penetration numbers, dry density, effective SPT area and the use of geostatistical techniques.

Keywords: geostatistics, kriging, layering, variogram, Mashhad, SPT.

1. Introduction

In conventional methods of geotechnical study, identification of sub-surface layers and determination of the layers profile are carried out indirectly through seismic methods and directly with drilling, insitu and laboratory tests (Low & Zaccheo, 1990).

Determination of the depth and materials of the sub-surface layers is usually done with respect to the results of insitu tests, such as inside borehole seismic tests indirectly and some local tests such as penetrometric measurement with SPT method directly, in areas with drilling information and it is done using interpolation methods and engineering judgment in areas without drilling information. In these cases, surveys are mainly based on visual observation and comparison of the results of these tests, which, of course, is a complex task and requires a lot of skill and experience (Huntley, 1990). Using geostatistical methods increased in recent years for this purpose (Taj al-Din, 1997).

Geostatistics is a branch of practical statistics science that is able to provide a wide range of statistical estimators for the desired property at areas without sampling data, using information from the areas with sampling information (Bahri & Khosravi, 2017; Davidovic *et al.*, 2010; Hengl, 2007). Due to geological conditions, data are not independent in geostatistics and have correlation to a certain distance. This branch of statistics has been widely devel-

oped around the world from a few decades ago, especially in countries with mining technology and has proven its efficiency in many cases (Taj al-Din, 1997).

Although the main part of geostatistics studies has been concerned with the issue of estimating mineral deposits, different practical research has been done in various geological sciences, geophysics and recently in geotechnics (Madani, 1994).

2. Research Method

Here it is necessary to explain some of the important concepts of geostatistics. In geostatistics, if the difference between the different values of a sample is to be associated with their location, it is called the region variable, which is represented by $Z(x)$. The region variable is a variable which has been distributed in three dimensional space and has spatial dependence and can be discussed in geostatistical studies.

One of the most important hypotheses in geostatistics is the inherent assumption. Based on this assumption, the variance of the differences between two regionalized variables is constant in one given direction for every distance h and does not depend on their location. For example, suppose two variables, Z_1 and Z_2 , for two points at a distance h in one given direction (*e.g.* north-south) on the ground and ΔZ being the difference between them. If for any other two points at a distance h in this direction, we determine values

Mahin Etemadifar, M.Sc., Abpouy Consulting Engineering Company, Mashhad, Iran. e-mail: etemadifar.net7@gmail.com.

Nasibeh Sadat Vaziri, M.Sc. Student, Department of Geology, Faculty of Science, Ferdowsi University of Mashhad, Mashhad, Iran. e-mail: nasibeh@gmail.com.

Iman Aghamolaie, Ph.D. Student, Department of Geology, Faculty of Science, Ferdowsi University of Mashhad, Mashhad, Iran. e-mail: imaneng189@gmail.com.

Naser Hafezi Moghaddas, Ph.D., Professor, Department of Geology, Faculty of Science, Ferdowsi University of Mashhad, Mashhad, Iran. e-mail: nhafezi@um.ac.ir.

Gholamreza Lashkaripour, Ph.D., Professor, Department of Geology, Faculty of Science, Ferdowsi University of Mashhad, Mashhad, Iran. e-mail: lashkaripour@um.ac.ir.

Submitted on May 4, 2017; Final Acceptance on May 16, 2018; Discussion open until December 31, 2018.

DOI: 10.28927/SR.412193

of $Z(x)$, variance of the difference between these two variables ΔZ will be constant and do not depend on their location in which:

$$\text{var}[z(x+h) - z(x)] = 2\gamma(h) \tag{1}$$

$\gamma(h)$ which is typically called variogram is variance which depends on distance. It is one of the most important concepts in geostatistics and some definitions and concepts of geostatistics are explained based on it. If we have $N(h)$ pairs of samples with a distance of “ h ” from each other then the experimental variogram function will be given by Eq. 2.

$$\gamma(h) = \frac{1}{2n(h)} \sum_{i=1}^{N(h)} [Z(x_i) - Z(x_i + h)]^2 \tag{2}$$

Of course it should be noted that the above function is a vector function hence its values along different direction are computable. In order to calculate $\gamma(h)$, it is better sampling to be done on a regular basis and at approximately equal intervals in each direction as much as possible.

In the variogram model, the value of $\gamma(h)$ often increases by increasing the distance h , and this condition continues to a certain distance (sill), from then the values will be fixed (Fig. 1). This indicates the dependence of the samples to a certain distance. In the sill $\gamma(h)$ remains constant with increasing distance.

A distance within which samples are related on each other is called the effective area. The maximum value $\gamma(h)$ in the effective area is called the variogram sill.

In geostatistics, in the effective area domain, statistical estimators are used for determining the desired variables in such a way that the estimate has the lowest mean error. The ordinary kriging, one of the most important estimators in geostatistics (which is used in this research), is based on estimating with the lowest variance of the estimation error.

The semi-variogram is one of the main tools of geostatistics for investigating the spatial changes and properties of parameters. Any semi-variogram is determined by

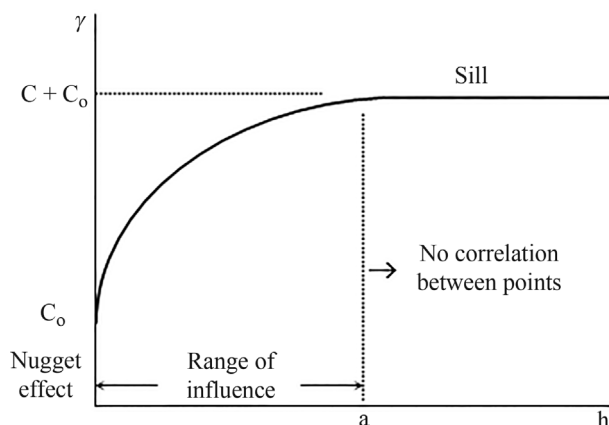


Figure 1 - Different parts of a variogram curve.

its parameters, *i.e.* nugget effect, effective area or effective radius and sill. After calculating the experimental directional semi-variograms and before the estimating operation, it is necessary to fit the most suitable theoretical models to them and get a continuous model valid for all possible directions.

In this study, the main goal is to determine from what distance from the borehole for every direction around a given borehole as a base point, no considerable variations in layering occurs (*i.e.* the vicinity radius along the desired direction) and also to specify the area that has the same layering as the base point.

It should be noted that in this paper, along any direction, in which no significant variation in the layering occurs, is called the effective distance and a surface which has a layering similar to the base point is called the effective surface. For example, with respect to Fig. 2, if the effective distance along 1, 2, ..., n directions are d_1, d_2, \dots, d_n then the hatched region shows the effective area.

According to Fig. 2 if the effective distances along 1, 2, ..., n directions are d_1, d_2, \dots, d_n then the hatched region shows the effective surface.

3. Discussion

The study area, with longitude 59°20' to 60°8' East and latitude 35°40' to 36°3' North, and is located from Azadi Highway to the west of Mashhad. In Fig. 3, the location of 192 studied boreholes is shown on the map.

4. Drawing Variogram for SPT

For a regionalized variable with a spatial structure, the distribution is in such a way that the similarity of regional values is greater for points that are closer together than for distant points.

Therefore, by increasing the spatial distance between samples, we determine the effective radius, beyond which the value of the region variable does not have much effect, and the value of the variogram no longer changes signifi-

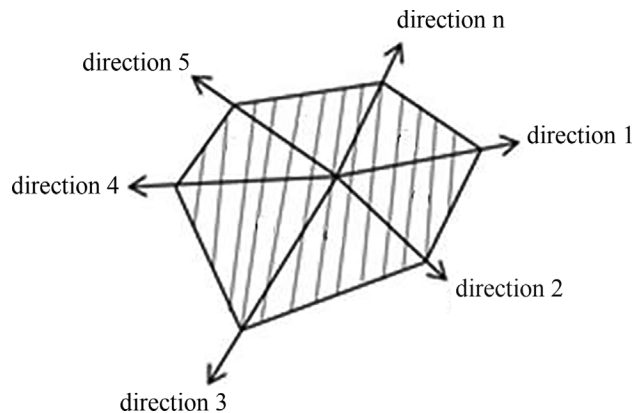


Figure 2 - Plan of base point location (x_0) and the effective distance along different directions which results in the determination of the effective surface (the hatched region).

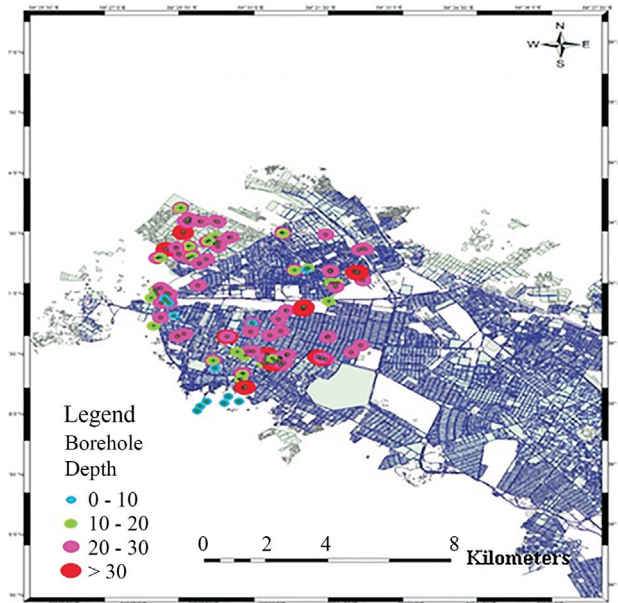


Figure 3 - Distribution map of boreholes, West Mashhad.

cantly. After determining the effective radius along different directions, the effective area is plotted. With its help, we can observe the uniformity of the parameter values of SPT in the study area (west of Mashhad).

The experimental variogram not only investigates and determines the structural characteristics of regionalized variables and explains how they change, it also has a role of data summarization.

As the number of probability distribution models is limited in classical statistics, a few practical models are also available for the experimental variogram. These theoretical models are divided into two groups:

1. Variograms in which $\gamma(h)$ value increases with h and does not approach a constant sill.
2. Variograms in which $\gamma(h)$ value at first increases with h and then reaches a constant limit which is the variogram's sill.

The present study on SPT variogram parameters shows that these variograms are among the second type. We can attribute different models for these variograms but with respect to the study carried out, the best fitted model to the variograms related to SPT is spherical.

The general equation for this model is written as Eqs. 3 and 4.

$$\gamma(h) = C \left(\frac{h}{a} - 0.5 \frac{h^3}{a^3} \right) \quad h < a \quad (3)$$

$$\gamma(h) = C \quad h < a \quad (4)$$

in which C is the threshold limit and a is the effective area.

4.1. Variograms drawn for standard penetration numbers in West of Mashhad

For this reason, at first the study area is divided into four sections and after that, SPT data are used for the estimation of variogram's effective radius for 10 and 20 m depth in every section. The results are shown in Figs. 4 and 5.

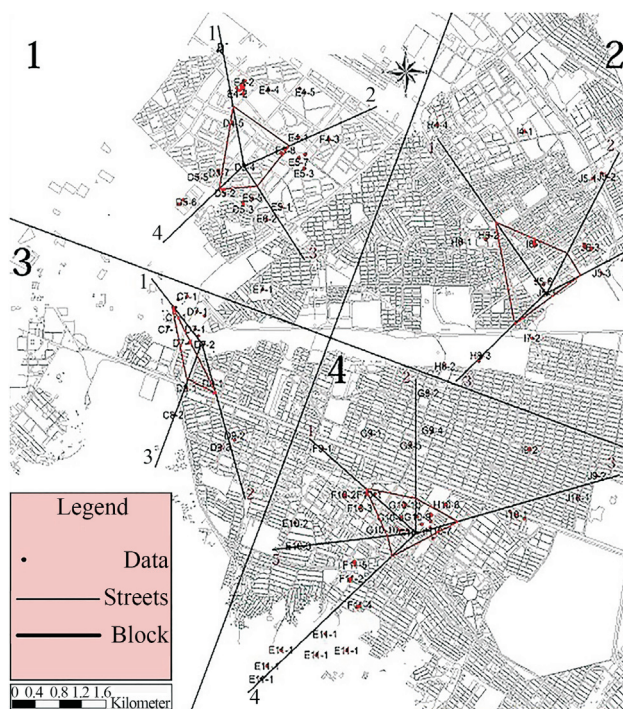


Figure 4 - Effective SPT area for depths of 0-10 m.

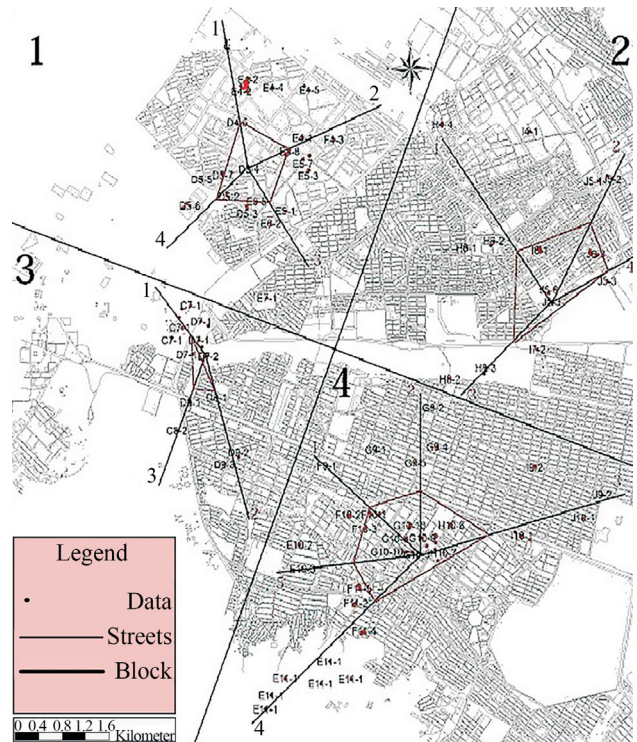


Figure 5 - Effective SPT area for depths of 10-20 m.

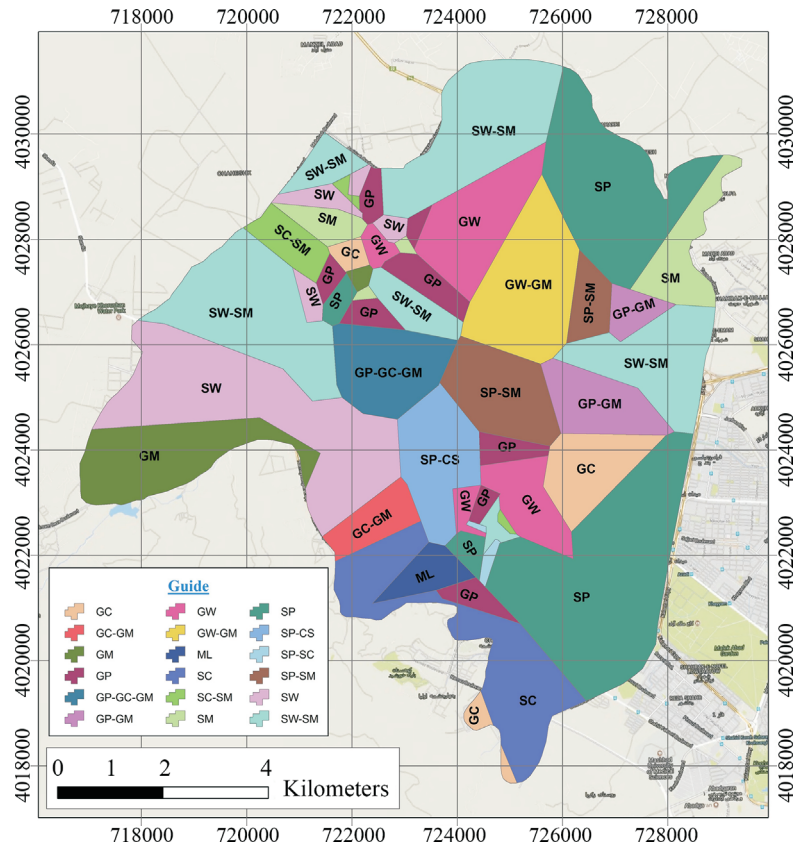


Figure 7 - Kriging map of soil texture for depth of 5-10 m.

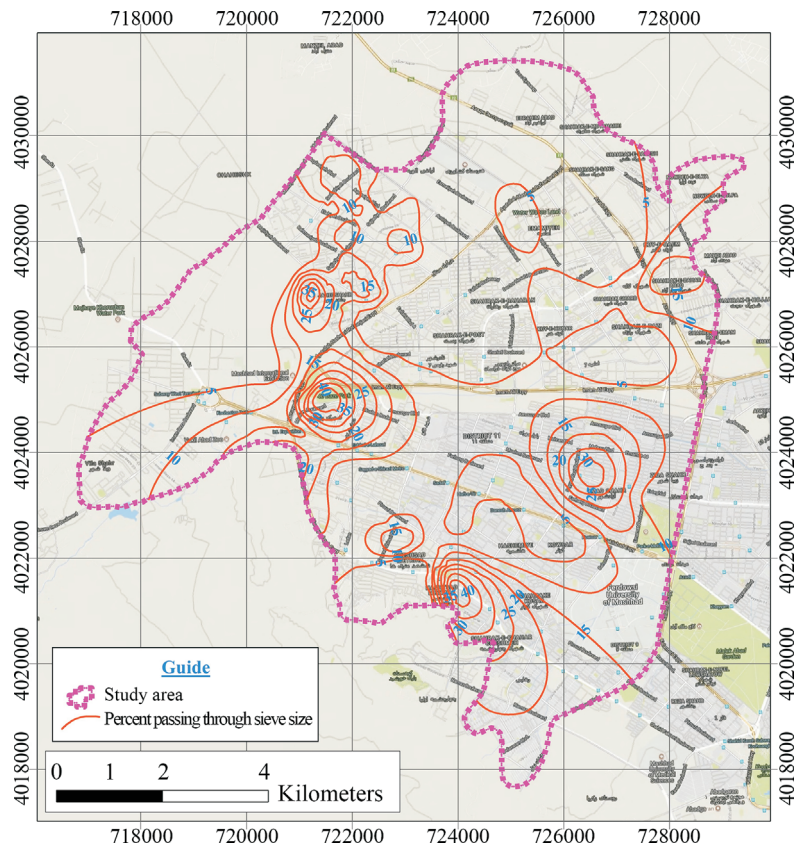


Figure 8 - Kriging map of passing no. 200 sieve at depth of 0-5 m.

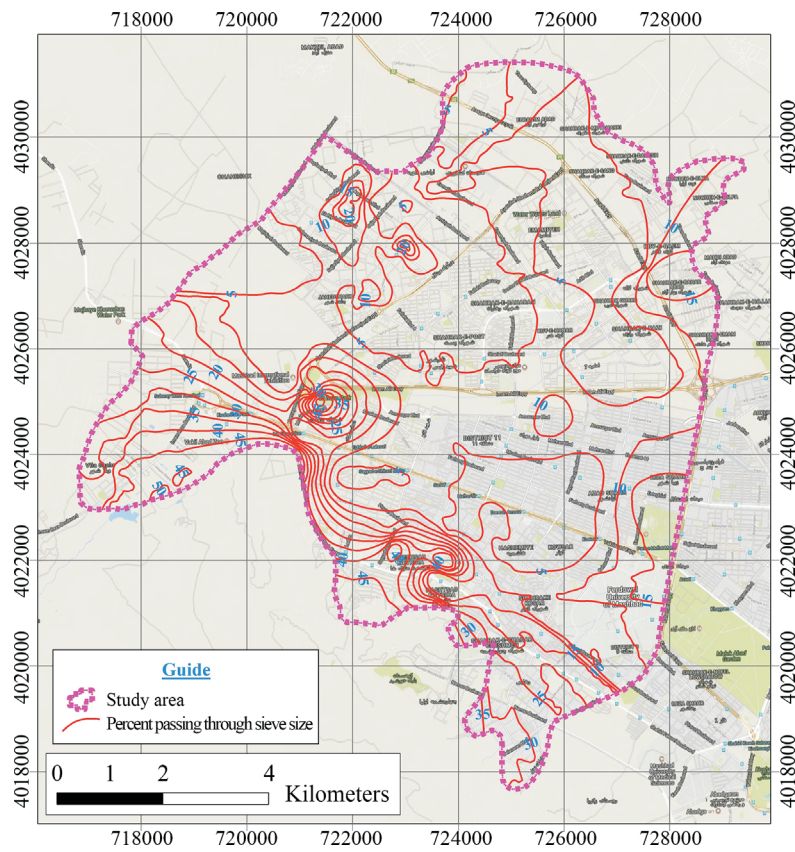


Figure 9 - Kriging map of passing no. 200 sieve at depth of 5-10 m.

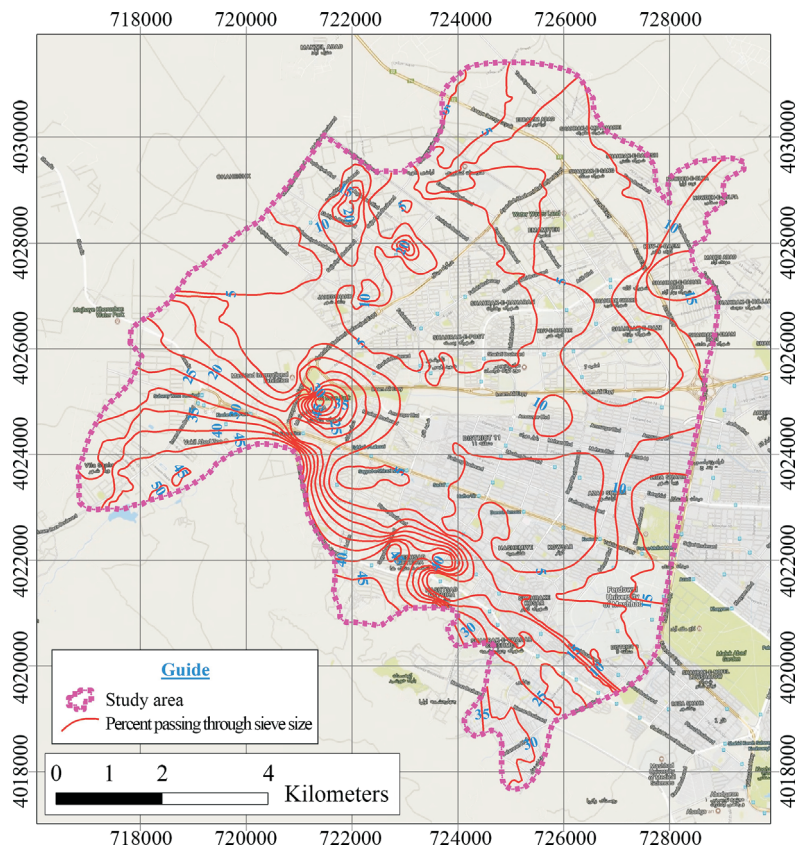


Figure 10 - Kriging map of SPT-N at depths of 0-5 m.

The closer spacing of curves in the specified area can be due to one of the following reasons:

- The sedimentation basin has had drastic energy changes (for example, the area has been part of an alluvial fan or flood plain).
- The area is tectonically active (however this is not true for the West of Mashhad because this region doesn't have impressive tectonic activity).
- The type of sediment load which is transferred by the river is different (this case is also not true for the West of Mashhad because the area is not active).
- Seasonal flooding in the region (this can be the most important factor).
- Incorrect pick up and human errors.

The kriging map of standard penetration numbers is shown in Fig. 11 for depth of 5-10 m. which could indicate that the SPT-N values have increased with increasing depth, which is to be expected due to increasing overhead pressure with increasing depth.

The kriging map of standard penetration numbers is shown in Fig. 12 for depths of 10-15 m which could indicate that SPT values still increase with increasing depth.

As shown in Fig. 13, the dry density increases from 1.65 (in West of Mashhad) to 1.95 (in Eastern Mashhad) at depth of 0-5 m due to the change in the texture of the soil

from coarse grain to fine grain (from west to East), which is justified by the loose and semi-compacted nature of the West soils in compared to the Eastern soils. The proximity of the curves indicates the transition zones and heterogeneity of the soil in that location, which can be coarse grained in the middle and fine grained around or vice versa, which depends on the increasing or decreasing trend of the contours.

In Fig.14 the density value is shown at depth of 5-10 m which is evidence of the above interpretation. Transition zones are still present, but the dry density values have increased due to increasing overpressure and density.

Figure 15 illustrates dry density values at depth of 10-15 m within which transition zones are still present, but density values have increased due to increasing overpressure and compaction. Of course, the increase of dry density is not as impressive as shown in Fig. 14 for a depth of 5-10 m.

5. Conclusions

The main purpose of this paper is to determine the specification of areas without borehole logs. Based on the knowledge of drilled boreholes in the study area, using the interpolation method, assessment the drawn kriging maps and using geostatistical techniques, the following main conclusions emerged from this study:

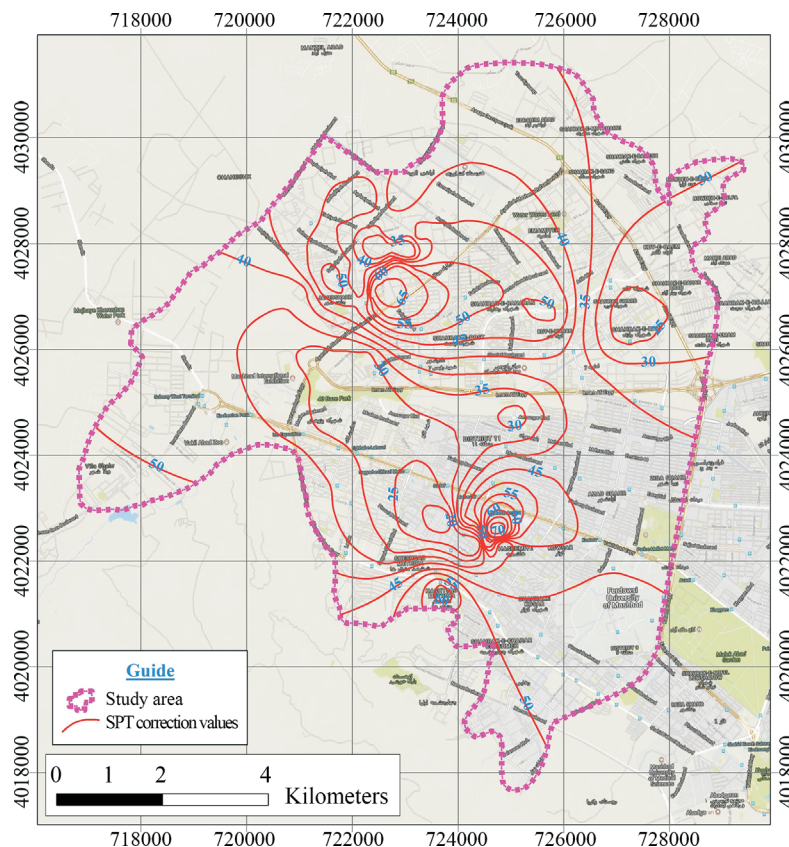


Figure 11 - Kriging map of SPT-N at depths of 5-10 m.

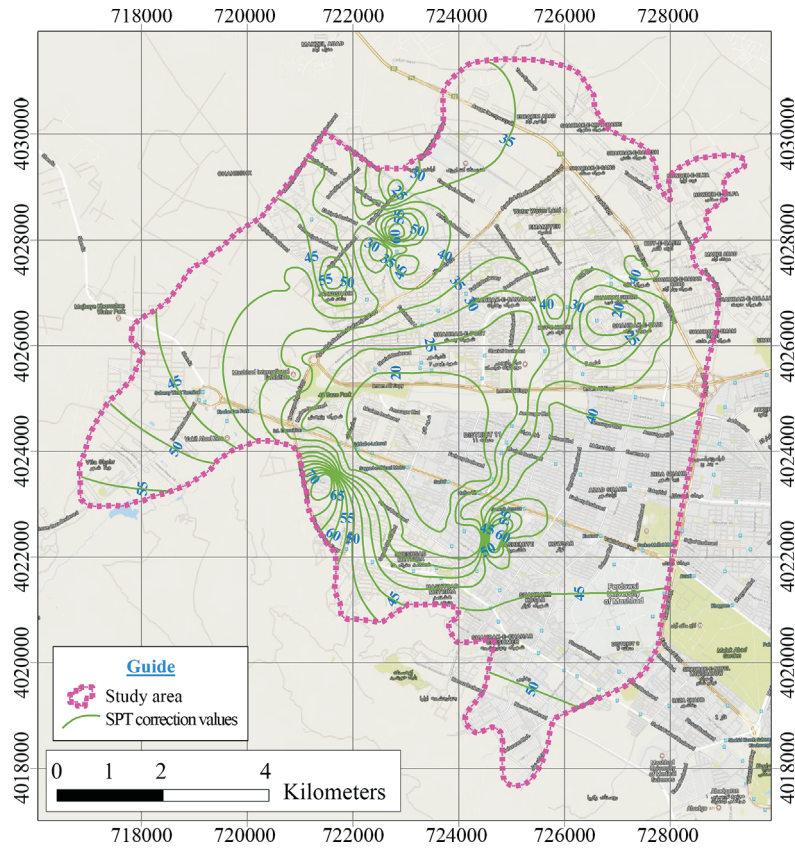


Figure 12 - Kriging map of SPT-N at depths of 10-15 m.

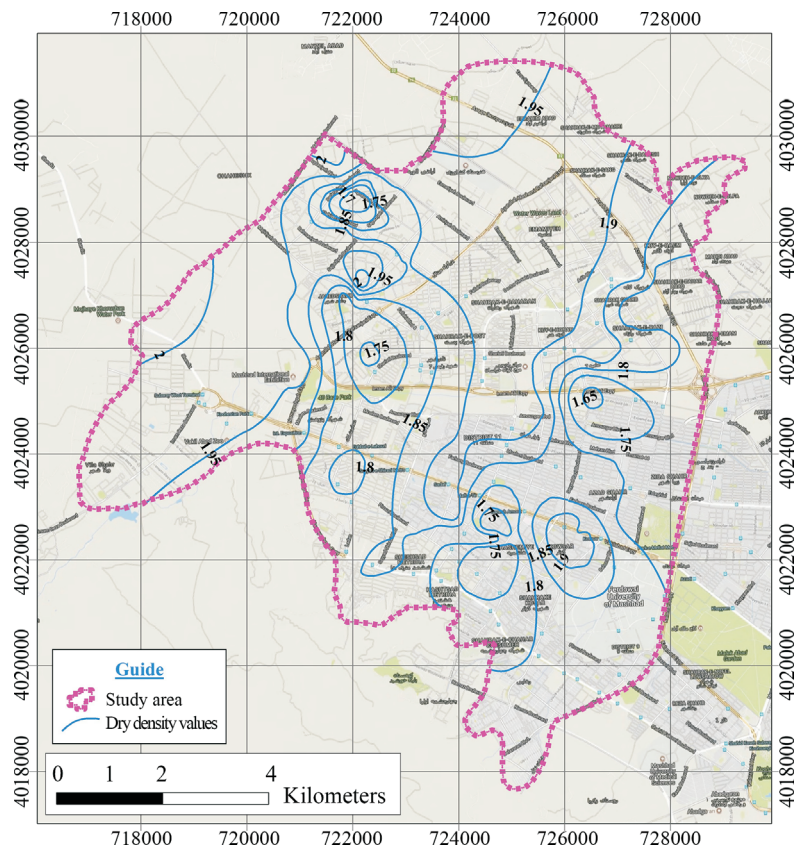


Figure 13 - Kriging map of dry density at depth 0-5 m.

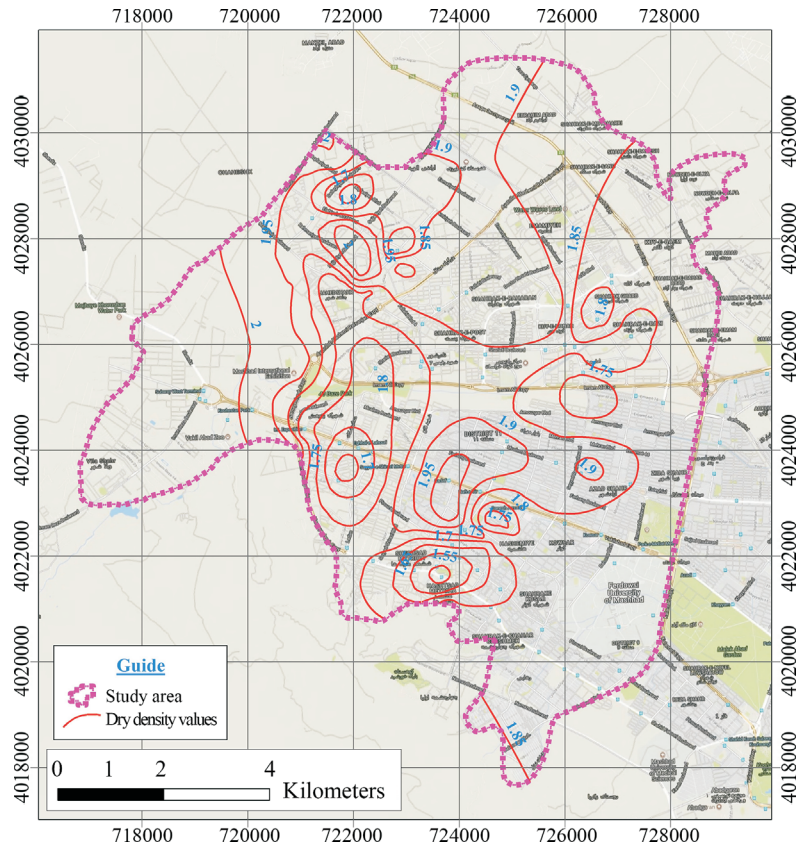


Figure 14 - Kriging map of dry density at depth of 5-10 m.

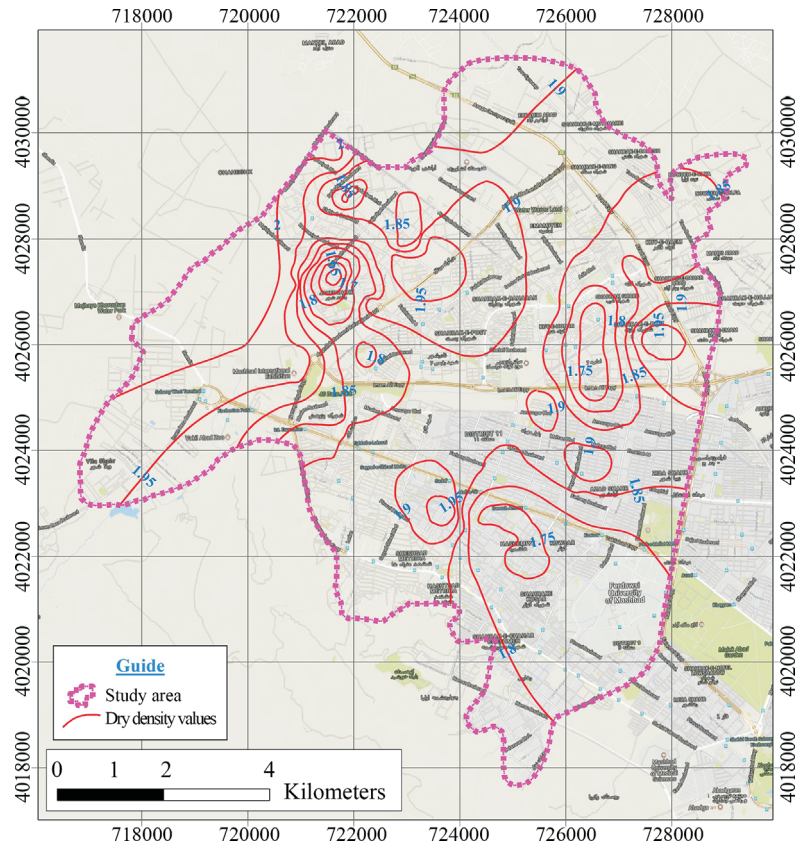


Figure 15 - Kriging map of dry density at depth of 10-15 m.

1. According to the soil texture maps and the percentage of passing no. 200 sieve, we can see that more than 80% of the specimens have less than 10% of clay and silt values in the study area, which indicates the high energy content of the sedimentation environment.
2. Also, soil texture kriging maps show that with increasing depth, the soil texture extends to the coarse grains mainly, which indicates the high energy of streams in the old sedimentation environment.
3. The investigation of plotted variograms to show the effective SPT area, indicates that with increasing depth to a certain value (in the case study 10 m), the effective area shows a significant decreasing trend generally, and the increase of overhead pressure with increasing depth and the homogeneity of the soil texture proves this to be expectable.
4. Also evaluation of the effective SPT area variograms, near the surface, is an evidence of soil-resistance heterogeneity in the east-west direction (along with the sedimentation of the rivers).
5. The drawn variograms to display the effective SPT area indicate that outside the effective area the occurrence of irregular changes to this parameter represent the impact of local events in the basin.
6. With increase of depth beyond a specific range (in this study, past 10 m), the effective range does not show a significant change due to density of sediments. Investigations have shown that SPT-N values at these depths are generally higher than 50.
7. The proximity of curves in kriging maps of dry density indicates the transition zones and heterogeneity of soil in that location. Locations other than the transition zones, which have coarse grained soils, are often river channels.
8. Generally, dry density increases from West to East of Mashhad which is due to changes of soil texture from coarse grain to fine grain (from West to East) which is justified due to the loose and semi-compacted nature

of the West soils in compared to the Eastern soils. And it also shows a slight increase with increasing depth.

9. The neighbouring radius decreases in a certain direction due to layering changes with increasing depth. In other words, with increasing depth, the influence of soils from surrounding areas becomes smaller.

References

- Bahri, A. & Khosravi, T. (2017). A review of spatial analysis and their application in the environment. Fourth International Conference on Environmental Planning and Management, Tehran, Faculty of Environment, University of Tehran.
- Chiasson, P.; Lafleur, J.; Soulié, M. & Law, K.T. (1995). Characterizing spatial variability of a clay by geostatistics. *Canadian Geotechnical Journal*, 32(1):1-10.
- Davidovic, N.; Prolovic, V. & Stojic, D. (2010). Modeling of soil parameters spatial uncertainty by geostatistics. *Facta Universitatis-Series: Architecture and Civil Engineering*, 8(1):111-118.
- Hengl, T. (2007). *A Practical Guide to Geostatistical Mapping of Environmental Variables*. European Commission, Joint Research Centre. Institute for Environment and Sustainability, Italy.
- Huntley, S.L. (1990). Use dynamic penetrometer as a ground investigation and design tool in Hertfordshire, field testing in engineering geology. *Geological Society Engineering Geology Special Publication*, 6:145-149.
- Low, I.J. & Zaccaro, P.F. (1990). *Subsurface Explorations & Sampling*. Foundation Engineering Handbook. Fang, Y.H. (eds), Chapman & Hall Publishers, Boca Raton, pp. 12-14.
- Madani, H. (1994). *Geostatistics Fundamentals*. Amirkabir University of Technology, Amirkabir 66 p.
- Taj Al-Din, R. (1997). *3D Distribution Statistical Modeling of Soil Geotechnical Properties*, Soil and Foundation Mechanics. Master Dissertation, Civil Engineering Department, College of Engineering, University of Tehran, 209 p.

Case Study: Stability Assessment in Underground Excavations at Vazante Mine - Brazil

L.T. Figueiredo, A.P. Assis

Abstract. Currently, most studies on stability of underground excavations include two separate analyses: the elastoplastic behavior of rock masses and/or kinematic analysis of possible wedges and blocks formed in the excavation walls. This paper presents a case study carried out at the Vazante Zinc Mine in Minas Gerais, Brazil, where studies on stability of underground excavations in discontinuous media included survey reports, laboratory tests and *in-situ* collected data. In this context, where galleries and mining stopes are excavated in discontinuous media, collapse events caused by the presence of discontinuities are common. First, the spatial orientation, geometric arrangement and mechanical characteristics of the discontinuities intercepted by the core samples were collected. The spatial orientation was based on guide layers, which are discontinuities with known dip direction and variable and dip. The geotechnical characteristics of the discontinuities were obtained by correlation with the roughness degree and the nature and weathering degree of the filling material. From there, the geological-geotechnical models were developed, which were the basis for the finite element analysis in discontinuous media of the designed excavations in the sections 13225 and 13300, between levels 210 and 345 of the mine. For comparison and complementation, wedge kinematic analysis and finite element analysis in equivalent continuous media were performed and, later, an arrangement for the reinforcement system was suggested. The results of these studies show that, in general, continuous models tend to be more conservative and have wider deformation zones, while discontinuous models are able to show in more detail where the displacements occur, and how the families of discontinuities affect the stability of excavations.

Keywords: discontinuities, discontinuous media, displacements, mining stope, reinforcement systems, underground excavations.

1. Introduction

Stability studies of underground excavations are mostly conducted using numerical methods that consider rock masses as continuous media, such as the finite element method, and/or wedge kinematic analysis. Basically, numerical methods use elastic and plastic geotechnical parameters of the material, and the discontinuous media (with joints, beddings and geological faults) are commonly correlated to continuous media through equivalent geotechnical parameters. The kinematic analysis is used to evaluate the equilibrium of the wedges and blocks formed by the intersection of the discontinuities in the walls of the excavations, based only on the geotechnical parameters of the joint families. Both methods have intrinsic limitations.

The numerical analysis by continuous media does not reproduce the mechanical behavior of the discontinuities present in the rock mass, while in the kinematic analysis only the blocks and wedges located in the excavation surface are evaluated. Over the last decade, many codes with mixed concepts were created, making it possible to reproduce a scenario closer to reality, where the geotechnical behavior of rock and discontinuities are simultaneously evaluated.

This study deals with the most common methodologies for characterization and geological-geotechnical modeling of discontinuous rock masses, and proposes a methodology for stability studies in such environments. For that purpose, a case study was carried out in a certain region of the Vazante Underground Mine, in Brazil, where collapse events related to the formation of slabs and blocks are recurring.

The city of Vazante is located in the northwest region of the State of Minas Gerais, approximately 504 km from Belo Horizonte and 354 km from Brasilia, federal district of Brazil. The Vazante Mine is located in the geological context of a shear zone, through which mineralized fluids have percolated and zinc minerals and other associated minerals have crystallized. The residual rocks of the Vazante Zinciferous Reservoir correspond to a dolomite, marl and phyllite sequence, susceptible to an accelerated weathering process that has generated cavities, often carrying mud and water under pressure. This association of factors is negative from the geotechnical point of view since it generates risk for the excavations. As shown in Fig. 1, the ore-bearing rocks are pink dolomites interspersed with metapelitic rocks, usually marls and slates, in addition to the dolomitic and Fe-carbonate breccias (siderite and ankerite).

Lucas Torrent Figueiredo, M.Sc., Anglo American Iron Ore Brazil (previously at Votorantim Metais Zinc), Belo Horizonte, MG, Brazil. e-mail: torrent.figueiredo@gmail.com.

André Pacheco de Assis, Ph.D., Professor Titular, Departamento de Engenharia Civil e Ambiental, Universidade de Brasilia, Brasilia, DF, Brazil. e-mail: aassis@unb.br.

Submitted on June 20, 2017; Final Acceptance on June 6, 2018; Discussion open until December 31, 2018.

DOI: 10.28927/SR.412203

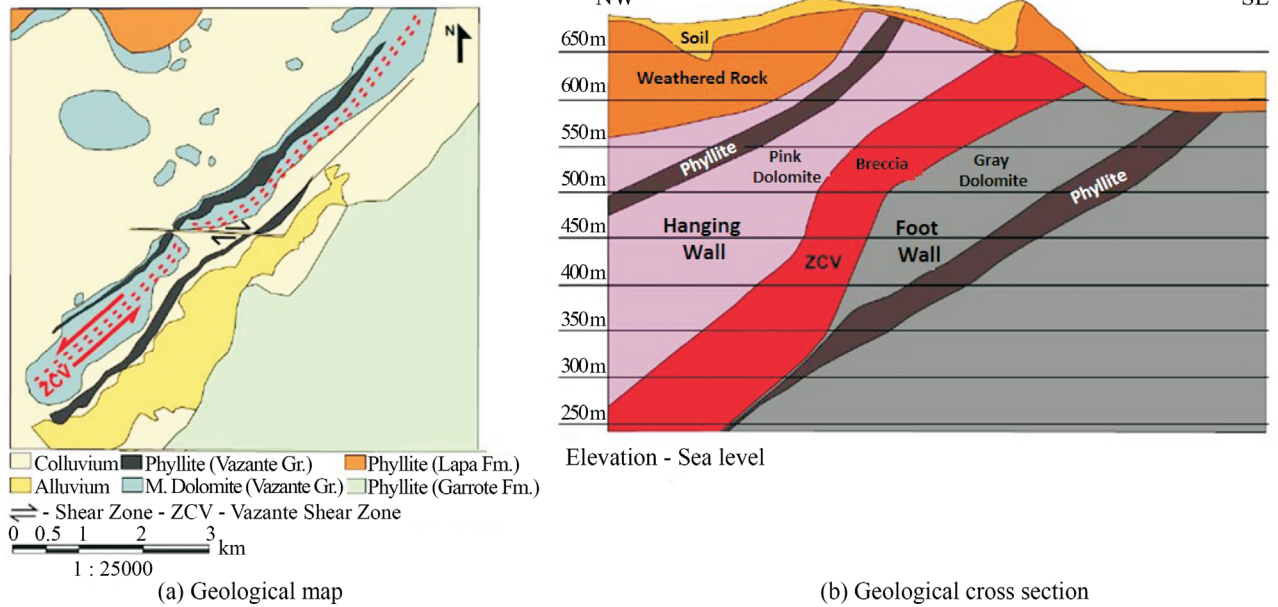


Figure 1 - Vazante Shear Zone Geology - (a) Geological Map and (b) Geological Cross Section (modified from Charbel, 2015).

The relationship between the preferential planes of bedding, faults and fractures, as well as the definition of water flow in the rock mass, can also represent risks associated with displacement and collapses during the underground excavation of galleries and mining stopes. Therefore, the purpose of this study is to identify and model such areas, and to indicate a long-term stabilization system to be adopted for each particular case. For that end, data from drillings in the studied area, located between the profiles 13.200 and 13.350 and the elevations 210.00 to 345.00 m, as well as survey data, previous laboratory test data and field data were used in this study. The drilling campaign was made from the gallery 345 GP-Shaft (Research Gallery), totaling 23 holes in 4 profiles.

Based on the drillhole core samples, the mean spatial orientations and spacing of the discontinuities were described, and also the roughness characteristics and the weathering degree of the filling material.

2. Spatial Orientation of Discontinuities

The orientation of the discontinuities (joints, fault and beddings) intercepted by the drillholes during the Vazante Mine exploration campaign was obtained by a preset dip direction value for the dolomite and marl bedding (S_0) family, in addition to the Vazante Fault (FVZ). Several authors, as Rostirolla *et al.* (2002), Bhering (2009) and Charbel (2015), have found that these two structural features show little variation in the dip direction, based on measurements obtained on the surface and underground, at various depths, both in the north (Sucuri Mine) and in the south (Lumia-deira Mine).

Rostirolla *et al.* (2002) summarized the mean orientation values of the discontinuities in the open pit area, correlating them with the deformation phases, established by the

same authors, and the mean values of S_0 and Vazante Fault, with very close dip directions, of 317 and 316, respectively.

Bhering (2009) obtained measurements for the S_0 family and the FVZ in mappings of transverse galleries at sites near the study area, at levels 388 and 345, between profiles 11.000 and 13.000. The mean orientation measured at these locations was 332/16 for beddings, and the average for the Vazante Fault was 326/73.

Charbel (2015) mapped several transverse galleries in regions next to the area of studies, at levels 345 and 388, between profiles 12.500 and 13.100. The dip direction obtained for S_0 varied between 280 and 345, with dip between 10° and 50°. The dip directions of the Vazante Fault varied between 300 and 335, with dip between 50° and 80°. Figure 2 shows one of the mappings performed on a transverse gallery that passes through the hanging wall and the foot wall of the fault, showing the strong dip direction trend to NW of the S_0 and Vazante Fault.

Based on the premise that guide layers (with little variation in the dip direction) are frequent in the rock mass of Vazante Mine, the orientation of the discontinuities around them was obtained from the α and β angles, introduced in the literature by R.E. Goodman in 1976. The smaller angle between the axis of the hole and the straight line of maximum gradient of the plane is called α angle. The β angle is determined between the bottom line of the hole, formed by the points of minimum elevation in the orthogonal sections with respect to the axis of the core sample and the apical trace, which is the extension of the major axis of the discontinuity in the section, in the side of the core sample. Figure 3 schematically shows the angles required for orientation of the discontinuities in core samples.

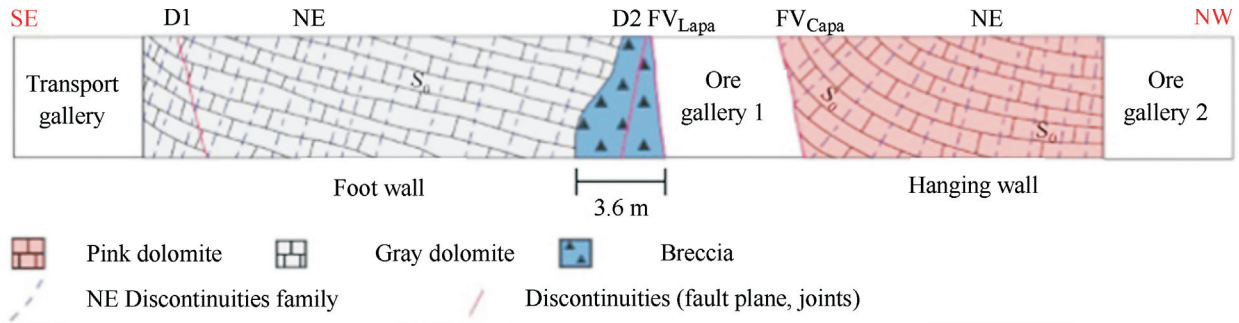


Figure 2 - 12850 transverse gallery mapping, at level 345, near the study area (modified from Charbel, 2015).

In the study area, all the drillholes were planned at azimuth 136, arranged in sections with several dips, every 25.00 m, depending on the average dip direction of the

Vazante Fault (azimuth 316), recorded in the study of Rostirolla *et al.* (2002). Thus, the drillholes intercepted the Vazante Fault frontally, as well as the dolomite and marl bedding (S_0) with average dip direction of 317. Therefore, all bedding planes and Vazante Fault (FVZ) were recorded with dip direction to the azimuth 316, and with the angle β being 0° or 180° , as a function of the inclination of the hole. The dip of S_0 and Vazante Fault varied according to angle α found in the core sample. Figure 4 relates stereonet and typical features of the main families of discontinuities in the study area.

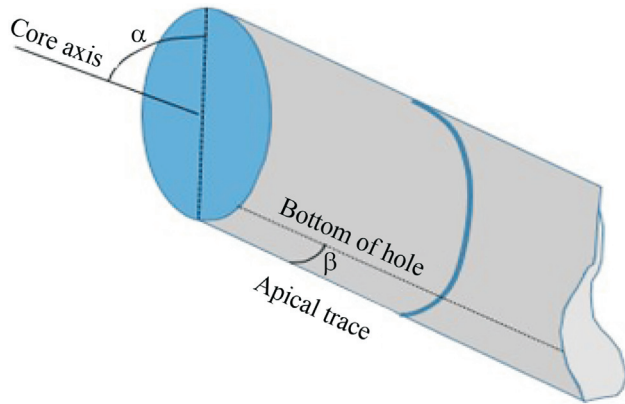


Figure 3 - Schematic image of a drill core and the α e β angles.

3. Geotechnical Parameters

In the study area, the rock mass is geotechnically classified as class II and class III (RMR System). In other words, it is controlled by the set of discontinuities and their characteristics. The material between the discontinuities is correlated to the intact rock. The geotechnical parameters of the intact rock are related to the study of Charbel (2015),

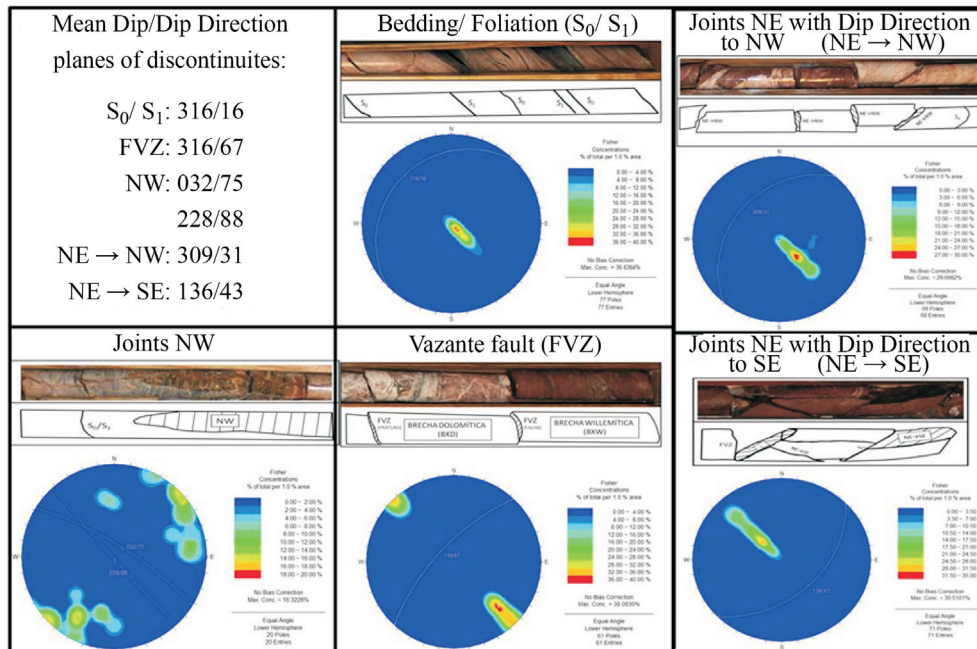


Figure 4 - Stereonet and typical features of the main families of discontinuities seen in core samples of the study area.

who compiled the data of uniaxial compression strength (σ_{ci}) and elastic modulus (E_i) of intact rock collected by IPT (1994b) and Bhering (2009), making the statistical treatment of these values for dolomites, dolomitic breccia and willemite breccia. Then, the Hoek-Brown strength criterion for intact rocks was applied, using the elastic constant of the material, m_i , equal to 9, the rock quality parameter s and the constant a , equal to 1.0 and 0.5, respectively. The equation of the Hoek-Brown criterion is shown in Table 1.

The Poisson coefficients (ν) adopted for dolomites and breccias are between 0.2 and 0.4, while the unit weights (γ) are provided by density tests in core samples.

For the stability analysis of rock masses in equivalent continuous media, the equivalent deformation modulus E_{mr} was determined from the elastic deformation modulus of the intact rock (E_i) and the Hoek-Brown parameters for equivalent rock masses m_b , s and a . Therefore, the determination of the GSI (Geological Strength Index) is essential.

The mass disturbance factor “D” was estimated to be 0.8, considering that the excavation method disturbs the rock mass, mainly due to the lack of control in the quantity and sequencing of explosives. Table 2 summarizes the Hoek-Brown parameters for equivalent continuous media analyses.

The shear strength of the discontinuities in the rock mass of the Vazante Mine was obtained from five fundamental parameters: basic friction angle (ϕ_b) and residual friction angle of the filling material (ϕ_r), roughness (JRC and Jr), weathering degree of the infill material (Ja), uniaxial compressive strength of the discontinuity wall (JCS) and fill height (Hp).

Based on the data mentioned above, it was possible to determine the shear strength (τ) by the Barton-Bandis and Mohr-Coulomb methods for each geotechnical group of discontinuities.

The discontinuities with the same characteristics of shear strength (τ) were separated into “Geotechnical Groups”. These groups are basically defined by the domi-

nant factor of resistance (L-filling, R-Rock and M-Mix), filling material (CA-Carbonates, MG-Marl, A-Clay), weathering degree (J1, J2, J3 and J4), and, only for the mixed discontinuities, the roughness degree (R1, R2 and R3), as shown in Fig. 5.

The values of the weathering degree of the fillings are correlated with the values of Ja of Barton, in other words, for Ja equal to 1, the degree is J1, if Ja is equal to 2, the degree is J2, and so on until J4.

The roughness degree (R1, R2 and R3) varies according to the JRC value, with R1 having JRC values between 4 and 6, R2 for JRC between 8 and 10, and R3 for JRC values above 12.

Before the presentation of the shear strength equations for each geotechnical group of discontinuities, the basic friction angle (ϕ_b), unconfined wall compression strength of the discontinuity, and the stiffness coefficients Kn and Kh, will be related. These parameters are required for the calculations to be developed.

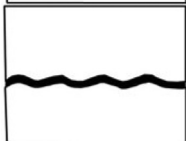
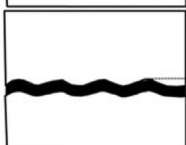
	Dominant factor	Hp/ Hr	ϕ_r
	R (Rock)	Hp/ Hr < 0.5	ϕ_r (Rock)
	M (Mix)	$0.5 \leq Hp/Hr < 1.0$	$\phi_r = \text{tg}^{-1} (Jr/ Ja)$
	L (Filling)	Hp/ Hr ≥ 1.0	ϕ_r (Filling)

Figure 5 - Table of comparison between discontinuities with shear strength controlled by rock, fillings and mix, where Hp/Hr is the relation between fill height and roughness height and ϕ_r is the residual friction angle of the filling material.

Table 1 - Values of m_i , σ_{ci} and Hoek-Brown equation for each intact rock.

Rock	m_i	σ_{ci} (MPa)	$\sigma'_1 = \sigma'_3 + \sigma_{ci} [m_i (\sigma'_3 / \sigma_{ci}) + s]^a$	Poisson (ν)	γ (kN/m ³)
Dolomite	9	124.00	$\sigma'_1 = \sigma'_3 + 124 [9(\sigma'_3/124)+1]^{0.5}$	0.2	27.00
Dolomitic Breccia (BXD)	9	101.00	$\sigma'_1 = \sigma'_3 + 101 [9(\sigma'_3/101)+1]^{0.5}$	0.2	30.00
Willemite Breccia (BXW)	9	108.00	$\sigma'_1 = \sigma'_3 + 108 [9(\sigma'_3/108)+1]^{0.5}$	0.2	35.00

Table 2 - Hoek-Brown geotechnical parameters of the Vazante Mine rock masses.

Rock mass	m_i	E_i (GPa)	σ_{ci} (MPa)	GSI	D	m_b	s	a	E_{mr} (GPa)
Dolomites	9	58	124	70	0.8	1.509	0.0106	0.5	18.97
D. Breccia (BXD)	9	55	101	50	0.8	0.5	0.0005	0.5	5.0
W. Breccia (BXW)	9	63	108	50	0.8	0.5	0.0005	0.5	5.8

For the evaluation of the basic friction angles (ϕ_b), tilt-tests were performed with BQ core samples of dolomites, breccias and marls.

Schmidt hammer tests were performed on discontinuities of carbonate rocks (dolomites and breccias), with weathering degrees varying from J1 to J4. According to Barton & Choubey (1977), who formulated the first version of the Barton-Bandis shear strength criterion, the method is applicable to unfilled discontinuities; it means rock-to-rock contact in the walls of the discontinuities. Therefore, rebound values of the Schmidt hammer (r) were collected for discontinuities of carbonate rocks, without filling, in several galleries of the Vazante Mine. The frequency histograms of the r measurements for discontinuities with intact wall and weathered wall are shown in Fig. 6.

The mean value of “R” for discontinuities with intact walls (J1) is 60, and for weathered discontinuities (J4), “r” is equal to 24. The “r/R” expression value (Barton & Choubey, 1977) for intact walls is equal to 1. The values of “r/R” on the walls with weathering degree equal to J4 is 0.4, and thus the “r/R” values were obtained by linear regression, for the intermediate weathering degrees (J2 and J3), as seen in Fig. 7. This procedure is based on the study of Karzulovic, published in Hoek & Karzulovic (2000), which showed, through rock tests under different weathering degrees, that the loss of resistance to uniaxial compression has a near linear relation with the weathering degrees of the minerals in joint walls.

With the data of “r”, the values of σ_c and E for the unfilled discontinuities from carbonated rocks of the Vazante Mine were obtained through the empirical equations. These values were compared to σ_c and E data obtained in laboratory tests in order to define which equations are more appropriate to the rocks analyzed in this study.

For obtaining σ_c from “r”, the Kahraman equation (1996) reproduced values closer to the data of laboratory tests performed in the Vazante Mine, while the equation of Yagiz (2008), for the calculation of E , has shown the best results.

In the literature, the shear strengths of the discontinuities filled with marl and clay were determined by the resid-

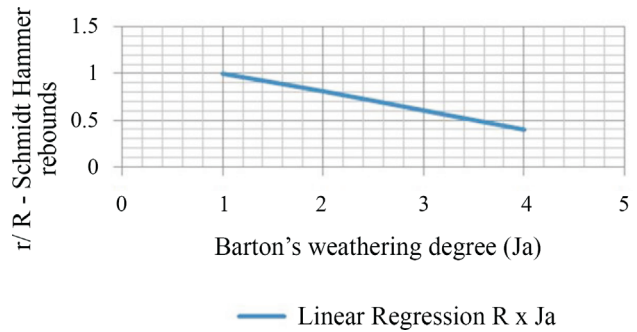


Figure 7 - Linear regression with values of intact rock (Ja = 1) and highly weathered rock (Ja = 4).

ual friction angle (ϕ_r) and cohesion (c) values for application of the Mohr-Coulomb criterion, since there is no data of Schmidt hammer tests for these materials.

The geotechnical parameters of the clays, which mainly fill the faults and fractures of the Vazante Shear Zone, were defined from the values reported by Barton (1970, 1974) and Wyllie & Mah (2004).

The normal stiffness (K_n) and shear stiffness (K_s) are coefficients that represent the stress required for a unit displacement of the discontinuities, both in the normal direction and tangentially to the plane, adopted from the equations proposed by Barton (1972), Goodman *et al.* (1968) and data obtained by Kulhawy (1975).

The rough discontinuities are mainly present in breccia and have their shear strength controlled by the material before the joint wall due to the smoothing tendency of the surface when subjected to high stresses. On the other hand, the shear strength of the smooth discontinuities is mechanically controlled by the material of the joint wall and it is typical of the bedding planes of dolomites and marls, as well as fault planes and joints in the Vazante Shear Zone and low angle faults. These features can be met or not, and the shear strength depends directly on this factor. The Barton-Bandis criteria will be applied to unfilled discontinuities, with contact between walls, in dolomites and breccias. Table 3 presents the Barton-Bandis equations for the geotechnical groups in which the shear strength depends on the degree of discontinuity of the walls.

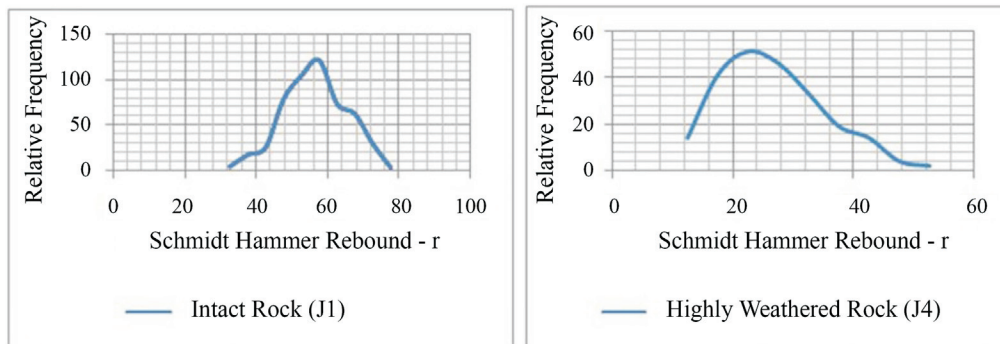


Figure 6 - Frequency histogram of the Schmidt hammer rebounds (r) measured in breccias and dolomites. Intact rock, on the left, and highly weathered rock, on the right.

Table 3 - Geotechnical parameters and Barton-Bandis equations for shear strength for rough (material before the joint wall) and smooth (material of the joint wall) discontinuities.

Geotechnical group	γ (kN/m ³)	r	r/R	JRC	ϕ_b (°)	* ϕ_r (°)	**JCS (MN/m ²)	$\tau = \sigma_n \cdot \tan[\phi_r + JRC \cdot \log_{10}(JCS/\sigma_n)]$
RCAJ1 / LCAJ1	27	60	1	1	35	35	272.65	$\tau = \sigma_n \cdot \tan[36 \cdot \log_{10}(272.65/\sigma_n)]$
RCAJ2 / LCAJ2	27	48	0.8	1	35	31	414.41	$\tau = \sigma_n \cdot \tan[32 \cdot \log_{10}(414.41/\sigma_n)]$
RCAJ3 / LCAJ3	27	36	0.6	1	35	27	73.34	$\tau = \sigma_n \cdot \tan[28 \cdot \log_{10}(73.34/\sigma_n)]$

* $\phi_r = (\phi_b - 20) + 20 (r/R)$ - Barton & Choubey (1977).
 **JCS = $10^{(0.00088 \cdot \gamma \cdot r + 1.01)}$ - Barton & Choubey (1977).

In the smooth and filled discontinuities, the Mohr-Coulomb criterion will be used, with the geotechnical parameters of the filling material according to the Table 4.

The mixed discontinuities are those in which ϕ_r is calculated as a function of roughness and weathering degree. Therefore, the relations of Barton ($\tan^1 Jr/Ja$) were used according to those parameters, and for Barton & Choubey according to the Schmidt hammer rebound values “r”. Next, in Table 5, the geotechnical parameters and the shear strength equations of Barton & Bandis are related for each group of discontinuities.

4. In Situ Stress

The principal directions of the stresses acting in the Vazante Group were estimated by some authors such as

Table 4 - Geotechnical parameters and Mohr-Coulomb for the smooth discontinuities filled with marl and clay.

Geotechnical group	Filling material	ϕ_r (°)	c (kPa)	$\tau = c + \sigma_n \cdot \tan \phi_r$
LA	Clay	12	0	$\tau = \sigma_n \cdot \tan 12$
LMGJ3	Marl	20	0	$\tau = \sigma_n \cdot \tan 20$
LMGJ4	Marl	12	0	$\tau = \sigma_n \cdot \tan 12$

Table 5 - Geotechnical parameters and Barton-Bandis equations for shear strength for mix discontinuities.

Geotechnical group	γ (kN/m ³)	r (r/R)	JRC(Jr)	Ja	ϕ_b (°)	* ϕ_r (°)	**JCS (MN/m ²)	$\tau = \sigma_n \cdot \tan[\phi_r + JRC \cdot \log_{10}(JCS/\sigma_n)]$
MCAJ2R1	27	48(0.8)	6 (1.5)	2	35	31	141.41	$\tau = \sigma_n \cdot \tan[37 \cdot \log_{10}(141.41/\sigma_n)]$
MCAJ2R2	27	48(0.8)	8 (2)	2	35	33	141.41	$\tau = \sigma_n \cdot \tan[41 \cdot \log_{10}(141.41/\sigma_n)]$
MCAJ3R1	27	36(0.6)	6 (1.5)	3	35	27	73.34	$\tau = \sigma_n \cdot \tan[33 \cdot \log_{10}(73.34/\sigma_n)]$
MCAJ3R2	27	36(0.6)	8 (2)	3	35	30	73.34	$\tau = \sigma_n \cdot \tan[38 \cdot \log_{10}(73.34/\sigma_n)]$
MCAJ3R3	27	36(0.6)	10 (3)	3	35	33	73.34	$\tau = \sigma_n \cdot \tan[43 \cdot \log_{10}(73.34/\sigma_n)]$
MCAJ4R1	27	24(0.4)	6 (1.5)	4	35	23	38.04	$\tau = \sigma_n \cdot \tan[29 \cdot \log_{10}(38.04/\sigma_n)]$
MCAJ4R2	27	24(0.4)	8 (2)	4	35	27	38.04	$\tau = \sigma_n \cdot \tan[35 \cdot \log_{10}(38.04/\sigma_n)]$
MCAJ4R3	27	24(0.4)	10 (3)	4	35	30	38.04	$\tau = \sigma_n \cdot \tan[40 \cdot \log_{10}(38.04/\sigma_n)]$

* Values according to the following equations:
 $\phi_r = (\phi_b - 20) + 20 (r/R)$ – Barton & Choubey (1976);
 $\phi_r = \tan^1(Jr/Ja)$ - Barton (2002).
 ** JCS = $10^{(0.00088 \cdot \gamma \cdot r + 1.01)}$ - Barton & Choubey (1976).

Pinho (1990), Rostirolla *et al.* (2002), Dardenne (2000), Dardenne & Schobbenhaus (2001) and Charbel (2015), from the geotectonic evolution of the Tocantins Province. In general, the arrangement of the vectors of *in situ* stresses suggested by these authors is the same, but with divergences in relation to which directions correspond to σ_1 , σ_2 and σ_3 .

According to Charbel (2015), as to what regards to the magnitude of the *in-situ* stresses in the Vazante Mine, there are geological indicators of achievement of a low rate.

In the present work, the guidelines for calculating the stresses will be those adopted by Charbel (2015) as the stress indicators in the Vazante Underground Mine suggested by him are in agreement with the observations made by this authors.

The vertical stress (σ_v), corresponding to σ_1 , can be calculated from the following equation.

$$\sigma_1 = \sigma_v = \gamma H \tag{1}$$

where γ is the unit weight of the rock, assuming 0.027 MN/m³, and H is the thickness of the column of rock mass above the point where it is desired to measure σ_v .

The horizontal stresses σ_H and σ_h , which correlate to σ_2 and σ_3 , respectively, have a correlation rate of $\sigma_H/\sigma_h = 1.4$.

5. Stability Analysis

The sections 13225 and 13300 were selected for the stability analysis, and the drillholes 1, 3, 5, 7 and 9 of each section were logged in order to obtain the geological and geotechnical classifications.

After modeling of the discontinuities, shown in Fig. 8, 2D sections were drawn for the finite element analysis.

Wedge kinematic analyses were made to verify the stability of the excavations walls. The studies were performed using the software Unwedge®, version 4.0, developed by Rocscience. In order to effectively evaluate the results, the Safety Factor (FS), regarding the resisting forces vs. the destabilizing forces, was used, with the adopted critical value of 1.5, following a tendency observed in failed wedges in the Vazante Mine as well as in tutorials and case studies of the software used.

The kinematic analyses of the ore galleries (GM) were used to assist in the adoption of a reinforcement system aimed to guarantee the safety of operations, besides retaining the waste material, causing a greater blasting efficiency.

The tiebacks used to retain the wedges have characteristics similar to those routinely used in the Vazante Mine. The bars have tensile strength of 0.27 MN/m, with a cement-rock adhesion of 0.34 MN/m, with 3.00 m length (1.00 m anchored), and a distance of the lines of 1.50 m. Several geometrical arrangements of the lines were tested, and the most efficient one was used, being very similar to the one used in the Mine of Vazante today.

In the transportation galleries (GT), the transit of people and equipment, often for an extended period of time, makes the retainment system very important for the safety of mine operations in general.

Figure 9 shows the stability analysis for the 300-GM2 gallery and for the 210-GT gallery, in the section 13300, where the wedges with the most critical safety factors were detected.

The mining stopes at the Vazante Mine are generally retained through the hanging wall of the ore body with cables in order to avoid operational dilution from the blasting of the waste material. The safety of people and machinery are also a motivation for the stabilization of unstable zones of mining stopes.

The modelled sections show that the ore bodies assume different angulations in different zones of the mineralization and, consequently, mining stopes with different angles and stress concentration. The locations where the lower angulations are verified, between 40° and 60°, are related to the Low Angle Fault Zone, where there is a fault that displaces the ore body between the levels 326 and 270. The other stopes above the level 326 and below the level 270 have in general an inclination between 60° and 80°.

The different inclinations of the mining stopes lead to different instability conditions, where in general the less inclined stopes showed unstable wedges on the hanging wall and the footwall of the ore body, whereas in stopes with higher inclinations, unstable wedges are limited by the hanging wall zone. Therefore, two retainment patterns were initially adopted, one with stabilization only of the hanging wall, and the other with stabilization of the hanging wall and the footwall. The cables used for the studies are the same as those currently adopted at Vazante Mine, with a diameter of 15.00 mm, a young modulus of 200 GPa and a tensile strength of 0.27 MN, as well as variable lengths between 6.00 and 20.00 m, and line spacing of 1.50 m.

Figure 10 shows the kinematic analyses of wedges, with cable arrangement and FS, for the stopes 270-300, and 240-270 in section 13300, where the most critical wedges were detected.

The finite element analyses were performed using Rocscience's Phase2® software, version 9.0, and allowed

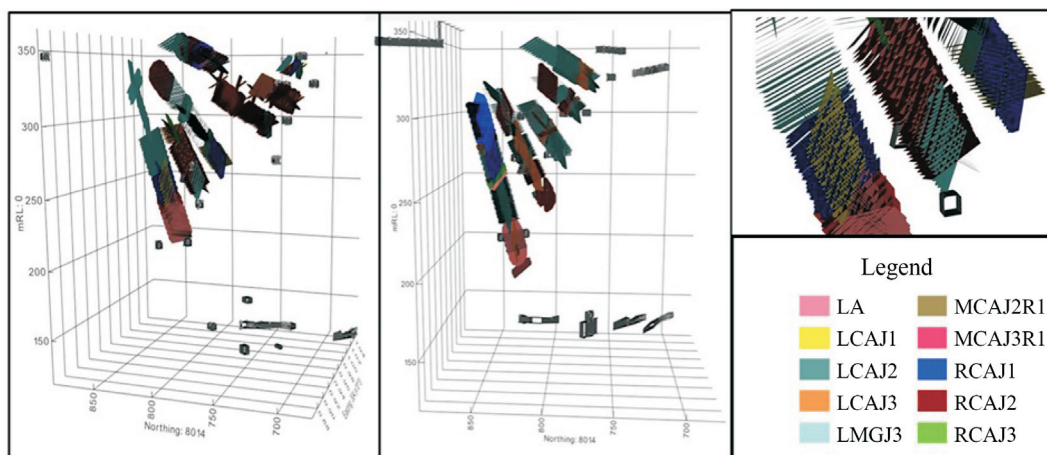


Figure 8 - 3D schematic image showing different views of the modelled discontinuities in the study area.

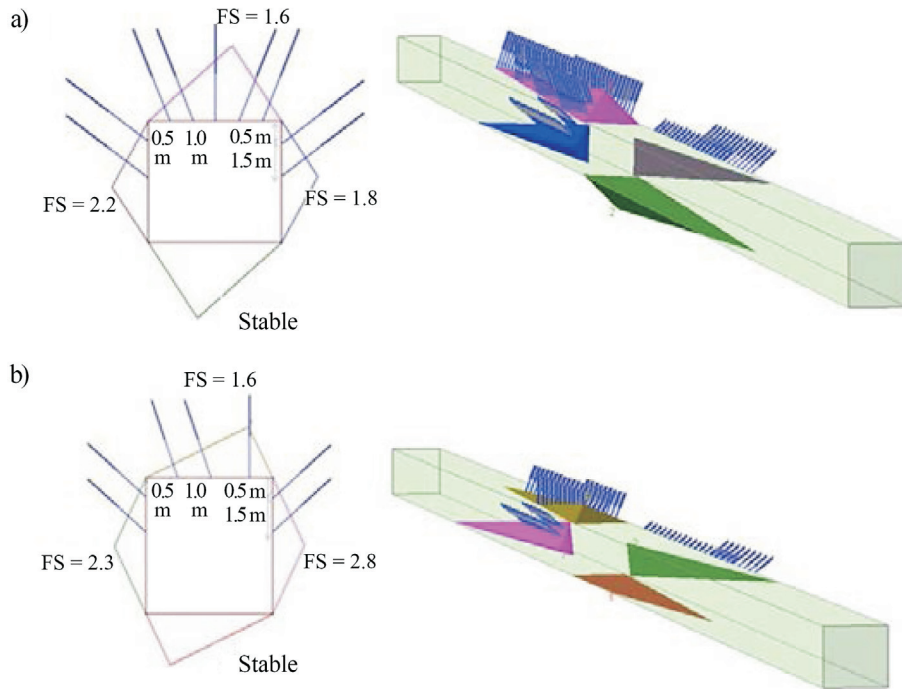


Figure 9 - a) Kinematic stability analysis of wedges, in 2D and 3D - Gallery 300 GM2, on section 13300, b) Kinematic stability analysis of wedges, in 2D and 3D - Gallery 210 GT, in section 13300.

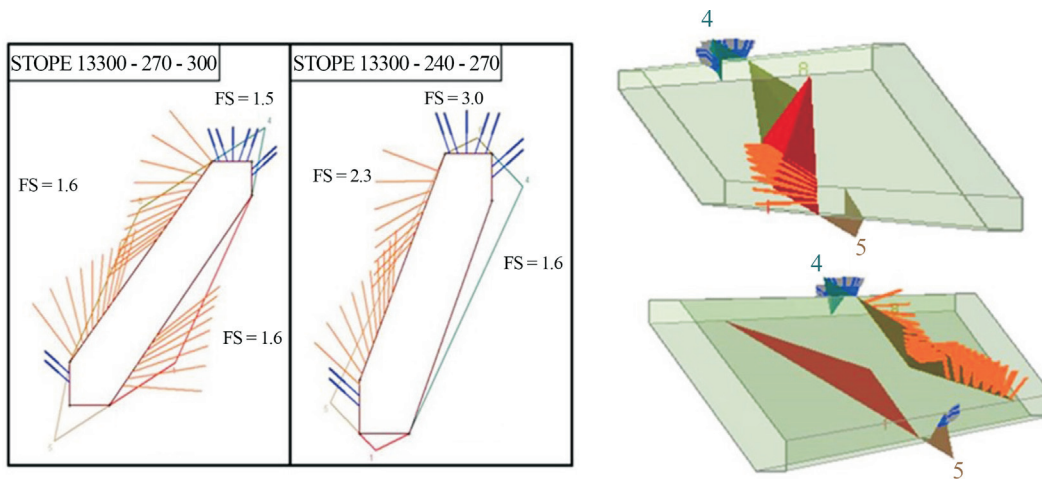


Figure 10 - Kinematic stability analysis of wedges, in 2D and 3D - Stopes 240-270 and 270-300, in section 13300.

the analysis of the stress concentrations induced in the excavations designed for the study area. Discontinuous models were developed, with the modeling of the discontinuities present in each region, and for the purpose of comparison, continuous models were also produced and analyzed with the adoption of equivalent parameters for the rock masses.

According to Curran *et al.* (2008) and Azami *et al.* (2013), the geotechnical parameters of the rock mass in the discontinuous models should be close to the values for the intact rock. Thus, the parameters of Hoek-Brown for a GSI of 90 for the waste rocks (Pink and Gray Dolomites), and an GSI of 80 for the Dolomitic and Willemite Breccias were

assumed. The assumption of GSI of 80 for the breccias comes from the difficulty of representation of localized discontinuities, without persistence in the Vazante Fault Zone. The Hoek-Brown parameters, for continuous media and discontinuous media, are summarized in Table 6.

The sections 13225 and 13300 were split into upper and lower sections, in other words, into four sections of analysis, two sections between levels 345 and 300, and two between levels 210 and 300. All sections have an orientation from NW to SE, approximately. The stress-strain analysis induced in the designed excavations was simulated in stages, according to the order of execution. In this way, it was possible to analyze the stability of the excavations un-

Table 6 - Geotechnical Hoek-Brown parameters and Young Modulus of the rock masses, for continuous and discontinuous media.

Rock mass		σ_{ci} (MPa)	E_i (GPa)	m_i	GSI	m_b	s	a	D	E_{eq} (GPa)
Continuous media	Dolomite	124	56	9	70	1.5	0.01	0.5	0.8	16.4
	Marl	35	6	6	70	1.0	0.01	0.5	0.8	1.8
	Dolomitic Breccia	101	55	9	50	0.5	0.0005	0.5	0.8	5.0
	Willemite Breccia	108	63	9	50	0.5	0.0005	0.5	0.8	5.8
Discontinuous media	Dolomite	124	56	9	90	5.0	0.22	0.5	0.8	30.3
	Marl	35	6	6	90	4.2	0.33	0.5	0.8	5.8
	Dolomitic Breccia	101	55	9	80	2.7	0.05	0.5	0.8	23.3
	Willemite Breccia	108	63	9	80	2.7	0.05	0.5	0.8	26.7

der stress conditions closer to reality, taking into account the interferences generated by neighboring excavations. In addition, it was possible to evaluate basic assumptions for the design of the mining stopes, such as the possibility of application of the VRM method, with direct connection between the top and base galleries of the stopes, and subsequent filling, or if a sill pillar is required, and which thickness is required.

Next, in Fig. 11, the geological model and excavations for the upper 13300 section, chosen to illustrate the methodology, are shown with the final solutions for the design of the mining stopes. The analysis steps presented are from the excavation of the galleries (step 2), and the first stage of analysis consists in the stress distribution in the rock mass without the excavations.

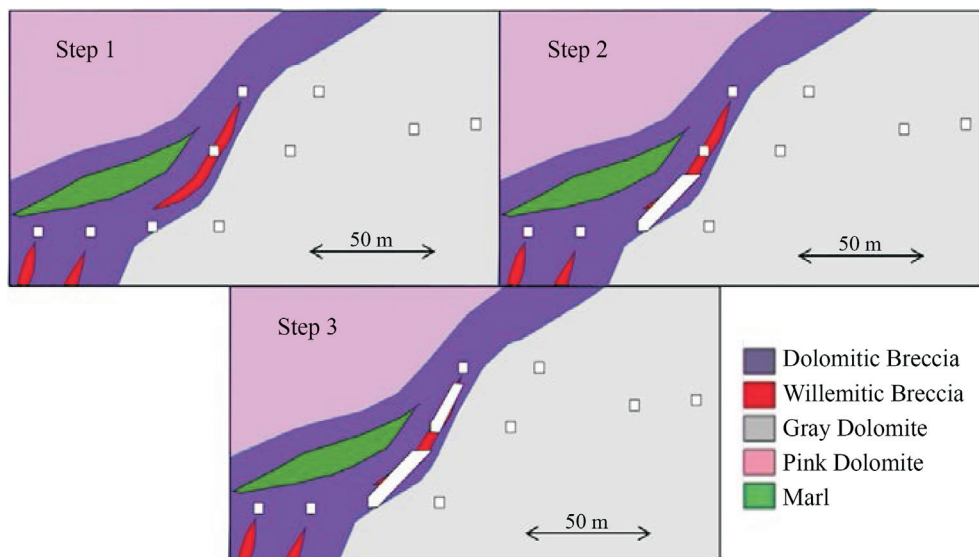
From relations between vertical and horizontal *in-situ* stresses shown before ($\sigma_v = \sigma_H = 1.4 \sigma_n$), the values adopted for the top section of profile 13300 were $\sigma_v = \sigma_H = 9.5$ MPa and $\sigma_n = 7$ MPa.

An elastoplastic constitutive model was adopted, with residual geotechnical parameters of the rock masses

estimated, based on values reported by Crowder & Bawden (2006), obtained through the GSI of the material. For materials with GSI above 70, the residual Hoek-Brown parameters are m_r equal to 1, s equal to 0, and dilation of 0. For materials with GSI less than 50, the m_r value assumed is equal to $0.5 \times m_b$, s equal to 0, and dilation also 0. It is worth remembering that to obtain the residual or post-peak geotechnical parameters of rock masses is extremely difficult and the best way to acquire these data would be through instrumentation, which does not exist in the Vazante Mine, and subsequent back analysis.

In order to simulate the effect of the strain that occurs prior to the installation of the tiebacks in the galleries, an internal pressure of 50% of the stress induced externally to the excavations was assumed against the walls when the tiebacks were installed. In this way, the tiebacks begin to act after half the strain has already occurred, which simulates a situation closer to reality.

The total critical displacement was used to evaluate the strain state of the excavation walls and corresponds to the displacement value in the rock mass from which the dis-

**Figure 11** - Geological interpretation of the section 13300 and analysis steps, in the upper bound, between the levels 300 and 345.

placement process begins; in this study a value of 2.00 cm was assumed. This value is based on the studies developed by Charbel (2015), based on back analysis of mining stopes with great operational dilution, reaching values of up to 60% at level 388 of Vazante Mine.

The characteristics of the tiebacks and cables used to retain the excavations in the finite element analysis are the same as those used in the wedge kinematic analysis.

The finite element meshes used in the analysis for the discontinuous media followed a standard, and the discretization used the intersection points of the discontinuities between them, and with the walls of the excavations and lithological contacts. In addition, other points were created along the lines of the discontinuities, lithological contacts, excavation walls and containment elements, where a distance greater than 0.50 m was observed between the pre-established points. The meshes adopted for the equivalent continuous media models followed a simpler pattern, with pre-definition of the distance between the discretization points, and densification of the points on the walls of the excavations, lithological contacts and along the retaining elements.

All ore galleries (GM) located in the study area were analyzed for their stability by valuation of the total displacements in the rocky masses around the excavations in continuous and discontinuous media.

The 326 GM gallery of section 13300 was chosen to demonstrate the results obtained in the finite element stability studies. The results of the analysis by continuous and discontinuous media showed similarities, with displacements exceeding 2.00 cm in the roof of the gallery.

By observing the strain zones formed in the non-reinforced excavations, it is evident that the interaction between the discontinuities and the rock blocks, reproduced in the discontinuous analysis, details more efficiently where the largest accumulations of stress will occur. In that analysis, the largest displacements are verified within a wedge shape formed in the roof, which resembles the wedges found in the wedge kinematic analysis. In the analysis made after the installation of the tiebacks, the verified displacements are below 2.00 cm, validating the efficiency of the reinforcement system, as can be seen in Fig. 12.

As previously described, the transport galleries (GT) are used for long periods during the life of the mine, leading to the analysis of long-term displacements, caused by suc-

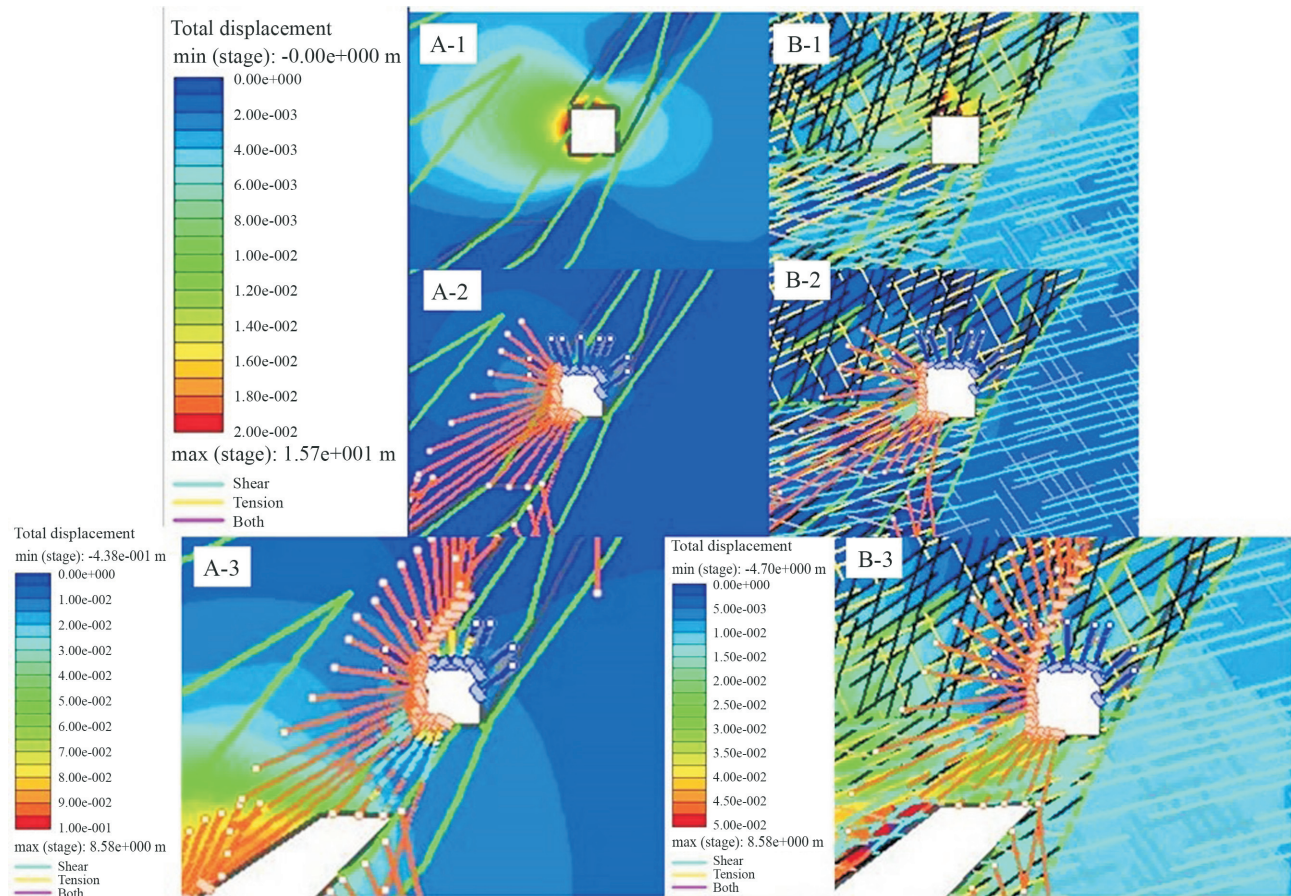


Figure 12 - Finite element analysis of the gallery 326 GM, section 13300. On the left, the analyses by continuous media, and, on the right, the analyses by discontinuous media. A-1 and B-1 are the analyses without the tiebacks, while A-2, B-2 are the analyses in the moment of the installation of the tiebacks and A-3, B-3 after the installation of the tiebacks.

cessive excavations of the mining stopes. Therefore, the studies to be presented below show the stability situation after the excavation of all stopes (most critical situation), and the behavior of the anchorage system in the same analysis step.

The 300 GT gallery studies, in the section 13300, indicated very close results for the models without reinforcement, with displacements from 2.50 to 3.00 cm. The application of the tiebacks limited these displacements to 1.50 cm in the discontinuous model, and it is considered that it practically did not work in the analysis by continuous media, with the same 2.50 cm, compared to the analysis without tiebacks.

In addition to providing safety for persons and equipment during the operating activities of the mine and retaining waste material, reinforcements in the mining stopes work restricting the strain zone generated by the concentration of stresses at certain points of the rock mass around the excavation, so that they have as less influence on the neighboring excavations (galleries and other mining stopes) as possible.

The design of the reinforcement system was determined through wedge kinematic analysis, and reevaluated in the study of stress vs. strains.

The analyzed stope, section 13300, is between the levels 326 and 345, with inclination of approximately 60°, and height just over 15.00 m. The upper sill pillar is 5.00 m, below the gallery 345 GM, and the lower one is 7.00 m, below the gallery 326 GM.

The total displacements observed in this stope were close for the continuous and discontinuous analyses, with-

out the application of the reinforcement system, with values between 4.50 and 5.50 cm. With the application of the reinforcement, the total displacements were reduced to values between 3.00 and 4.00 cm in the analysis by continuous media, and to values below 2.00 cm in the analysis by discontinuous media.

The total displacements observed in the sill pillars remained in the same order of value in relation to the analyses by continuous media, with and without the installation of the cables, while there was a reduction of values close to 3.00 cm, for values of 1.50 cm with the cables applied.

Figure 13 illustrates the continuous and discontinuous media analyses of the stopes between the GM and GM galleries 326.

The results obtained in all the finite element analysis made on sections 13300 and 13225 for the galleries in continuous and discontinuous media can be briefly seen in Fig. 14 and Fig. 15. Figure 16 highlights the results of the analysis and stopes only for section 13300.

6. Conclusions and Recommendations

In general, it can be concluded that the purposes of the study were achieved as all the possible information from the drill core surveys of the studied region was obtained, which provided data for the analysis of the stability of the excavations in discontinuous media. Previous knowledge of the local geological-structural framework, and of the geotechnical behavior of the rock masses, were also essential for the geological-geotechnical modeling.

The total displacements of the rock masses on the walls of the galleries, after the installation of the set of

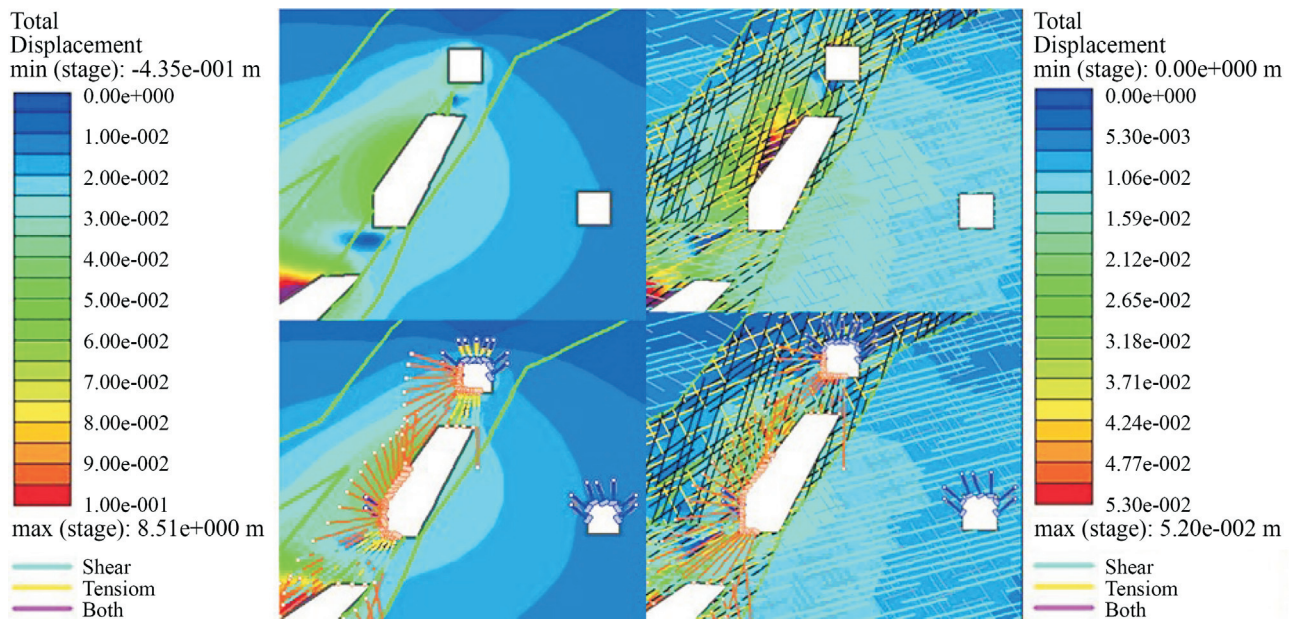
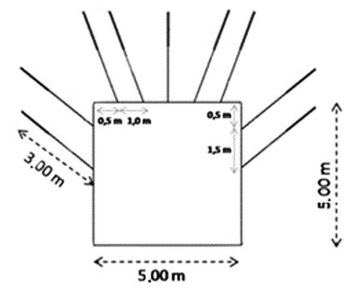


Figure 13 - Finite element analysis of the stope between the galleries 326 GM and 345 GM, on section 13300. On the left, the analysis by continuous media, and, on the right, the analysis by discontinuous media. Above, the analysis without the cables, while below the analysis with the cables, just after the excavation.

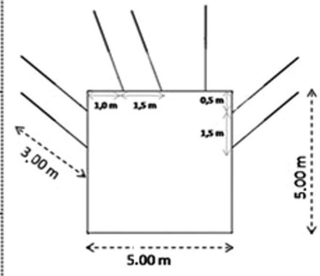
Gallery	Rock Mass	Discontinuities			*FS of Wedges -Kinem. analysis	**Total displacements (Finite Element)		Excavations design / Reinforcement System
		Spacing (m)	Orientation	Class		Continuous Means	Discontinuous Means	
13225	GM-210, GM-240, GM-270 BXD /BXW	0,5	316/68	LA	Between 1,4 e 2,2	No tiebacks 3 to 3,5 cm; With tiebacks 2 to 2,5 cm	No tiebacks 1,5 to 2 cm; With tiebacks < 1 cm	Tiebacks: 3.00 m (anchored length 1.00 m), D=20 mm, tension strength-270KN, Spacing = 1.5 m
		1,0	045/60	LA				
		1,0	341/64	RCAJ2				
		0,5	316/38	RCAJ1				
	GM-300, GM-326, GM-345 BXD /BXW	0,5	316/39	LA	Between 1,4 e 2,2	No tiebacks 3 to 3,5 cm; With tiebacks 1 to 1,5 cm	No tiebacks 1,5 to 2 cm; With tiebacks < 1 cm	
		1,0	136/42	LCAJ2				
		0,5	272/43	RCAJ2				
		1,0	316/00	RCAJ3				
13300	GM-210, GM-240, GM-270 BXD /BXW	0,5	316/78	LA	Between 1,4 e 2,2	No tiebacks 3,5 to 4 cm; With tiebacks 2 to 2,5 cm	No tiebacks 1,5 to 2 cm; With tiebacks < 1 cm	
		2,0	045/60	LA				
		1,0	316/25	LCAJ2				
		1,0	267/81	RCAJ1				
	GM-300, GM-326, GM-345 BXD /BXW	0,5	316/45	LA	Between 1,4 e 2,2	No tiebacks 3 to 3,5 cm; With tiebacks 2 to 2,5 cm	No tiebacks 2,5 to 3 cm; With tiebacks 1,5 to 2 cm	
		1,0	316/81	LCAJ2				
		3	136/70	LCAJ3				
		1	267/81	RCAJ1				
		1	136/30	RCAJ1				



* Factor of Safety after the application of the tiebacks
 ** Displacements with and without the application of the tiebacks

Figure 14 - Summary of the characteristics of the rock masses, results of the analysis and reinforcement system of the ore galleries.

Gallery	Rock Mass	Discontinuities			*FS of Wedges -Kinem. analysis	**Total displacements (Finite Element)		Excavations design / Reinforcement System
		Spacing (m)	Orientation	Class		Continuous Means	Discontinuous Means	
13225	GT-210, GT-240, GT-270 DCZ	2	045/60	LA	Between 1,5 e 2,3	No tiebacks 3,5 to 4 cm; With tiebacks 2,5 to 3 cm	No tiebacks 2,5 to 3 cm; With tiebacks 1 to 1,5 cm	Tiebacks: 3.00 m (anchored length 1.00 m), D=20 mm, tension strength-270KN, Spacing = 1.5 m
		1,0	136/40	LCAJ3				
		1,0	316/20	LMGJ3				
		2	136/52	RCAJ1				
	GT-300, GT-326, GT-345 DCZ	1,0	316/88	LCAJ2	Between 1,5 e 2,4	No tiebacks 1,5 to 2 cm; With tiebacks 1,5 to 2 cm	No tiebacks 1,5 to 2 cm; With tiebacks 1 to 1,5 cm	
		1	316/20	LMGJ3				
13300	GT-210, GT-240, GT-270 DCZ	2	045/60	LA	Between 1,5 e 2,5	No tiebacks 2,5 to 3 cm; With tiebacks 2 to 2,5 cm	No tiebacks 1,5 to 2 cm; With tiebacks 1 to 1,5 cm	
		1,0	136/64	LCAJ2				
		1,0	316/15	LMGJ3				
		1	136/20	RCAJ2				
	GT-300, GT-326, GT-345 DCZ	1,0	136/64	LCAJ2	Between 1,5 e 2,6	No tiebacks 2 to 2,5 cm; With tiebacks 1,5 to 2 cm	No tiebacks 1,5 to 2 cm; With tiebacks 1 to 1,5 cm	
		1,0	316/15	LMGJ3				
		1	136/20	RCAJ2				
		2	045/60	LA				



* Factor of Safety after the application of the tiebacks
 ** Displacements with and without the application of the tiebacks

Figure 15 - Summary of the characteristics of the rock masses, results of the analysis and reinforcement system of the transport galleries.

tiebacks, remained close to the limit of 2.00 cm, a value considered critical for rupture processes according to back analysis of overbreaking stopes. In the discontinuous models, all the displacements were below 2.00 cm after the ap-

plication of the tiebacks. In the continuous model, some displacements reached approximately 2.50 cm. Anyway, this result is considered satisfactory, because of the conservative nature of the method. Therefore, the tieback systems

Stope	Rock Mass		Discontinuities			*FS Wedge Kinem. Anal.	**Total displacements (Finite Element)		Excavations design / Reinforcement System	
	Hang. Wall	Foot Wall	Spacing (m)	Orientation	Class		Continuous Means	Discontinuous Means		
13300	*** 240-270 270-300 (GM) 270-300 (GM2)	BXD	BXD	0.5	316/78	LA	From 1.5 to 2.3	240-270 and 270-300 (GM2)	240-270 and 270-300 (GM2)	
				2.0	045/60	LA		HW: No cable > 10cm Cable: 8 - 9 cm FW: No cable: 8 - 9 cm Cable: 8 - 9 cm	HW: No cable: 4 - 6 cm Cable: 3 - 3.5 cm FW: No cable: 4 - 6 cm Cable: 3 - 4 cm	
				1.0	316/25	LCAJ2		270-300 (GM)	270-300 (GM)	
				1.0	267/81	RCAJ1		HW: No cable > 10cm Cable: 8 - 9 cm FW: No cable 8 - 9 cm Cable: 8 - 9 cm	HW: No cable: 3 - 3.5cm Cable: < 1.5 cm FW: No cable: 3.5 - 4cm Cable: 2.5 - 3 cm	
				2.0	136/30	RCAJ2				
13300	300-326 326-345	BXD	DCZ	0.5	316/45	LA	From 1.5 to 2.3	Hang. Wall: No Cable 6 to 9 cm; With tiebacks 4 to 7 cm	Hang. Wall: No tiebacks 4 to 6 cm; With tiebacks 3 to 3.5 cm	
				1.0	316/81	LCAJ2		Foot Wall No tiebacks 2.5 to 3 cm; With tiebacks 2.5 to 3 cm	Foot Wall No tiebacks 1.5 to 2 cm; With tiebacks 1.5 to 2 cm	
				3.0	136/70	LCAJ3				
				1.0	267/81	RCAJ1				
				1.0	136/30	RCAJ1				

* Factor of Safety after the application of the tiebacks
 ** Displacements with and without the application of the cables
 *** The stope between the galleries 270 GM and 300 GM was the last to be excavated

Figure 16 - Summary of the characteristics of the rock masses, results of the analysis and reinforcement system of the mining stopes.

initially suggested by the wedge kinematic analysis for the GM's and GT's can be considered satisfactory for all the analyzed galleries.

The mining stopes had their reinforcement system initially defined by the kinematic analysis of the critical wedges, in the same way as the galleries. These analyses indicated wedges with a safety factor lower than 1.3 on the hanging wall, foot wall and roof of the stopes, which were stabilized with cables, in order to reach a FS of 1.5.

The thickness of the sill pillars varied according to the inclination of the stopes, having 5.00 m in excavations with inclinations greater than 60°, and 7.00 m for stopes with an inclination lower than 60°. In the presence of parallel stopes, as occurs in the lower portion of section 13300, sill pillars of 7.00 m are also suggested.

The results obtained for the finite element analysis, by continuous media and by discontinuous media, were very different for the studies of the mining stopes, contrary to the analysis made in the galleries. The total displacements observed, with and without the installation of the reinforcement system, are much greater in continuous models. In the analysis by discontinuous media, the majority of the results of total displacements, after the application of the cables, showed values close to 2.00 cm, whereas in the

analysis by continuous media the displacements exceeded significantly the 2.00 cm in almost all the cases.

Local geological contexts were also of great importance for the evaluation of the efficiency and the need for reinforcement. In the stopes in which the foot wall area of the ore body is composed of gray dolomite, the displacements are much reduced, being below 2.00 cm in all cases, regardless of the inclination and height of the stopes. In the stopes where the foot wall is composed of dolomitic breccia, according to the analysis made, it is required to apply a cable as the total displacements exceeded 2.00 cm, and the largest deformation areas were verified in the stopes with inclination less than 60°. The presence of thick bundles of marl in the hanging wall region also induce high total displacements, as evidenced in the analysis of the stopes between the levels 300 and 326, in section 13300.

Therefore, the cable system applied in the mining stopes was considered satisfactory for the analysis of critical wedges, with safety factors greater than 1.5, and for finite element analysis with discontinuous media, with total displacements close to 2.00 cm. However, in the analysis by finite elements by continuous media, the observed displacements were high, even after the application of the reinforcement system, with values between 7.00 and 10.00 cm.

Finally, complementary studies are recommended, namely for comparison of the results obtained with the actual results of the excavations to be executed in the study region, so that the methodology and the parameters are calibrated for the analysis by discontinuous media. In addition, the post-peak, or plastic, geotechnical parameters of the rock masses involved in the analysis should be better studied through instrumentation and back analysis. Stability studies by distinct elements are also indicated, since the geotechnical characterization of the discontinuities performed in this work provides enough information for that, in order to compare the results obtained in the finite element analysis and wedge kinematic analysis. The shearing and axial stresses in the cables can also be better studied through the discontinuous models as it is possible to evaluate relative movements between blocks delimited by the discontinuities present in the rocky masses.

References

- Azami, A.; Yacoub, T.; Curran, J.H. & Wai, D. (2013). A Constitutive Model for Jointed Rock Mass. www.roscience.com.
- Bandis, S.C.; Lumsden, A.C. & Barton, N. (1983). Fundamentals of Rock Joint Deformation. *International Journal of Rock Mechanics, Mining Sciences & Geomechanics*, 20(6):249-268.
- Barton, N. (1970). A low strength material for simulation of the mechanical properties of intact rock in rock mechanics models. *Proc. 2nd Congress International Society for Rock Mechanics*, Belgrade, Theme 3, Paper 15, 12 p.
- Barton, N. (1972). A model study of rock-joint deformation. *International Journal of Rock Mechanics and Mining Sciences & Geomechanics*, 9(5):579-602.
- Barton, N. (1974). Estimating the shear strength of rock joints. *Proc. 3rd Congress International Society for Rock Mechanics*, Denver, 2A:219-220.
- Barton, N. & Choubey, V. (1977). The shear strength of rock joints in theory and practice. *Rock Mechanics*, 1(2):1-54.
- Barton, N. & Bandis, S. (1980). Some effects of scale on the shear strength of joints. *International Journal of Rock Mechanics and Mining Sciences & Geomechanics*, 17(1):69-73.
- Bhering, A.P. (2009). Classificação do Maciço Rochoso e Caracterização das Brechas de Mina Subterrânea de Vazante-MG. Dissertação de Mestrado, Departamento de Engenharia Civil da Universidade Federal de Viçosa, Viçosa, 176 p.
- Charbel, P.A. (2015). Gerenciamento de Risco Aplicado à Diluição de Minério. Tese de Doutorado, Departamento de Engenharia Civil, Universidade de Brasília, Brasília, 406 p.
- Crowder, J.J. & Bawden, W.F. (2006). The Estimation of Post-Peak Rock Mass Properties: Numerical Back Analysis Calibrated using In Situ Instrumentation Data. www.roscience.com.
- Curran, J.H.; Hammah, R.E.; Yacoub, T. & Corkum, B. (2008). The practical modelling of discontinuous rock masses with finite element analysis. 42nd US Rock Mechanics Symposium and 2nd U.S.-Canada Rock Mechanics Symposium, ARMA 8-180.
- Dardenne, M.A. (2000). The Brasilia Fold Belt. *Proc. 31st International Geological Congress - Tectonic evolution of South America*, Rio de Janeiro, 1:231-263.
- Dardenne, M.A. & Schobbenhaus, C. (2001). *Metagênese do Brasil*. Editora Universidade de Brasília, Brasília, 392 p.
- Goodman, R.E.; Taylor, R.L. & Brekke, T.L.; (1968). A model for the mechanics of jointed rock. *Journal of the Soil Mechanics and Foundations Division*, 94(SM3):637-659.
- Goodman, R.E. (1976). *Method of Geological Engineering in Discontinuous Rocks*. West Publishing Company, San Francisco, 467 p.
- Hoek, E. & Karzulovic, A. (2000). Rock mass properties for surface mines. *Slope Stability in Surface Mining*, Society for Mining, Metallurgical and Exploration (SME), Colorado, 1:59-70.
- IPT (1994). Ensaios laboratoriais de mecânica de rochas em amostras provenientes das minerações subterrâneas de Vazante e Morro Agudo, MG. Report N° 31 663, 272 p.
- Kahraman, S.; Korkmazve, S. & Akcay, M. (1996). The Reliability of Using Schmidt Hammer and Point Load Strength Test in Assessing Uniaxial Compressive Strength, K.T.U. Department of Geological Engineering 30th Year Symposium, Trabzon, 1:362-369.
- Kulhawy, F.H. (1975). Stress deformation properties of rock and rock discontinuities. *Engineering Geology*, 9(4):327-350.
- Pinho, J.M.M. (1990). *Evolução Tectônica da Mineralização de Zinco de Vazante-MG*. Dissertação de Mestrado, Instituto de Geociências, Universidade de Brasília, Brasília, 212 p.
- Rostirolla, S.P.; Mancini, F.; Reis Neto, J.M.; Figueira, E.G.; & Araújo, E.C. (2002). Análise estrutural da mina de Vazante e adjacências: geometria, cinemática e implicações para a hidrogeologia. *Revista Brasileira de Geociências*, 32(1):59-68.
- Wyllie, D.C. & Mah, C.W. (2004). *Rock Slope Engineering*. 4th ed. Spon Press, London, 431 p.
- Yagiz, S. (2008). Predicting uniaxial compressive strength, modulus of elasticity and index properties of rocks using the Schmidt hammer. *Bulletin of Engineering Geology and the Environment*, 68(1):55-63.

A Case History with Combined Physical and Vacuum Preloading in Colombia

D.G. Yanez, F. Massad

Abstract. The scope of this paper is the back analysis of soft soil treatment case studies in which prefabricated vertical drains together with physical and vacuum surcharge were applied. Initially, the vacuum surcharge systems in vertical drains used worldwide are reviewed. The radial consolidation theory specifically developed for vacuum and physical surcharges is presented, highlighting the influence of the vacuum efficiency parameter. This parameter represents whether or not there is a loss of vacuum pressure in depth. In the second moment, the local geological-geotechnical parameters of the construction are presented, from which data were used as case studies. This characterization was based on the study of regional geology, field geotechnical tests, the collection of undisturbed samples and further laboratory tests. Based on the specific consolidation theory and the geological-geotechnical characterization carried out, detailed analyzes are presented for 2 specific sites of the case study. The detailed analysis is composed of two steps of numerical modeling. The first step analyzes the vacuum loss in depth, as presented in the literature review and the second step is used to check the geotechnical parameters interpreted by the investigation campaign. At the end, comments and considerations are made about the vacuum consolidation theory and the soil characteristics in the case studies.

Keywords: consolidation theories, sample quality, settlement back analysis, soft soil, vacuum surcharge.

1. Introduction

There are several constructive methodologies for improving soft soil, such as partially or completely removing and substituting the soft soil layer; building light embankments; using stability berms; building piled embankments and embankments reinforced with geosynthetics; building in stages; preloading with temporary surcharge; installing Prefabricated Vertical Drains (PVDs) along with the use of preloading; and using PVDs together with both embankment and vacuum surcharge combined. The most adequate solution depends on: the geological-geotechnical characteristics of the deposits; the use of the constructed area and its vicinity; the time available for construction; and the cost of construction. (Almeida & Marques, 2010). Partially or completely removing and substituting the soft soil layer has been less and less applicable because of its high cost and the environmental impact given the need for both borrow and spoil banks. Staged construction is often an economical approach, but the time required for consolidation is often incompatible with the available schedule. PVDs can be installed to improve drainage conditions and geosynthetic reinforcement, *i.e.* geogrids or geotextiles, used to increase the embankment height in every stage, thus reducing the consolidation time, but sometimes it is not enough to meet modern construction restraints.

A current alternative to preloading in embankments on soft soil is vacuum surcharge, which results in negative pore pressure (suction) on the soil that is approximately

100 kPa next to sea level - a value that is lower in practice. Differently from a traditional embankment, suction does not lead to an increase in total stress, risking stability. Vacuum suction can also be used to accelerate consolidation time compared to conventional surcharge, even with PVD. The vacuum preloading technique was presented by Kjellman (1952) after initial tests in the 1940s. Kjellman's system consisted in applying vacuum in a sand layer on the surface with an impermeable membrane over it. This impermeable membrane needs to completely isolate the area where vacuum is to be applied, therefore, it can be necessary to build a peripheral trench in the area, maintained with a water or slurry seal. Despite the knowledge available regarding the vacuum application theory (Holtz & Wager, 1975), it was only after the 1980s that this method became popular, especially in the Asian (Choa, 1989; Qian *et al.*, 1992) and European geotechnical communities (Massé *et al.*, 2001), due to advances in vacuum pump technology. The main advantages of vacuum surcharge (sometimes also called "virtual" surcharge) in relation to physical surcharge are the following, as presented by Pilot (1981): (i) there are no problems with embankment instability to be considered; (ii) it eliminates the need for material quarries for temporary surcharge, which are usually expensive and/or unavailable in modern projects; and (iii) the installation, application and removal of vacuum surcharge are quickly carried out. In opposition, vacuum surcharge adds more variables to the already complex problem of soft soil treatment with PVDs and preloading. So much is that Indraratna *et al.*

Diego Gazolli Yanez, M.Sc. Student, Escola Politécnica, Universidade de São Paulo, Av. Prof. Almeida Prado 271, trav. 2, São Paulo, SP, Brazil. e-mail: gazolli@usp.br. Faïçal Massad, Ph.D., Full Professor, Escola Politécnica, Universidade de São Paulo, Av. Prof. Almeida Prado 271, trav. 2, São Paulo, SP, Brazil. e-mail: faissal@usp.br. Submitted on July 25, 2016; Final Acceptance on May 16, 2018; Discussion open until December 31, 2018. DOI: 10.28927/SR.412217

(2005) developed a specific radial consolidation theory for vacuum surcharge which can (or not) describe a linear suction pressure decrease with depth.

A vacuum suction system was used as preloading in a highway duplication in Colombia where alluvial soft soil is present. This deposit formation gives the soil a heterogeneous profile in which the stratigraphy includes erratic peat deposits with very low shear strength, eventual fine sands and the upper layers are affected by seasonal desiccation. Vacuum surcharge was especially attractive in this case because the existing highway lane's operation could be compromised if the new embankment were to cause instability. Two sites 900 m apart from each other were chosen to be presented in this paper, namely A and B. SPT and piezocone testing were executed in the former and a complete investigation, including laboratory consolidation tests, was conducted at the latter. Better settlement predictions were expected to arise from the parameters measured at the latter site B but, given the heterogeneous nature of the soft soil, they did not. Thus, in order to provide reliable results and interpretations, back analysis was carried out to infer the vacuum efficiency and representative soil parameters.

2. Practical Systems for Applying Vacuum Currently in Use

There are currently two well-known systems for applying vacuum on soft soil: the “membrane” and the “drain-to-drain” systems, as shown in Fig. 1. The former, an older system, uses an impermeable membrane mounted on a sand blanket over a peripheral trench in the whole area to be treated, just like the system created by Kjellman (1952), as is commercially employed in Europe and several Asian countries, especially China and Japan. In some cases, it is necessary to dig an impervious slurry wall below the peripheral trench in order to isolate sand lenses and permeable layers, whereas the more recent system allows intermediate sealing sheets to be used (Chai *et al.*, 2008). The

second system connects vacuum straight to the PVDs and was developed in the Netherlands in the early 1990s (Sandroni *et al.*, 2012). In both systems, it is common to temporarily lower the water table during the operation of vacuum, which leads to superficial dehydration and occasionally to tension cracks.

One of the advantages of the “drain-to-drain” system in comparison with the “membrane” one is that the former can be used in terrains where there are intermediate sand layers in the soil. In this case, any sand layers below as well as above the water level must be isolated from the vacuum by blind stretches of the drains in order not to lose efficiency of the vacuum, avoiding the need for the impervious slurry wall around the area to be treated in the “membrane” system. If the lower layer is a draining one, the PVD must remain approximately 1.0 m above this stratum, forming a lower impermeable zone. Contrarily, one possible disadvantage of the “drain-to-drain” method regards its suction reach. In the “membrane” system, vacuum pressure is applied in the sand blanket and to the soil through the vertical drains, while in the “drain-to-drain” system vacuum is only applied directly inside the vertical drains. Hence, as Li *et al.* (2011) verified in laboratory with samples whose diameter was 30 cm and 1 m high, the “membrane” system was slightly more efficient than the “drain-to-drain” one, possibly due to the application of vacuum not only in the vertical drain, but also on the surface, resulting in both radial and vertical suction combined. However, when the soft soil is too thick, this effect is negligible.

The highest vacuum pressure that can be applied is limited by atmospheric pressure, which is higher than 90 kPa up to an altitude of 1,000 m. In practice, however, the highest feasible pressures are between 60 and 80 kPa, due to vacuum losses in the system (in the vacuum pumps, connections, hoses, vertical drains, etc.) and on the soil. A nominal suction (p_v) of 80 kPa is usually associated with vacuum consolidation and, when the necessary surcharge

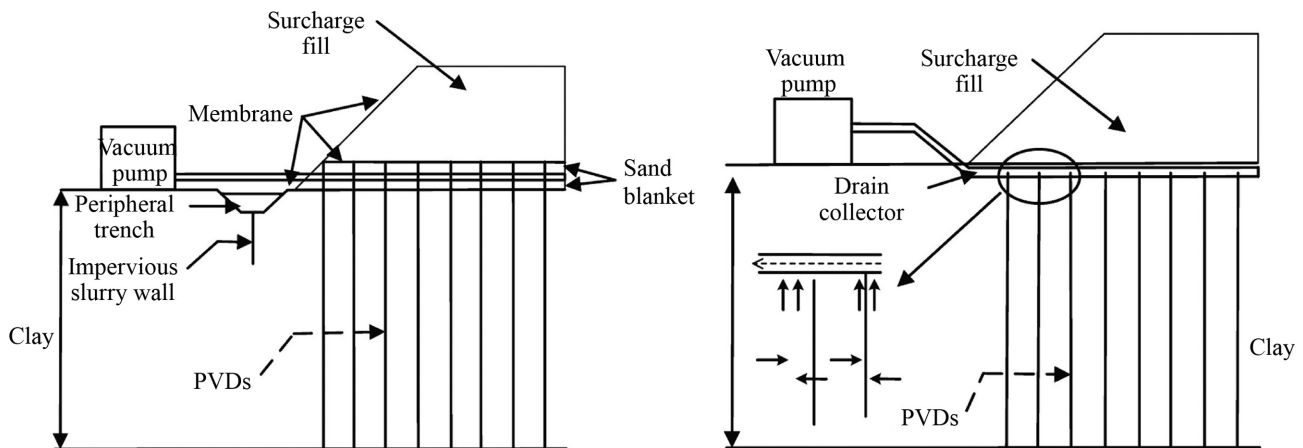


Figure 1 - Systems for applying vacuum on the field (a) with membrane, and (b) drain to drain (or “membraneless”). Source: Indraratna (2010).

for the construction is higher than 80 kPa, physical preloading is also employed. When the vacuum pump is located above the level where suction is applied, part of the pressure dissipates throughout the suction height (H_s). It is possible to observe the relationship between atmospheric pressure, suction height - or the difference between the elevation of the vacuum pump and the water table level - and the vacuum pressure effectively applied on the soil, as shown in Eq. 1 and Fig. 2.

$$\sigma_{vac} = p_v - H_s \cdot \gamma_w \quad (1)$$

3. Radial Consolidation Theory with Vacuum, Focusing on its Distribution in Depth

Indraratna *et al.* (2005) presented a theory of radial consolidation with physical and vacuum surcharge through the overlapping of their effects. Their theory stems from the radial consolidation described by Barron (1948) and Hansbo (1979) and adopts a distribution of vacuum pressure according to what is presented in Fig. 3, where vertical and radial vacuum pressure can be affected by the reduction factors k_1 and k_2 , respectively. Corresponding pore pressure excess is shown in Eq. 2. These factors, as well as spacing ratio ($n = D/d_w$), define the efficiency of vacuum preloading (G) indicated in Eqs. 2, 3 and 4. This vacuum distribution was adopted based on laboratory studies, with large-scale consolidation equipment and vertical drains, which indicated vacuum losses of up to 25% in 1 m of drain, from the top to the bottom of the sample. Other authors, such as Massé *et al.* (2001), consider that vacuum pressure as constant with depth, being limited only by the maximum depth at which PVDs can be installed, *i.e.*, approximately 45 m.

$$\Delta u = \sigma_{vac,0} \cdot G(n) + [q - \sigma_{vac,0} \cdot G(n)] \cdot e^{\frac{8T_v}{F(n)+F_v+F_r}} \quad (2)$$

or

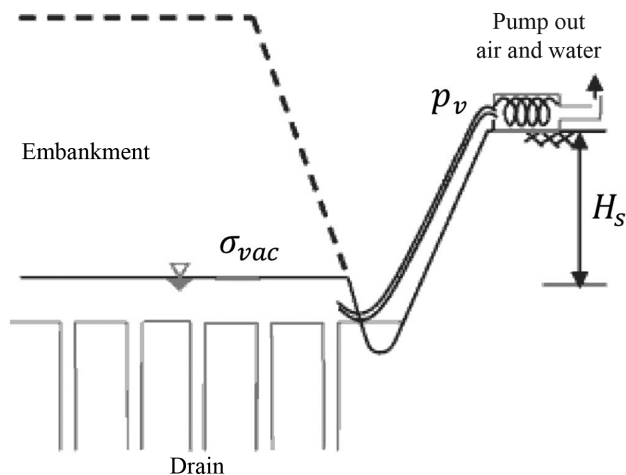


Figure 2 - Vacuum pressure applied to the soil. Source: adapted from Chai *et al.* (2014).

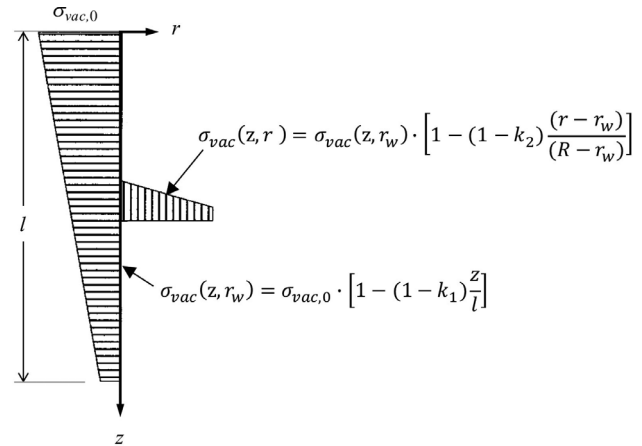


Figure 3 - Vacuum pressure distribution. Source: adapted from Indraratna *et al.* (2005).

$$\Delta u = \sigma_{vac,0} \cdot G(n) + [q - \sigma_{vac,0} \cdot G(n)] \cdot U_h \quad (3)$$

where

$$G(n) = \frac{(1 + k_1)[n(1 + 2k_2) + (2 + k_2)]}{6(n + 1)} \quad (4)$$

$G(n)$ efficiency of vacuum preloading, q conventional surcharge, n spacing ratio, D diameter of the effective influence zone of the drain, d_w diameter of the drain (well), $\sigma_{vac,0}$ vacuum pressure applied at the top of the drain ($\sigma_{vac,0} < 0$), k_1 vacuum reduction factor in the vertical direction, k_2 vacuum reduction factor in the horizontal direction.

To assess vacuum distribution in real practice, Indraratna *et al.* (2005) used field data to compare their theory of radial consolidation with vacuum considering four cases:

- Case A: vacuum pressure is constant in both directions ($k_1 = k_2 = 1$);
- Case B: vacuum pressure is constant throughout the vertical drain and varies linearly down to 0 in the radial direction ($k_1 = 1, k_2 = 0$);
- Case C: vacuum pressure is constant in the radial direction and varies linearly down to 0 throughout the vertical drain ($k_1 = 0, k_2 = 1$); and
- Case D: vacuum pressure varies linearly down to 0 in both vertical and radial directions ($k_1 = k_2 = 0$).

The one that came closer to the data measured in the field was Case C, in which the vacuum pressure adopted is constant in the radial direction and varies linearly up to 0 throughout the vertical drain ($k_1 = 0, k_2 = 1$, therefore $G(n) = 0.5$). In Case A, the vacuum pressure adopted is constant in both the vertical and radial directions, so $G(n) = 1.0$. In Eq. 2 and 3 it is easy to observe that the efficiency of vacuum preloading ($G(n)$) directly determines the amount of negative pressure that remains at the end of the vacuum consolidation process, therefore also determining the difference in pore pressure that dissipates during settlement. It is possible to notice that when $G(n) = 1.0$ (Case A), Eq. 2 is

the same as presented by Hansbo (1979). Despite the difference in the amount of pore pressure dissipation in the soil among the cases assessed, the rate of radial consolidation with vacuum, expressed by the relation $U_h \times T_h$, is the same as the traditional radial consolidation by Hansbo (1979) and Barron (1949).

4. Local Geological-Geotechnical Characteristics of the Case Study

4.1. Alluvial origin of the soft soil

The construction case history analyzed in this paper is the duplication of the Ruta del Sol highway in Colombia, officially called Ruta Nacional 45. The highway runs through five Colombian departments: Cundinamarca, Boyacá, Santander, Cesar and Magdalena, between the cities of Villeta (Cundinamarca) and Ciénaga (Magdalena). More details on the geotechnical parameters and the soft soil treatment can be seen in Yanez (2016). Regional and local geology are described according to CONSOL (2015).

During construction, alluvial soil deposits were found in the low areas next to the Magdalena River, where drainage is insufficient and organic matter and fine compressible soil accumulate. Figure 4 presents the kinds of soil that are formed in these geological conditions. Alluvial soils can also be highly dehydrated during periods of drought.

The Magdalena River begins in southwestern Colombia and runs throughout the country, ending in the Caribbean Sea. It is about 1,550 km long and its average streamflow amounts to approximately 7,000 m³/s. In comparison, the Tietê River, in Brazil, has an average streamflow of about 2,500 m³/s. Differently from marine soft soil, alluvial soils are generated according to the action and intensity of the waters that flow in a river. Rivers that meander in lowlands undergo a random sedimentation process throughout time, varying according to the streamflow and rain intensity over a period of hundreds of years.

The aforementioned construction is located near the equator, in the Intertropical Convergence Zone with a biannual rain pattern. Average annual precipitation amounts to 2,150 mm. Temperatures in the area vary between 27 and 35 °C and relative humidity varies between 75% and 80%. The Magdalena River Basin valley is located between 185 and 800 m altitude in relation to sea level. Rocks from the Paleogene and Neogene periods (both from the Tertiary) of continental origin are found in this area. They usually correspond to conglomerates, sandstones and argillites with the addition of other unconsolidated deposits from the Quaternary period. The region's relief is moderate, with mounts and hills formed due to the erosion that acted on the sedimentary rocks of the Neogene and landscapes smoothed by recent alluviation, resulting from weathering in the highest areas.

Alluvial deposits originated from the Magdalena River dynamics form terraces elevated some meters above the original streambed, characterized by a lowland morphology slightly inclined in the direction of the body of water. These terraces present slopes that are between 3 and 5 m high on the river banks. On the surface, they are mainly comprised of brown clayey silt to sandy silt and an occasional bedding of rounded gravel and sand with some fines. These regions where drainage is insufficient are frequently flooded and often accumulate fine materials and decomposing vegetation, which generate the soft soil identified in the case study.

4.2. Geotechnical investigations

All borings were located according to the highway stationing, called ST and each ST corresponds to one kilometer along the axis. Initial investigations were carried out by SPT borings. Disturbed samples were collected from all SPT borings in every meter to carry out characterization tests in laboratory (grain size by sieving, water content, specific gravity and Atterberg Limits). Samples with N

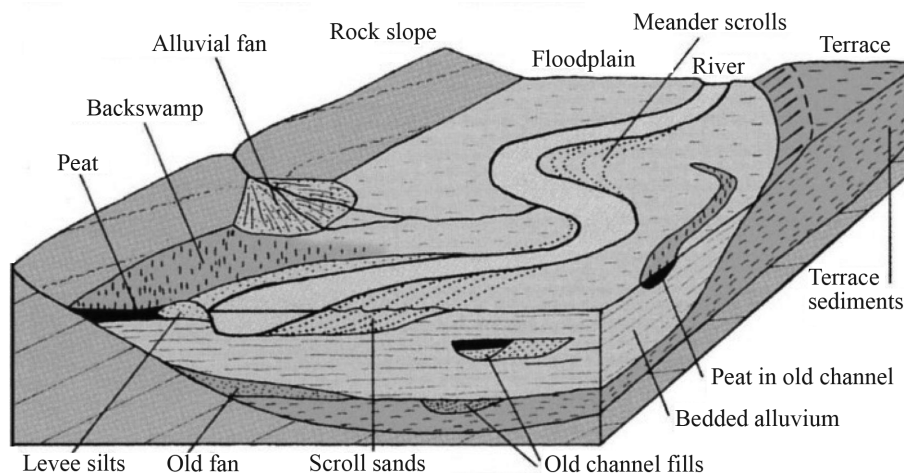


Figure 4 - Geotechnical formation of alluvial soils. Source: Waltham (2001).

(number of blows) between five and ten blows were found in the middle of a larger soft soil *stratum* in several borings, which might have been influenced by the presence of twigs and decomposing organic matter in the compressible alluvial layer. Additional geotechnical tests were carried out in sites where the soft soil was thicker than 6 m. Undisturbed samples were collected with 4” Shelby tubes for laboratory consolidation tests, and piezocone tests were conducted with pore pressure dissipation in more than one depth.

Overall, 51 consolidation tests were performed with the undisturbed samples collected ranging from ST 68 to 112 and grouped in a database parameter. Geotechnical assessment was based on all *in situ* testing and restricted to fair, good, very good and excellent undisturbed samples. Quality analysis of the samples is described in item 4.2.1 ahead and the geotechnical parameters that raised from it described in item 4.2.3.

4.2.1. Quality of the consolidation test samples

Undisturbed sample quality was assessed according to Lunne *et al.* (1997). This method is based on Eq. 5, that relates the initial void ratio of the sample (e_0) and the void ratio measured in the consolidation test in the effective stress in its natural state (e). Table 1 presents the sample disturbance criterion.

$$\frac{\Delta e}{e_0} = \frac{e_0 - e}{e_0} \tag{5}$$

In most cases, sample disturbance between collection and transportation to the laboratory were so significant that caused unusable test results. It is possible to observe the analysis of the quality of the 4” Shelby samples submitted to consolidation testing in Fig. 5.

4.2.2. Stress history through piezocones

Preconsolidation stress measured by piezocones (CPTu), according to Mayne & Brown (2003), was compared to the preconsolidation stress obtained through laboratory tests. Figure 6 presents this calibration comparison performed in three sites.

In the laboratory, preconsolidation stress was obtained using the method by Silva (1970). Preconsolidation stress estimates presented by the company that owns the piezocone equipment, by Mayne & Brown (2003), were fairly similar to the values obtained in the consolidation tests, as can be observed in Fig. 6. In general, the stress his-

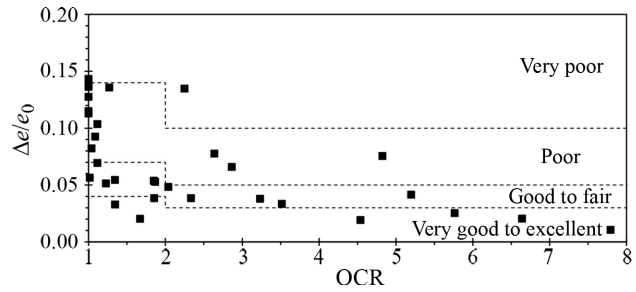


Figure 5 - Quality index of the consolidation tests according to Lunne *et al.* (1997). Source: Yanez *et al.* (2015).

tory observed in the alluvial soil in the case history and presented in the sequence is like what is shown in Fig. 6: an occasional top weathered crust (possibly by dehydration) followed by normally consolidated compressible soil.

4.2.3. Geotechnical parameters

Yanez *et al.* (2015) obtained preliminary geotechnical parameters from the parameter database comparing the resulting water content and measured compressibility at the laboratory. Poor and very poor samples were not considered in this assessment. It is possible to notice that data regarding compressibility $C_c/(1 + e_0)$ as a function of water content are very sparse (Fig. 7b), differently from data concerning C_c as a function of w (Fig. 7a).

Table 2 shows regional geotechnical parameters representative of the soil in the case history divided into two groups, as presented by Yanez *et al.* (2015). The first group consists of clayey silt, with soft to medium consistency and water content (w) between 30% and 100%. The second group is considerably more compressible and peaty, with very soft consistency and higher water content. Geotechnical parameters of soil from the alluvial lowlands in the city of São Paulo are presented for comparison.

4.2.4. Representative borings

In Figs. 8 and 9 it is possible to observe representative borings of two sites in the case history. The borings also contain data on natural water content and Atterberg limits. The SPT-336 (Fig. 8a) and the CPTu-5 were carried out close to each other.

At Site A, two pore pressure dissipation tests were performed, analyzed according to Houlsby & Teh (1988). Figure 10 presents the pore pressure dissipation test done 3.1 m deep in CPTu-5.

Table 1 - Sample disturbance criterion. Source: Lunne *et al.* (1997).

Overconsolidation ratio	$\Delta e/e_0$			
	Very good to excellent	Good to fair	Poor	Very poor
1-2	< 0.04	0.04-0.07	0.07-0.14	> 0.14
2-4	< 0.03	0.03-0.05	0.05-0.10	> 0.10

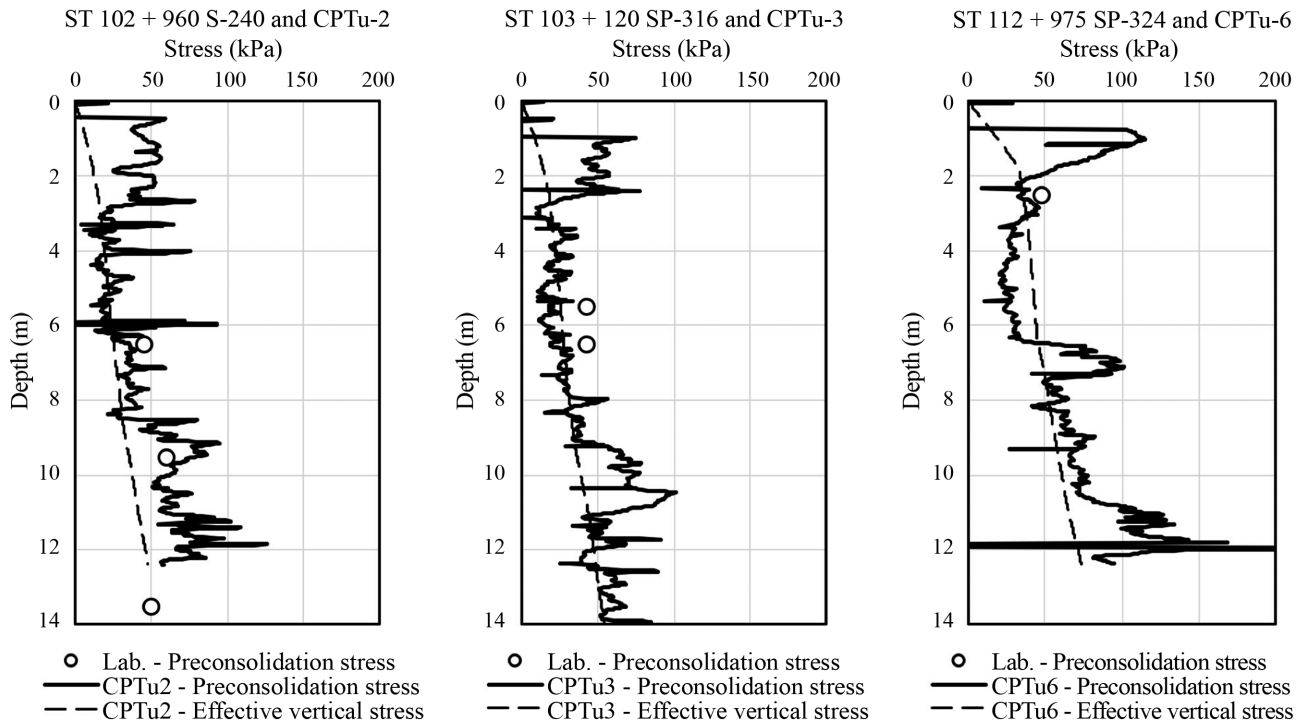


Figure 6 - Comparison between the preconsolidation stress measured with piezocones and in laboratory tests.

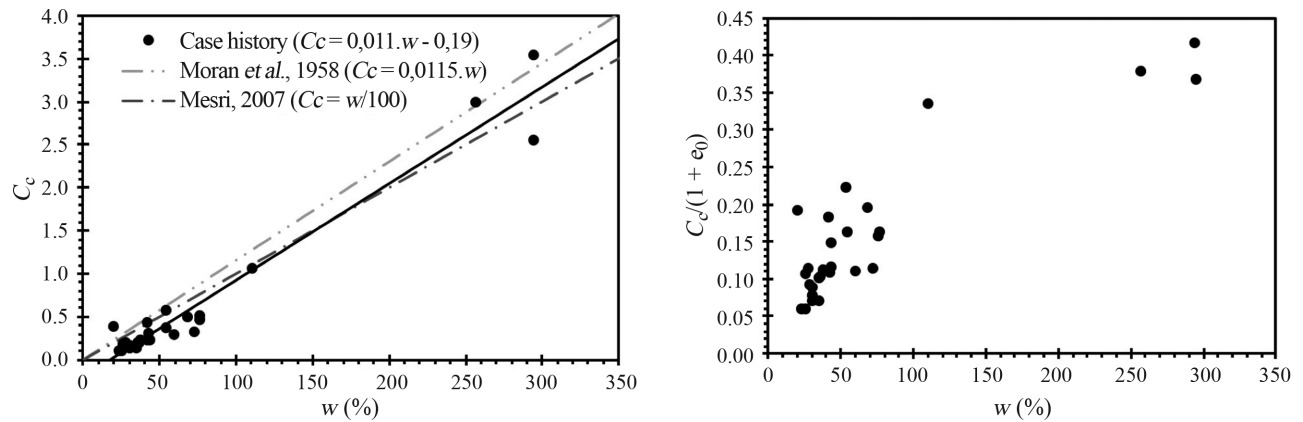


Figure 7 - Results of the geotechnical tests between w with (a) C_c and (b) $C_c/(1 + e_0)$. Source: Yanez *et al.* (2015).

The result of the pore pressure dissipation tests with piezocones can be observed in Table 3, which summarizes data from 3 dissipation tests conducted in Site A and 6 in Site B. It is possible to notice that the consolidation ratio measured using piezocones (Table 3) is consistent with the one measured in laboratory tests (Table 2) for Group 1, clayey silts.

5. Embankment Instrumentation

Many instruments were installed at the case study site to monitor the construction of the embankments. Namely, settlement plates (marked as PR), inclinom-

eters and standpipe piezometers were widely used. Settlement plates were installed to monitor vertical displacements during embankment construction. These settlement instruments consist of 1 m square metal plates connected to threaded rods and placed on top of the original ground before the embankment heightening. PVC pipes were installed around the rods to prevent friction between the rods and the compacted fill. Benchmarks were also installed several meters away from the settled area.

Standpipe piezometer measurements were not reliable due to dehydration of the instruments by vacuum suc-

tion and poor installation procedures. Furthermore, inclinometers and piezometers readings are not discussed in this article. More details on the geotechnical instruments and monitoring can be seen in Yanez (2016).

Table 2 - Geotechnical parameters of the alluvial soft soil. Source: Yanez *et al.* (2015, p. 1602).

Characteristics	Case history		Lowland soil in the city of São Paulo*
	Group 1 clayey silts	Group 2 Peat	
Thickness (m)	6-21	< 5	≤ 5
Consistency	Very soft to medium	Very soft	Very soft to soft
$\sigma'_p - \sigma'_{v0}$	0-20	0-40	N/A
SPT	0-6	0-2	0-4
LL (%)	40-80	70	30-100
PI (%)	10-35	30	10-35
% < 5 μm	-	-	30-75
γ_s (kN/m ³)	26.0	19.0	N/D
γ_{clay} (kN/m ³)	14.5-16.5	11-15	11.0-18.0
w (%)	30-100	> 200	30-300
e_0	1-2	> 6	1-6
S_u (kPa)	20-40	10-20	5-25
OMC (%)	1-10	> 20	N/A
C_{ae} (%)	-	-	3
C_{v-EDO} (cm ² /s)	(1-50).10 ⁻⁴	(1.5-3.0).10 ⁻⁴	(30-50).10 ⁻⁴
$C_f/(1+e_0)$	0.10-0.35	0.40-0.45	0.15-0.35(0.25)
C_f/C_c (%)	10-25	12-15	10

* According Massad, F. (2003). Obras de Terra: Curso Básico de Geotecnia. Oficina de Textos, São Paulo, 170 p.

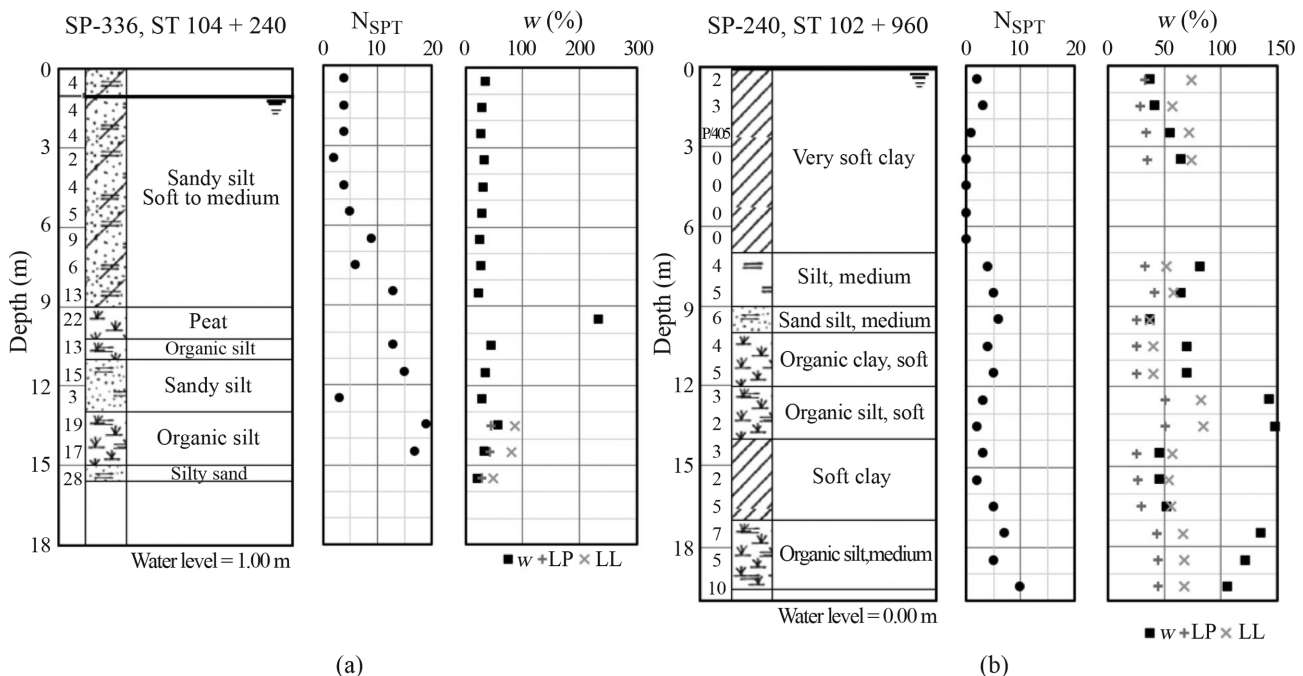


Figure 8 - Example of representative borings in Sites A and B, respectively.

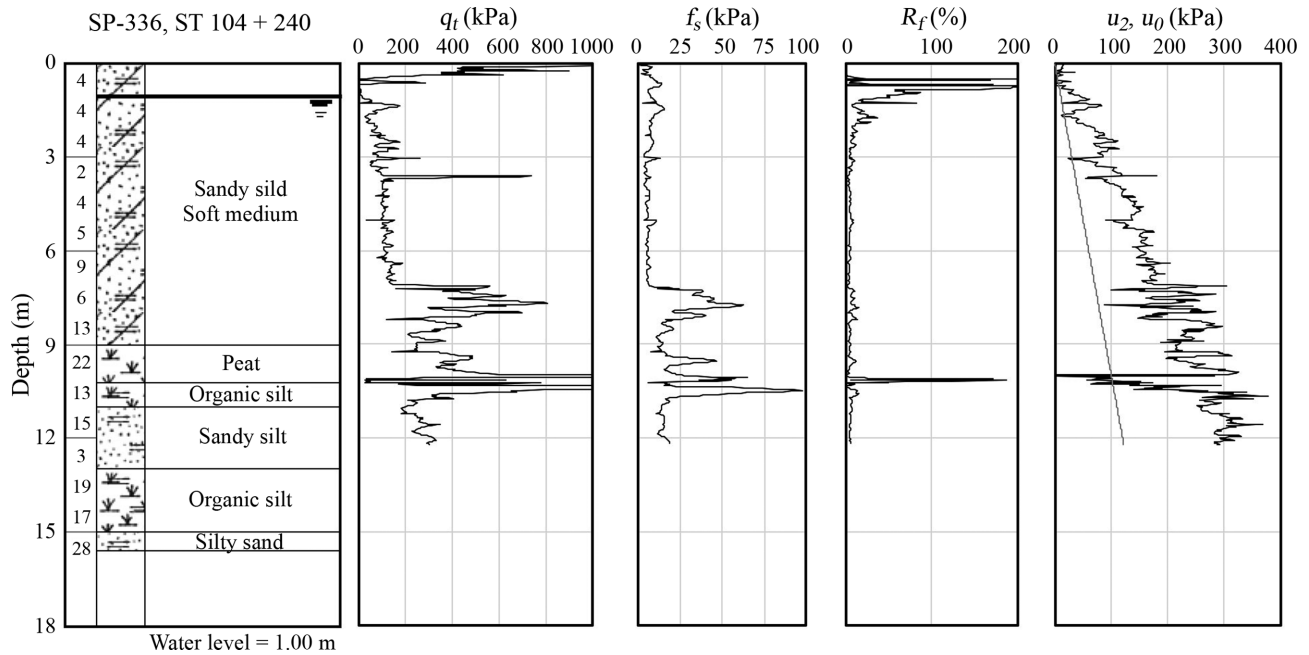


Figure 9 - Piezocone test CPTu-4 carried out in Site A.

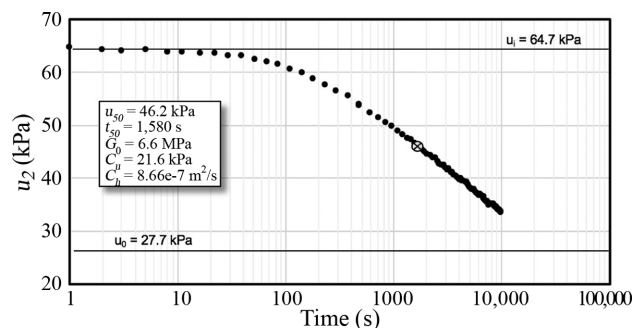


Figure 10 - Pore pressure dissipation at 3.1 m in CPTu-5, Site A in the Case history.

6. Sites Analyzed

6.1. Site A

In Figure 11 it is possible to observe Site A plan with the location of the three SPT borings and the two CPTu tests carried out. In this specific site, no undisturbed samples were collected for additional laboratory tests.

Table 3 - Coefficients of consolidation measured in Sites A and B using piezocones.

Parameter	Coefficients of consolidation (m ² /s)	
	Site A	Site B
c_a (NC)	2.3E-7	4.7E-7
c_v (NA)	1.1E-7	2.3E-7
c_a (Piezocone)	1.5E-6	3.1E-6

Figure 12 shows the geological-geotechnical profile of this site and the location of the settlement plates (PR-01 to PR-06).

The stress history interpreted using piezocones can be seen in Fig. 13. From these tests, the soft soil next to CPTu-5 (Fig. 13(b)) was interpreted as preconsolidated approximately 20 kPa above the effective initial stress and normally consolidated next to CPTu-4 (Fig. 13(a)).

Between stationing ST 104 + 040 and ST 104 + 400 of the new lane, the soft soil was treated with PVDs installed in a triangular pattern, 1.30 m distant from each other and vacuum preloading. Geotechnical instruments began to be read in June 2014. Vacuum surcharge was applied for approximately five months.

6.2. Site B

Site B is located about 1 km away from Site A. PVD and vacuum surcharge was applied in this site between stations ST 102 + 780 and ST 103 + 240. As can be observed in

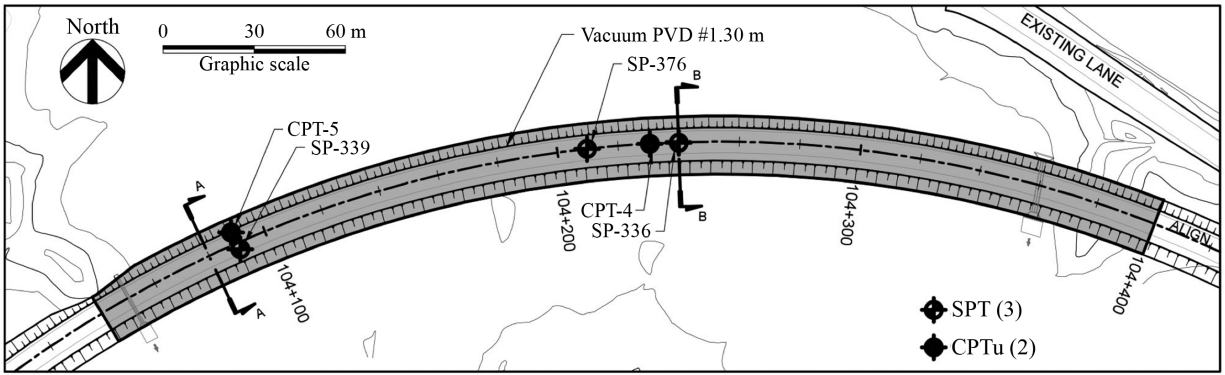


Figure 11 - Site A plan and its corresponding geotechnical tests.

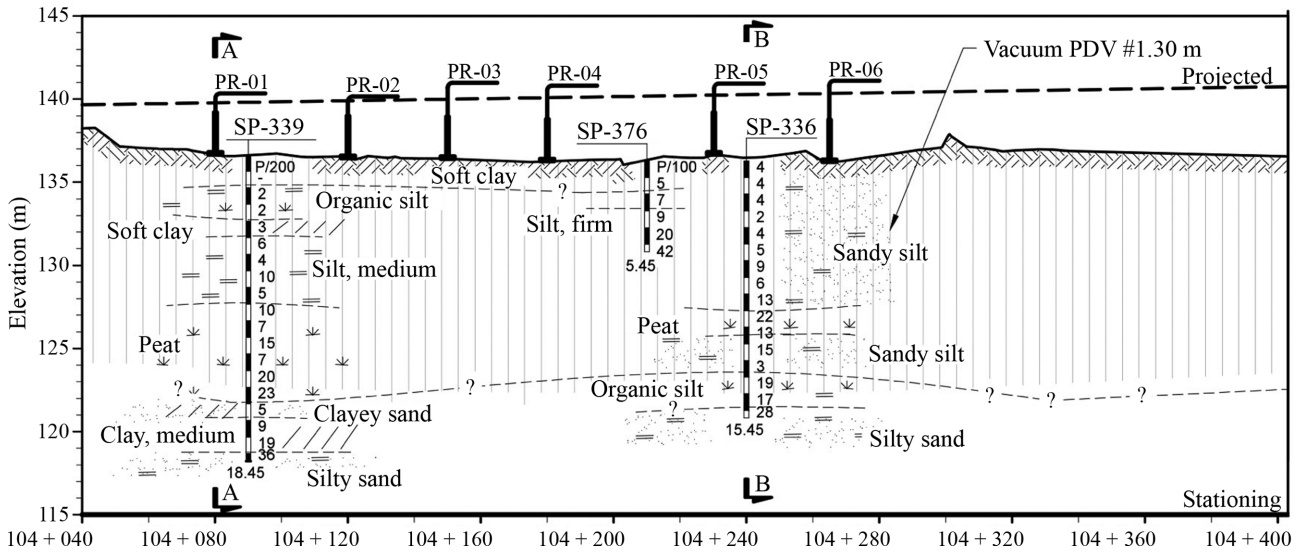


Figure 12 - Geological-geotechnical profile of Site A.

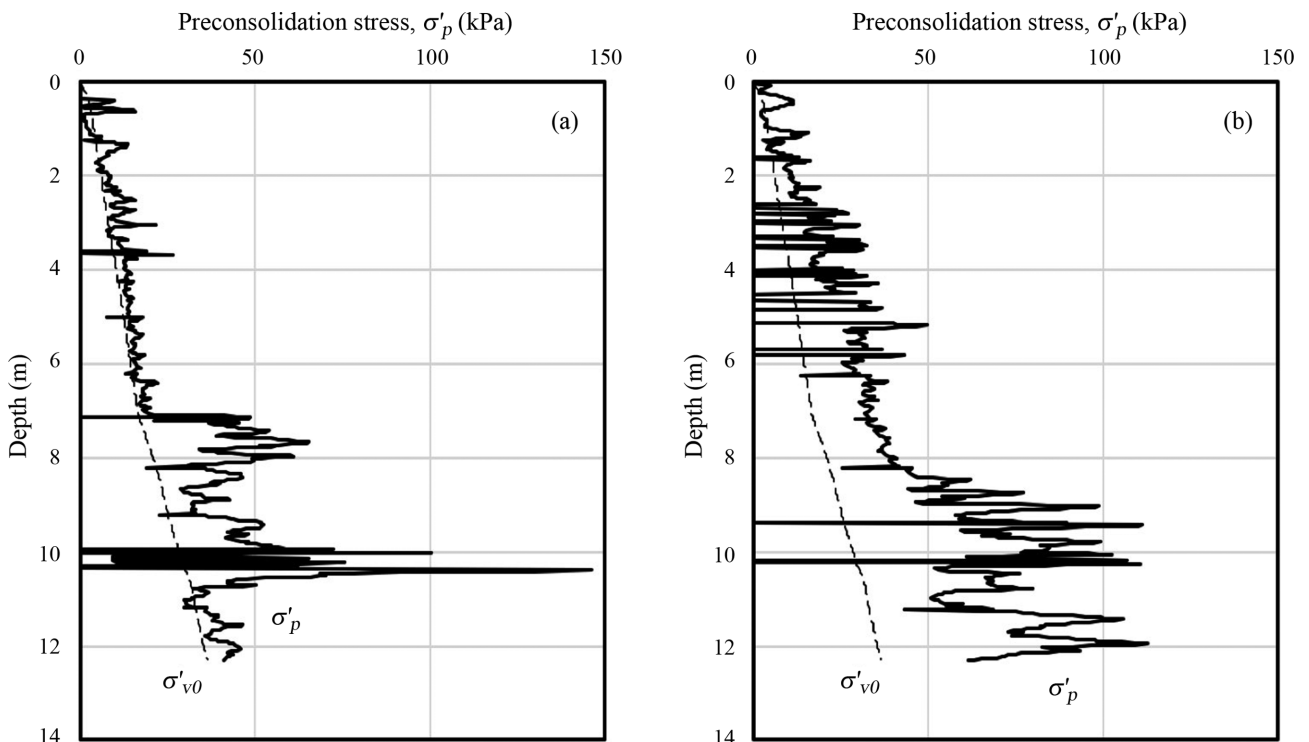


Figure 13 - Preconsolidation and effective vertical stresses in depth interpreted from the piezocone tests in Site A (a) CPTu-4, (b) CPTu-5.

Fig. 14, treatment with PVDs was interrupted about 20 m away from three buried piping (oil and gas pipelines) and a bridge abutment. The figure also presents the location plan of the five SPT borings and the three CPTu tests performed, as well as the plan location of the undisturbed samples collected next to borings SP-240 and SP-316.

Figure 15 presents the geological-geotechnical profile of the south lane axis and the location of the settlement plates in the new lane axis.

In this site, five undisturbed samples were collected for laboratory tests. Geotechnical instruments began to be read in August 2014. Vacuum surcharge was applied for approximately 5.5 months. PVDs were installed in a triangular pattern, 1.30 m distant from each other.

The stress history interpreted using piezocones can be seen in Fig. 16. The results in Fig. 16 (b) and (c) indicate a top weathered crust about 2 m thick and great soil variability below this depth, which can be interpreted as normally consolidated. The previously mentioned Figs. 6(a) and (b) also show the stress history measured at this site using

piezocones, compared with the value measured in laboratory tests.

At first glance, it seems that CPTu-2 [Fig. 16(b)] indicates an underconsolidated soil; the values of σ_{v0} (dashed line) were figured out by the executor of the test assuming water table at a 1.2 m depth. But, supposing water table at the surface, as indicated by boring SP-240 [see Figs. 8(b) and 14], the σ_{v0} would be represented by the line with dashes and dots of Fig. 16-b.

7. Numerical Modeling

7.1 Software used in numerical modeling

RocScience's Settle3D v. 2 software was used to calculate time-settlement curves considering embankment construction stages and stratigraphy according to the available borings.

Firstly, effective stress in the specified terrain is calculated by the software algorithm and afterwards it computes the resulting deformations according to the type of material adopted for each soil layer. Terzaghi's unidimen-

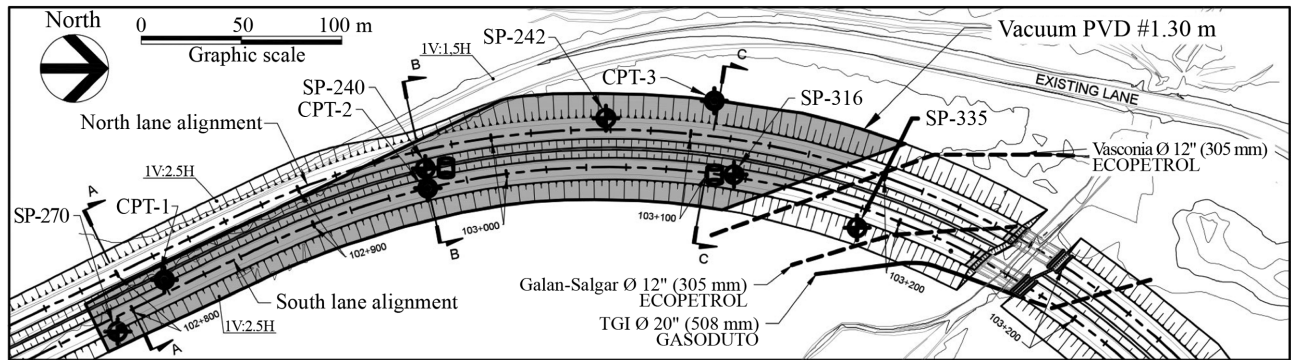


Figure 14 - Site B plan and its corresponding geotechnical tests.

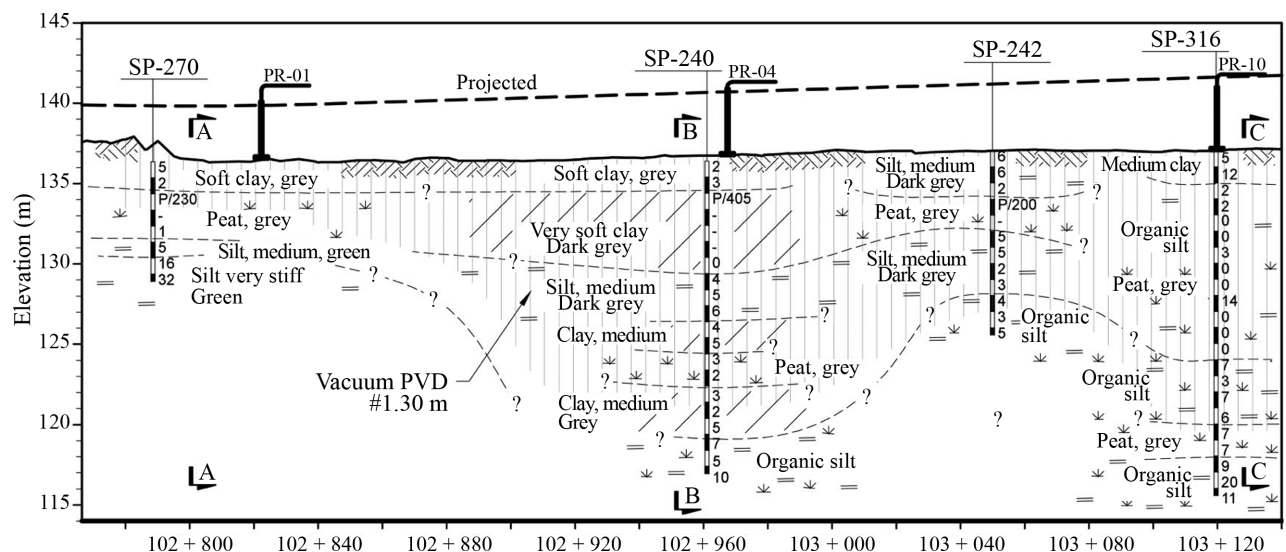


Figure 15 - Geological-geotechnical profile of Site B.

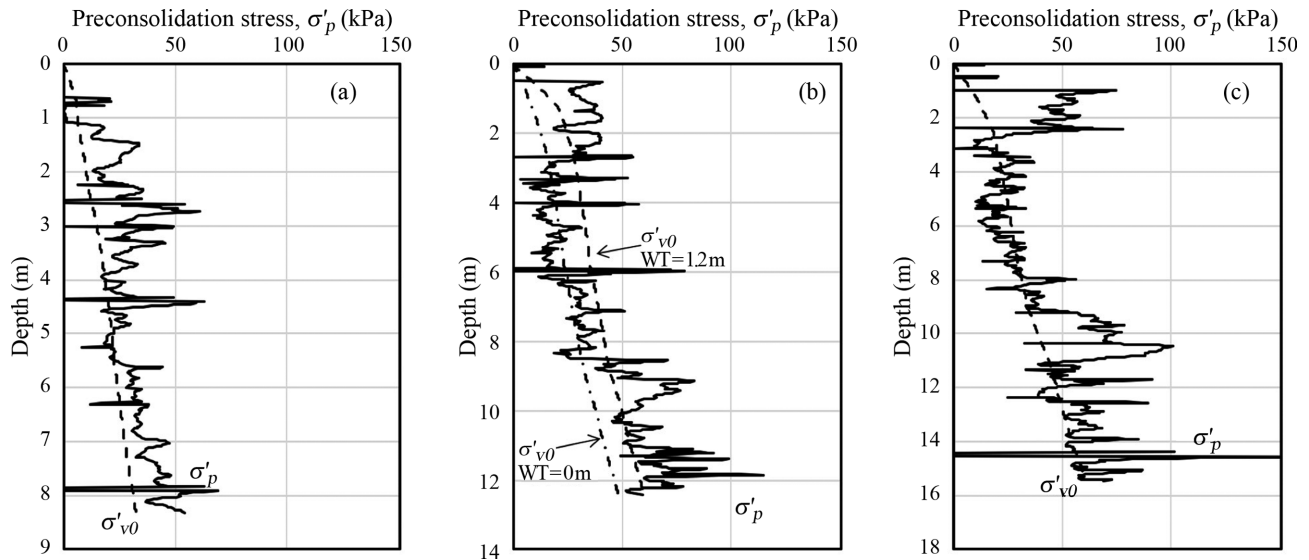


Figure 16 - Preconsolidation and vertical effective stress in depth interpreted from the piezocone tests in Site B (a) CPTu-1, (b) CPTu-2 and (c) CPTu-3.

sional consolidation theory is used for vertical flow and Hansbo (1979) radial consolidation theory for radial flow (RocScience, 2009). Pore pressure dissipation is obtained through a numerical approach with finite differences, according to the boundary conditions imposed in the model. A nonlinear model for consolidation settlement that accurately considers the relation e - $\log \sigma'_v$ is adopted by the software for calculating both compressibility and pore pressure dissipation. Eq. 6 is thus used to calculate permeability as a function of depth. Also, it is possible to specify different values for the coefficient of consolidation in the normally consolidated and overconsolidated branches.

$$k_v = \frac{c_v \cdot C_c \cdot \gamma_w}{2.3(1 + e_0) \cdot \sigma'_{v0}} \quad (6)$$

By incorporating Eq. 6 in its algorithm, the software adopts the same assumptions of the consolidation theory by Janbu (1965) and Mikasa (1965), in which settlement develops faster than in the Terzaghi's traditional theory.

7.2. Numerical modeling assumptions

Numerical modeling considered the following assumptions:

- In terms of compressibility an equivalent single and homogeneous soil layer was adopted to account for the profile variability.
- Different coefficient of consolidation values were specified for the normally and overconsolidated branches.
- Compressible soft soil thickness in each model was determined based on the SPT borings next to the settlement plates analyzed.
- Two vacuum distributions in depth were considered in the numerical simulations:
 - constant with depth: $G(n) = 1.0$, widely used; and

- linear decrease with depth: $G(n) = 0.5$, according to Indraratna *et al.* (2005), as shown in Fig. 3.

A surcharge at the surface of the terrain equal to the vacuum pressure effectively applied on the top of the vertical drain, as shown in Eq. 1, and multiplied by the efficiency of vacuum preloading, given by Eq. 3. Nominal vacuum pressure (p_v) for this construction was specified as 54 kPa, indicated in Table 4, and 2.0 m suction height (H_v) considered. Therefore, $\sigma_{vac} = 34$ kPa.

- PVDs length was adopted 1 m shorter than the compressible soil layer.
- By lack of specific information, the ratio of horizontal and vertical coefficients of consolidation was adopted 2.0 and equal to the ratio of horizontal and vertical permeability, indicated in Table 4.
- Embankment buoyancy effect and stress correction due to the layer thickness reduction was considered in all numerical analyses.
- Noncohesive and sandy material, occasionally with gravel, was used for the compacted embankment. Its unit

Table 4 - Values adopted in the numerical modeling.

Parameter	Value	Unit
k_h/k_v	2.0	-
C_r/C_c	0.15	-
d_w (m)	0.028	m
d_s/d_w	2.5	-
k_h/k_s	2.5	-
γ_{clay}	15.5	kN/m ³
$\gamma_{embankment}$	20	kN/m ³
P_v	54	kPa

weight varied from 19 to 21 kN/m³, according to the quarries used. Since there were no specific records available of the deposits used in each site, 20 kN/m³ was adopted as its unit weight.

- Secondary consolidation settlement was not considered in the numerical simulations.

Settle3D v2.0 considers horizontal soil profiles with no spatial variation of the soil layer thickness. Therefore, stratigraphic variations in the transversal sections were not considered. Embankments were modeled according to data provided by the instruments, regarding transversal width, slope angle and corresponding construction stages over time. Other values of geotechnical parameters adopted are indicated in Table 4.

8. Settlement Analysis

8.1. Analysis with the parameters of the geotechnical investigations

8.1.1. Site A

For this site, the following measured geotechnical parameters and conditions were assumed:

- void ratio approximately equal to 1 for silts and between 4 and 6 in the thin and randomly occurring peat strata;
- top and bottom drainage;
- vertical coefficient of consolidation, in the normally consolidated and overconsolidated ranges, of 1.1E-7 m²/s and 7.5E-7 m²/s, respectively, based on pore pressure dissipation tests by piezocones (Table 3);
- 20 kPa preconsolidated stress margin shown in CPTu-5, concerning plates PR-01 through PR-04 and normally

consolidated soil as shown in CPTu-4, concerning plate PR-06;

- soft soil thickness based on borings and surveying:
 - PR-01: 16 m;
 - PR-02: 17 m;
 - PR-04: 15 m; and
 - PR-06: 12 m
- a 0.12 compression ratio $C_c/(1 + e_0)$ was adopted for the equivalent homogeneous soil layer because it is the arithmetic average of the compressibility obtained in the regional parameter database of the consolidation tests (see item 4.2.3) for clayey silts, the predominant soil in this site; and
- water level 0.5 m below the surface, based on the SPT and piezocone borings performed.

The result of the numerical simulations for the first four settlement plates can be observed in Figs. 17 and 18, in comparison with the measured settlement.

Settlement plates PR-01 and PR-02 had their stress history based on CPTu-4, next to them. It is possible to notice that total settlement estimated using numerical modeling was fairly coherent in relation to the results measured through instrumentation. Contrarily, measured settlement in plate PR-04 was higher than estimated by numerical models. It is possible that stress history around PR-04 is different than plates PR-01 and PR-02. PR-06 measured settlement was also higher than estimated by numerical analyses, even considering vacuum constant with depth.

8.1.2. Site B

The following conditions and measured geotechnical parameters were considered in Site B based on the geotechnical surveys:

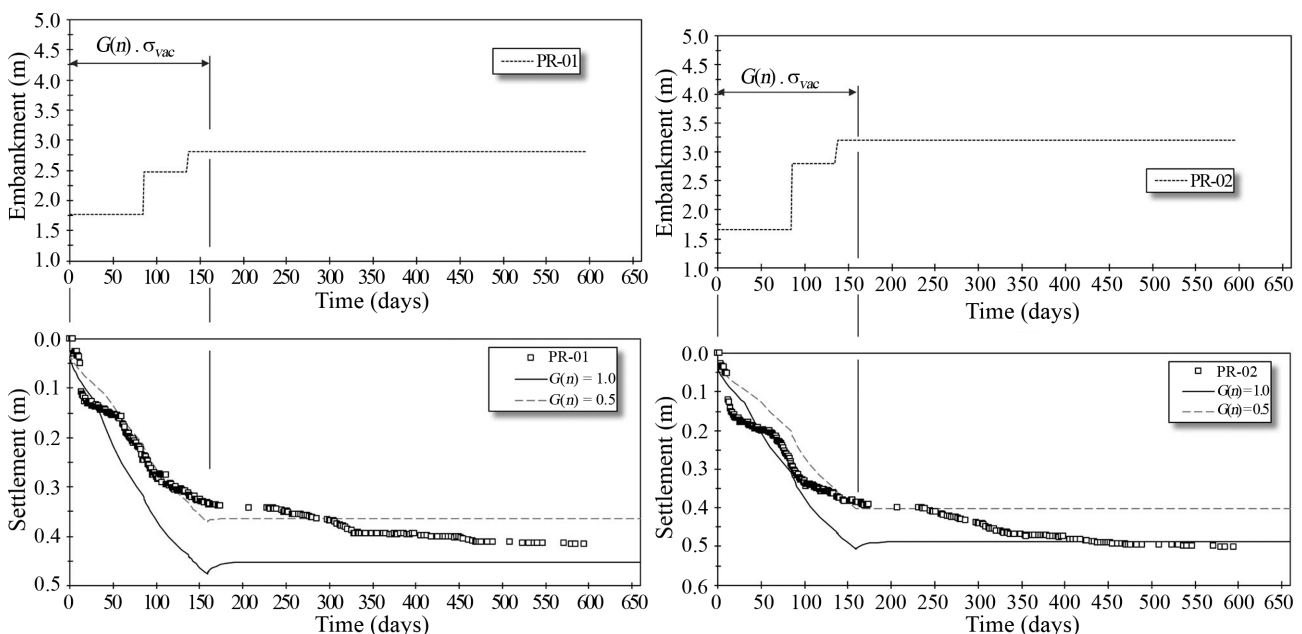


Figure 17 - Settlement measured and calculated - Site A - PR-01 and PR-02.

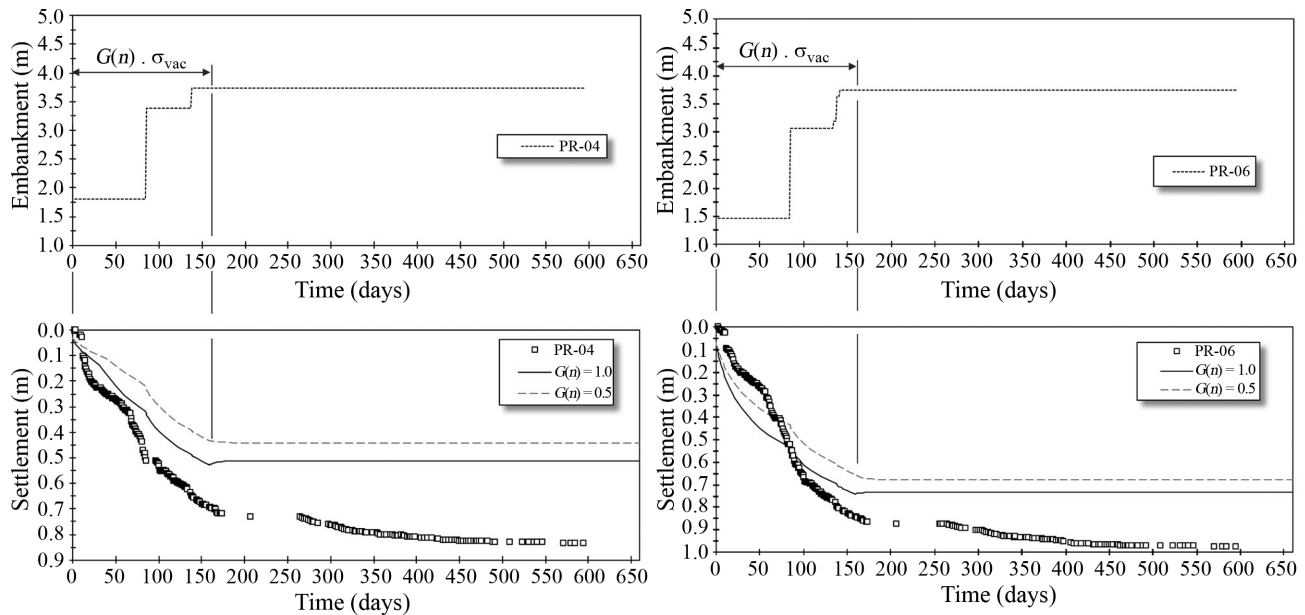


Figure 18 - Settlement measured and calculated - Site A - PR04 and PR06.

- void ratio approximately equal to 1 for silts and between 3 and 6 in the peat strata, of thinner thickness;
- top drainage, based on the SPT borings;
- vertical coefficient of consolidation $2.3E-7 \text{ m}^2/\text{s}$ and $1.5E-6 \text{ m}^2/\text{s}$, in the normally and overconsolidated ranges, respectively, based on pore pressure dissipation tests indicated in Table 3;
- 30 kPa preconsolidated stress margin down to 2 m deep and normally consolidated soil above this depth;
- soft soil thickness based on nearby borings:
 - PR-04: 17 m;
 - PR-10: 20 m; and
 - PR-11: 11.5 m
- compression ratio $C_c/(1 + e_0)$ equal to 0.16 based on the good to fair quality consolidation test performed with an undisturbed sample collected at this site; and
- water level 0.5 m below the surface, based on the SPT and CPTu borings.

The result of the numerical simulations for these settlement plates can be observed in Figs. 19 and 20, also in comparison with measured settlement.

In plates PR-10 and PR-11 (Fig. 20), additional embankment heights of 2.76 m and 1.94 m were constructed about 100 and 165 days after vacuum pressure ceased, respectively. These new loadings resulted in additional consolidation settlement, as can be seen in the measured and presented data. The later embankment loading was about 55 and 38 kPa for plates PR-10 and PR-11, respectively. Numerical simulations with $G(n) = 1.0$ assumed a temporary surcharge of 34 kPa for vacuum loading, hence the numerical simulation for plate PR-11 does not show the development of significant settlement after 345 days, disagreeing with what was registered by the settlement plate.

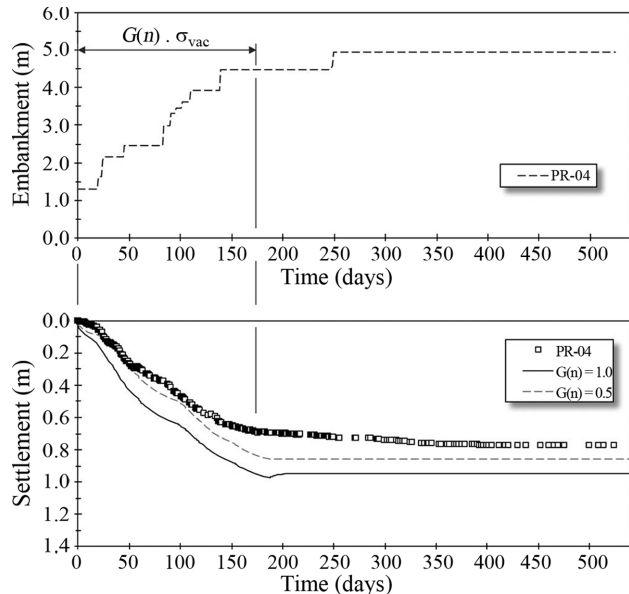


Figure 19 - Settlement measured and calculated - Site B - PR04.

All plates in Site B presented higher settlement than estimated by numerical analyses, including the ones considering vacuum constant in depth. In like manner, plates PR-04 and PR-06 from Site A also measured higher settlement than modeled. It is interesting to observe that the accuracy of the predictions in Site B was lower than that in Site A, despite the larger amount of geotechnical investigations available, including a good quality consolidation test.

8.2. Parameters obtained by back analyzing settlements

Based on the numerical models described in item 8.1, it was possible to adjust parameters $C_c/(1 + e_0)$ and c_v ,

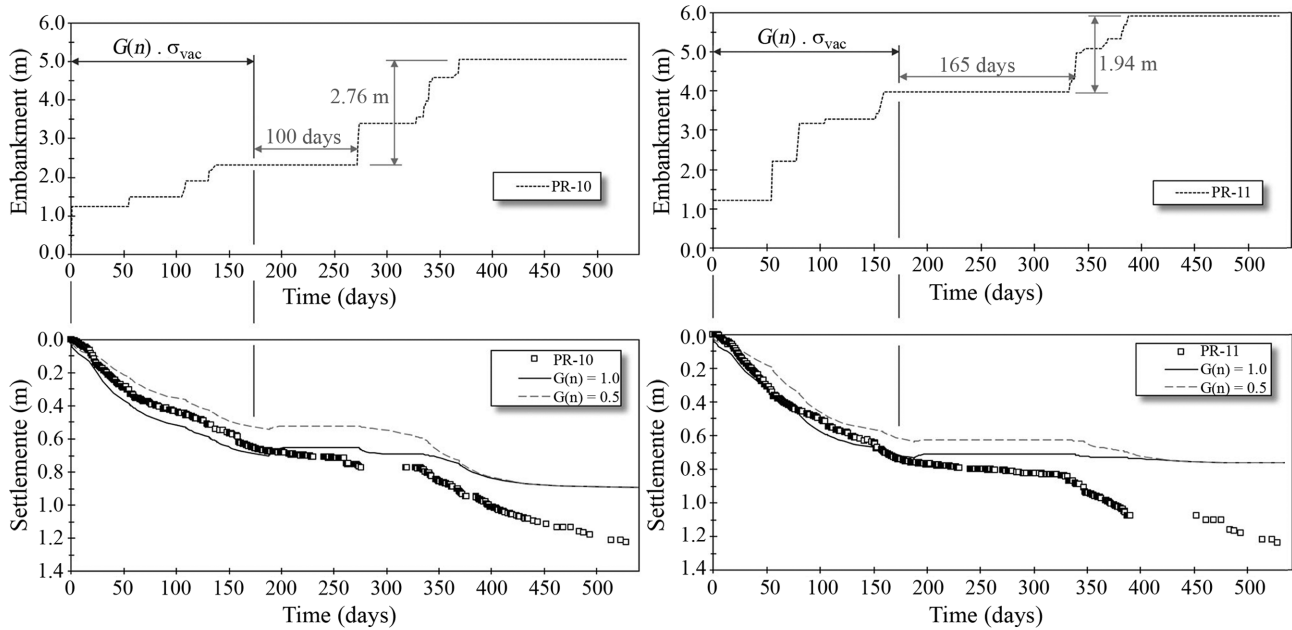


Figure 20 - Settlement measured and calculated - Site B - PR10 and PR-11.

through back analysis to the best fit between calculated and measured data. A twofold adjustment was performed for each settlement plate. In the first step, parametric analyses regarding soil compressibility were carried out until total modeled settlement was best adjusted to measured data. The next step was a parametric analysis of the soil coefficient of consolidation looking for best adjustment regarding the shape of the curve. Settlement plates were adjusted for both considerations of vacuum distribution in depth: constant when $G(n) = 1.0$ and decreasing when $G(n) = 0.5$.

8.2.1. Site A

Stress history in the top layer was revised from pre-consolidated to normally consolidated in plate PR-04. The other plates stress history was not revised. Resulting adjustments performed can be observed in Figs. 21 and 22.

In Site A, the adjustment tended towards higher compressibility parameters than the ones measured by geotechnical investigations. On the other hand, the coefficient of consolidation was adjusted for a lower number than measured by dissipation tests.

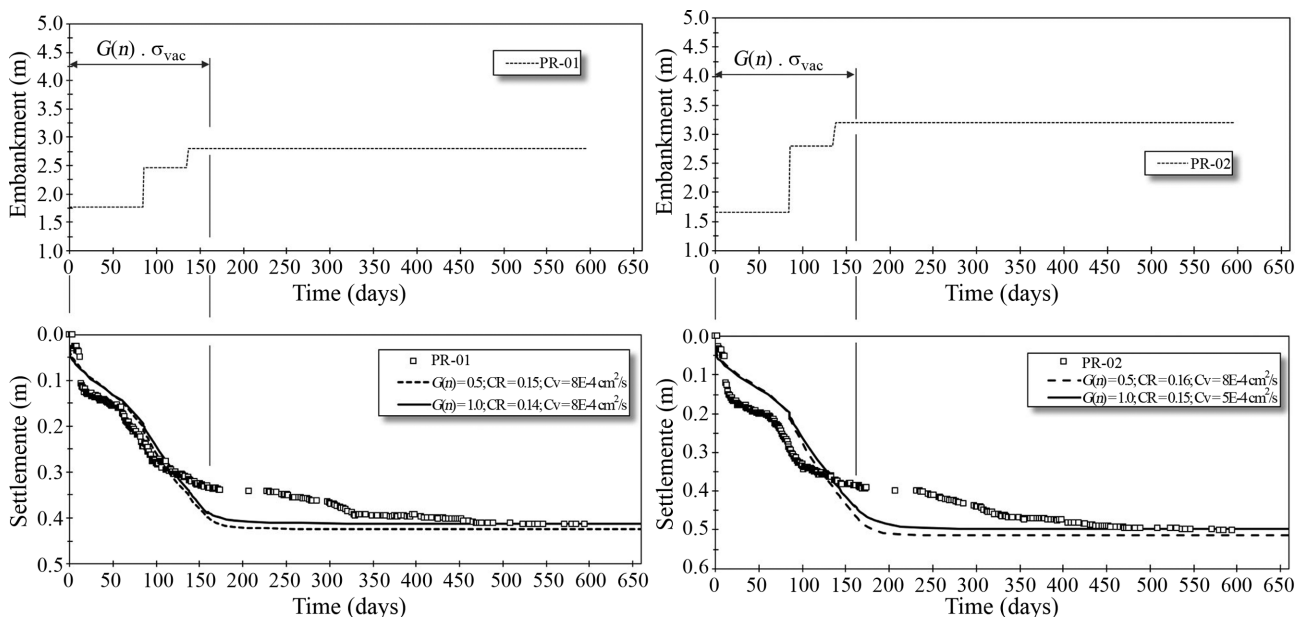


Figure 21 - Adjustment through back analysis - Site A, Plates PR-01 and PR-02.

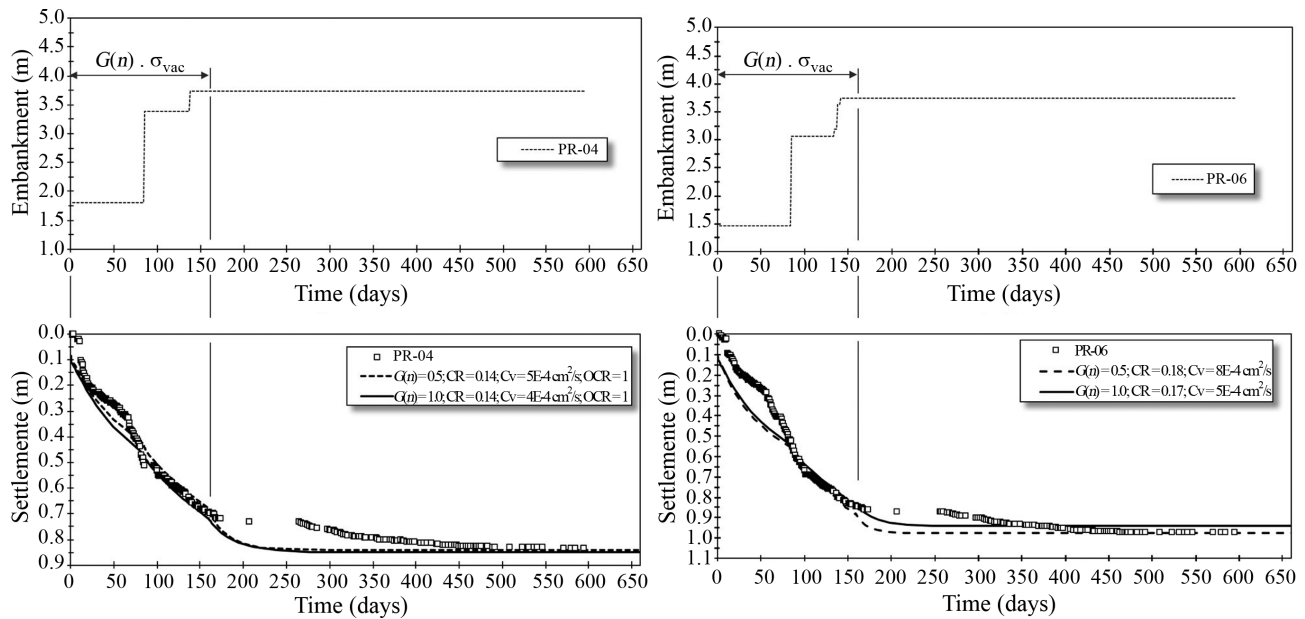


Figure 22 - Adjustment through back analysis - Site A, Plates PR-04 and PR-06.

Based on the coefficient of consolidation back analyzed, it was possible to calculate the time necessary to reach 95% of primary consolidation if no PVDs were installed. Using Terzaghi’s theory for vertical consolidation and considering Taylor’s solution for embankment construction time (variable loading), maximum and minimum times required would be 52.6 and 16.5 years for settlement plates PR-02 and PR-06, respectively. It is thus possible to notice that the installation of PVDs was effective regarding the time required for primary settlement to develop.

8.2.2. Site B

Stress history was not revised for any plate in Site B. Likewise Site A, compressibility adjustment through back analysis in Site B tended towards higher parameters than ones measured through geotechnical surveying. Resulting adjustments performed are presented in Figs. 23 and 24.

Plate PR-10 compressibility parameter analyzed was higher than expected for local organic silts and closer to expected for peat. Furthermore, coefficient of consolidation was adjusted to a lower figure than measured by dissipation tests, as was the case at Site A.

Again, using Terzaghi’s theory for vertical consolidation and considering Taylor’s solution for embankment construction time, the maximum and minimum times required for 95% of the primary consolidation to be concluded if no PVDs were installed at Site B would be 32.5 and 181.8 years for settlement plates PR-11 and PR-10, respectively.

9. Final Remarks

For the development of this paper, firstly an investigation campaign with 51 laboratory consolidation tests

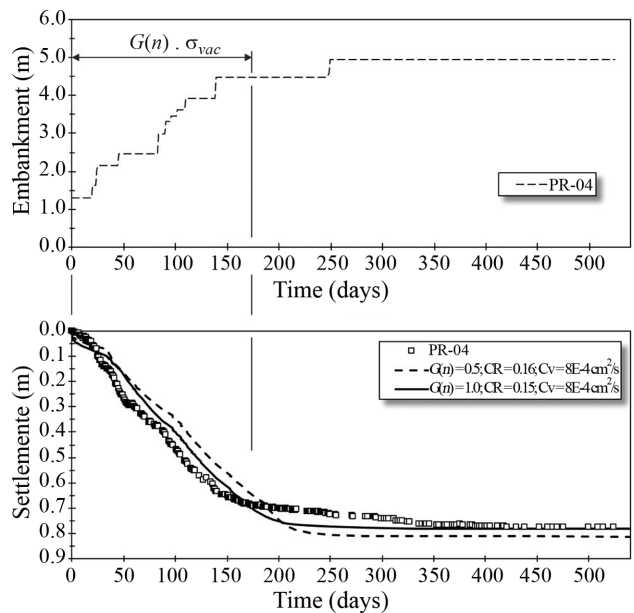


Figure 23 - Adjustment through back analysis - Site B, Plate PR-04.

were analyzed regarding regional geotechnical parameters. Afterwards, in 2 different sites, 7 settlement plates were chosen for a more thorough analysis of vacuum consolidation theory and settlement predictions. Corresponding geotechnical parameters were inferred from field investigations and calibrated through back analysis. Concerning the analyses carried out, the following conclusions were reached:

- Geotechnical soil parameters were inferred by tests that presented a good or higher quality and calibrated through

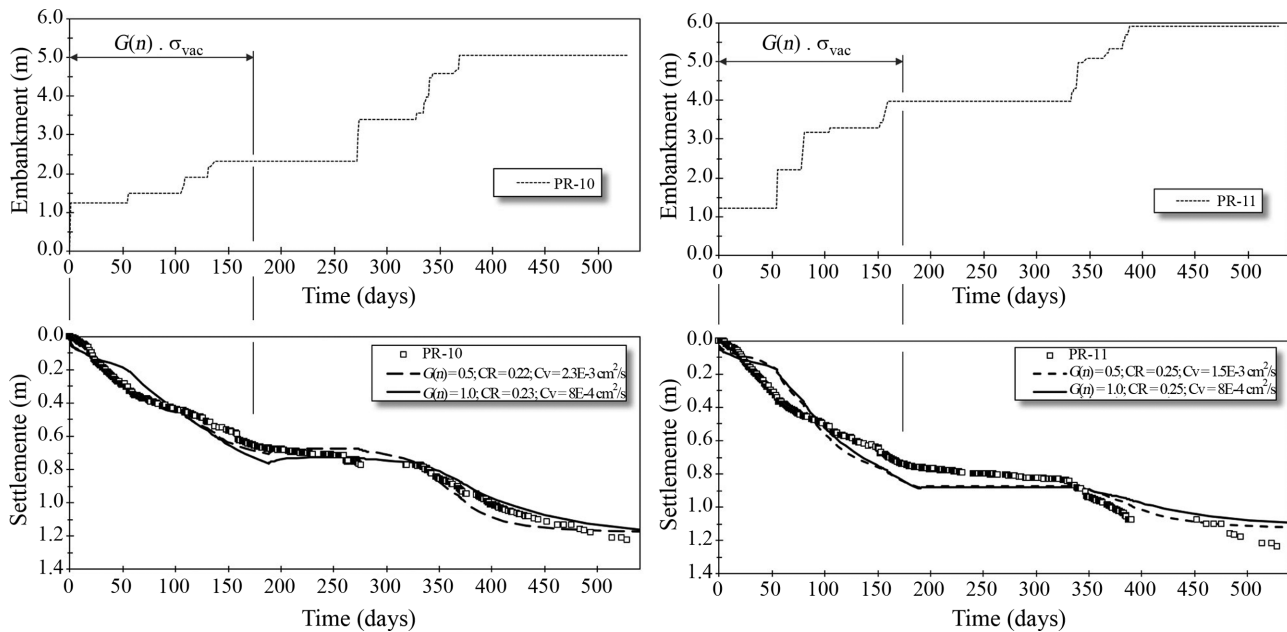


Figure 24 - Adjustment through back analysis - Site B, Plates PR-10 and PR-11.

back analysis of the measured settlement. Results obtained showed that back analyzed compressibility might have been influenced by the random presence of peat and organic matter, since it was systematically higher than what was obtained through consolidation tests.

- Preconsolidation stress estimates presented by the owner company of the piezocone equipment adjusted fairly well to the values obtained in the consolidation tests. Observed stress history was usually normally consolidated but also presented an occasional top crust with a low preconsolidation stress margin. Due to the loading imposed by the compacted embankment and vacuum combined pressures, stresses beyond the preconsolidation pressure may have been reached.
- The coefficient of horizontal consolidation (c_h) of the soft soil, inferred through back analyses based on the geotechnical instrumentation, resulted in values systematically lower than the ones measured using piezocones. This might be related to the alluvial composition of the soil, which presents sandy and silty fractions that could have affected the measurements made using piezocones. This hypothesis is related to the quality of the investigations and to the representativeness of this coefficient (c_h) for the equivalent soil as a whole.
- When the present research was being developed, two different theories of consolidation with vacuum surcharge (σ_{vac}) were compared, namely σ_{vac} constant with depth - more widely used - and σ_{vac} decreasing with depth - according to Indraratna *et al.* (2005). In Site A, the more widely used theory resulted in better accuracy, whereas in Site B the results were basically the same.
- The assessment of the theory that considers vacuum decreasing with depth depends on the availability of piezo-

cones perfectly installed between geodrains and capable of measuring the reduction of pore pressure imposed by vacuum, including negative values.

Acknowledgments

The authors would like to thank the Polytechnic School of the University of São Paulo (EPUSP) for supporting this research, as well as the companies Tecnogeo, Geoprojetos and CONSOL for providing the necessary information for the analysis carried out.

References

- Almeida, M.S.S.A. & Marques, M.E.S. (2010). Aterros Sobre Solos Moles - Projeto e Desempenho. Oficina de Textos, São Paulo, 254 p.
- Barron, R. (1948). Consolidation, 74(6):718-742.
- Chai, J.; Liu, M.D. & Carter, J.P. (2014). Methods of vacuum consolidation and their deformation analyses. Proc. of the ICE - Ground Improvement, 167(1):35-46.
- Chai, J.; Miura, N. & Bergado, D. (2008). Preloading clayey deposit by vacuum pressure with cap-drain: Analyses vs. performance. Geotextiles and Geomembranes, 26(3):220-230.
- Choa, V. (1989). Drains and vacuum preloading pilot test. Proc. 12th Int. Conf. on Soil Mech. and Found. Engn., ISSMGE, Rio de Janeiro, v. 2, pp. 1347-1350.
- CONSOL (2015). Estudio de Geología para Ingeniería y Geotécnica. Report, Consorcio Constructor Ruta del Sol, Colombia, 423 p.
- Hansbo, S. (1979). Consolidation of clay by band-shaped prefabricated drains. Ground Engineering, 12(5):16-27.

- Holtz, R. & Wager, O. (1975). Preloading by vacuum: current prospects. Transportation Research Board, 548:26-29.
- Houlsby, G. & Teh, C. (1988). Analysis of the piezocone in clay. Proc. of the International Symposium on Penetration Testing, Rotterdam, pp. 777-783.
- Indraratna, B. (2010). Recent advances in the application of vertical drains and vacuum preloading in soft soil stabilisation. Australian Geomechanics Journal, 45(2):1-43.
- Indraratna, B.; Sathananthan, I.; Rujikiatkamjorn, C. & Balasubramaniam, A. (2005). Analytical and numerical modeling of soft soil stabilized by prefabricated vertical drains incorporating vacuum preloading. International Journal of Geomechanics, 5(2):114-124.
- Janbu, N. (1965). Consolidation of clay layers based on non linear stress-strain. Proc. 6th Int. Conf. on Soil Mech. and Found. Eng., ISSMFE, Montreal, v. 2, pp. 83-87.
- Kjellman, W. (1952). Consolidation of clay soil by means of atmospheric pressure. Proc. Conf. on Soil Stabilization, MIT, Massachusetts, pp. 258-263.
- Li, B.; Wu, S.; Chu, J. & Lam, K.P. (2011). Evaluation of two vacuum preloading techniques using model tests. Proc. Geo-Frontiers 2011: Advances in Geotechnical Engineering, ASCE, Dallas, Texas, United States, pp. 636-645.
- Lunne, T.; Berre, T. & Strandvik, S. (1997). Sample disturbance effects in soft low plastic Norwegian clay. Proc. International Symposium on Recent Developments in Soil and Pavement Mechanics, Rio de Janeiro, Brazil, pp. 81-102.
- Massé, F.; Spaulding, C.A.; Wong, I.C. & Varaksin, S. (2001). Vacuum consolidation: a review of 12 years of successful development. Proc. Geo-Odyssey, ASCE, Blacksburg, VA, 23 p.
- Mayne, P. & Brown, D. (2003). Characterization of Piedmont residuum of North America. Characterization and Engineering Properties of Natural Soils, 2:1323-1339.
- Mikasa, M. (1965). Discussion. Proc. 6th Int. Conf. on Soil Mech. and Found. Eng., ISSMFE, Montreal, v. 3, pp. 459-460.
- Pilot, G. (1981). Methods of improving engineering properties. Brand, E.W. & Brenner, R.P. (eds) Soft Clay Engineering: Developments in Geotechnical Engineering. Elsevier, New York, pp. 637-696.
- Qian, J.; Zhao, W.; Cheung, Y. & Lee, P. (1992). The theory and practice of vacuum preloading. Computers and Geotechnics, 13(2):103-118.
- Rocscience (2009). Settle3D - Settlement and Consolidation Analysis - Theory Manual. [Online] Available at: https://rocscience.com/help/settle3d/webhelp/pdf_files/theory/Settle3D_Theory.pdf, accessed 23 March 2016.
- Sandroni, S.; Andrade, G.G. & Odebrecht E. (2012). Uso de vácuo como sobrecarga de aterro sobre solo mole: uma primeira experiência de campo. Anais COBRAMSEG, ABMS, Porto de Galinhas, 8 p. CD-ROM.
- Silva, P. (1970). Uma nova construção gráfica para determinação da tensão de pré-adensamento de uma amostra de solo. Anais IV Congresso Brasileiro de Mecânica dos Solos, ABMS, Rio de Janeiro, v. 2, pp. 219-223.
- Waltham, T. (2001). Foundations of engineering geology. CRC Press, New York, 104 p.
- Yanez, D.G. (2016). Estudo Probabilístico Sobre Estimativas de Recalques de Aterros Sobre Solos Moles, Com Drenos Verticais e Sobrecarga Física e de Vácuo. Master's Thesis, Departamento de Estruturas e Geotecnia, Escola Politécnica da Universidade de São Paulo, São Paulo, 441 p.
- Yanez, D.G.; Massad, F. & Correa, M.R.B. (2015). Soft soil geotechnical properties in a case study of a large alluvial soft soil improvement in Latin America. Proc. of the 15th Congreso Panamericano de Mecánica de Suelos e Ingeniería Geotécnica, IOS Press, Buenos Aires, pp. 1599-1606.

List of Symbols

- B_q : CPTU pore pressure ratio
 C_c : compression index
 c_h : coefficient of horizontal consolidation
 CR : compression ratio
 C_r : swelling index
 c_u : undrained shear strength
 c_v : coefficient of vertical consolidation
 D : diameter of the effective influence zone of the drain
 d_s : diameter of the smear zone
 d_w : diameter of the drain (well)
 e : void ratio
 e_0 : initial void ratio
 $F(n)$: drain spacing factor
 F_r : drainage resistance factor
 f_s : cone lateral friction
 F_s : soil disturbance factor
 $G(n)$: efficiency of vacuum preloading
 H : compressible layer thickness
 k_h : horizontal permeability in the undisturbed zone
 k_s : horizontal permeability in the disturbed or smear zone
 k_v : vertical permeability
 n : spacing ratio
 q_c : cone tip resistance
 q_w : drain discharge capacity
 R : radius of the cone
 t : time
 T_h : horizontal time factor
 T_v : vertical time factor
 U : percentage or degree of average primary consolidation
 u : pore pressure
 u_0 : initial pore pressure
 z : depth
 γ : natural specific weight of the soil

γ_s : specific gravity weight
 γ' : submerged weight
 γ_w : specific weight of water

σ'_p : preconsolidation pressure
 σ'_v : effective vertical stress
 σ'_{v0} : initial effective vertical stress

SOILS and ROCKS

An International Journal of Geotechnical and Geoenvironmental Engineering

Publication of

ABMS - Brazilian Association for Soil Mechanics and Geotechnical Engineering

SPG - Portuguese Geotechnical Society

Volume 41, N. 2, May-August 2018

Author index

Aghamolaie, I.	193	Mascarenha, M.M.A.	157
Assis, A.P.	203	Massad, F.	75, 217
Barbosa, M.G.T.	17	Matos, T.H.C.	157
Bim, R.	61	Moghaddas, N.H.	193
Carraro, J.A.H.	149	Morgenstern, N.R.	107
Cavalcante, A.L.B.	17	Nascimento, P.N.C.	3
Chagas, J.V.R.	157	Nunes, G.B.	61
Consoli, N.C.	149	Odebrecht, E.	179
Cordão Neto, M.P.	157	Oliveira, O.M.	61
Cunha, R.P.	91	Pacheco, M.P.	171
Curado, T.S.	49	Passini, L.B.	103
Danziger, B.R.	171	Pedrini, R.A.A.	133
Etemadifar, M.	193	Poulos, H.G.	91
Figueiredo, L.T.	203	Póvoa, L.M.M.	3
Garcia, R.S.	17	Rezende, L.R.	157
Giacheti, H.L.	133	Rocha, B.P.	133
Godoy, V.B.	149	Rosenbach, C.M.D.C.	149
González, A.A.M.	103	Sales, M.M.	49
Higashi, R.A.R.	61	Santa Maria, F.C.M.	33
Kormann, A.C.M.	103	Santa Maria, P.E.L.	33
Lashkaripour, G.R.	193	Scheuermann Filho, H.C.	149
Leão, M.F.	171	Schnaid, F.	179
Ludemann, S.M.	17	Valverde, R.M.	75
Maia, P.C.A.	3	Vaziri, N.S.	193
		Yanez, D.G.	217

BUILDING A BETTER WORLD



TPF

PLANEGE CENOR



Engineering and Architectural Consultancy

Geology, Geotechnics, Supervision of Geotechnical Works
Embankment Dams, Underground Works, Retaining Structures
Special Foundations, Soil Improvement, Geomaterials



www.tpfplanegecenor.pt



- > **Prospecção Geotécnica**
Site Investigation
- > **Consultoria Geotécnica**
Geotechnical Consultancy
- > **Obras Geotécnicas**
Ground Treatment-Construction Services
- > **Controlo e Observação**
Field Instrumentation Services and Monitoring Services
- > **Laboratório de Mecânica de Solos**
Soil and Rock Mechanics Laboratory

Certificada ISO 9001 por



Geocontrole



Parque Oriente, Bloco 4, EN10
2699-501 Bobadela LRS
Tel. 21 995 80 00
Fax. 21 995 80 01
e.mail: mail@geocontrole.pt
www.geocontrole.pt


Geocontrole
Geotecnia e Estruturas de Fundação SA



COBA

GEOLOGY AND GEOTECHNICS

Hydrogeology • Engineering Geology • Rock Mechanics • Soil Mechanics • Foundations and Retaining Structures • Underground Works • Embankments and Slope Stability
Environmental Geotechnics • Geotechnical Mapping



- Water Resources Planning and Management
- Hydraulic Undertakings
- Electrical Power Generation and Transmission
- Water Supply Systems and Pluvial and Wastewater Systems
- Agriculture and Rural Development
- Road, Railway and Airway Infrastructures
- Environment
- Geotechnical Structures
- Cartography and Cadastre
- Safety Control and Work Rehabilitation
- Project Management and Construction Supervision



PORTUGAL

CENTER AND SOUTH REGION
Av. 5 de Outubro, 323
1649-011 LISBOA
Tel.: (351) 210125000, (351) 217925000
Fax: (351) 217970348
E-mail: coba@coba.pt
www.coba.pt

Av. Marquês de Tomar, 9, 6.º.
1050-152 LISBOA
Tel.: (351) 217925000
Fax: (351) 213537492

NORTH REGION

Rua Mouzinho de Albuquerque, 744, 1.º.
4450-203 MATOSINHOS
Tel.: (351) 229380421
Fax: (351) 229373648
E-mail: engico@engico.pt

ANGOLA

Praceta Farinha Leitão, edifício nº 27, 27-A - 2.º Dto
Bairro do Maculusso, LUANDA
Tel./Fax: (244) 222338 513
Cell: (244) 923317541
E-mail: coba-angola@netcabo.co.ao

MOZAMBIQUE

Pestana Rovuma Hotel. Centro de Escritórios.
Rua da Sé nº114. Piso 3, MAPUTO
Tel./Fax: (258) 21 328 813
Cell: (258) 82 409 9605
E-mail: coba.mz@tdm.co.mz

ALGERIA

09, Rue des Frères Hocine
El Biar - 16606, ARGEL
Tel.: (213) 21 922802
Fax: (213) 21 922802
E-mail: coba.alger@gmail.com

BRAZIL

Rio de Janeiro
COBA Ltd. - Rua Bela 1128
São Cristóvão
20930-380 Rio de Janeiro RJ
Tel.: (55 21) 351 50 101
Fax: (55 21) 258 01 026

Fortaleza

Av. Senador Virgílio Távora 1701, Sala 403
Aldeota - Fortaleza CEP 60170 - 251
Tel.: (55 85) 3261 17 38
Fax: (55 85) 3261 50 83
E-mail: coba@esc-te.com.br

UNITED ARAB EMIRATES

Corniche Road - Corniche Tower - 5th Floor - 5B
P. O. Box 38360 ABU DHABI
Tel.: (971) 2 627 0088
Fax: (971) 2 627 0087



Conheça mais:
www.geobrugg.com/pt/taludes



Safety is our nature

TECCO® SYSTEM³ com fio de aço de alta resistência

**SISTEMA ECOLOGICAMENTE
CORRETO PARA ESTABILIZAÇÃO
DE TALUDES**

Reliable solutions with **technology, quality,** and **innovation** for Civil Engineering proposes



MACCAFERRI POLIMAC

New polymeric coating with high performance
PoliMac™



Long-life galvanising
GalMac® 4R

Intermetallic coating

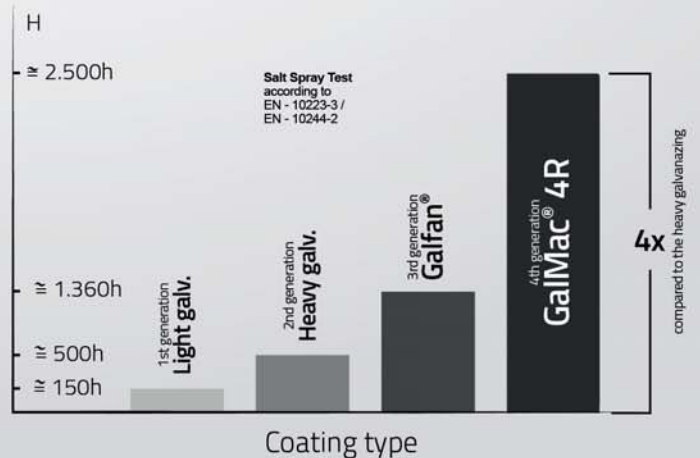
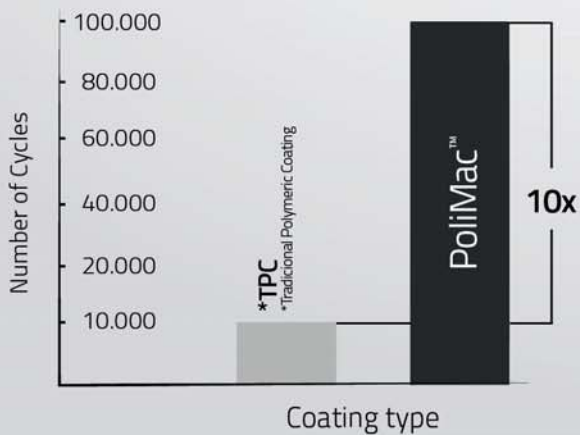
Steel wire LCC*
*Low Carbon Content



The **PoliMac™** in controlled abrasion resistance tests, it showed its excellent performance by resisting up to 100,000 cycles in the standard tests **ABNT NBR 7577** and **EN 10223-3**; about **10x more** than the traditional coating.



The **GalMac® 4R** coating complies with the main national and international standards such as: **EN 10223-3: 2013**, **ASTM B860** and **NBR 8964**.



Follow us on our **social media**



/maccaferri



/maccaferriatriz



@Maccaferri_BR



+MaccaferriWorld

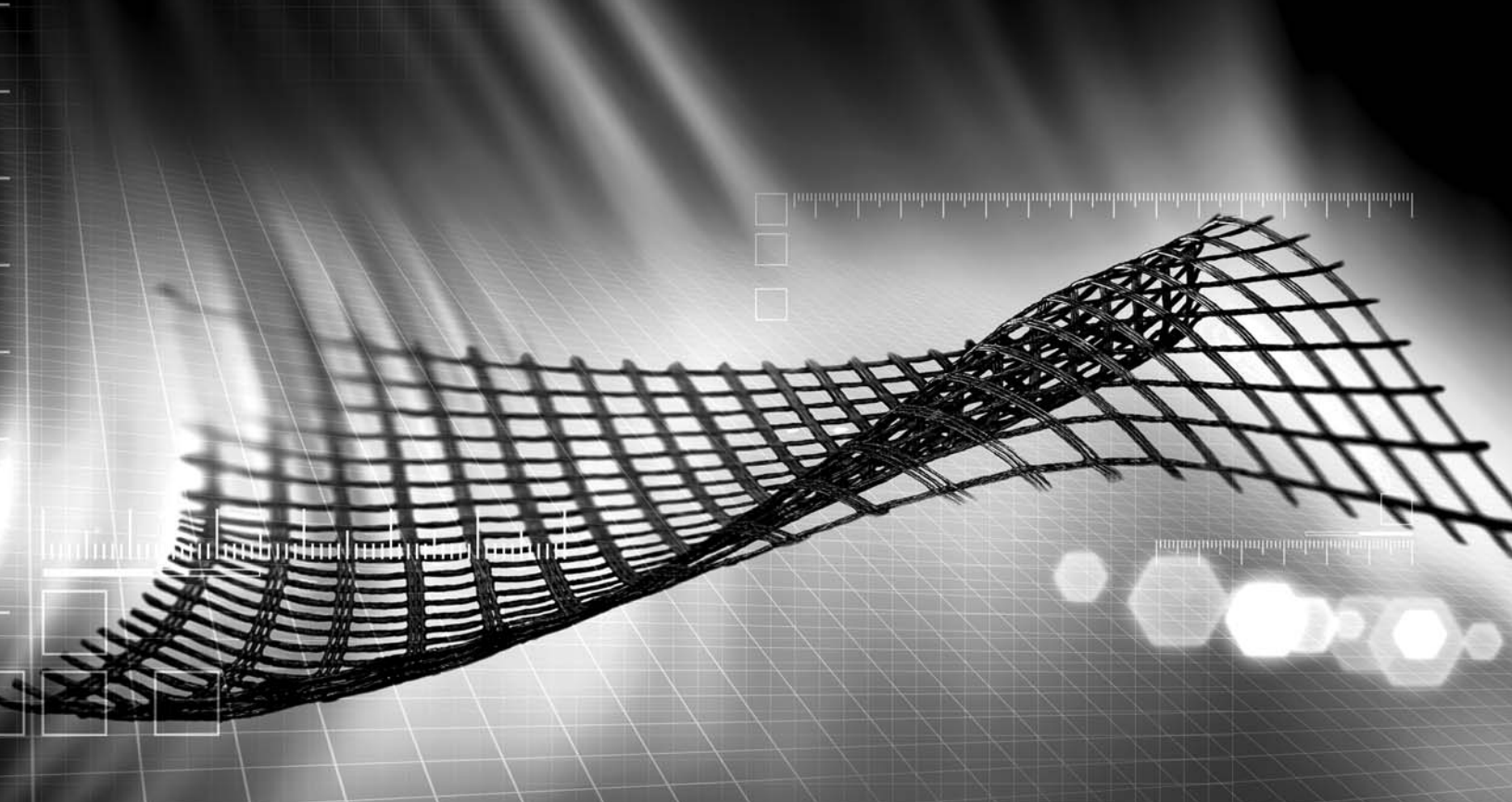


/maccaferriworld



MACCAFERRI

www.maccaferri.com/br



A strong, lasting connection.

With a history of over 150 years of pioneering in geosynthetics, we strive to create solutions for the most diverse engineering challenges.

Our business areas:



**Earthworks and
Foundations**



**Environmental
Engineering**



Roads and Pavements



Hydraulic Engineering

Talk to HUESKER Brasil:
www.HUESKER.com.br
HUESKER@HUESKER.com.br
+55 (12) 3903 9300

Follow HUESKER Brasil in social media:



HUESKER
Ideen. Ingenieure. Innovationen.



Geotechnic and Rehabilitation

TEIXEIRA DUARTE
ENGENHARIA E CONSTRUÇÕES, S.A.

- Head Office
Lagoas Park - Edifício 2
2740-265 Porto Salvo - Portugal
Tel.: (+351) 217 912 300
Fax: (+351) 217 941 120/21/26

- Angola
Alameda Manuel Van Dunen 316/320 - A
Caixa Postal 2857 - Luanda
Tel.: (+34) 915 550 903
Fax: (+34) 915 972 834

- Algeria
Parc Miremont - Rua A, Nº136 - Bouzareah
16000 Alger
Tel.: (+213) 219 362 83
Fax: (+213) 219 365 66

- Brazil
Rua Iguatemi, nº488 - 14° - Conj. 1401
CEP 01451 - 010 - Itaim Bibi - São Paulo
Tel.: (+55) 112 144 5700
Fax: (+55) 112 144 5704

- Spain
Avenida Alberto Alcocer, nº24 - 7° C
28036 Madrid
Tel.: (+34) 915 550 903
Fax: (+34) 915 972 834

- Mozambique
Avenida Julyus Nyerere, 130 - R/C
Maputo
Tel.: (+258) 214 914 01
Fax: (+258) 214 914 00

Instructions for Submission of Manuscripts

Category of the Papers

Soils and Rocks is the international scientific journal edited by the Brazilian Association for Soil Mechanics and Geotechnical Engineering (ABMS) and the Portuguese Geotechnical Society (SPG). The aim of the journal is to publish (in English) original research and technical works on all geotechnical branches.

According to its content the accepted paper is classified in one of the following categories: Article paper, Technical Note, Case Study or Discussion. An article paper is an extensive and conclusive dissertation about a geotechnical topic. A paper is considered as a technical note if it gives a short description of ongoing studies, comprising partial results and/or particular aspects of the investigation. A case study is a report of unusual problems found during the design, construction or the performance of geotechnical projects. A case study is also considered as the report of an unusual solution given to an ordinary problem. The discussions about published papers, case studies and technical notes are made in the Discussions Section.

When submitting a manuscript for review, the authors should indicate the category of the manuscript, and is also understood that they:

- assume full responsibility for the contents and accuracy of the information in the paper;
- assure that the paper has not been previously published, and is not being submitted to any other periodical for publication.

Manuscript Instructions

Manuscripts must be written in English. The text is to be typed in a word processor (preferably MS Word), **single column**, using ISO A4 page size, left, right, top, and bottom margins of 25 mm, Times New Roman 12 font, and line spacing of 1.5. All lines and pages should be numbered. The text should be written in the third person.

The first page of the manuscript must include the title of the paper followed by the names of the authors with the abbreviation of the most relevant academic title. The affiliation, address and e-mail must appear below each author's name. An abstract of 200 words follows after the author's names. A list with up to six keywords at the end of the abstract is required.

Although variations on the sequence and title of each section are possible, it is suggested that the text contains the following sections: Introduction, Material and Methods, Results, Discussions, Conclusions, Acknowledgements, References and List of Symbols. A brief description of each section is given next.

Introduction: This section should indicate the state of the art of the problem under evaluation, a description of the problem and the methods undertaken. The objective of the work should be clearly presented at the end of the section.

Materials and Methods: This section should include all information needed to the reproduction of the presented work by other researchers.

Results: In this section the data of the investigation should be presented in a clear and concise way. Figures and tables should not repeat the same information.

Discussion: The analyses of the results should be described in this section.

Conclusions: The content of this section should be based on the data and on the discussions presented.

Acknowledgements: If necessary, concise acknowledgements should be presented in this section.

References: References to other published sources must be made in the text by the last name(s) of the author(s), followed by the year of publication, similarly to one of the two possibilities below:

...while Silva & Pereira (1987) observed that resistance depended on soil density... or It was observed that resistance depended on soil density (Silva & Pereira, 1987).

In the case of three or more authors, the reduced format must be used, e.g.: Silva *et al.* (1982) or (Silva *et al.*, 1982). Two or more citations belonging to the same author(s) and published in the same year are to be distinguished with small letters, e.g.: (Silva, 1975a, b, c.). Standards must be cited in the text by the initials of the entity and the year of publication, e.g.: ABNT (1996), ASTM (2003).

Full references shall be listed alphabetically at the end of the text by the first author's last name. Several references belonging to the same author shall be cited chronologically. Some examples are listed next:

Papers: Bishop, A.W. & Blight, G.E. (1963). Some aspects of effective stress in saturated and unsaturated soils. *Geotechnique*, 13(2):177-197.

Books: Lambe, T.W. & Whitman, R.V. (1979). *Soil Mechanics*, SI Version. John Wiley & Sons, New York, 553 p.

Book with editors: Sharma, H.D.; Dukes, M.T. & Olsen, D.M. (1990). Field measurements of dynamic moduli and Poisson's ratios of refuse and underlying soils at a landfill site. Landva, A. & Knowles, G.D. (eds), *Geotechnics of Waste Fills - Theory and Practice*, American Society for Testing and Materials - STP 1070, Philadelphia, pp. 57-70.

Proceedings (printed matter or CD-ROM): Jamiolkowski, M.; Ladd, C.C.; Germaine, J.T. & Lancellotta, R. (1985). New developments in field and laboratory testing of soils. Proc. 11th Int. Conf. on Soil Mech. and Found. Engn., ISSMFE, San Francisco, v. 1, pp. 57-153. (specify if CD ROM).

Thesis and dissertations: Lee, K.L. (1965). *Triaxial Compressive Strength of Saturated Sands Under Seismic Loading Conditions*. PhD Dissertation, Department of Civil Engineering, University of California, Berkeley, 521 p.

Standards: ASTM (2003). *Standard Test Method for Particle Size Analysis of Soils - D 422-63*. ASTM International, West Conshohocken, Pennsylvania, USA, 8 p.

Internet references: *Soils and Rocks* available at <http://www.abms.com.br> and downloaded on August 6th 2003.

On line first publications must also bring the digital object identifier (DOI) at the end.

Figures shall be either computer generated or drawn with India ink on tracing paper. Computer generated figures must be accompanied by the corresponding digital file (.tif, .jpg, .pcx, etc.). All figures (graphs, line drawings, photographs, etc.) shall be numbered consecutively and have a caption consisting of the figure number and a brief title or description of the figure. This number should be used when referring to the figure in text. Photographs should be black and white, sharp, high contrasted and printed on glossy paper.

Tables shall be numbered consecutively in Arabic and have a caption consisting of the table number and a brief title. This number should be used when referring to the table in the text. Units should be indicated in the first line of the table, below the title of each column. Acronyms should be avoided. When applicable, the units should come right below the corresponding column heading. Additional comments can be placed as footnotes.

Equations shall appear isolated in a single line of the text. Numbers identifying equations must be flushed with the right margin. International System (SI) units must be used. The definitions of the symbols used in the

equations must appear in the List of Symbols. It is recommended that the symbols used are in accordance with Lexicon in 8 Languages, ISSMFE (1981) and the ISRM List of Symbols.

The text of the submitted manuscript (including figures, tables and references) intended to be published as an article paper or a case history should not contain more than 30 pages, formatted according to the instructions mentioned above. Technical notes and discussions should have no more than 15 and 8 pages, respectively. Longer manuscripts may be exceptionally accepted if the authors provide proper explanation for the need of the required extra space in a cover letter.

Discussion

Discussions must be written in English. The first page of a discussion should contain:

The title of the paper under discussion;

Name of the author(s) of the discussion, followed by their position, affiliation, address and e-mail. The author(s) of the discussion should refer to himself (herself/themselves) as the reader(s) and to the author(s) of the paper as the author(s).

Figures, tables and equations should be numbered following the same sequence of the original paper. All instructions previously mentioned for the preparation of article papers, case studies and technical notes also apply to the preparation of discussions.

Editorial Review

Each paper will be evaluated by reviewers selected by the editors according to the subject of the paper. The authors will be informed about the results of the review process. If the paper is accepted, the authors will be required to submit a version of the revised manuscript with the suggested modifications. If the manuscript is rejected for publication, the authors will be informed about the reasons for rejection. In any situation comprising modification of the original text, classification of the manuscript in a category different from that proposed by the authors, or rejection, the authors can reply presenting their reasons for disagreeing with the reviewer comments.

Submission

The author(s) must upload a digital file of the manuscript to the Soils and Rocks website.

Follow Up

The online management system will provide a password to the corresponding author, which will enable him/her to follow the reviewing process of the submitted manuscript at the Soils and Rocks website.

Volume 41, N. 2, May-August 2018**Table of Contents***VICTOR DE MELLO LECTURE**Geotechnical Risk, Regulation, and Public Policy*

N.R. Morgenstern

107

*ARTICLES**The Up-Hole Seismic Test Together with the SPT: Description of the System and Method*

R.A.A. Pedrini, B.P. Rocha, H.L. Giacheti

133

Durability of RAP-Industrial Waste Mixtures Under Severe Climate Conditions

N.C. Consoli, H.C. Scheuermann Filho, V.B. Godoy, C.M.D.C. Rosenbach, J.A.H. Carraro

149

Effects of the Addition of Dihydrate Phosphogypsum on the Characterization and Mechanical Behavior of Lateritic Clay

M.M.A. Mascarenha, M.P. Cordão Neto, T.H.C. Matos, J.V.R. Chagas, L.R. Rezende

157

Stress-Strain Analysis of a Concrete Dam in Predominantly Anisotropic Residual Soil

M.F. Leão, M.P. Pacheco, B.R. Danziger

171

Assessment of the Stress History of Quaternary Clay from Piezocone Tests

E. Odebrecht, F. Schnaid

179

*CASE STUDIES**Heterogeneity Evaluation of Soil Engineering Properties Based on Kriging Interpolation Method.**Case Study: North East of Iran, West of Mashhad*

M. Etemadifar, N.S. Vaziri, I. Aghamolaie, N.H. Moghaddas, G.R. Lashkaripour

193

Case Study: Stability Assessment in Underground Excavations at Vazante Mine - Brazil

L.T. Figueiredo, A.P. Assis

203

A Case History with Combined Physical and Vacuum Preloading in Colombia

D.G. Yanez, F. Massad

217